

University of Massachusetts Medical School

eScholarship@UMMS

GSBS Dissertations and Theses

Graduate School of Biomedical Sciences

2020-07-14


Anti-CRISPR Proteins: Applications in Genome Engineering

Jooyoung Lee

University of Massachusetts Medical School

Let us know how access to this document benefits you.

Follow this and additional works at: https://escholarship.umassmed.edu/gsbs_diss

 Part of the [Biotechnology Commons](#), [Genetics and Genomics Commons](#), [Microbiology Commons](#), and the [Other Biomedical Engineering and Bioengineering Commons](#)

Repository Citation

Lee J. (2020). Anti-CRISPR Proteins: Applications in Genome Engineering. GSBS Dissertations and Theses. <https://doi.org/10.13028/xxj4-6a50>. Retrieved from https://escholarship.umassmed.edu/gsbs_diss/1091

Creative Commons License



This work is licensed under a [Creative Commons Attribution 4.0 License](#).

This material is brought to you by eScholarship@UMMS. It has been accepted for inclusion in GSBS Dissertations and Theses by an authorized administrator of eScholarship@UMMS. For more information, please contact Lisa.Palmer@umassmed.edu.

Anti-CRISPR Proteins: Applications in Genome Engineering

A Dissertation Presented

By

Jooyoung Lee

Submitted to the Faculty of the University of Massachusetts Medical School

Graduate School of Biomedical Sciences, Worcester

in partial fulfillment of the requirements for the

degree of

DOCTOR OF PHILOSOPHY

July 14th, 2020

Anti-CRISPR Proteins: Applications in Genome Engineering

A Dissertation Presented
By
Jooyoung Lee

The signatures of the Dissertation Defense Committee signify completion and approval as to style and content of the Dissertation

Erik J. Sontheimer., Ph.D., Thesis Advisor

Scot A. Wolfe, Ph.D., Member of Committee

Wen Xue, Ph.D., Member of Committee

Guangping Gao, Ph.D., Member of Committee

Victor Ambros, Ph.D., Member of Committee

Blake Wiedenheft, Ph.D., External Member of Committee

The signature of the Chair of the Committee signifies that the written dissertation meets the requirements of the Dissertation Committee

Scot A. Wolfe, Ph.D., Member of Committee

The signature of the Dean of the Graduate School of Biomedical Sciences signifies that the student has met all graduation requirements of the school.

Mary Ellen Lane, Ph.D., Dean of the Graduate School of Biomedical Sciences

Interdisciplinary Graduate Program
July 14th, 2020

Acknowledgment

My Ph.D. training would not have been possible without the tremendous support from many people. A five-year journey has taught me to grow not only as a scientist but also as a person. First, I would like to thank my advisor, Dr. Erik Sontheimer, for giving me the opportunity to fledge scientifically in a nurturing environment. He gave me the freedom to gain independence and confidence when I seek guidance in times of feeling lost. Erik is not only a phenomenal mentor but also a thoughtful and caring person. I am very fortunate to have learned professionalism, humor, and a kind heart from him. I also would like to thank the members of my thesis research advisory and dissertation examination committees: Drs. Scot Wolfe, Wen Xue, Guangping Gao, Victor Ambros, and Blake Wiedenheft. My thesis committee members helped me navigate my research with their keen scientific minds and ample resources. I would like to especially thank Scot and Wen and their lab members for making me feel welcomed in their labs and Guangping for generous resources. I am also grateful for having had the opportunities to collaborate with many labs within and outside of UMass: Phil Zamore lab, Craig Mello lab, Guangping Gao lab, and Karen Maxwell/Alan Davidson labs. I feel lucky to have gotten to know and work with many amazing colleagues as well as administrators at the RTI and UMass community.

I would like to extend my acknowledgments to all the past and current members of Sontheimer Lab. I will cherish our memories of pursuing “work hard and play

hard” together. I would like to give so much credit to our lab mom, Nadia, for her everyday scientific guidance but, more importantly, life advice. I also would like to thank Aamir, Ali, Daniel, and Raed, “the OGs,” who have been alongside me the longest, for their genuine friendship and support. You guys are like brothers to me. I also thank all the other Sontheimerians, especially Tomás, for finding the best deals for me.

My Ph.D. experience would not have been the same without the classmates and friends outside of the lab to enjoy the little things in life together. From close and far, I want to thank everyone who has provided me with the mental support and countless pep talks that have kept me going throughout my graduate school.

Last but not least, I would like to thank my family. Their support and encouragement made me stay positive and happy even at the difficult times, and for that, I am forever grateful. Thank you for understanding and supporting my decision to be apart for almost a decade in a foreign country without the family. Even when we do not have as much bonding time together as a family, you have always rooted for me and, most importantly, believed in me.

Abstract

Clustered, regularly interspaced, short palindromic repeats and CRISPR-associated proteins (CRISPR-Cas) constitute a bacterial and archaeal adaptive immune system. The ongoing arms race between prokaryotic hosts and their invaders such as phages led to the emergence of anti-CRISPR proteins as countermeasures against the potent antiviral defense. Since the first examples of anti-CRISPRs were shown in a subset of CRISPR-Cas systems, we endeavored to uncover these naturally-occurring inhibitors that inactivate different types of CRISPR-Cas systems. In the first part of my thesis, we have identified and characterized Type II anti-CRISPR proteins that inactivate several Cas9 orthologs. We share mechanistic insights into anti-CRISPR inhibition and show evidence of its potential utility as an off-switch for Cas9-mediated mammalian genome editing. Although the RNA programmability of Cas9 enables facile genetic manipulation with great potential for biotechnology and therapeutics, limitations and safety issues remain. The advent of anti-CRISPR proteins presents opportunities to exploit the inhibitors to exert temporal, conditional, or spatial control over CRISPR. In the second part of my thesis, we demonstrate that anti-CRISPR proteins can serve as useful tools for Cas9 genome editing. In particular, we have demonstrated that anti-CRISPRs are effective as genome editing off-switches in the tissues of adult mammals, and we further engineered anti-CRISPR proteins to achieve tissue-specific editing *in vivo*. Taken together, my thesis research aimed to mine for natural anti-CRISPR protein inhibitors and

repurpose these proteins to complement current Cas9 technologies in basic and clinical research.

Preface

The following publications are included in this thesis as a whole or in part:

Pawluk, A., Amrani, N., Zhang, Y., Garcia, B., Hidalgo-Reyes, Y., **Lee, J.**, Edraki, A., Shah, M., Sontheimer, E. J., Maxwell, K. L., & Davidson, A. R. (2016). Naturally Occurring Off-Switches for CRISPR-Cas9. *Cell*, 167(7), 1829-1838.e9.

Mir, A., Edraki, A., **Lee, J.**, & Sontheimer, E. J. (2018). Type II-C CRISPR-Cas9 Biology, Mechanism, and Application. *ACS Chemical Biology*, 13(2), 357-365.

Lee, J.*, Mir, A.* , Edraki, A., Garcia, B., Amrani, N., Lou, H. E., Gainetdinov, I., Pawluk, A., Ibraheim, R., Gao, X. D., Liu, P., Davidson, A. R., Maxwell, K. L., & Sontheimer, E. J. (2018). Potent Cas9 Inhibition in Bacterial and Human Cells by AcrIIIC4 and AcrIIIC5 Anti-CRISPR Proteins. *mBio*, 9(6).
<https://doi.org/10.1128/mBio.02321-18>

Lee, J., Mou, H., Ibraheim, R., Liang, S.-Q., Liu, P., Xue, W., & Sontheimer, E. J. (2019). Tissue-restricted genome editing *in vivo* specified by microRNA-repressible anti-CRISPR proteins. *RNA*, 25(11), 1421-1431.

Garcia, B., **Lee, J.**, Edraki, A., Hidalgo-Reyes, Y., Erwood, S., Mir, A., Trost, C. N., Seroussi, U., Stanley, S. Y., Cohn, R. D., Claycomb, J. M., Sontheimer, E. J., Maxwell, K. L., & Davidson, A. R. (2019). Anti-CRISPR AcrIIIA5 Potently Inhibits All Cas9 Homologs Used for Genome Editing. *Cell Reports*, 29(7), 1739-1746.e5.

Davidson, A. R., Lu, W.-T., Stanley, S. Y., Wang, J., Mejdani, M., Trost, C. N., Hicks, B. T., **Lee, J.**, & Sontheimer, E. J. (2020). Anti-CRISPRs: Protein Inhibitors of CRISPR-Cas Systems. *Annual Review of Biochemistry*.
<https://doi.org/10.1146/annurev-biochem-011420-111224>

The following publications were contributed but are not included in this thesis:

Stone, N. P., Hilbert, B. J., Hidalgo, D., Halloran, K. T., **Lee, J.**, Sontheimer, E. J., & Kelch, B. A. (2018). A Hyperthermophilic Phage Decoration Protein Suggests Common Evolutionary Origin with Herpesvirus Triplex Proteins and an Anti-CRISPR Protein. *Structure*, 26(7), 936-947.e3.

Iyer, S., Mir, A., VegaBadillo, J., Roscoe, B., Ibraheim, R., Zhu, L.J., **Lee, J.**, Liu, P., Luk, K., Mintzer, E., Soares de Brito, J., Zamore, P., Sontheimer, E. J., and Wolfe, S.A. (2019). Efficient Homology-directed Repair with Circular ssDNA Donors., *bioRxiv 864199*; doi: <https://doi.org/10.1101/864199>

Chatterjee, P., **Lee, J.**, Nip, L., Koseki, S. R. T., Tysinger, E., Sontheimer, E. J., Jacobson, J. M., & Jakimo, N. (2020). A Cas9 with PAM recognition for adenine dinucleotides. *Nature Communications*, 11(1), 2474.

Chatterjee, P., Jakimo, N., **Lee, J.**, Amrani, N., Rodríguez, T., Koseki, S. R. T., Tysinger, E., Qing, R., Hao, S., Sontheimer, E. J., & Jacobson, J. (2020). An engineered ScCas9 with broad PAM range and high specificity and activity. *Nature Biotechnology*. <https://doi.org/10.1038/s41587-020-0517-0>

Copyright Information

Chapter 2

Chapter 2 is a body of work that describes the discovery and characterization of anti-CRISPR proteins which are published.

1. **Sections 2.2.1 - 2.2.3** are part of a collaborative study conducted in the labs of Maxwell/Davidson at the University of Toronto and the Sontheimer led by April Pawluk with significant contributions from, Nadia Amrani, Yan Zhang, Bianca Garcia, Alireza Edraki, Yuri Hidalgo-Reyes and myself.

Pawluk, A., Amrani, N., Zhang, Y., Garcia, B., Hidalgo-Reyes, Y., **Lee, J.**, Edraki, A., Shah, M., Sontheimer, E. J., Maxwell, K. L., & Davidson, A. R. (2016). Naturally Occurring Off-Switches for CRISPR-Cas9. *Cell*, 167(7), 1829-1838.e9.

No permission is required for reprints as the author of this Elsevier article.

2. **Sections 2.2.4 - 2.2.7** are part of a collaborative study conducted in the labs of Maxwell/Davidson at the University of Toronto and the Sontheimer with an equal contribution (*) from Aamir Mir and myself and significant contributions from Alireza Edraki, Bianca Garcia, Nadia Amrani, and Hannah E. Lou.

Lee, J.*, Mir, A.*, Edraki, A., Garcia, B., Amrani, N., Lou, H. E., Gainetdinov, I., Pawluk, A., Ibraheim, R., Gao, X. D., Liu, P., Davidson, A. R., Maxwell, K. L., & Sontheimer, E. J. (2018). Potent Cas9 Inhibition in Bacterial and Human Cells by AcrIIIC4 and AcrIIIC5 Anti-CRISPR Proteins. *mBio*, 9(6).

<https://doi.org/10.1128/mBio.02321-18>

This is an open-access article distributed under the terms of the Creative Commons CC BY license.

3. **Sections 2.2.8 - 2.2.9** are part of a collaborative study conducted in the labs of Maxwell/Davidson at the University of Toronto and the Sontheimer led by Bianca Garcia with significant contributions from Alireza Edraki, and myself.

Garcia, B., **Lee, J.**, Edraki, A., Hidalgo-Reyes, Y., Erwood, S., Mir, A., Trost, C. N., Seroussi, U., Stanley, S. Y., Cohn, R. D., Claycomb, J. M., Sontheimer, E. J., Maxwell, K. L., & Davidson, A. R. (2019). Anti-CRISPR AcrIIIA5 Potently Inhibits All Cas9 Homologs Used for Genome Editing. *Cell Reports*, 29(7), 1739-1746.e5.

This is an open-access article distributed under the CC BY-NC-ND license (<http://creativecommons.org/licenses/by-nc-nd/4.0/>).

Chapter 3

Chapter 3 is a body of work that describes different applications of anti-CRISPR proteins. None of the data presented in this chapter is published.

1. **Section 3.2.1** reports a method of using cell-cycle-dependent degrons to regulate anti-CRISPR expression to improve HDR efficiency. Experiments were conducted in the Sontheimer lab by Samantha Goetting, a summer undergraduate researcher, under my guidance.
2. **Section 3.2.2** is a part of a collaborative study conducted in the Sontheimer lab led by Nadia Amrani with contributions from Raed Ibraheim and myself.

Chapter 4

Chapter 4 describes a strategy for achieving tissue-restricted genome editing by Cas9 using miRNA-repressible anti-CRISPR proteins. Except for a small part of section 4.2.7, all of the work presented in this chapter is published as follows:

Lee, J., Mou, H., Ibraheim, R., Liang, S.-Q., Liu, P., Xue, W., & Sontheimer, E. J. (2019). Tissue-restricted genome editing *in vivo* specified by microRNA-repressible anti-CRISPR proteins. *RNA*, 25(11), 1421-1431

1. **Sections 4.2.1 - 4.2.6** are part of a collaborative study conducted in the labs of Xue and Sontheimer at the University of Massachusetts Medical School with significant contributions from Haiwei Mou and Shun-Qing Liang in the Xue lab for mouse experiments.

No permission is required for reprints as the author of this article.

2. **Section 4.2.7** ELISA experiment (Figure 4.7B-C) is not published. This experiment was performed by Cole Pero, a rotation student in the Sontheimer lab, under my guidance.

Appendix

None of the studies and data presented in the appendices is published.

Appendix 1 describes Type II-C anti-CRISPR proteins that have not yet been characterized by the labs of Maxwell/Davidson and Sontheimer. Unpublished data was acquired by myself.

Appendix 2 is a follow-up study on the miRNA-repressible anti-CRISPR strategy presented in Chapter 4. None of the data is published. Experiments were carried out by Jiayi Catherine Wang, an exchange medical student from West China School of Medicine, Sichuan University, under my guidance. Small RNA sequencing experiments and analyses were performed by Ildar Gainstenov from the Zamore lab at the University of Massachusetts Medical School.

Appendix 3 is a follow-up study on the immunogenicity of anti-CRISPR proteins related to Chapter 4.2.7. None of the data is published. The study was conducted with assistance from Greg Cottle from the Department of Animal Medicine and Yueying Cao from the Xue lab for mouse work and ELISA experiments were performed by Carolyn Kraus in the Sontheimer lab under my guidance.

Appendix 4 is an extension of the miRNA-repressible anti-CRISPR platform presented in Chapter 4. The preliminary data is to establish a foundation for a new project for achieving therapeutic muscle-specific genome editing for Duchenne's Muscular Dystrophy. None of the data is published. Experiments were performed by myself.

List of Third Party Copyrighted Material

The following figures were modified and reproduced with permission from the publisher:

Figure 1.1 Classifications of CRISPR-Cas systems
Springer Nature License # 4850981131049

Figure 1.2 A schematic of three major stages of CRISPR-Cas immunity
Springer Nature License # 4850981427280

Figure 1.3 Overview of class 2 CRISPR-Cas systems
Springer Nature License # 4850990100985

Figure 1.4 Applications of catalytically impaired CRISPR-Cas effectors
Elsevier License # 4850990338398

Figure 1.5 Therapeutic editing using CRISPR-Cas effectors
Elsevier License # 4850990338398

Figure 1.6 A summary of delivery modalities for CRISPR-Cas9
Elsevier License # 4850990583561

Figure 1.7 Viral mechanisms to evade CRISPR-Cas immunity
Springer Nature License # 4850981427280

Figure 1.8 Different approaches for anti-CRISPR discovery
Annual Reviews, Inc. License ID # 1042479-1
Elsevier License # 4851470351745

Figure 1.9 Functions and mechanisms of anti-CRISPR proteins
Annual Reviews, Inc. License ID # 1042527-1

Figure 1.10 Application and regulation of anti-CRISPR proteins
Springer Nature License # 4851480703079

List of Figures

Chapter 1

Figure 1.1	Classifications of CRISPR-Cas systems·····	4
Figure 1.2	A schematic of three major stages of CRISPR-Cas immunity·····	7
Figure 1.3	Overview of class 2 CRISPR-Cas systems·····	9
Figure 1.4	Applications of catalytically impaired CRISPR-Cas effectors·····	18
Figure 1.5	Therapeutic editing using CRISPR-Cas effectors·····	25
Figure 1.6	A summary of delivery modalities for CRISPR-Cas9·····	31
Figure 1.7	Viral mechanisms to evade CRISPR-Cas immunity·····	39
Figure 1.8	Different approaches for anti-CRISPR discovery·····	50
Figure 1.9	Functions and mechanisms of anti-CRISPR proteins·····	58
Figure 1.10	Application and regulation of anti-CRISPR proteins·····	70

Chapter 2

Figure 2.1	Three families of anti-CRISPR proteins inhibit Nme1Cas9·····	80
Figure 2.2	AcrIIC1-3 inhibit Nme1Cas9 genome editing in mammalian cells·····	82
Figure 2.3	AcrIIC3 can be used for a dNme1Cas9 application·····	85
Figure 2.4	Identification and validation of two Type II-C anti-CRISPRs·····	88
Figure 2.5	Characterization of new Type II-C Cas9 orthologs·····	91
Figure 2.6	AcrIIC4 and AcrIIC5 inhibit genome editing in human cells·····	93
Figure 2.7	Mechanistic insights into AcrIIC4 and AcrIIC5 inhibition·····	96
Figure 2.8	AcrIIA5 is a broad-spectrum inhibitor of Type II Cas9 proteins·····	98
Figure 2.9	AcrIIA5 prevents DNA binding and leads to sgRNA cleavage·····	103

Chapter 3

Figure 3.1	Cell-cycle dependence of DSB repair pathways·····	129
Figure 3.2	Control of Cas9 and anti-CRISPR with cell cycle degrons·····	132
Figure 3.3	AcrIIA5-hCdt1 and TEG donor improve HDR efficiency·····	135
Figure 3.4	Type II-C anti-CRISPRs inhibit Nme1Cas9-pDBD fusion·····	137
Figure 3.5	Anti-CRISPRs inhibit orthogonal Cas9-Cas9 fusion·····	140

Chapter 4

Figure 4.1	Overview of the microRNA-repressible anti-CRISPR system·····	158
Figure 4.2	Regulation of anti-CRISPR expression <i>in vitro</i> by miRNAs·····	160
Figure 4.3	Hepatocyte-specific genome editing by Cas9 orthologs·····	163
Figure 4.4	Cas9 inhibition by anti-CRISPR is released by miR-122 <i>in vivo</i> ·····	166
Figure 4.5	miRNA-repressible AcrIIC3 inhibits Cas9 in a non-target tissue···	169
Figure 4.6	Confirmation of Nme2Cas9 expression and Acr transcripts·····	171
Figure 4.7	Anti-CRISPR expression <i>in vivo</i> has no overt adverse effects·····	173

Appendix

Figure A1.1	Type II-C anti-CRISPR inhibition of Nme1Cas9 and Nme2Cas9··	195
Figure A2.1	Experimental overview of miRNA profiling for <i>in vitro</i> studies·····	198
Figure A2.2	Effects of miRNA and target abundance on silencing activity·····	200
Figure A2.3	Comparison of full-length vs. g2-g16 MREs on silencing activity··	204
Figure A2.4	Acr repression by full-length or g2-g16 MREs leads to editing·····	206
Figure A3.1	Immunization assay with recombinant Cas9 and anti-CRISPR·····	210
Figure A3.2	IgG immune response against Nme2Cas9 and SpyCas9·····	212
Figure A3.3	IgG immune response against anti-CRISPR proteins·····	214
Figure A4.1	Two strategies for therapeutic gene editing in DMD·····	220
Figure A4.2	Exon skipping strategy: a design of target sites and validation·····	222
Figure A4.3	Exon deletion strategy: design of a scAAV with two guides·····	224

List of Tables

Appendix Table 1.....	227
Appendix Table 2.....	228

List of Abbreviations

AAV: adeno-associated virus

Aca: anti-CRISPR associated

Acr: anti-CRISPR

Cas: CRISPR associated

CRISPR: clustered, regularly interspaced, short palindromic repeats

crRNA: CRISPR RNA

dCas9: nuclease-dead Cas9

DMD: Duchenne's muscular dystrophy

DSB: double-strand break

dsDNA: double-stranded DNA

ELISA: enzyme-linked immunosorbent assay

ESE: exonic splicing enhancer

gDNA: genomic DNA

HDR: homology-directed repair

HITI: homology-independent targeted integration

Indels: insertions and deletions

ITR: inverted terminal repeats

MGE: mobile genetic element

miRNA: microRNA

MRE: miRNA response element

nCas9: nickase Cas9

NHEJ: non-homologous end-joining

NLS: nuclear localization signal

NmeCas9: *Neisseria meningitidis* Cas9

ORF: open reading frame

PAM: protospacer adjacent motif

PID: PAM-interacting domain

pDBD: programmable DNA binding domain

pegRNA: prime editing guide RNA

rAAV: recombinant adeno-associated virus

RNP: ribonucleoprotein

RT: reverse transcriptase

sgRNA: single-guide RNA

SpyCas9: *Streptococcus pyogenes* Cas9

scAAV: self-complementary rAAV

ssAAV: single-stranded rAAV

ssDNA: single-stranded DNA

T7E1: T7 Endonuclease 1

TALEN: transcription activator-like effector nuclease

TIDE: tracking of indels by decomposition

tracrRNA: trans-activating crRNA

ZFN: zinc-finger nuclease

ZFP: zinc-finger protein

Table of Contents

Acknowledgment	iii
Abstract	v
Preface	vii
Copyright Information	ix
List of Third Party Copyrighted Material	xii
List of Figures	xiii
List of Tables	xv
List of Abbreviations	xvi
Table of Contents	xix
Chapter 1 Introduction	xxi
1.1 Introduction to CRISPR-Cas systems	1
1.1.1 The diversity and biology of CRISPR-Cas systems	1
1.1.2 Class 2 CRISPR-Cas systems	8
1.2 CRISPR-Cas systems for genome engineering	13
1.2.1 Applications of CRISPR-Cas	13
1.2.2 Therapeutic gene editing using CRISPR-Cas effectors	23
1.2.3 <i>Ex vivo</i> and <i>in vivo</i> delivery for gene editing	26
1.2.4 Challenges of CRISPR-mediated therapeutic editing	29
1.3 Introduction to anti-CRISPR proteins	37
1.3.1 Evolutionary arms race between prokaryotic hosts and their invaders	38
1.3.2 Functions of anti-CRISPR proteins in a host-pathogen arms race	42
1.3.3 The origins of anti-CRISPR proteins	48
1.3.4 Discovery approaches for anti-CRISPR proteins	49
1.3.5 Mechanisms of anti-CRISPR protein inhibition	57
1.3.6 Applications of anti-CRISPR proteins	69
Chapter 2 Discovery and characterization of anti-CRISPR proteins	76
2.1 Introduction	76
2.2 Results	78

2.2.1 The discovery of anti-CRISPR proteins for Cas9	78
2.2.2 Anti-CRISPRs inhibit Cas9 genome editing in mammalian cells	81
2.2.3 Anti-CRISPRs inhibit a dCas9 application in mammalian cells	83
2.2.4 Type II-C anti-CRISPRs are found in diverse bacterial species	86
2.2.5 Characterization of two new Type II-C Cas9 orthologs	89
2.2.6 AcrIIIC4 and AcrIIIC5 inhibit genome editing in human cells	92
2.2.7 AcrIIIC4 and AcrIIIC5 prevent stable DNA binding by Nme1Cas9	94
2.2.8 AcrIIIA5 inhibits Cas9 from both Type II-A and -C systems	97
2.2.9 AcrIIIA5 activity prevents DNA binding and leads to sgRNA cleavage	101
2.3 Discussion	105
2.4 Materials and Methods	110
Chapter 3 Applications of anti-CRISPR proteins for genome engineering	121
3.1 Introduction	121
3.1.1 Precise gene editing using HDR is inefficient	122
3.1.2 Enhancing target specificity often requires engineering nucleases	125
3.2 Results	127
3.2.1 Anti-CRISPRs with cell-cycle-dependent degrons improve HDR	127
3.2.2 Application of anti-CRISPR proteins for Cas9 fusion platforms	136
3.3 Discussion	143
3.4 Materials and Methods	148
Chapter 4 Tissue-restricted genome editing <i>in vivo</i> by miRNA-repressible anti-CRISPRs	151
4.1 Introduction	151
4.1.1 Background on AAV	153
4.1.2 Enhancing tissue-specificity of transgene expression	154
4.1.3 A strategy for miRNA-mediated transgene de-targeting	155
4.2 Results	156
4.2.1 A strategy for microRNA-regulated anti-CRISPR proteins	156
4.2.2 In vitro validation of microRNA-repressible anti-CRISPR vectors	159
4.2.3 Acr repression by miR-122 precludes inhibition in hepatocytes	162
4.2.4 MiR-122-dependent genome editing conferred by Acrs <i>in vivo</i>	164
4.2.5 MiRNA-repressible anti-CRISPR inhibits off-tissue genome editing	167

4.2.6 Lack of editing <i>in vivo</i> is not due to lack of Nme2Cas9 expression	169
4.2.7 Expression of anti-CRISPRs <i>in vivo</i> does not elicit adverse effects	172
4.3 Discussion	174
4.4 Materials and Methods	177
Chapter 5 Discussion	183
5.1 The prospects of CRISPR genome engineering	183
5.1.1 A summary of CRISPR-Cas applications	183
5.1.2 Considerations for human therapeutics	185
5.1.3 Heritable germline editing and ethics	187
5.2 The new and emerging field of anti-CRISPRs	189
5.2.1 The biology of anti-CRISPRs	189
5.2.2 A summary of anti-CRISPR protein applications	191
Appendix	192
Appendix 1 Characterization of additional Type II-C anti-CRISPRs	193
Appendix 2 Optimization of the miRNA-repressible anti-CRISPR system	196
A2.1 Transgene repression requires a threshold level of miRNAs	197
A2.2 Optimizing the length of the MRE to bypass the TDMD pathway	201
A2.3 Future directions	207
Appendix 3 Immunogenicity of anti-CRISPR proteins	209
A3.1 No IgG immune response against anti-CRISPR proteins is detected	211
A3.2 Future directions	216
Appendix 4 Muscle-specific genome editing <i>in vivo</i> for DMD	218
A4.2 Background on Duchenne's Muscular Dystrophy	218
A4.2 Exon skipping strategy for therapeutic editing in DMD	221
A4.3 Exon deletion strategy for therapeutic editing in DMD	223
A4.4 Future directions	225
Appendix Table 1. Protein sequences of anti-CRISPR and Cas9	227
Appendix Table 2. Plasmids used in Chapters 2, 3, and 4	228
References	229

Chapter 1 Introduction

1.1 Introduction to CRISPR-Cas systems

1.1.1 The diversity and biology of CRISPR-Cas systems

Clustered, regularly interspaced, short palindromic repeats (CRISPR)-CRISPR associated (Cas) is an adaptive immune system found in archaea and bacteria that protects against mobile genetic elements (MGEs) such as phages by targeting and destroying their nucleic acids (Barrangou et al., 2007; Brouns et al., 2008; Marraffini & Sontheimer, 2008). Distributions of CRISPR-*cas* loci are represented in a substantial majority of archaea (~90%), including almost all hyperthermophiles, and in ~40% of bacteria, underscoring the prevalence and importance of their existence (Makarova et al., 2020). Although CRISPR-Cas systems are highly abundant and diverse, they share core architectural and functional similarities. A typical CRISPR locus consists of *cas* genes and a CRISPR array, a series of identical repeat sequences interspaced by short spacer sequences, which are fully or partially complementary to foreign genetic elements called protospacers. The spacer and repeat sequences are typically transcribed into a long precursor CRISPR RNA (pre-crRNA), which is further processed into mature CRISPR RNAs (crRNAs). Proteins involved in different processes of CRISPR-mediated immunity are encoded by *cas* genes in the vicinity of the CRISPR array (Makarova et al., 2020). In the biological context,

crRNAs and Cas proteins from the CRISPR locus function together hand-in-hand to form an RNA-guided effector protein complex to target matching protospacers when encountered by MGEs.

The diversity of CRISPR-Cas systems

Although an increasing wealth of genomic and metagenomic data will likely continue the expansion of the CRISPR-Cas systems, current systems are broadly grouped into two classes and further categorized into 6 types and 33 subtypes (Makarova et al., 2020) (Figure 1.1). A number of *cas* genes encoding important proteins in the CRISPR-Cas pathway have been identified to date and divided into functional modules: adaptation, expression, interference, and ancillary. Although no genes are shared by all CRISPR-Cas systems, the only proteins that are almost universal are Cas1 and Cas2, which are key enzymes that function in the adaptation module. In most class 1 systems, Cas6 is directly involved in processing crRNAs. In class 2 systems, some Cas proteins (such as in subtype V-A and type VI) can have RNase activity and process their own crRNAs while Type II (and some Type V subtypes) systems rely on the bacterial host RNase III. The latter types are also distinguished from the rest by having an additional RNA component, known as a trans-activating RNA (tracrRNA). The partial pairing between the direct repeat region of a crRNA and tracrRNA forms a stable duplex that is processed by RNase III (E. Charpentier et al., 2015; Deltcheva et al., 2011). This mature guide RNA (crRNA-tracrRNA) remains

bound to an effector protein for interference. The effector protein(s) in the interference module is extremely diverse and forms the basis for classification schemes of different CRISPR systems. In the case of class 1 systems, multiple proteins form a complex with crRNA for interference step while class 2 CRISPR systems use a single, multi-domain effector protein that essentially serves the same purpose of an entire effector complex of class 1. The ancillary module is composed of genes that are linked or predicted to be associated with CRISPR but are not yet fully explored.

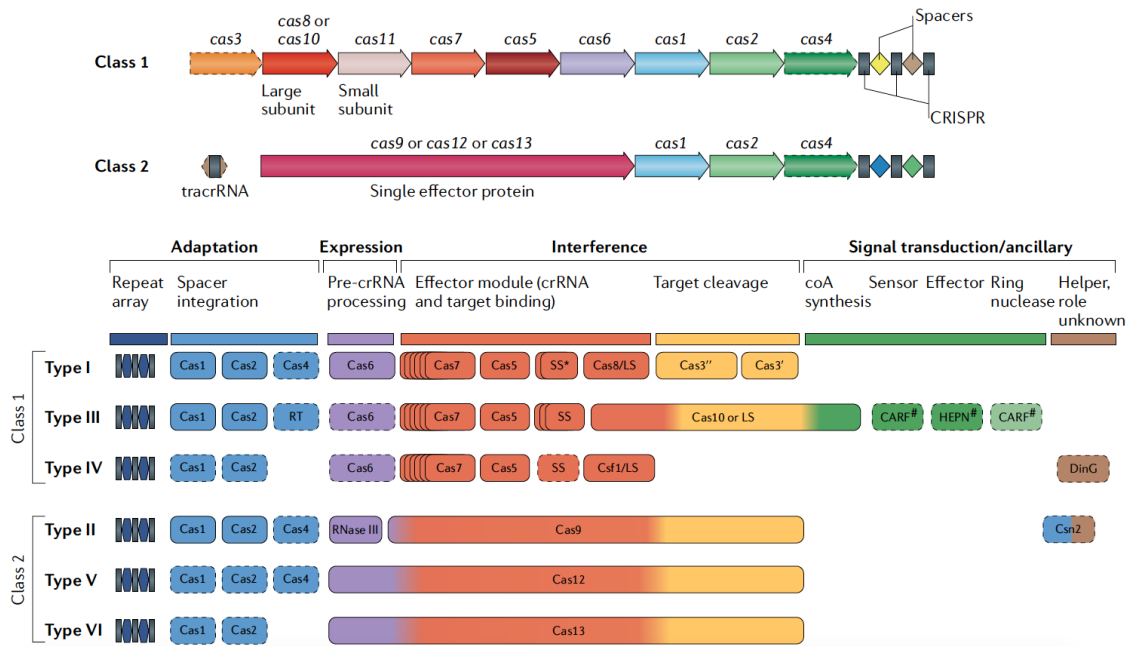


Figure 1.1 Classifications of CRISPR-Cas systems. Top: a generic organization of class 1 and 2 CRISPR loci. Two classes are distinguished by either a multi-effector complex or single effector protein. Bottom: each class is further divided into six types based on the genetic, structural, and functional organizations: class 1 includes Types I, III, and IV while class 2 includes Types II, V, and VI. Figure adapted from Makarova et al. with permission (see the List of Third Party Copyright Information) (Makarova et al., 2020).

The biology of CRISPR-Cas systems

CRISPR-Cas systems function against invading genetic materials in three key steps: adaptation, biogenesis, and interference (Figure 1.2). Adaptation is a key aspect of CRISPR-Cas adaptive immunity that provides hosts with protection from continuous invasions by MGEs. This is facilitated by adaptation in which hosts acquire new spacers from the foreign genetic materials by incorporating them into CRISPR loci (McGinn & Marraffini, 2019). The acquisition of spacers from the previous encounter serves as a memory reservoir to effectively destroy the invading genome upon future infection (Brouns et al., 2008; Garneau et al., 2010; Hale et al., 2009; Rouillon et al., 2013; Sapranaukas et al., 2011). Most CRISPR loci make a single long transcript of pre-crRNA that must be processed into individual crRNAs during the expression stage (Brouns et al., 2008; Carte et al., 2008; E. Charpentier et al., 2015; Deltcheva et al., 2011). The processing is mediated by either Cas protein(s) or host RNases depending on different CRISPR systems (Carte et al., 2008; Deltcheva et al., 2011; Haurwitz et al., 2010). During the interference step, the complementarity between the spacers of crRNAs and protospacer sequences of invading genomes such as viruses or plasmids triggers the cleavage of nucleic acid targets by Cas nuclease(s). In some systems such as Type I and II, a PAM flanking the target sequence is required for cleavage of the protospacer sequence in the invading nucleic acids. PAMs also serve an important role in protecting host's own genome by avoiding "self-targeting," which is the cleavage of the spacer sequence in the CRISPR

array (Deveau et al., 2008; Mojica et al., 2009). This is a simplified summary of key functionalities of CRISPR-Cas systems but there are many details and aspects that are unique for different systems.

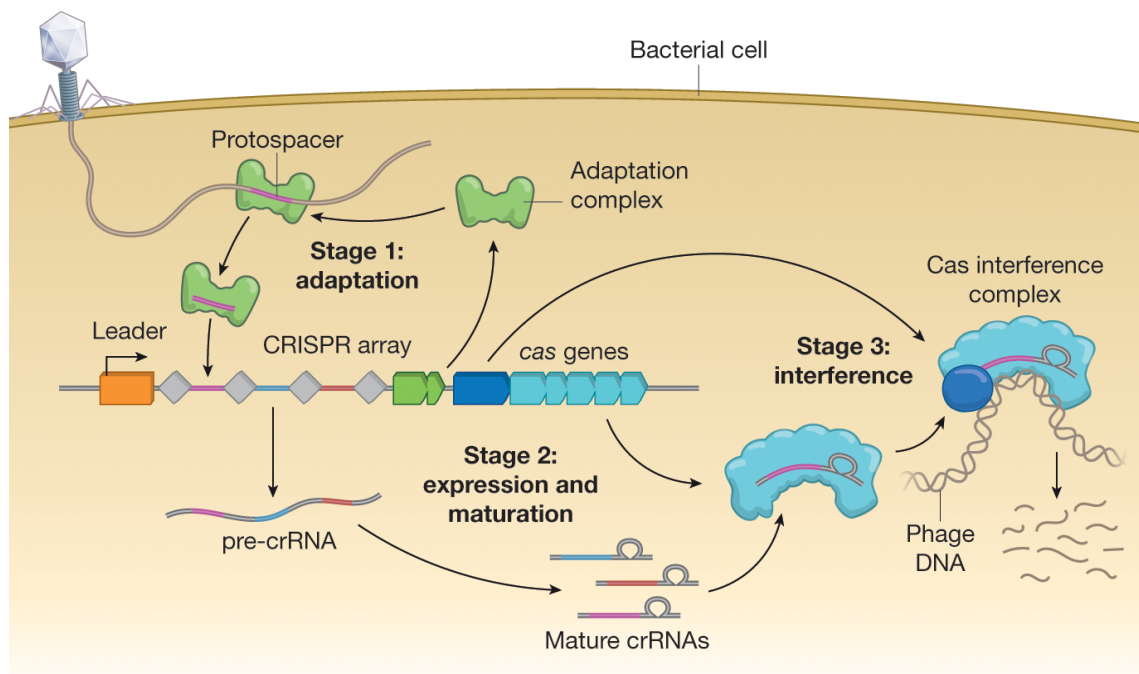


Figure 1.2 A schematic of the three major stages of CRISPR-Cas immunity. Step 1: Adaptation is the acquisition of a protospacer from invading MGEs and integration as a spacer into the CRISPR array. Step 2: expression and maturation involve transcription of pre-crRNAs containing spacer sequences and processing into mature forms. Step 3: interference is executed by Cas effector protein(s) guided by crRNAs to target the protospacers in the invading genome. Figure adapted from Hampton et al. with permission (see the List of Third Party Copyright Material) (Hampton et al., 2020).

1.1.2 Class 2 CRISPR-Cas systems

Although class 1 is far more abundant than class 2 in most groups of bacteria and archaea, class 2 remains nearly exclusive to bacteria. The near-absence of class 2 in archaea can be partly explained by the absence of RNase III, which is required for crRNA processing in many class 2 systems. Class 2 effector proteins, especially those from Type II systems, are known to play important roles in adaptation, crRNA processing, and interference steps. In particular, Cas9, Cas12, and Cas13 are the signature effector proteins from Types II, V and VI, respectively, that have gained great attention for their biotechnological uses (Figure 1.3). Each of these types is discussed in more detail below.

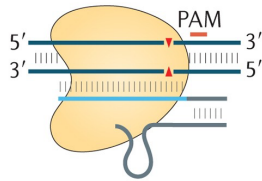
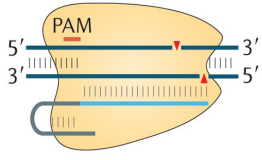
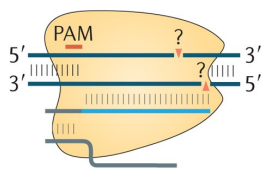
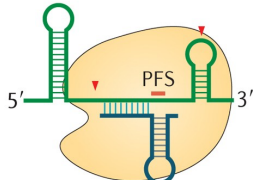
		Nuclease domains	tracrRNA	PAM	Substrate	Cleavage pattern
Type II Cas9		RuvC and HNH	Yes	3', GC-rich	dsDNA	Blunt ends
Type V-A Cas12a (Cpf1)		RuvC and Nuc	No	5', AT-rich	dsDNA	Staggered ends, 5' overhangs
Type V-B Cas12b (C2c1)		RuvC	Yes	5', AT-rich	dsDNA	Staggered seven-nucleotide cut of target DNA
Type VI-A Cas13a (C2c2)		2 HEPN domains	No	5', non-G PFS	ssRNA	Cleaves ssRNA near uracil and collateral activity

Figure 1.3 Overview of class 2 CRISPR-Cas systems. A schematic of the effector complex consisting of protein, target DNA, crRNA and tracrRNA (for Types II, V and VI) is shown. Red bars indicate a PAM (protospacer adjacent motif) or a PFS (protospacer flanking sequence). Red triangles show cut sites in the target DNA or RNA. dsDNA, double-stranded DNA; ssRNA, single-stranded RNA. Nuclease domains, canonical PAM/PFS preferences, target substrates, and cleavage patterns are summarized. Figure adapted from Shmakov et al. with permission (see the List of Third Party Copyright Material) (Shmakov et al., 2017).

Type II

Cas9 is an effector protein of Type II systems that became a focus of the CRISPR field relatively early. A Cas9 ribonucleoprotein (RNP) complex with crRNA and a trans-activating (tracrRNA) cleaves DNA in an RNA-guided fashion (Gasiunas et al., 2012; Jinek et al., 2012). Cas9 contains two nuclease domains, an HNH (His-Asn-His) domain and a RuvC-like domain, that are responsible for creating a double-strand break (DSB) by cleaving the target strand that pairs with the spacer and the displaced non-target strand, respectively.

Cas9 is one of the best-studied CRISPR-Cas systems because of its initial demonstration as a programmable RNA-guided genome editing platform using a Type II-A Cas9 from *Streptococcus pyogenes* (*S. pyogenes* Cas9 - SpyCas9) (Cho et al., 2013; Cong et al., 2013; W. Y. Hwang et al., 2013; W. Jiang, Bikard, et al., 2013; Jinek et al., 2013; Mali et al., 2013). Today, many Type II Cas9 orthologs have been repurposed as tools for genome engineering. Type II CRISPR systems are further subdivided into three subtypes based on the degree of homology between Cas9 proteins, and the presence or absence of an additional Cas protein involved in adaptation. Type II-A and II-B systems include Csn2 and Cas4, respectively, while most Type II-C systems are characterized by a lack of both Cas4 and Csn2 (Mir, Edraki, et al., 2018). [An additional variant of Type II-C CRISPR system (type II-C2) has been identified in archaea that shares similarity with Type II-C Cas9s but also contains Cas4 (Burstein et al., 2017)].

Moreover, Type II-C CRISPR arrays have internal promoters embedded in each repeat sequence, generating nested pre-crRNAs as a source of mature crRNAs instead of processing a single pre-crRNA transcript (Y. Zhang et al., 2013).

Another feature of all Type II Cas9s is the requirement of a PAM sequence in the target DNA. PAM recognition by a Cas9 is thought to be required prior to the initiation of unwinding and cleavage of double-stranded DNA (dsDNA) at a sequence upstream of PAM. Although PAM lengths and sequences are unique to each Cas9, most are GC-rich.

Type V

Type V systems differ fundamentally from Type II by the domain architecture of effector proteins. While Type II effector proteins contain two nuclease domains, Type V effectors (Cas12) only have RuvC-like domains that are responsible for DSB induction. Although effectors of subtypes V-A (Cas12a) and V-B (Cas12b) have been investigated in detail, there are currently 10 subtypes of Type V.

Various Cas12 effectors possess different properties, including dsDNA cleavage and nicking and collateral cleavage of single-stranded DNA and RNA (Yan et al., 2019). In particular, Cas12a (formerly known as Cpf1) is a prototype Type V effector protein that has been extensively studied structurally and functionally. A key distinction of Cas12a is its ability to process its own crRNA and its lack of a tracrRNA. Cas12a also differs from most Cas9s by generating a staggered

dsDNA cleavage pattern; furthermore, it cleaves distal from the PAM sequence, which tends to be AT-rich.

Type VI

The Type VI effector protein, Cas13, is the first and thus far only variant in class 2 to target only RNA, presumably transcripts of invading genomes since RNA viruses are less common than those with DNA genomes. It is characterized by the presence of two HEPN (Higher Eukaryotes and Prokaryotes Nucleotide-binding) RNase domains that possess RNA cleavage and binding activities instead of a DNA-targeting mechanism. In addition, target RNA recognition of Cas13-crRNA complex triggers its nonspecific RNase activity, and collateral RNA degradation induces dormancy in hosts infected with the targeted virus (Meeske et al., 2019). Type VI systems seem to be less diverse and less abundant than Types II and V, although new subtypes may be discovered in the future.

1.2 CRISPR-Cas systems for genome engineering

1.2.1 Applications of CRISPR-Cas

Due to its ease of programmability and simplicity, different Cas proteins have been repurposed for genome engineering applications in many heterologous contexts. It has successfully been used for genetically modifying plants and animals, for gene therapy for human diseases, and development of research and diagnostic tools (Doudna, 2020; Pickar-Oliver & Gersbach, 2019; Porteus, 2019).

To date, most applications of CRISPR systems have focused on the programmable DNA-targeting activity of Cas9. The cleavage activity of Cas9 can be harnessed for genome editing while catalytically inactive ('dead') variants of Cas9 (dCas9) have been used for transcriptional control, epigenetic manipulation, and chromatin imaging. Most recently, nickase versions of Cas9 (nCas9) have been used in base editing as well as prime editing (Anzalone et al., 2019; Komor et al., 2018; Rees & Liu, 2018a). All of these advances also have their own limitations, such as the potential for off-target effects and challenges that are associated with delivery (Doudna, 2020). Thus, alternative tools for CRISPR technologies are in high demand.

The diversity of CRISPR systems such as in the nature of their targets (DNA vs. RNA), PAM specificities and sizes provide opportunities for enhancing and expanding the capabilities of our toolbox for biomedical research and

biotechnology. For example, Cas12a from Type V-A lacks a tracrRNA and has an AT-rich PAM, yielding in a simpler, single crRNA-guided and highly specific enzyme that can target AT-rich genomes. Cas13a from Type VI also opens a door for RNA-targeting technologies that enable us to manipulate RNA transcripts in cells. Both Cas12a and Cas13a have been used in diagnostics for viral infection (Ackerman et al., 2020; J. S. Chen et al., 2018; Gootenberg et al., 2017).

Outcomes of CRISPR-Cas gene editing repair

In engineered systems, the crRNA and tracrRNA can be fused into a single-guide RNA (sgRNA) (Jinek et al., 2012). Cas9 can use an sgRNA to target virtually any sequence next to a cognate PAM and introduce a DSB. As DSBs are inherently detrimental for genomic integrity, they are resolved by cellular repair pathways. In most mammalian cells, DSBs are repaired via non-homologous end-joining (NHEJ) that can sometimes introduce insertions and deletions (indels) at the cut site by imprecise repair process, which may inactivate the target gene. When the NHEJ machinery restores the original sequence by directly ligating the blunt ends of DNA without indels, the intact sequence is subjected to Cas9-mediated cleavage again, ultimately resulting in indels. Indels may be useful for knocking out a gene of interest or perturbing functional elements of a gene. An alternative major repair pathway known as homology-directed repair (HDR) requires a template DNA that has sequences homologous to the region surrounding the DSB. The source of a template DNA can be an endogenous allele or an exogenous donor. The donor DNA can be used to introduce a precise modification such as correction, insertion, or deletion into the target DNA. However, HDR has limitations in its availability in dividing cells only, and in its inefficiency compared to NHEJ. Unlike NHEJ, which operates throughout the cell cycle, HDR is largely restricted to the S and G2 phases of the cell cycle (Hustedt & Durocher, 2016).

Although the two major DSB repair pathways, NHEJ and HDR, are dominant in the repair of a conventional DSB, there are other alternative DSB repair pathways that are less prevalent. DSBs introduced by Cas9 result in different repair outcomes depending on the types of repair machinery that are available, genomic context, cell types, cell-cycle stages, and target sites. Therefore, editing efficiencies and outcomes vary considerably from site to site, depending on sgRNA expression, DNA accessibility, and other factors (Scully et al., 2019).

Cas9 applications based on DNA binding

There are numerous applications that can be harnessed without introducing DSBs (Figure 1.4). A catalytically impaired dCas9 with both nuclease domains inactivated can be fused to an effector protein such as a transcriptional regulator or an epigenetic modifier for gene expression, as well as fluorescent proteins for live-cell imaging (Adli, 2018). A nickase Cas9 with only one nuclease domain active can cleave only one strand of dsDNA. Cas9 nickases fused to accessory enzymes such as deaminases or reverse transcriptases have opened up new, emerging technologies such as base editing and prime editing (Anzalone et al., 2019; Rees & Liu, 2018a).

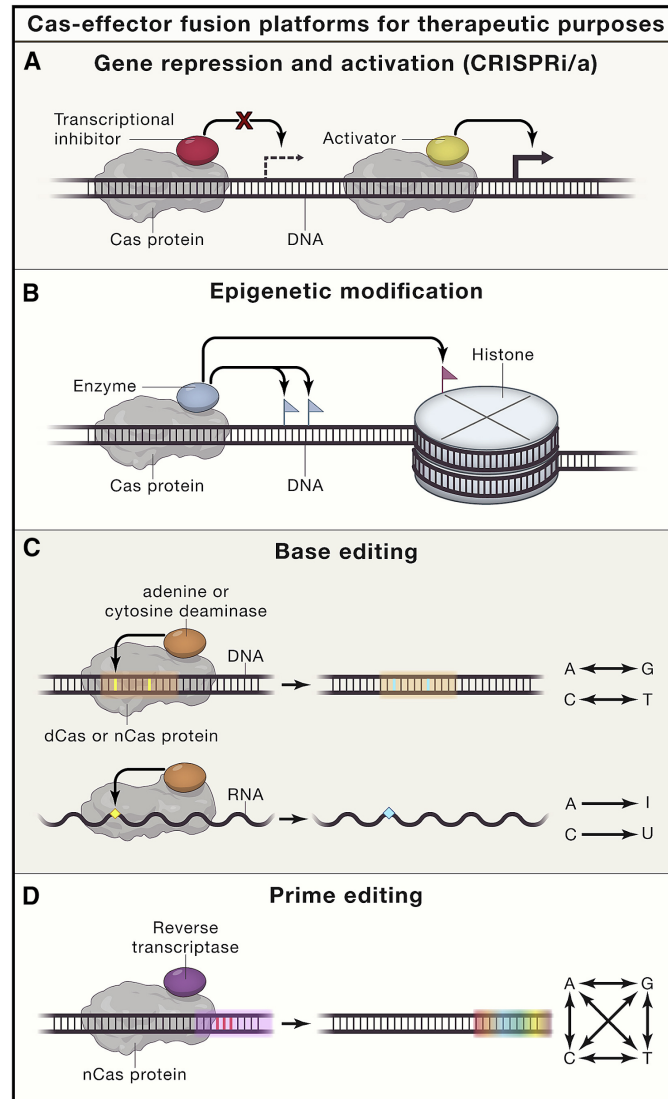


Figure 1.4 Applications of catalytically impaired CRISPR-Cas effectors. (A) Gene regulation using transcription activators or repressors. **(B)** Epigenome editing deposits epigenetic markers such as methylation and histone modifications. **(C)** Deaminases fused to either dead Cas9 (dCas9) or nickase Cas9 (nCas9) allow base editing. **(D)** In prime editing, a reverse transcriptase is fused to a nCas9 and uses a prime editing guide RNA (pegRNA) as a template to encode new genetic information. Figure adapted from Wang et al. with permission (see the List of Third Party Copyright Material) (D. Wang et al., 2020).

CRISPR interference and activation (CRISPRi/a)

Once dCas9 binds strongly to the DNA target sequence, this tight binding can interfere with the activity of other endogenous DNA binding proteins such as transcription factors and RNA polymerases (Qi et al., 2013). This has been exploited to develop the CRISPR interference (CRISPRi) approach in which dCas9 binding activity blocks the transcriptional process, resulting in gene knockdown (Qi et al., 2013). The downregulation of gene expression can be further enhanced by fusing a strong repressor complex such as Kruppel-associated Box (KRAB) to dCas9 (Gilbert et al., 2013). Similarly, the dCas9-targeting platform can be repurposed for transcriptional activation (CRISPRa). To achieve robust induction of gene expression, different transactivation domains such as VP64 (composed of four tandem copies of VP16) or improved complexes such as those composed of VP64, p65, and Rta (VPR) proteins, have been used (Cheng et al., 2013; Maeder et al., 2013; Mali et al., 2013; Perez-Pinera et al., 2013).

Epigenome editing

The epigenome is defined as regulatory elements such as post-translational modifications and other chromatin features that change genome function in a manner that does not involve changes in DNA sequence. Epigenetic markers such as DNA methylation and histone modifications play crucial roles in proper gene expression and genome organization. To better understand the functional

roles of various epigenomic features, the programmable capacity of dCas9 has been exploited to recruit epigenetic writers and erasers to specific loci. DNA methylation is well-studied in chromatin biology to regulate gene expression (Razin & Riggs, 1980). Generally, DNA methylation at promoters or distal regulatory elements is associated with transcriptional repression. To manipulate gene expression through DNA methylation, the dCas9 system has been used to both deposit DNA methylation marks using a catalytic domain of DNA methyltransferase such as DNMT3A (Amabile et al., 2016) and to remove DNA methylation using catalytic domains of endogenous demethylases such as ten-eleven translocation (TET) proteins: TET1, TET2, and TET3 (X. S. Liu et al., 2016). In addition to understanding chromatin biology, these types of technologies may provide an opportunity to manipulate aberrant disease-associated DNA methylation. For example, dCas9 fused to a DNA demethylation enzyme TET1 was used to demethylate the CGG trinucleotide repeat expansion in fragile X syndrome that results in silencing of the *FMR1* gene due to hypermethylation of CGG repeats (X. S. Liu et al., 2018).

Base editing

A prominent advance in the field is the development of a base editing platform that enables the installation of desired nucleotide changes independently of DSBs and HDR. A DNA base editor consists of a catalytically disabled nuclease fused to a deaminase enzyme, and in some cases, a DNA glycosylase inhibitor

(Komor et al., 2016). Upon binding to its target site in genomic DNA, base pairing between the guide RNA and target DNA strand forms a displaced single-stranded DNA (ssDNA) known as an “R-loop,” which is subjected to deamination enzymes. Two classes of base editors, adenine BE (ABE) and cytosine BE (CBE), convert an A•T base pair to a G•C base pair and C•G base pair into a T•A base pair, respectively. Using a nickase Cas9 improved the efficiency by generating a nick in the unedited strand and thus directing cells to repair the non-edited strand using the edited strand as a template (Gaudelli et al., 2017; Komor et al., 2016; Nishida et al., 2016). Collectively, CBEs and ABEs can mediate all four possible transition mutations ($C \rightarrow T$, $A \rightarrow G$, $T \rightarrow C$, and $G \rightarrow A$). RNA base editors achieve similar targeted adenosine conversion to inosine using Cas13-guided RNA-targeting methods (Cox et al., 2017). Although some bystander editing within a window of several base pairs and Cas9-dependent off-target editing may cause undesired changes, newer generations of base editors have emerged from extensive efforts to refine the editing window and increase editing precision (Thuronyi et al., 2019). Overall, programmable DNA and RNA base editors greatly expanded the CRISPR-based toolbox for a diverse array of animal, plant, and microbial organisms.

Prime editing

The latest game-changer is prime editing (Anzalone et al., 2019), which allows gene editing beyond the capabilities of base editors to include additional point

mutations (including transversions) as well as insertions and deletions. In prime editing, Cas9 nickase is fused to a reverse-transcriptase (RT) enzyme and the guide RNA is re-engineered as a prime editing guide RNA (pegRNA) to contain the sequence intended to correct the mutations. Like conventional sgRNA, pegRNA dictates target DNA specificity. However, it also hybridizes with the nicked single-stranded DNA to provide a template for reverse transcription, thereby encoding the desired sequence information. The fusion enzyme nicks the DNA and the upstream ssDNA of the nick binds to the extended portion of the pegRNA in accordance with Watson-Crick base pairing, and then RT uses the pegRNA as a template to synthesize corrected DNA. Cellular factors mediate removal of the flap containing the redundant portion of the original DNA and ligation of the two ends of ssDNA, and then the mismatch repair machinery corrects the unedited, complementary DNA strand using the edited strand as a template. Prime editing is an unprecedented, versatile genome editing platform that enables not only transition and transversion point mutations but also small indel mutations. This opens the possibility of highly precise and efficient repairing mutations in human diseases (Urnov, 2020).

1.2.2 Therapeutic gene editing using CRISPR-Cas effectors

The idea of gene therapy to treat genetic diseases has been around for decades. However, delivering a functional gene copy to replace a mutated protein is not always applicable to other types of diseases, for example, those that are caused by gain-of-function pathogenic mutations. Directly correcting a mutated gene, thereby restoring the gene's function, in its natural context may address some of the limitations of traditional gene therapy (High & Roncarolo, 2019). This led to a rise of gene-editing tools such as zinc-finger nucleases (ZFNs), transcription activator-like effector nucleases (TALENs), and other types of meganucleases (Zheng et al., 2020). The rise of CRISPR-Cas9 has contributed tremendously to basic research but also holds enormous therapeutic potential for human diseases.

Therapeutic gene editing strategies

Many therapeutic editing strategies currently employed use nuclease activities of Cas effector proteins (Figure 1.5). Simply targeting a mutated gene and inducing NHEJ can have a therapeutic benefit by knocking down or out a dysfunctional protein, inducing the skipping of a mutated exon to rescue partially functional protein, and other strategies (D. Wang et al., 2020). Furthermore, by exploiting the predictable and reproducible indel spectra at many target sites, frameshift and microduplication mutations can be restored in-frame (Iyer, Suresh, et al., 2019; Shen et al., 2018; van Overbeek et al., 2016). With the capability of multiplexing sgRNA, Cas9 can be deployed for larger genomic DNA rearrangements (Mani & Chinnaiyan, 2010). Precise repair by HDR is another option to directly correct disease-causing mutations by supplying a corrected DNA template (Jasin & Rothstein, 2013). However, HDR is less efficient than NHEJ and is ineffective in non-dividing cells (Lieber, 2010). An alternative approach known as homology-independent targeted integration (HITI) methods have been developed for insertion of exogenous DNA sequences into the genome (Suzuki et al., 2016).

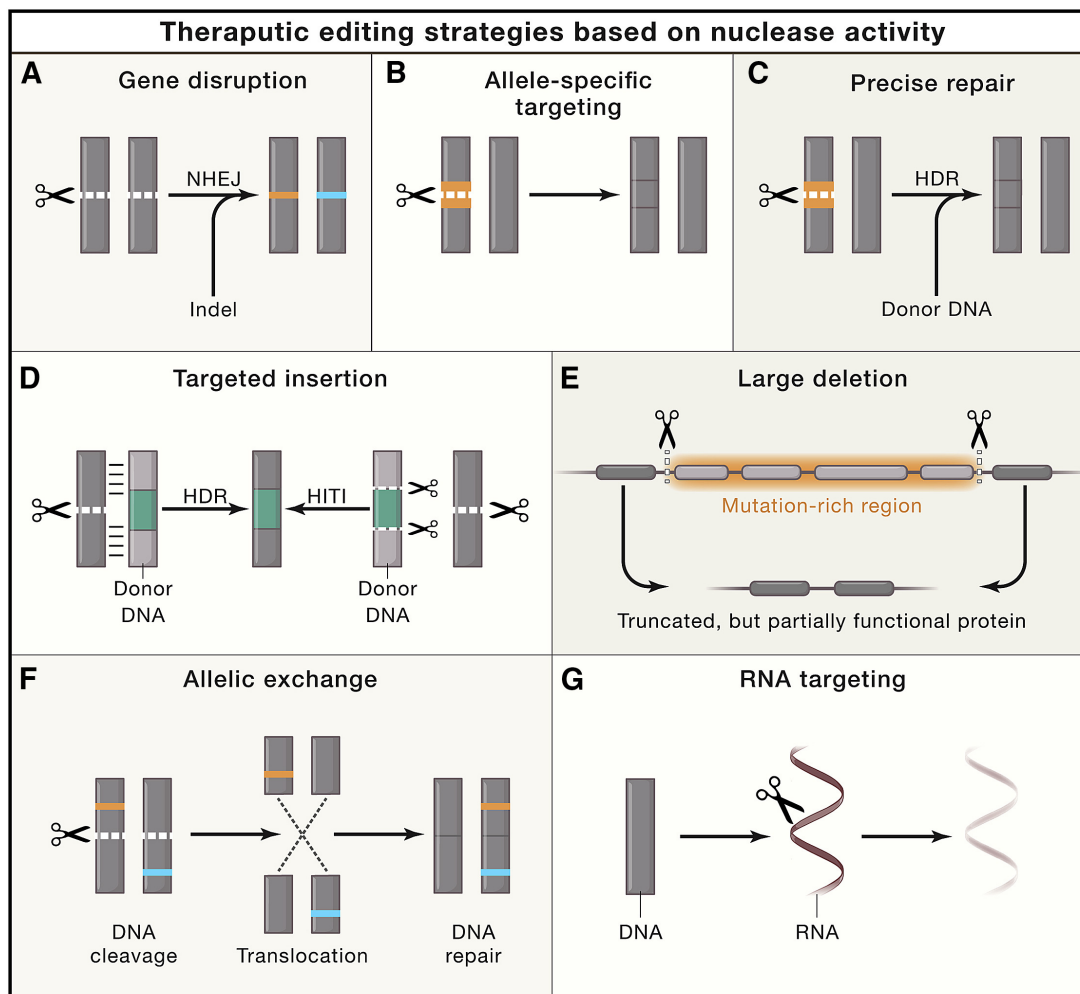


Figure 1.5 Therapeutic editing using CRISPR-Cas effectors. (A) Indels via NHEJ can knock out a gene. **(B)** In some cases, targeting can be directed to a specific mutant allele without affecting the wild-type allele. **(C)** Precise repair of a mutation mediated by HDR in the presence of a donor. **(D)** Seamless knock-in of a therapeutic gene can be achieved by either HDR or HITI. **(E)** Two simultaneous targeting events can result in a segmental deletion of a gene harboring a mutation. **(F)** Targeting intronic sequences can induce allelic exchange through translocation between homologous chromosomes to convert a compound heterozygous genotype to heterozygous. **(G)** RNA targeting achieves gene silencing by degrading RNA instead of DNA. Figure adapted from Wang et al. with permission (see the List of Third Party Copyright Material) (D. Wang et al., 2020).

1.2.3 *Ex vivo* and *in vivo* delivery for gene editing

***Ex vivo* gene editing**

In *ex vivo* delivery, genome editing reagents are first introduced into human cells (either from a patient or a healthy donor) in a dish, and an expanded cell population carrying the desired genetic modification(s) is then grafted back into patients (Doudna, 2020; High & Roncarolo, 2019). *Ex vivo* delivery provides a few advantages: 1) existing robust delivery methods such as lentivirus transduction and RNP electroporation can make a gene modification easy and efficient, 2) the ability to select cells that meet the efficiency and accuracy requirements can help ensure safety and efficacy when introduced in patients, and 3) a host immune response to Cas9 proteins can be avoided. Due to these reasons, many preclinical and clinical studies employ CRISPR-Cas9 *ex vivo* gene editing approaches for targeting multiple blood disorders such as disrupting *CCR5* in T cells for HIV infection, engineering immune cells to combat cancer, and editing the *BCL11A* gene in hematopoietic stem cells for treating hemoglobinopathies (Y. Li et al., 2020; Porteus, 2019).

***In vivo* delivery by AAV vectors**

Ex vivo approach is limited to cell types that can be isolated, manipulated, and re-engrafted, but most cell types are differentiated, post-mitotic, and only functional *in vivo*. Deploying CRISPR-based therapeutics directly into the human body holds great promise for treating a broader range of diseases that cannot be addressed by the *ex vivo* approach. However, efficient delivery is a hurdle for any *in vivo* gene editing platform. Currently, the adeno-associated virus (AAV) vector is the leading delivery modality for *in vivo* delivery (D. Wang et al., 2019, 2020).

An engineered AAV, known as a recombinant AAV (rAAV), is composed of a viral protein capsid and a single-stranded DNA genome that encodes a therapeutic gene expression cassette in place of viral protein-coding sequences. The AAV genome is also flanked by inverted terminal repeats (ITRs) of viral origin that are necessary for genome replication and packaging. A traditional gene therapy approach has successfully used rAAVs to deliver functional proteins in patients, paving the road for *in vivo* CRISPR-gene editing (D. Wang et al., 2019, 2020).

A key to the success of *in vivo* genome editing is the safe and effective delivery of genome editing reagents to target tissues and cell types, and AAV offers many desired advantages: well-characterized tissue tropism, safety, and efficient expression.

The tissue tropism of AAV is largely determined by the interaction between the viral capsid and target cell surface receptors such as glycoproteins. A

combinatorial recognition of co-receptors may also participate in cell entry. Different AAV serotypes are presumed to facilitate spatial distribution across different tissue- and cell- types. New natural variants of AAV and engineered capsids may diversify tissue tropism profiles for either broad or specific *in vivo* delivery.

The safety profile of AAV is one of its most promising attributes. AAVs are known for low genotoxicity and minimal immunogenicity. The prevailing thought is that AAV genomes remain predominantly episomal without host genome integration, although the integration of the AAV genome may be facilitated by ITRs in some cases (Miller et al., 2004). This may result in varying frequencies of integration events that have been detected at on-target DSBs (Hanlon et al., 2019; Jarrett et al., 2017; Maeder et al., 2019; McCullough et al., 2018; Nelson et al., 2019). Moreover, it is presumed that the lack of coding sequences of viral origin contributes to their low immunogenicity and cytotoxicity when delivered *in vivo*.

Efficient expression is important to achieve durable therapeutic efficacy in gene therapy. Although the AAV vector genome largely remains episomal inside host cells, it can mediate long-term, stable transgene expression. The AAV genome undergoes circularization and concatemerization to stabilize its presence as episomal DNA, resulting in persistent expression in postmitotic cells (D. Duan et al., 1998, 1999).

1.2.4 Challenges of CRISPR-mediated therapeutic editing

Therapeutic gene editing using CRISPR-Cas9 has rapidly moved into clinical studies for the treatment of cancer (ClinicalTrials.gov Identifier: NCT03399448), β -thalassemia (NCT03655678), and sickle cell disease (NCT03745287). The first human application using AAV delivery directly to the eye targets a *CEP290* mutation that encodes a faulty protein resulting in Leber congenital amaurosis-10 (LCA10), a leading cause of blindness in childhood (Maeder et al., 2019). In addition, clinical trials to use genome editing for degenerative diseases such as muscular dystrophies are on the rise. Although the success and long-term outcomes remain to be evaluated in the future, currently CRISPR gene editing is by no means devoid of challenges.

Delivery

Despite the promising outlook for current CRISPR technologies, efficient delivery of editing components to the intended cell and tissue types has remained challenging. Currently, the most popular form of *ex vivo* delivery is the electroporation of Cas9-sgRNA RNP (Fajrial et al., 2020). *In vivo* delivery, which is the biggest bottleneck for somatic-gene editing, has both viral (e.g. AAVs) and non-viral (e.g. lipid nanoparticles carrying Cas9 mRNA and sgRNA) approaches (D. Wang et al., 2019; Yin et al., 2014). Each delivery modality offers different advantages and suffers from its own limitations (Figure 1.6).

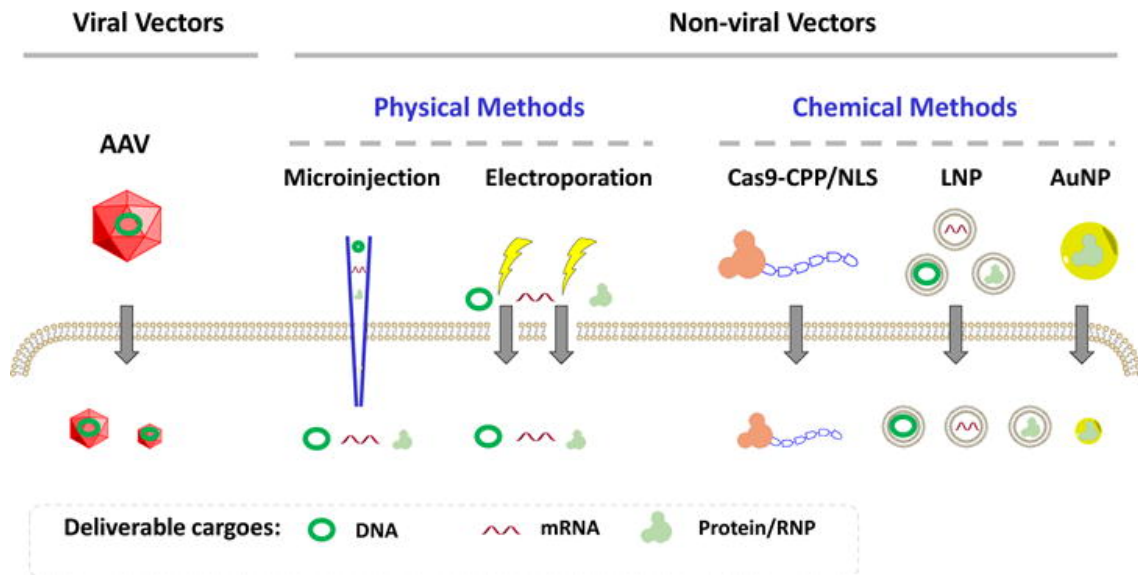


Figure 1.6 A summary of delivery modalities for CRISPR-Cas9. Deliverable Cas9 cargo may be DNA or mRNA molecules or it may be delivered as a functional ribonucleoprotein (RNP). A variety of viral and nonviral methods have been derived to achieve successful delivery across the cell membrane. CPP, cell-penetrating peptide; NLS, nuclear localization signal; LNP, lipid nanoparticle, AuNP, gold nanoparticle. Figure adapted from Glass et al. with permission (see the List of Third Party Copyright Material) (Glass et al., 2018).

Two major drawbacks of AAV delivery are the limited genome-packaging capacity of the AAV vector and potential undesired editing from prolonged expression in non-target cell or tissue types. The packaging size for the AAV genome is limited to the maximal length of ~4.7 kb for the transgene expression cassette. A widely used SpyCas9 alone is ~4.2 kb without any regulatory elements such as a promoter and a polyadenylation signal. Other genome editing components like sgRNA and HDR/HITI donor must be packaged into another AAV. This dual-vector AAV delivery system is adopted for many applications but potentially limits efficacy to the cells that have taken up both vectors. To circumvent this limitation, smaller Cas9s that are amenable to all-in-one AAV delivery have been either naturally discovered or engineered (Edraki et al., 2018; Ibraheim et al., 2018; E. Kim et al., 2017; Konermann et al., 2018; J.-J. Liu et al., 2019; Ran et al., 2015; Teng et al., 2018). A Type II-A *Staphylococcus aureus* (SauCas9) has a gene size of 3.2 kb, allowing a single AAV vector to express SauCas9 together with one or two sgRNAs (Ran et al., 2015). Recently, an all-in-one AAV was reported to express a DNA donor template as a third component in a single AAV vector (Krooss et al., 2020). In particular, Type II-C Cas9 orthologs are attractive due to their naturally high accuracy and compact size: Nme1Cas9 [1,082 amino acids (aa)] (Amrani et al., 2018; Esvelt et al., 2013; Hou et al., 2013; Ibraheim et al., 2018), CjeCas9 (984 aa) (E. Kim et al., 2017), GeoCas9 (1,087 aa) (Harrington, Paez-Espino, et al., 2017), and AceCas9 (1,138 aa) (Hand et al., 2018, 2019; Tsui et al., 2017). Despite their advantages, some of

these Cas9 orthologs also are limited by a longer and more complex PAM requirement (Mir, Edraki, et al., 2018). Recently, Nme2Cas9 has been reported to have a shorter (5'-N₄CC3') PAM and is efficient for *in vivo* gene editing after all-in-one AAV delivery (Edraki et al., 2018). Cas-effector fusion platforms such as base editors and prime editors exceed the cargo size and cannot be delivered in a single AAV. To overcome such a barrier, strategies have been developed to split the large transgene into two or more segments into AAV vectors and reconstitute the functional, full-length proteins (Tornabene & Trapani, 2020).

A benefit of stable transgene expression from AAV in traditional gene therapy is actually a disadvantage for CRISPR-gene editing since a mutation is permanently corrected after gene editing. Long-term expression is unnecessary and a safety concern since it has been shown to increase off-target cleavage (Zuris et al., 2015). Transient expression is preferred and, to this end, non-viral delivery methods may be useful (F. Chen et al., 2020; Finn et al., 2018; Wan et al., 2019; C.-F. Xu et al., 2019; Yin et al., 2014). In addition to controlling the duration of gene editing, avoiding the exposure of editing reagents to unintended tissues and cell types will be necessary to ensure clinical safety profiles that are suitable for *in vivo* therapeutics. Although different AAV serotypes provide a spectrum of tissue tropism, they often differ only in the tropism strength but not absolute specificity.

Safety

To ensure safety in clinical applications, the specificity of gene editing and immunogenicity in hosts must be addressed. Specificity can be defined by the accuracy and precision of editing. While the accuracy refers to the ratio of on- versus off-target site editing, the precision is achieving the desired modification at the on-target site compared to other types of mutations as a product of gene editing. Cas9 may result in various sequence changes at the desired site due to a mixture of repair outcomes or even induce larger, more complex genomic rearrangements or deletions (Kosicki et al., 2018; Maddalo et al., 2014).

Development of thorough detection methods will be required to monitor and evaluate both the accuracy and precision of genome editing in clinical settings and ultimately to eliminate undesired editing outcomes. Extensive efforts have been put forth in making the CRISPR gene editing platform safer by engineering Cas9 to be more accurate to minimize the off-target activity (D. Kim et al., 2019). In addition, platforms such as base editing and prime editing that do not require DSBs have been developed as an alternative approach, although these strategies face delivery challenges due to their larger size.

The host immune responses to AAV vectors complicate the safety profile of *in vivo* gene delivery (Mingozzi and High, 2013). Furthermore, the immunogenicity of bacterially derived Cas9 proteins, as well as pre-existing antibodies against Cas9 orthologs derived from bacteria that colonize the human population, may

also compromise the safety and efficacy of CRISPR gene editing *in vivo* (Charlesworth et al., 2019; Crudele & Chamberlain, 2018; A. Li et al., 2020; Simhadri et al., 2018; Wagner et al., 2019). In an adaptive immune response, antibodies are important for coating pathogens to block their entry into cells and to mark them for destruction by the immune system. However, the actual killing of cells expressing foreign proteins is mediated through cellular immune responses (Crudele & Chamberlain, 2018). Activation of CD8⁺ cytotoxic T cells could lead to the killing of Cas9-expressing cells, rendering the gene therapy ineffective.

To evade humoral immunity and T-cell responses, patients with neutralizing antibodies can be excluded from the clinical trials or immunosuppression drugs can be administered (Mingozzi and High 2013). Although there seems to be no apparent adversity reported to date after expressing Cas9 *in vivo* (L. Xu et al., 2019), the immunogenicity issues can be circumvented by immune-orthogonal or less immunogenic Cas9 orthologs (Moreno et al., 2019). Genome-editing therapies that involve *ex vivo* editing are not as affected by either immunogenicity or pre-existing antibodies to Cas9 as the host will not be exposed to Cas9 due to the short half-life of residual Cas9 RNPs in edited cells *ex vivo*.

Altogether, many hurdles ahead of CRISPR-mediated therapeutic gene editing seem conquerable with continuous efforts in enhancing and expanding the

current capabilities to eventually pave the way for the development of safe and effective clinical applications.

1.3 Introduction to anti-CRISPR proteins

Bacteria are under constant attack from their invaders such as bacteriophages, which drives the evolution of numerous innate and adaptive immune systems to cope with this pressure. Bacteriophages have also evolved countermeasures to combat diverse anti-phage mechanisms and survive in co-existence with their bacterial hosts. The discovery and exploitation of CRISPR-Cas systems have concurrently led to the identification and characterization of novel anti-immunity mechanisms such as anti-CRISPR (Acr) proteins. Understanding the dynamics of their interactions in this ongoing arms race has spurred numerous implications, from understanding the microbial ecology and evolution to the development of biotechnological tools.

1.3.1 Evolutionary arms race between prokaryotic hosts and their invaders

In 2013, Bondy-Denomy and Davidson et al. discovered a strange phenomenon in *Pseudomonas aeruginosa* susceptible to viral infection despite having active CRISPR-Cas systems targeting the phage genome (Bondy-Denomy et al., 2013). This led to their identification of “anti-CRISPR” proteins responsible for thwarting CRISPR interference. In the initial phase of anti-CRISPR discovery, most anti-CRISPR proteins inactivated Types I-F and I-E systems (Bondy-Denomy et al., 2013; Pawluk et al., 2014). Since then, the relatively young field of anti-CRISPRs has rapidly evolved, leading to the discovery of additional anti-CRISPR proteins, the understanding of their functional roles in nature, and the dissection of their inhibitory mechanisms, as well as how to repurpose them for genome engineering applications.

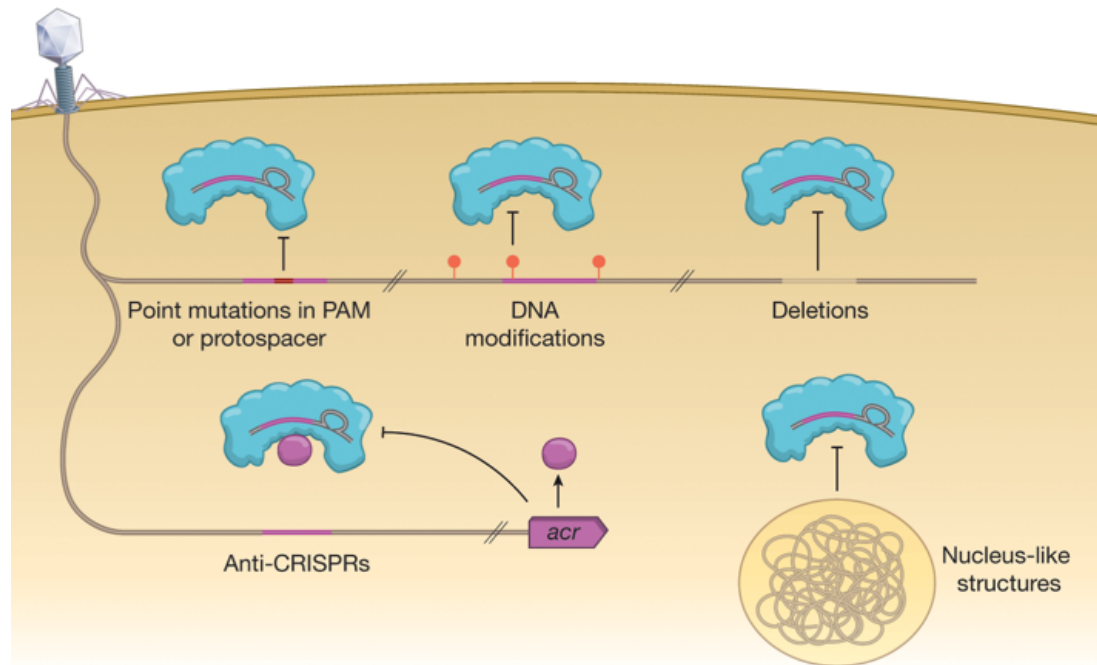


Figure 1.7 Viral mechanisms to evade CRISPR-Cas immunity. To overcome CRISPR-Cas defenses, phages make point mutations in the PAM or protospacer sequence, or modify or delete the DNA so that the DNA cannot be bound by Cas complexes. Phages can also encode anti-CRISPR proteins that inactivate CRISPR immunity. Jumbo phages produce a nucleus-like structure as a physical barrier to exclude Cas complexes. Figure adapted from Hampton et al. with permission (see the List of Third Party Copyright Material) (Hampton et al., 2020).

The adaptive nature of CRISPR-Cas systems may be expected to provide a powerful barrier to the propagation of MGEs in bacteria, including phages, plasmids, and integrative and conjugative elements. Phages are unable to evade a CRISPR-Cas system by mutations alone when targeted by multiple and diverse CRISPR spacers; hence other types of mechanisms must be employed, such as the deployment of anti-CRISPR proteins or formation of a physical barrier that resembles a nucleus (Figure 1.7) (Malone et al., 2020). In particular, anti-CRISPR proteins are remarkably effective in phage survival in that carrying at least one *acr* gene can prevent phage elimination in hosts carrying CRISPR-Cas systems (van Houte et al., 2016). While Type I CRISPR-Cas immune systems can eliminate lytic phages effectively, temperate phages capable of entering a lysogenic state cannot be eliminated in the bacterial population. In fact, imperfect matching of spacers to the prophage sequence imparts a fitness disadvantage, driving the loss of CRISPR-Cas systems from bacteria. In such circumstances, *acr* genes that suppress the host immune system provide a strong selective benefit for both the phage and the host (Rollie et al., 2020). The selective pressure from fitness costs may explain the loss or inactivation of *cas* genes in CRISPR loci and non-uniform distribution in bacteria phyla. Furthermore, the high diversity observed in CRISPR-Cas systems may be partly driven by the presence of equally diverse anti-CRISPR proteins and vice versa. This may also explain the occurrences of multiple CRISPR-Cas systems belonging to different types and/or subtypes in a single bacterial strain as well as anti-CRISPR proteins.

These and other studies underscore the fitness costs and benefits associated with CRISPR-Cas systems and anti-CRISPR proteins (W. Jiang, Maniv, et al., 2013; Westra et al., 2015).

1.3.2 Functions of anti-CRISPR proteins in a host-pathogen arms race

Role of an Aca protein as a transcriptional regulator

Anti-CRISPR associated (Aca) proteins are frequently encoded downstream of the *acr* gene and are highly conserved in MGEs. To date, there are seven families of Aca proteins that share homology at the N-terminus of the HTH DNA-binding domain (Marino et al., 2018; Pawluk, Amrani, et al., 2016; Pawluk, Staals, et al., 2016). Recently the function of Aca proteins in regulating the *acr* operon has been elucidated. It was speculated that *acr* genes must be expressed very rapidly to confer phage survival. Not surprisingly, the expression of *acr* genes were quickly ramped up in the early infection stage, driven by a strong promoter immediately upstream of *acr* genes (Stanley et al., 2019). In the same study, it was shown that Aca1 protein subsequently represses this high level of transcription. Lack of Aca repression resulted in phage lethality because the uncontrolled transcription from the strong Acr promoter disrupted the transcription of downstream genes (Stanley et al., 2019). Another study reported that a dimer of Aca2 proteins similarly binds to the promoter and regulates *acr* genes in the same operon (Birkholz et al., 2019). Altogether, the conserved role of Aca proteins is to mitigate the deleterious effects of strong constitutive transcription from *acr* promoters (Birkholz et al., 2019; Stanley et al., 2019).

Interestingly, some anti-CRISPR proteins (AcrIIA1 and AcrIIA6) share N-terminal homology with Aca proteins, suggesting dual roles as both anti-CRISPR and Aca

proteins. Recently, it has been shown that AcrIIA1 indeed has a dual regulatory function (Osuna, Karambelkar, Mahendra, Sarbach, et al., 2020). The full-length AcrIIA1 uses its two-domain architecture to act as a “Cas9 sensor” and “anti-anti-CRISPR.” The AcrIIA1 HTH motif in the N-terminus (NTD) responsible for *acr* repression is highly conserved across Aca orthologs, yet it is completely dispensable for Acr activity. Instead, the motif responsible for the Acr activity resides in the C-terminal domain (CTD) (Osuna, Karambelkar, Mahendra, Christie, et al., 2020). The AcrIIA1-CTD is necessary and sufficient to perform the anti-CRISPR function by binding to the catalytic HNH domain of Cas9. This triggers Cas9 degradation during the lysogenic phase in which phages integrate into the bacterial chromosome (becoming prophages). During lytic infection, AcrIIA1 alone was insufficient to inactivate CRISPR targeting and required additional Acrs to rapidly inhibit Cas9. These two studies together show that AcrIIA1 is a bi-functional Acr protein that performs anti-CRISPR and anti-anti-CRISPR functions and shed light on how Acrs with varying inhibitory spectra (narrow vs. broad) play different roles in the lytic and lysogenic life cycles of phages.

Anti-CRISPR proteins provide phage resistance by cooperation

A conundrum of how anti-CRISPR proteins can accumulate to effective concentrations immediately upon phage infection has been partially resolved by the observation of rapid and high expression of *acr* genes from a strong promoter (Stanley et al., 2019). Nonetheless, many infections of CRISPR-resistant hosts fail initially. Instead, Acr-producing phages display cooperative behavior on a community scale. Acrs from the first phage infecting an immunosuppressed host may not provide full protection from CRISPR-Cas, but enable productive infection for successive phages (Borges et al., 2018; Landsberger et al., 2018). Initial infections by phages produce inadequate levels of Acr proteins to completely inactivate CRISPR-Cas systems. Nonetheless, consecutive and unsuccessful infections accumulate Acrs in the immunocompromised host until a critical threshold level is reached. Low levels of Acr proteins in sacrificial phages result in infection failures, and the density of the phages needed largely depends on the potency of Acr, for instance, weaker Acr proteins requiring higher phage densities. This may also explain why multiple distinct *acr* genes are often found within the same *acr* locus: to neutralize CRISPR-Cas in different ways to maximize the likelihood of successful infection. The co-existence of anti-CRISPR proteins of varying strengths is also explained by different advantages each strong and weak Acr provides in a heterogeneous population and how it influences the evolution of CRISPR-Cas. Phages carrying anti-CRISPR proteins cooperate with each other to outpace CRISPR-Cas immunity by not only leaving

behind immunosuppressed hosts but also by limiting the emergence of resistant hosts in the population.

Roles of weak and strong anti-CRISPR proteins

Anti-CRISPR proteins vary not only in their inhibitory spectra for different CRISPR-Cas systems but also in their potency in inhibiting the Cas proteins (Borges et al., 2017; Stanley & Maxwell, 2018). One possible explanation is that the strength of inhibition confers different advantages. For instance, strong Acrs enable bypass of CRISPR-Cas immunity against phages. At a community level, phages with Acrs benefit phages without the Acrs by limiting CRISPR resistance, thus providing indirect protection and allowing replication in the immunocompromised subpopulation of bacterial hosts (Nussenzweig & Marraffini, 2018). Since strong Acrs, but not weak Acrs, enable phages without the Acrs to exploit immunosuppressed CRISPR-resistant hosts, phages with the weaker Acrs provide greater advantages than stronger Acrs when competing with other phages without Acrs (Chevallereau et al., 2020). Therefore, in the early evolution of new *acr* genes, it is likely that weak Acrs would be more pervasive in the phage population. Nevertheless, this could be a transient phenomenon since in the longer-term, wherein phages with different Acrs have emerged and compete against each other, weak Acrs no longer provide the greatest fitness benefit. Strong Acr phages are favored in CRISPR-resistant hosts while both strong and weak Acr phages are equally fit in the CRISPR-sensitive population; however, since pre-existing CRISPR immunity is not common, both strong and weak Acrs probably co-exist in nature (Chevallereau et

al., 2020). Overall, different Acrs of varying inhibitory spectrum and potency may help shape the evolutionary dynamics of host-phage populations.

1.3.3 The origins of anti-CRISPR proteins

The sequence and structural plasticity of anti-CRISPR proteins make identifying the precursors of these proteins challenging. Although this is speculative, anti-CRISPR proteins may have sprung from sporadic mutations in phage proteins in a convergent, *de novo* protein evolution until their function provided fitness advantages from anti-CRISPR activity (Pawluk et al., 2018). This hypothesis is plausible given that phages have a rapid mutation rate and short generation time, and anti-CRISPRs are mostly very small and often encoded near viral structure genes. In support of this hypothesis, a study reported a potential evolutionary origin of AcrIIC1 in the phage decoration protein gp87 based on the structural similarity between the AcrIIC1 and a β tulip domain of gp87 (Stone et al., 2018). It is likely that phage decoration proteins predated the evolution of AcrIIC1. Unlike most other β tulip proteins, AcrIIC1 uses a different side of the β tulip domain to bind the Cas9 HNH domain (Harrington, Doxzen, et al., 2017), suggesting that the interaction with the Cas9 HNH nuclease may have evolved in a decoration protein without disrupting its structural role. Other Acr proteins may have evolved from phage proteins as well, but their structural homologies may have been masked by the rapid evolution and insertion of new structural elements. Future studies are needed to underpin the evolutionary origins and drivers in the context of phages and bacteria with CRISPR-Cas immune systems.

1.3.4 Discovery approaches for anti-CRISPR proteins

The diversity of anti-CRISPR sequences and structures noted above also impose challenges in the discovery of novel Acr proteins. To overcome these challenges, a number of approaches have been used to uncover anti-CRISPR proteins in nature: 1) guilt-by-association bioinformatics, 2) sequence-based searches for self-targeting spacers in bacterial genomes, 3) functional screens of virulent phages, 4) functional screening of metagenomic libraries, and 4) computational methods (Figure 1.8).

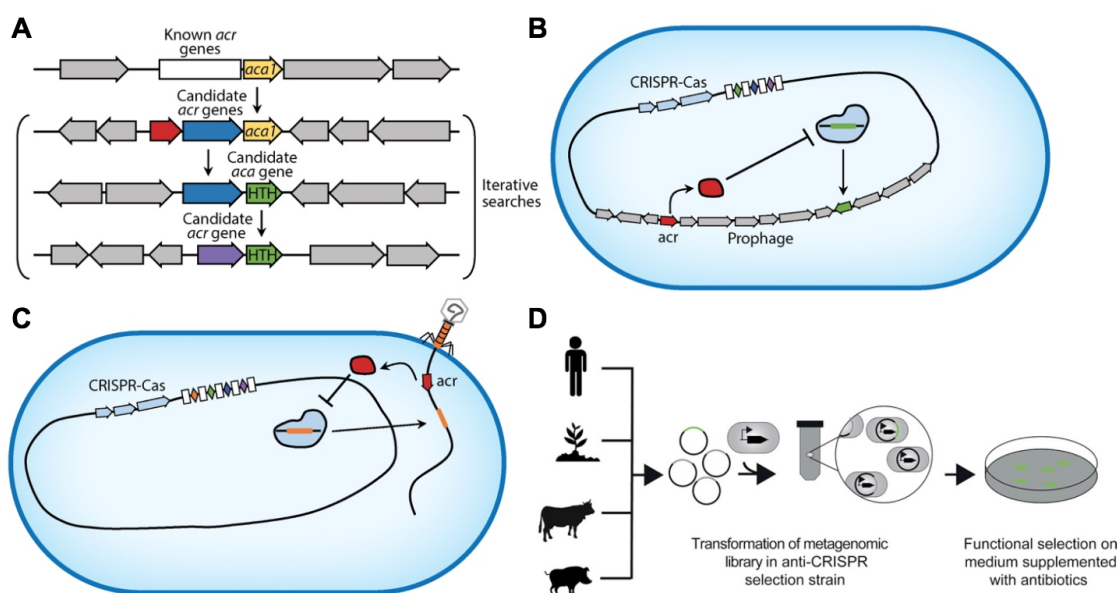


Figure 1.8 Different approaches for anti-CRISPR discovery. **(A)** A guilt-by-association bioinformatic approach uses experimentally validated anti-CRISPR genes in association with an anti-CRISPR-associated (*aca*) gene encoding a helix-turn-helix (HTH) motif-containing protein. **(B)** A self-targeting bioinformatic approach takes advantage of spacers matching prophages within the same host genome that, in theory, should target their own genome for destruction. The co-existence of a prophage and a self-targeting spacer indicates the presence of a possible anti-CRISPR within the prophage. **(C)** In phage screening assays, candidate *acr* genes are selected in phages that escape CRISPR targeting in the immunized bacteria strains carrying the spacers against the phage genome. **(D)** In functional assays, a high-throughput approach is used to discover anti-CRISPR genes from metagenomic libraries based on their functional activity rather than sequence homology or genetic context. Figure modified from Uribe et al. and Stanley and Maxwell with permission (see the List of Third Party Copyright Material) (Stanley & Maxwell, 2018; Uribe et al., 2019).

1. “Guilt-by-association” bioinformatics

One of the earliest methods used in the discovery of anti-CRISPR proteins is the guilt-by-association bioinformatics approach. This is a process of iterative BLAST searches using an *aca* gene as a bait that has co-occurrence with the existing anti-CRISPR genes. The first nine anti-CRISPRs found in *P. aeruginosa* were not similar to each other; however, they all shared a highly conserved gene downstream of the anti-CRISPR genes named as *anti-CRISPR-associated gene 1 (aca1)*. The *aca1* gene encodes a predicted protein containing a helix-turn-helix motif commonly found in transcriptional regulators. Using Aca1 as a bait in a series of BLAST searches, additional Types I-F and I-E *acr* genes were identified upstream of *aca1* genes in *P. aeruginosa* (AcrIF6-10) (Pawluk et al., 2014). The same BLAST searches with *aca2*, a homolog of *aca1*, led to the discovery of the first Type II anti-CRISPR proteins that act against Cas9 from *Neisseria meningitidis* harboring Type II-C CRISPR systems (AcrIIC1-3) (Pawluk, Amrani, et al., 2016). In pursuit of anti-CRISPR proteins in different types and subtypes, a similar set of “ping-pong” BLAST searches from one *acr* gene to another led to the discovery of both widespread anti-CRISPRs (*acrIF11* and *-12*) and new *aca* genes (*aca4* - *aca7*) (Marino et al., 2018).

2. Screening for self-targeting bacterial genomes

Another bioinformatic approach that has yielded a number of discoveries for different types of Acrs involves searching for bacterial genomes encoding both a functional CRISPR-Cas system and spacers that target sites within the same host genome. Survival of bacterial hosts despite the existence of a CRISPR-Cas system that can target its own genome suggests that there is an active mechanism that prevents self-targeting. This enabled the discovery of anti-CRISPR proteins in *Listeria monocytogenes* (AcrIIA1-4) that not only inhibited LmoCas9 but, in some cases, also inhibited the widely used SpyCas9 (Rauch et al., 2017). In combination with the guilt-by-association method, Marino et al. reported Types I-C and V anti-CRISPR proteins by using *acrIF11* that had a widespread occurrence as a bait to dissect *acr* loci in the genomes of bacteria that have the tolerance for self-targeting with Types I and V CRISPR-Cas systems (Marino et al., 2018). In particular, AcrVA1 (170 aa) found in *Moraxella* species is able to inhibit not only *Moraxella bovoculi* (Mb) Cas12a but also other commonly used Cas12a orthologs, AsCas12a and LbCas12a and (more modestly) FnCas12a from *Acidaminococcus* sp., *Lachnospiraceae* bacterium, and *Francisella novicida*, respectively (Marino et al., 2018). Concurrently, Watters et al. used a streamlined “Self-Targeting Spacer Searcher (STSS)” to uncover AcrVA1, AcrVA4, and AcrVA5 (Watters et al., 2018). Both AcrVA4 and AcrVA5 inhibit dsDNA cleavage for both MbCas12a and LbCas12a, but not

AsCas12a (Watters et al., 2018). The discovery of Type V-A anti-CRISPR proteins will be a useful tool for Cas12a-based genome editing applications.

3. Screening phages that escape CRISPR targeting

Some anti-CRISPR proteins were discovered in phages themselves rather than in a prophage genome. AcrIIA5 and AcrIIA6 were identified in virulent *Streptococcus thermophilus* phages (Hynes et al., 2017, 2018). When strains of *S. thermophilus* with an active Type II-A CRISPR-Cas system were challenged with phages, a library of genes in the escape phage was cloned and tested in *S. thermophilus* by expressing candidate anti-CRISPR proteins and checking for a restored titer of a CRISPR-sensitive phage. From this approach, *acrIIA5* and *acrIIA6* were identified in virulent *S. thermophilus* phages (Hynes et al., 2017, 2018). A similar phage screening approach was used to find the first archaeal anti-CRISPR that inactivates Type I-D CRISPR-Cas systems in a strain of *Sulfolobus islandicus* that harbors Types I-A, I-D, and III-B CRISPR-Cas systems (He et al., 2018). While the SIRV2 virus readily infected *S. islandicus* despite having a spacer, the SIRV2 mutant (SIRV2M) that lacked a fragment containing several genes failed to infect *S. islandicus*. By comparing and testing genes that are missing in SIRV2M, but are conserved in SIRV2 and SIRV3 that can infect *S. islandicus*, He et al. pinpointed *acrID* that supported the infectivity of the SIRV2M. AcrID1 inactivated the Type I-D CRISPR-Cas system by directly interacting with the Cas10d subunit.

4. Functional screening of metagenomics libraries

With the growing availability of large sequencing data, two independent studies were conducted to screen functional anti-CRISPR proteins in the human oral, gut, and soil metagenomic libraries (Forsberg et al., 2019; Uribe et al., 2019). Both studies employed a technique based on the ability of anti-CRISPR proteins to inhibit CRISPR-Cas systems and, therefore, allow bacteria to survive on antibiotics when challenged by CRISPR-Cas systems targeting a plasmid encoding the antibiotic resistance gene. Bacteria that grow in the antibiotic indicated a presence of anti-CRISPR protein in the tested library. The anti-CRISPR candidate genes were derived from various metagenomic samples. Four genes (AcrIIA7-AcrIIA10) inhibiting SpyCas9 were identified (Uribe et al., 2019). From human oral and fecal metagenomic library, Forsberg et al. reported 10 contigs that have confirmed inhibitory activity against SpyCas9 as well as AcrIIA11 (Forsberg et al., 2019). From a large library of candidate genes that have potential anti-CRISPR activity, both studies were able to narrow down to unique, non-overlapping genes distinct from previous studies. This suggests that there are plenty of new Acr genes to be uncovered that may have evolved independently from a variety of precursor proteins, which may be missed in the conventional methods described above.

5. Computational methods for prediction of anti-CRISPR proteins

Since known anti-CRISPR proteins rarely share any sequence or structural homology, predicting novel *acrs* has been a challenge. With an increasing number of anti-CRISPR proteins in the database, Eitzinger et al. recently reported a machine learning-based method (AcRanker) using only amino acid composition information to help identify additional families of Acrs (Eitzinger et al., 2020). The model can be used to predict candidate Acr proteins in the prophage regions within self-targeting bacterial genomes. These additional features are important as they can increase the probability of finding true anti-CRISPR proteins. Using this method, the authors have discovered and biochemically validated two previously unknown anti-CRISPR proteins: AcrIIA20 and AcrIIA21. In their studies, candidate anti-CRISPR proteins (ML1-10) were tested against *Streptococcus pyogenes*, *aureus*, and *iniae* Cas9. AcRanker may be used to complement existing strategies to uncover additional Acrs by prioritizing candidate proteins for empirical validation of their function. Other groups also reported a similar computational approach to predict anti-CRISPR proteins (J. Wang et al., 2020; Yi et al., 2020).

1.3.5 Mechanisms of anti-CRISPR protein inhibition

In less than a decade, numerous studies have reported detailed biochemical and/or structural characterization of anti-CRISPR proteins. Remarkably, among all known structures of anti-CRISPR proteins, there is little to no similarity, suggesting that the Acrs may have been derived from diverse and unique evolutionary origins. The diversity in sequences and structures of anti-CRISPR proteins is also reflected in the unique inhibitory mechanisms they employ to inactivate CRISPR-Cas systems (Figure 1.9). Some well-studied anti-CRISPR proteins' mechanisms of action are discussed below.

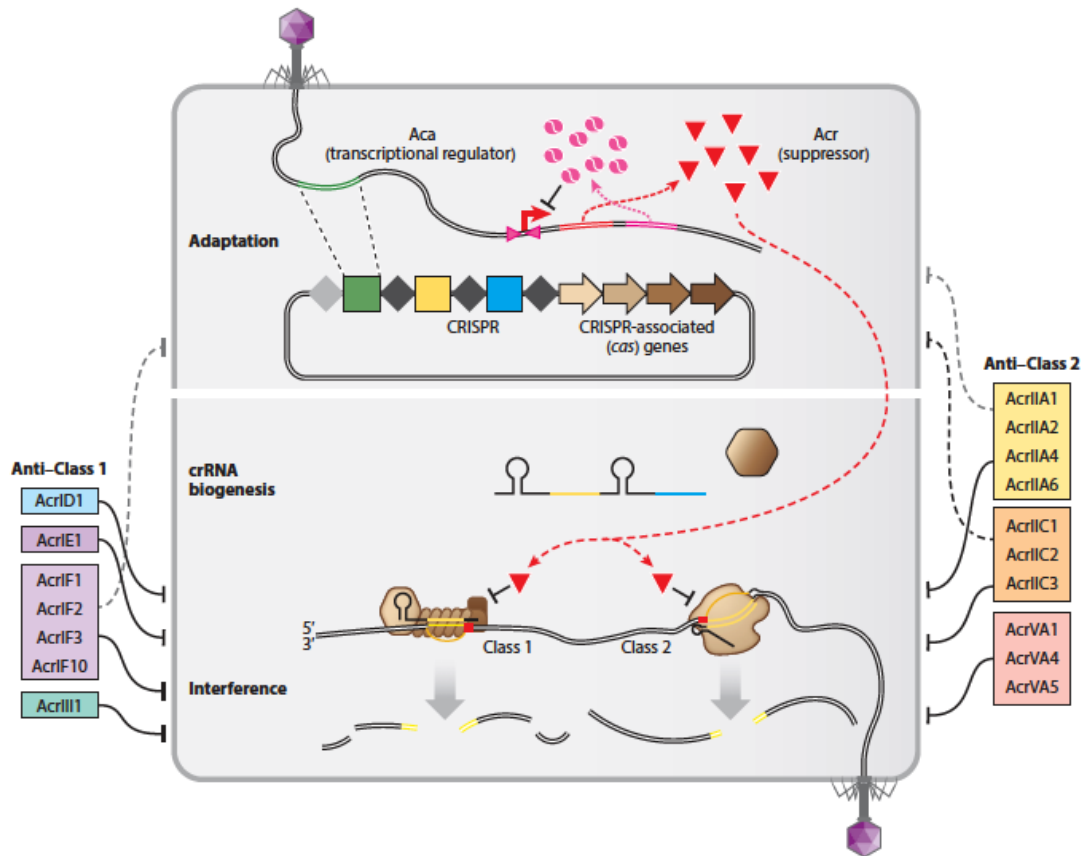


Figure 1.9 Functions and mechanisms of anti-CRISPR proteins. The Acrs with known structures and functions in CRISPR-Cas adaptive immune systems are indicated. Aca proteins (pink) repress Acr (red triangles) expression within the same operon. Most Acrs of class 1 (left) and 2 (right) immune systems target the surveillance complex and block DNA binding or nuclease activity. Figure adapted from Wiegand et al. with permission (see the List of Third Party Copyright Material) (Wiegand et al., 2020).

Anti-CRISPRs in DNA-targeting CRISPR Class 1 and 2 Systems

Class 1: Type I Systems

Types I-F and I-E in *P. aeruginosa* are characterized by a multi-effector Csy complex composed of a Cas5-Cas8 heterodimer, Cas6, and six subunits of Cas7. These proteins form a surveillance complex along with the 60-nt crRNA. Once the Csy complex binds and unwinds the target DNA strand flanked by a PAM, Cas3 nuclease is recruited to cleave the target DNA. AcrIF1, AcrIF2, and AcrIF10 bind to different binding surfaces of the Csy complex to prevent target DNA binding while AcrIF3 and AcrIE1 block Cas3 recruitment (Bondy-Denomy et al., 2015). Subtype I-D, a hybrid between Types I and III systems, encodes variants of signature proteins, Cas3 and Cas10, that are unique for each type. AcrID1 binds to Cas10d, the large subunit of the I-D CRISPR-Cas complex (He et al., 2018). It is unclear yet which step AcrID1 is involved in since Cas10d is the large subunit that forms an effector complex and participates in target-cleavage.

Class 2: Type II Systems

Type II anti-CRISPR proteins have been studied in the most detail due to their utility as off-switches for genome engineering applications.

Preventing target DNA binding

AcrIIA4 is a highly acidic protein that interacts with the PAM-interacting domain (PID) of sgRNA-loaded SpyCas9, thus occluding the PAM binding site and preventing target DNA binding (Dong et al., 2017; I. Kim et al., 2018; Shin et al., 2017; H. Yang & Patel, 2017). It weakly binds to apo-Cas9 suggesting that SpyCas9 must undergo conformational changes upon sgRNA loading to expose the binding site for AcrIIA4. This also makes sense for the anti-CRISPR protein to inactivate the loaded form of SpyCas9 since it would most likely encounter the sgRNA-Cas9 complex in a natural context. Similarly, AcrIIA2 binds to the PID of SpyCas9 although AcrIIA4 and AcrIIA2 differ drastically in their structures and sequences, showcasing a convergent evolution where two different proteins have co-opted to bind a sensible and effective site (F. Jiang et al., 2018; L. Liu et al., 2018). The PID is a suitable binding site for an Acr to inhibit as it can effectively prevent SpyCas9 binding to the target DNA.

Inhibiting target DNA cleavage

Some Acrs, however, still allow target DNA binding but instead inactivate nuclease function. AcrIIC1 identified in *N. meningitidis* has been shown to inhibit

other Type II-C Cas9 orthologs from *Campylobacter jejuni* and *Geobacillus stearothermophilus*, which are 42% and 36% identical to Nme1Cas9, respectively (Harrington, Doxzen, et al., 2017). AcrIIC1 binds to the HNH nuclease domain, one of the most conserved domains of Cas9s, and makes contact with highly conserved residues for catalysis, thus enabling inhibition of diverse Cas9 orthologs. AcrIIC1-bound Cas9 can still bind to the target DNA but is unable to cleave due to its interaction with the active site of the HNH nuclease domain.

Inhibition by dimerization

AcrIIC3 binds Nme1Cas9 and induces dimerization to form a 2:2 complex (Harrington, Doxzen, et al., 2017; Sun et al., 2019; Zhu et al., 2019). The dimerization is mediated by two AcrIIC3 proteins where one interacts with the HNH domain of the first Cas9 and the recognition (REC) domain of the second Cas9, while the other Acr does the opposite (Y. Kim et al., 2019; Zhu et al., 2019). AcrIIC3 binds to the opposite side of the HNH domain that AcrIIC1 binds to and keeps it in an inactive state away from its cleavage site (Sun et al., 2019). In addition to inactivating target DNA cleavage by binding to the HNH domain, the dimerization via AcrIIC3 interaction with the REC lobe, which is highly variable among Cas9 homologs, may reduce the binding affinity to the target DNA. This may explain earlier observations for preventing DNA binding

(Harrington, Doxzen, et al., 2017; Pawluk, Amrani, et al., 2016), although inhibition of target DNA binding is not absolute (Sun et al., 2019).

AcrIIC2 forms a homodimer with a negatively charged surface that interacts with the positively charged arginine-rich bridge helix (BH) domain that connects the REC lobe to the nuclease (NUC) lobe. The BH is also involved in sgRNA interaction (Thavalingam et al., 2019; Zhu et al., 2019). AcrIIC2, when bound to Nme1Cas9, prevents sgRNA loading, and cannot bind to a Cas9 that is already loaded by an sgRNA. Crystal structures and superimposition studies of AcrIIC2 bound to Nme1Cas9 show that the AcrIIC2 dimer occupies the BH sites that contact the sgRNA and likely prevent sgRNA loading by steric hindrance. Without the sgRNA bound, apo-Cas9 is also more susceptible to intracellular proteases. This may reduce the accumulation of Cas9 proteins in mammalian cells and contribute to the reduced Cas9 activity observed previously (J. Lee et al., 2018; Thavalingam et al., 2019). The inability to inhibit the loaded form of Cas9 may explain the low efficiency of AcrIIC2 in inhibiting Nme1Cas9, since co-expression of components allows some Cas9 to form active complexes for editing (Pawluk, Amrani, et al., 2016).

Class 2: Type V Systems

Type V anti-CRISPR proteins that inactivate Cas12a have also been reported with detailed mechanistic studies defined both structurally and biochemically. Cas12a is also a single effector protein that uses a crRNA and generates a staggered DNA cut using only RuvC-like nuclease domains. AcrVA1 can inhibit four Cas12a orthologs by occupying the PAM site in the cleft between REC and NUC lobes, and cleaves the crRNA bound to the Cas12 protein as a multi-turnover catalytic enzyme (Knott, Thornton, et al., 2019). AcrVA5, which has a narrower inhibitory spectrum than AcrVA1, also possesses enzymatic activity that adds a covalent modification to MbCas12a. AcrVA5 mediates acetylation of K635, an important residue in MbCas12a involved in PAM interaction, thus thwarting DNA binding. A crystal structure of AcrVA5 revealed similarities to acetyltransferases (Knott, Thornton, et al., 2019). AcrVA4 acts as an allosteric inhibitor of Cas12a by inhibiting conformational changes to prevent target DNA binding (Knott, Cress, et al., 2019; Knott, Thornton, et al., 2019; H. Zhang et al., 2019). The C-terminus of AcrVA4 binds to the REC domain where crRNA binds, while the N-terminus mediates a dimerization of Cas12a proteins, although the dimerization is not required for Cas12a inhibition (Knott, Cress, et al., 2019).

Despite sequence and structural diversity, Acrs across different types and subtypes share some mechanistic similarities. The most commonly used mode of action is to prevent DNA binding by directly interacting at or close to the PAM of Cas9. Blocking DNA cleavage is the second most common strategy used by Acrs that interact with the nuclease domains of Cas proteins. Although AcrIIIC2 can inhibit the formation of the guide-loaded Cas9 complex, Acrs generally are most effective if they can directly block the DNA binding and cleavage of the loaded CRISPR-Cas RNPs, as they would exist in nature when phages infect bacterial hosts. Another theme is the dimerization of some Acrs and Cas nucleases; however, why and how dimerization provides functional advantages is not fully understood. The Type V Acrs with enzymatic activities, such as crRNA cleavage and posttranslational modification, are very exciting, and new types of activities may surprise us in the future with the discovery and characterization of additional anti-CRISPR proteins.

Anti-CRISPRs in RNA-targeting CRISPR Class 1 and 2 Systems

Anti-CRISPR proteins inactivating RNA-targeting Types III and VI are less known when compared to DNA-targeting systems.

Type III CRISPR systems

Not many examples of anti-CRISPR proteins have been reported or studied for Type III systems, perhaps due to their complexity. Type III CRISPR systems recognize a viral RNA and activate the effector protein, Cas10. Cas10 has a HD nuclease domain responsible for the degradation of a viral DNA via ssDNA cleavage and a cyclase palm domain that synthesizes a signaling molecule, cyclic oligoadenylate (cOA; such as cA4 or cA6) (Kazlauskiene et al., 2017; Niewoehner et al., 2017). Cyclic nucleotides are important in the activation of RNases (Csm6 in Type III-A or Csx1 in Type III-B) that are not part of the RNP complex but trigger non-specific RNA degradation. The added complexity of the multi-step CRISPR interference is still subject to anti-CRISPR inhibition. For example, an anti-CRISPR (AcrIIIB1) encoded by a phage that infects *Sulfolobus* specifically inhibits subtype III-B complexes by interacting with the effector complex that synthesizes cOAs. This enables the inhibition of collateral RNase-related activities while Cas10 DNase and Cmr4 RNase activities remain unaffected (Bhoobalan-Chitty et al., 2019). The prevention of collateral RNA degradation likely prevents host cell entry into a dormant state that would otherwise suppress the viral life cycle (Rostøl & Marraffini, 2019). Soon after this

study was published, Athukoralage et al. reported the discovery of AcrIII-1, which targets the signaling molecule cA4 for degradation (Athukoralage et al., 2020). The viral ring nuclease AcrIII-1 binds the cA4 specifically, and uses a conserved active site for cA4 cleavage, allowing viruses to neutralize the Type III CRISPR defense system. Since AcrIII-1 family targets signaling molecules rather than CRISPR effector complexes, these Acrs have a broad host range as widely distributed in bacterial and archaeal viruses as well as proviruses (Athukoralage et al., 2020).

Type VI Systems

The Cas13 effector proteins from Type VI systems (class 2) provides new CRISPR-derived capabilities by virtue of its RNA targeting activity. This has enabled the development of RNA editing and post-transcriptional degradation approaches, as well as detection methods for viral RNAs (Abudayyeh et al., 2017; Ackerman et al., 2020; Cox et al., 2017; Gootenberg et al., 2017; Konermann et al., 2018; Myhrvold et al., 2018; Terns, 2018). Recently, Lin et al. took a comprehensive approach by integrating the STSS, guilt-by-association, and co-occurrence with known Acrs approaches to identify the AcrVIA1-7 proteins that can function as off-switches for Cas13a activity (P. Lin et al., 2020). Interestingly, the most potent of these, AcrVIA5, could prevent dCas13a-mediated RNA editing for A-to-I base editing using a fused ADAR (adenosine deaminase acting on RNA) enzyme, illustrating its use in controlling the nuclease during editing, knock-down and/or visualization of RNA molecules (P. Lin et al., 2020). Concurrently, Meeske et al. screened temperate phages from isolates of *Listeria spp.*, an organism that commonly harbors Type VI-A CRISPR-Cas systems, and landed on a prophage that encodes AcrVIA1 (Meeske et al., 2020). Based on a cryo-EM structure, AcrVIA1 interacts with the crRNA-exposed side of Cas13a, making contacts with both protein and crRNA residues to prevent binding of complementary target RNA in order to inhibit both target and non-specific RNase activities of Cas13a (Meeske et al., 2020). In its natural host, AcrVIA1 can completely neutralize Type VI-A CRISPR-Cas immunity against

ϕ LS46 listeriophage gradually. In Type VI CRISPR immunity, phage DNA is not cleared by hosts (Meeske et al., 2019), leading to continuous transcription and translation of AcrVIA1 until enough Acrs accumulate for Cas13a inactivation inside bacteria.

1.3.6 Applications of anti-CRISPR proteins

The rapidly expanding palette of CRISPR-Cas technologies has led to a corresponding motivation to develop tools to control and modulate their activities. Acr proteins targeting Type II (Cas9) and Type V (Cas12a) effectors have drawn particular interest as they may provide temporal, spatial, or conditional control over established genome-editing systems.

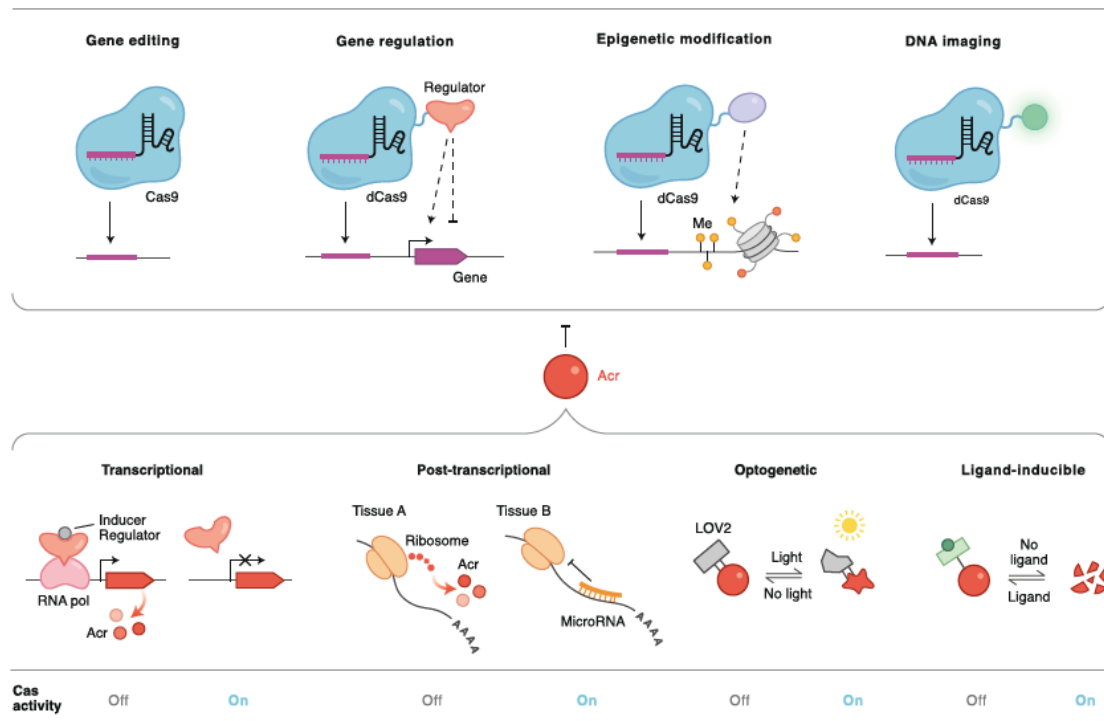


Figure 1.10 Application and regulation of anti-CRISPR proteins. Top: types of CRISPR applications that can be controlled by Acrs. Bottom: methods of regulating anti-CRISPR proteins with conditional, spatial, and temporal control. Figure adapted from Marino et al. with permission (see the List of Third Party Copyright Material) (Marino et al., 2020).

Uses for gene-editing technologies

One major application of Acr proteins is their use as off-switches for genome editing. Minimizing undesired off-target activity is important for CRISPR-Cas9 technology, especially for therapeutic use. Although extensive efforts have led to Cas9 variants with enhanced specificity (D. Kim et al., 2019), excessive or prolonged Cas9 activity may increase the likelihood of off-target editing or cytotoxicity, necessitating a means to shut down the Cas9 activity upon achieving a desired outcome. In combination with engineered Cas9 variants and means to regulate Cas9 expression, Acr proteins can act as an additional safeguard to reduce potential adverse effects of Cas9. For example, timed delivery of AcrIIA4 reduced the extent of off-target editing in cells by limiting the window of Cas9 activity and taking advantage of kinetic differences of Cas9 editing at on- versus off-target sites (Shin et al., 2017). CRISPR technology has also been applied to the development of gene drives, which are genetic elements that force super-Mendelian inheritance to disseminate desired traits in a population. A prominent example is the ongoing development of female sterility-inducing gene drives in mosquitoes to eradicate vector-borne diseases such as malaria (Nateghi Rostami, 2020). Effective control over the spread of a gene drive after its initial release is highly desirable as a safety measure. Acr proteins could be deployed to put a brake on the propagation of a CRISPR-based gene drive after the parental driver organisms are released into the relevant ecosystem. As a proof of concept, temporal control of AcrIIA2 and AcrIIA4 using an inducible promoter has

been demonstrated to halt or titrate the efficiency of a SpyCas9-based gene drive in yeasts (Basgall et al., 2018).

Uses for dCas9-based applications

Nuclease-inactive dCas9 can be used to tether or recruit various effector proteins to genomic sites of interest. For example, chromatin visualization and targeted gene regulation can be achieved via fusion of fluorescent proteins (FPs) and transcriptional activators or repressors to dCas9. Technologies based on dCas9 not only allow genome manipulation but also alteration of the epigenome via fusion of DNA demethylation enzymes (e.g., TET) or histone-modifying effectors (e.g., LSD1 or p300) (Adli, 2018). Acrs that limit DNA binding may also be used to regulate the activities of these functional domains. For example, Type II Acr proteins were used to control chromosome labeling by dCas9-FPs (Basgall et al., 2018; Bubeck et al., 2018; J. Lee et al., 2018; Pawluk, Amrani, et al., 2016; Rauch et al., 2017), as well as demethylation by dCas9-Tet1 fusions in induced pluripotent stem cells (X. S. Liu et al., 2018). Moreover, Acr proteins have enabled programmable and dynamic gene regulation by controlling CRISPRi and CRISPRa (Hoffmann et al., 2019; J. Li et al., 2018; Nakamura et al., 2019).

Engineering anti-CRISPR proteins

Acr proteins can often tolerate fusion to epitope tags and FPs without compromising their inhibitory potency. In the case of AcrIIIC1, insertion of an exogenous domain, such as a mCherry fluorescent protein, at carefully selected AcrIIIC1 surface sites dramatically improved the inhibition of Nme1Cas9 (Mathony et al., 2020). This offers opportunities to engineer Acr proteins through other domain insertions without losing the inhibitory activity. For instance, an AcrIIIA4 hybrid with a light-inducible LOV2 domain has been shown to control SpyCas9- and dSpyCas9 in optogenetics (Bubeck et al., 2018). A posttranslational control of Acr proteins was achieved by fusing an inducible destabilization domain that degrades the protein in the absence of an external ligand known as Shield1 (Nakamura et al., 2019). Acrs can be further engineered from a synthetic biology perspective to alter the specificity and potency of Acrs (Aschenbrenner et al., 2020; Mathony et al., 2020). Based on the structure of the Nme1Cas9 binding interface with AcrIIIC1, AcrIIIC1 can be converted from a Type II-C inhibitor to AcrIIIC1X that inhibits Type II-A SauCas9 (Mathony et al., 2020). Similarly, the inhibitory potency can be modulated by using artificially weakened Acr proteins to finetune Cas9 activity for achieving an optimal kinetic balance of retaining on-target editing and eliminating off-target editing events (Aschenbrenner et al., 2020).

Other uses of anti-CRISPR proteins

Inhibiting Cas9 can be a useful tool for the production of viral vectors that have been developed as a “self-cleaving” genome. A helper-dependent adenovirus (HDAd) vector for transient Cas9 expression in target cells, by design, encodes SpyCas9 and a guide that directs the cleavage of the vectors’ own genome after transduction of target cells, thereby allowing transient SpyCas9 expression and function (Palmer et al., 2019). However, self-cleavage during viral production also occurs, leading to genomic rearrangements that make virus production impossible. Anti-CRISPR proteins were used to inhibit SpyCas9 from initiating vector self-cleavage during the viral production, thus greatly improving yield (Palmer et al., 2019). Another potential use of Acr proteins is in the development of phage therapies as an alternative to antibiotics to treat bacterial infections (Nobrega et al., 2015). Phage therapies, however, may be compromised in pathogenic hosts with active CRISPR-Cas systems, such as *Pseudomonas* (van Belkum et al., 2015) and *Neisseria* (Y. Zhang, 2017). Because Acr proteins have been found in these and other pathogens, *acr* genes could be included in the engineering of therapeutic bacteriophages that circumvent multidrug resistance in pathogenic bacteria.

Chapter 2 Discovery and characterization of anti-CRISPR proteins

2.1 Introduction

Anti-CRISPR proteins of both Types I-E and I-F CRISPR-Cas systems (Bondy-Denomy et al., 2013; Pawluk et al., 2014) occur widely in MGEs (e.g. phages and conjugative elements) of diverse bacterial species (Pawluk, Staals, et al., 2016); however, Acrs outside of Type I systems have not yet been discovered. Since Acrs confer strong evolutionary advantages to MGEs encoding them, we hypothesized that Acrs must exist for other CRISPR-Cas systems. Thus, we employed the “guilt-by-association” bioinformatic approach that successfully identified Type I anti-CRISPRs to search for inhibitors of Type II systems. As described below, collaborative efforts among Maxwell, Davidson and Sontheimer labs led to the discovery of three distinct anti-CRISPR protein families that potently inhibit the *N. meningitidis* Type II-C CRISPR-Cas system. For the first time, we show that these proteins can function as off-switches for Nme1Cas9 genome engineering in mammalian cells (Pawluk, Amrani, et al., 2016).

Furthermore, our initial discovery of anti-CRISPR proteins for Type II CRISPR-Cas systems was a tip of the iceberg and the beginning of uncovering more Acrs that await our characterization. To this end, we took the working bioinformatics approach to identify two new Type II-C anti-CRISPRs and their cognate Cas9 orthologs, validated their functionality *in vitro* and in bacteria, and defined their inhibitory spectrum against a panel of Cas9 orthologs. We demonstrate that they

act before Cas9 DNA binding, and document their utility as off-switches for Cas9-based tools for mammalian genome engineering applications (J. Lee et al., 2018). Additionally, we characterized the Type II-A anti-CRISPR (AcrIIA5) in more detail to understand its broad-spectrum inhibition against both Type II-A and II-C Cas9 orthologs (Garcia et al., 2019). The identification of diverse anti-CRISPRs and definition of Acr inhibitory mechanisms afford deeper insight into the interplay between Cas9 orthologs and their inhibitors and provide a greater scope for exploiting Acrs for CRISPR-based genome engineering.

2.2 Results

2.2.1 The discovery of anti-CRISPR proteins for Cas9

The anti-CRISPR associated (*aca*) gene is often encoded downstream of known anti-CRISPR genes, which we used as a bait to search for candidate Acr proteins in the genomic localization of MGEs within the species harboring Type II systems. By conducting a series of BLAST searches with Aca1 and Aca2, we identified a candidate anti-CRISPR gene in a strain of *Brackiella oedipodis* lying directly upstream of the *aca2* gene (Figure 2.1A). The most frequently observed CRISPR-Cas system among the species encoding homologs of the candidate Acr protein was Type II-C. Since some homologs (such as AcrIIC1_{Nme} that shares 29% identity) were identified in the strains of *N. meningitidis*, we tested whether these proteins possess inhibitory functions against Nme1Cas9. AcrIIC1_{Boe} presumably inhibits BoeCas9 in its native context, but sufficient similarity with Nme1Cas9 (47% identical) may allow cross-species inhibition. We used the HTH-containing protein homologs (Aca3) downstream of *acrIIC1*_{Nme} as a new bait to uncover two additional *acrIIC2*_{Nme} and *acrIIC3*_{Nme} in the MGE-like genomic regions of *N. meningitidis* strain. To assess the effect of these candidate anti-CRISPRs on the enzymatic activity of Nme1Cas9, *in vitro* DNA cleavage assays were performed. While purified Nme1Cas9 loaded with *in vitro* transcribed sgRNA yielded in DNA cleavage without any Acr or with Type I-specific AcrE2, the addition of the *N. meningitidis* anti-CRISPRs (AcrIIC1-3) resulted in inhibition

of Nme1Cas9-catalyzed cleavage in a dose-dependent manner. DNA cleavage activity of SpyCas9 was not affected by the addition of any of the anti-CRISPRs since subtype II-A, which it belongs to is distantly related to Nme1Cas9 (Figure 2.1B).

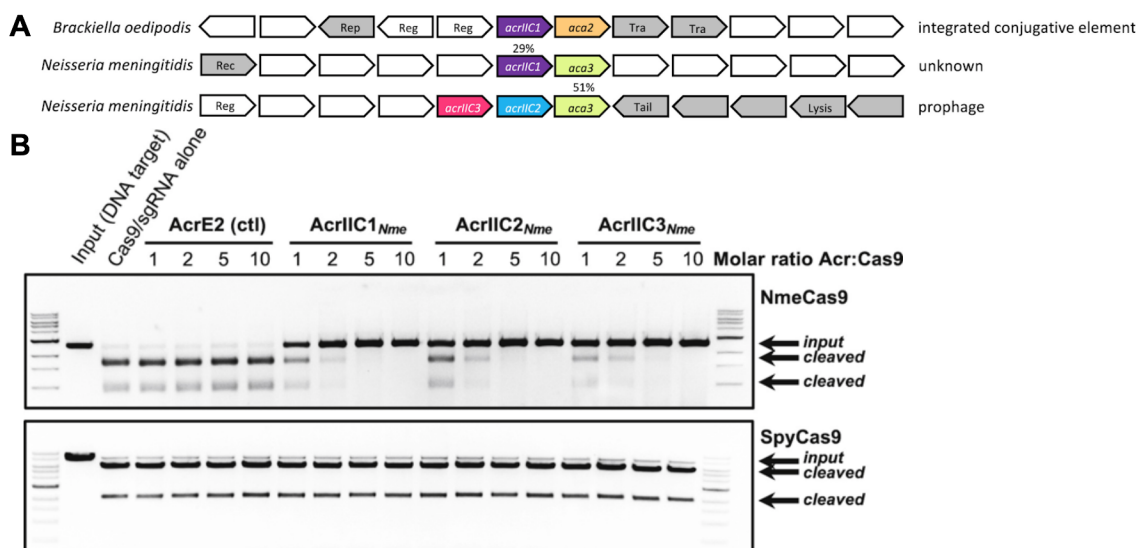


Figure 2.1 Three families of anti-CRISPR proteins inhibit Nme1Cas9. (A) A schematic of the genomic architecture of Type II-C *acr* and *aca* genes in *B. oedipodis* and *N. meningitidis*. Amino acid identity (%) for homologous genes are indicated. Known functions of genes annotated as the following: Rep, plasmid replication protein; Reg, transcriptional regulator; Tra, conjugal transfer protein; Rec, recombinase; Tail, phage tail structural protein; Lysis, phage lysis cassette; colored in gray, MGE-related functions and/or show clear evidence of horizontal transfer. Not drawn to scale. **(B)** *In vitro* cleavage of linearized plasmid DNA by purified, recombinant Nme1Cas9 (top) or SpyCas9 (bottom). Cas9 was pre-incubated with purified anti-CRISPR proteins and then with cognate sgRNA. Mobilities of input and cleaved DNAs are denoted on the right.

2.2.2 Anti-CRISPRs inhibit Cas9 genome editing in mammalian cells

Since Cas9 is widely adopted as a genome editing tool, we tested the possibility of using these anti-CRISPRs as off-switches for CRISPR-Cas9 genome editing in mammalian cells. We co-transfected HEK293T cells with three plasmids expressing Cas9, sgRNA, and each Acr, respectively. Genome editing efficiency was determined using an established T7 endonuclease 1 (T7E1)-based protocol. Each of the anti-CRISPRs greatly decreased the ability of Nme1Cas9 to create genomic lesions with AcrIIIC3_{Nme} appearing to be the most potent, although a variation in activities of Acrs may depend on their expression or stability in cells (Figure 2.2). Consistent with our *in vitro* results, the anti-CRISPRs had no effect on editing mediated by SpyCas9 targeting the same genomic site (Figure 2.2). In addition, AcrE2 had no significant inhibitory effect in any of these experiments. These results demonstrate the potential application of Type II anti-CRISPRs for controlling Cas9-mediated genome editing.

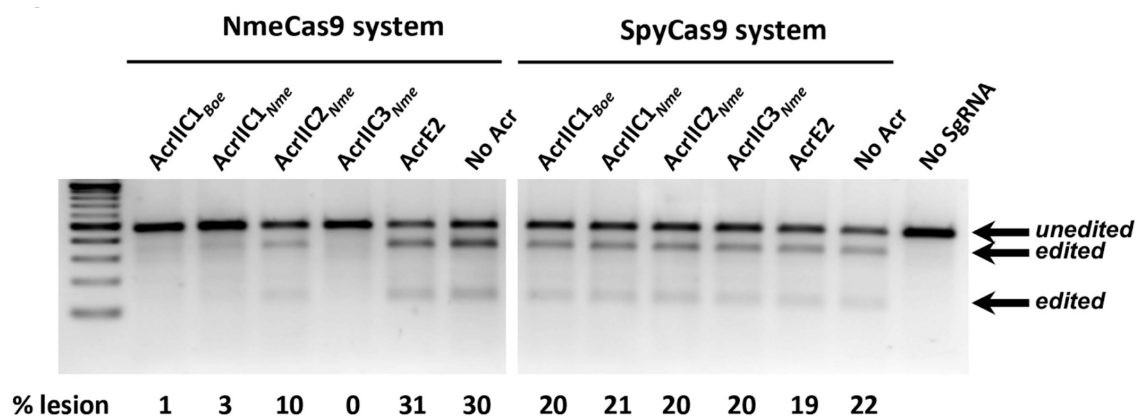


Figure 2.2 Type II-C anti-CRISPR proteins inhibit Nme1Cas9-mediated genome editing in mammalian cells. Co-expression of plasmids encoding AcrIIC1-3 families reduced genome editing indicated by T7E1 assays as shown for Nme1Cas9 (left), but did not affect SpyCas9 editing (right). Type I AcrE2 is used as a non-cognate anti-CRISPR that should not inhibit Type II Cas9 orthologs. Editing efficiencies (“% lesion”) are quantified based on the signal intensity of bands using densitometry.

2.2.3 Anti-CRISPRs inhibit a dCas9 application in mammalian cells

Encouraged by the anti-CRISPR functioning as an off-switch for gene editing, we explored the possibility of controlling other types of Cas9 applications. Nuclease-inactive dCas9 orthologs that do not catalyze DNA cleavage have proven to be exceptionally useful for RNA-guided DNA binding since a wide range of domains and functionalities can be fused or tethered to the DNA-bound dCas9-sgRNA complex (Adli, 2018). If anti-CRISPR inhibition occurs before the stable R-loop formation and cleavage, anti-CRISPR could be used as an off-switch not only for genome editing but also for dCas9 DNA binding applications such as CRISPRi and CRISPRa (Adli, 2018). To determine whether our most potent genome editing inhibitor (*AcrIIC3_{Nme}*) can prevent stable DNA binding by dNme1Cas9 in mammalian cells, we used a previously developed system in which superfolder (sf) GFP-labeled dNme1Cas9 and mCherry-labeled dSpyCas9 are simultaneously colocalized to telomeric loci by cognate sgRNAs upon co-transfection of their expression plasmids in U2OS cells (Ma et al., 2015) (Figure 2.3A). We readily observed colocalizing telomeric dNme1Cas9-(sfGFP)₃ and dSpyCas9-(mCherry)₃ foci as long as both of the telomere-directed sgRNAs were included for the two dCas9 orthologs (Figure 2.3B-D). When a third mTagBFP2-marked plasmid carrying an anti-CRISPR expression cassette was included, AcrE2 had no effect on telomeric co-localization, as expected (Figure 2.3E). In contrast, the co-expression of *AcrIIC3_{Nme}* prevented the formation of telomeric foci by dNme1Cas9-(sfGFP)₃ (Figure 2.3F). We scored only cells that exhibited

mTagBFP2 and sfGFP fluorescence as well as mCherry telomeric foci for the presence or absence of co-localizing dNme1Cas9-(sfGFP)₃ telomeric foci in a double-blinded fashion (Figure 2.3G). While telomeric dNme1Cas9-(sfGFP)₃ foci were observed in most cells in the presence of the negative control AcrE2 protein, we did not observe any co-localizing dNme1Cas9-(sfGFP)₃ telomeric foci when AcrIIC3_{Nme} was co-expressed. These results confirm the robust inhibitory effect of AcrIIC3_{Nme} on stable, sgRNA-programmed DNA binding by dNme1Cas9, and indicate that it can be used as a potent off-switch not only for Nme1Cas9 genome editing but also for dNme1Cas9-based applications in mammalian cells.

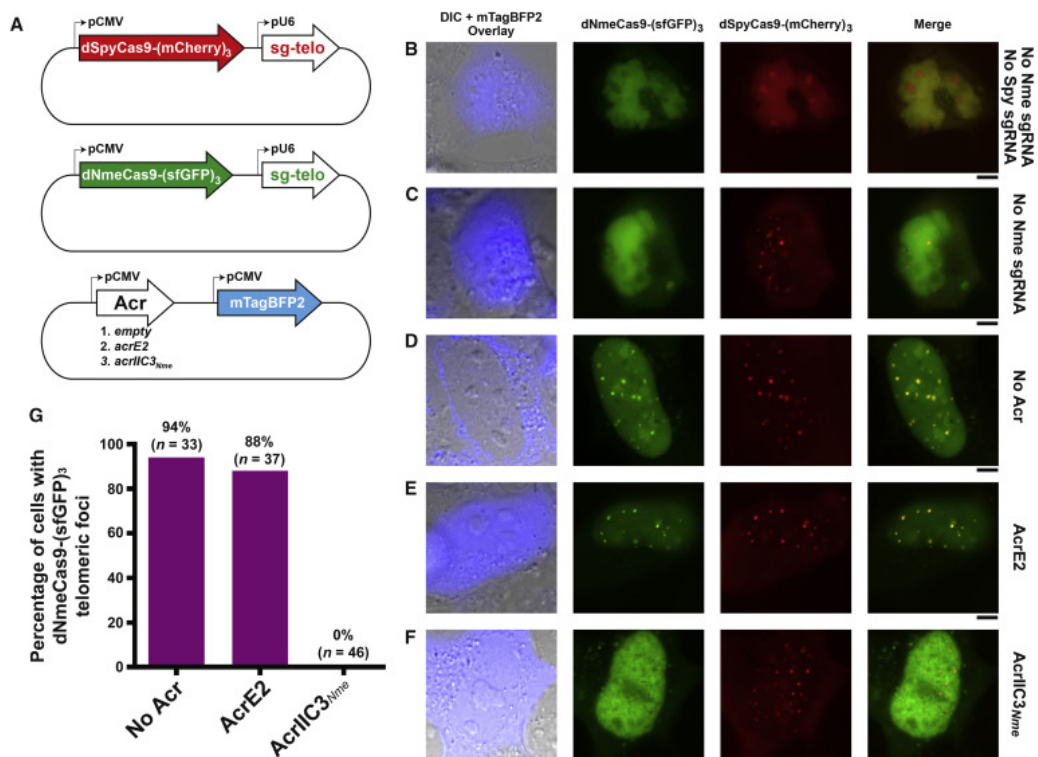


Figure 2.3 A potent Acrilc3_{Nme} can be used for a dNme1Cas9 application. (A) Schematic representation of plasmids used for expression of dNme1Cas9-(sfGFP)₃, dSpyCas9-(mCherry)₃, and their respective telomeric sgRNAs. The plasmid encoding the anti-CRISPR protein is marked with the mTagBFP2. (B-F) Fluorescence images of U2OS cells transiently transfected with plasmids depicted in (A). Each row represents different conditions indicated on the right side. Scale bars, 5 μ m. (G) Quantitation of dNme1Cas9-(sfGFP)₃ telomeric foci, as scored by co-localization with dSpyCas9-(mCherry)₃ telomeric foci. n, the number of cells that were evaluated in each condition.

2.2.4 Type II-C anti-CRISPRs are found in diverse bacterial species

In sections 2.2.4 - 2.2.7, we report two novel anti-CRISPR families in strains of *Haemophilus parainfluenzae* and *Simonsiella muelleri*, both of which harbor Type II-C CRISPR-Cas systems. Although these novel Acrs are found in different bacterial species, we show that they can inhibit Nme1Cas9, demonstrating cross-species inhibitory potential. Having identified functional anti-CRISPR proteins, we also speculated that these bacterial strains may harbor active CRISPR-Cas systems. We identified Cas9 orthologs from *H. parainfluenzae* and *S. muelleri* and demonstrated that the newly identified Acrs can inhibit Cas9 orthologs from these systems as well, and defined important features of their inhibitory mechanisms. The *S. muelleri* Acr (AcrIIC5_{smu}) is the most potent Nme1Cas9 inhibitor identified to date. Although anti-CRISPRs from *H. parainfluenzae* and *S. muelleri* revealed cross-species inhibition against Nme1Cas9, more distantly related Type II-C Cas9s were not inhibited by these proteins. The specificities of anti-CRISPRs and divergent Cas9s appear to reflect the coevolution of their strategies to combat or evade each other. Finally, we validate these new anti-CRISPR proteins as potent off-switches for Cas9 genome engineering applications.

Using the same bioinformatics approach that led us to the discovery of the first anti-CRISPR proteins for Nme1Cas9, we searched for open reading frames (ORFs) encoding uncharacterized small proteins immediately upstream of *aca2* orthologs in genomic regions near putative phage- or MGE-associated sequences. This led us to two putative Acr candidates in genomes of *H. parainfluenzae* strain and *S. muelleri* strain. Both are located upstream of apparent *aca2* orthologs (Figure 2.4A). Both strains encode predicted Type II-C CRISPR-Cas machinery with Cas9 orthologs that exhibit 59% and 62% identity with Nme1Cas9, respectively. Based on these similarities, we first tested whether these candidates prevent DNA cleavage by Nme1Cas9 *in vitro* (Figure 2.4B). As each of the purified candidate Acrs was added to parallel reaction mixtures, cleavage was inhibited in a concentration-dependent manner with AcrIIC5_{Smu} exhibiting the greatest potency (Figure 2.4B).

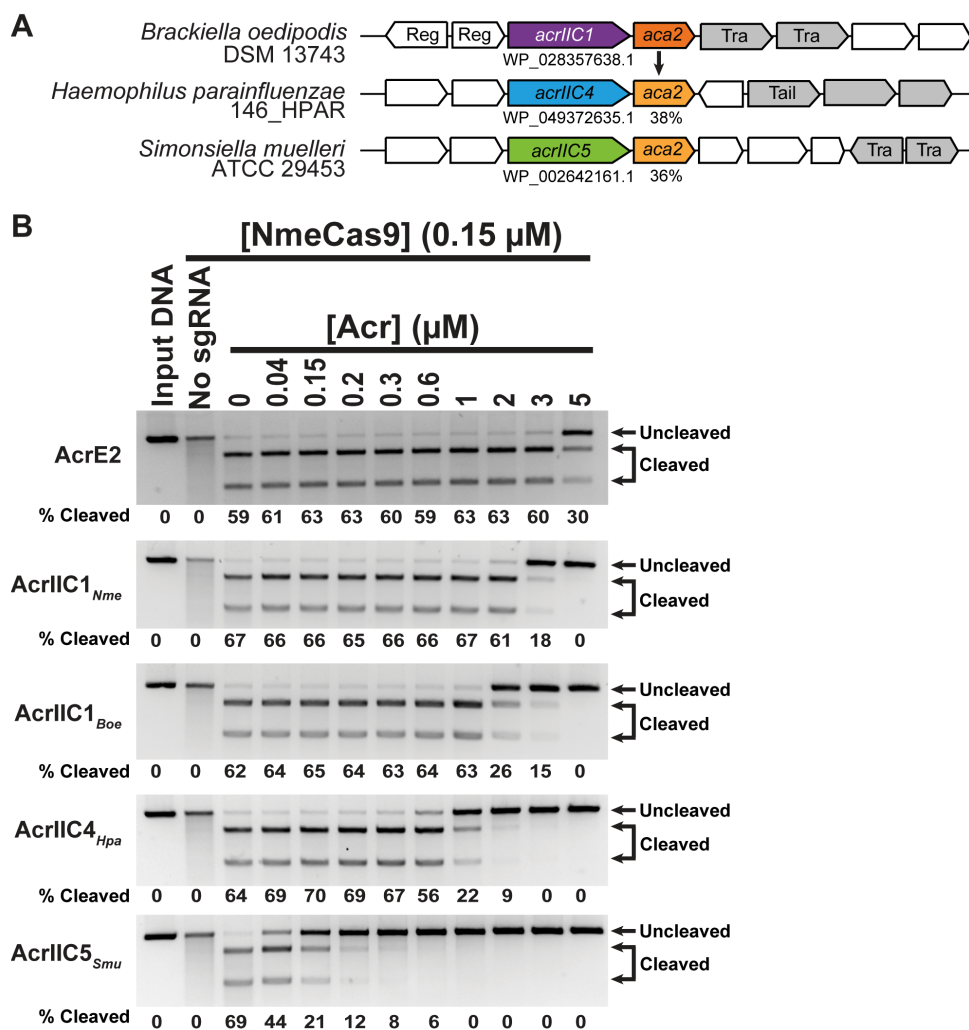


Figure 2.4 Identification and *in vitro* validation of two Type II-C anti-CRISPR proteins. (A) Schematic of candidate anti-CRISPR proteins and *aca2* genes in the genomic context of *H. parainfluenzae* and *S. muelleri*. Gray genes are associated with MGEs, and known gene functions are annotated as follows: Reg, transcriptional regulator, Tail, phage tail morphogenesis, and Tra, transposase. The *B. oedipodis aca2* gene is used as a query for BLAST searches, and percent identities of *aca2* orthologs are denoted. Not drawn to scale. (B) *In vitro* cleavage of target DNA by the Nme1Cas9-sgRNA complex in the presence of anti-CRISPR protein. Pre-formed Nme1Cas9-sgRNA RNP complex was incubated with purified anti-CRISPR proteins before the addition of a linearized plasmid with a protospacer and PAM sequence. Cleavage efficiencies estimated based on band intensity densitometry (“% cleaved”).

2.2.5 Characterization of two new Type II-C Cas9 orthologs

Since little was known about the Cas9 orthologs from *H. parainfluenzae* and *S. muelleri*, we characterized Type II-C CRISPR-Cas systems in these species (Figure 2.5A). We identified a *cas9* ORF for each and cloned for recombinant protein expression and purification for *in vitro* studies. Although we found *tracrRNA:crRNA* for HpaCas9, we could not detect *tracrRNA* for SmuCas9. Therefore, we took advantage of the nonorthogonality of sgRNAs to closely related Cas9 orthologs (Briner et al., 2014; Fonfara et al., 2014) and used the Nme1Cas9 sgRNA to test the cleavage activity of SmuCas9. To determine the PAM sequence for each ortholog, a library of short DNA fragments containing a unique protospacer flanked by 10-nt randomized PAM sequences was subjected to *in vitro* digestion using purified, recombinant Cas9 proteins and T7-transcribed sgRNAs. Next, digested products were gel purified and deep sequenced. PAM sequences were identified from the resulting sequencing data based on the frequency of nucleotides at each position of the digested products. We found that HpaCas9 had a strong preference for 5'-N₄GNTT-3' (Figure 2.5B) and SmuCas9 had a strong preference for the 5'-N₄C-3' PAM sequence (Figure 2.5C). This single cytosine at the 5th position from the protospacer appears to be the most critical PAM nucleotide by far, although moderate preferences for other nucleotides at other positions cannot be excluded from this analysis. We validated these putative PAMs by performing *in vitro* cleavage of a nondegenerate substrate and confirmed efficient cleavage (Figure 2.5B-C).

We next examined whether AcrIIC4_{Hpa} and AcrIIC5_{Smu} inhibit their native, cognate Cas9 proteins *in vitro* DNA cleavage and showed that AcrIIC4_{Hpa} and AcrIIC5_{Smu} indeed inhibit their cognate HpaCas9 and SmuCas9 (Figure 2.5B-C). Given that some Type II Acrs can inhibit orthologous Cas9 within the same subtype, we tested other Type II-C Acr families from *Neisseria* (AcrIIC1_{Nme}, AcrIIC2_{Nme}, and AcrIIC3_{Nme}) for inhibition of these two newly characterized Cas9 proteins. We found that all three of these previously characterized Acrs also inhibit the DNA cleavage activity of both HpaCas9 and SmuCas9 (Figure 2.5B-C).

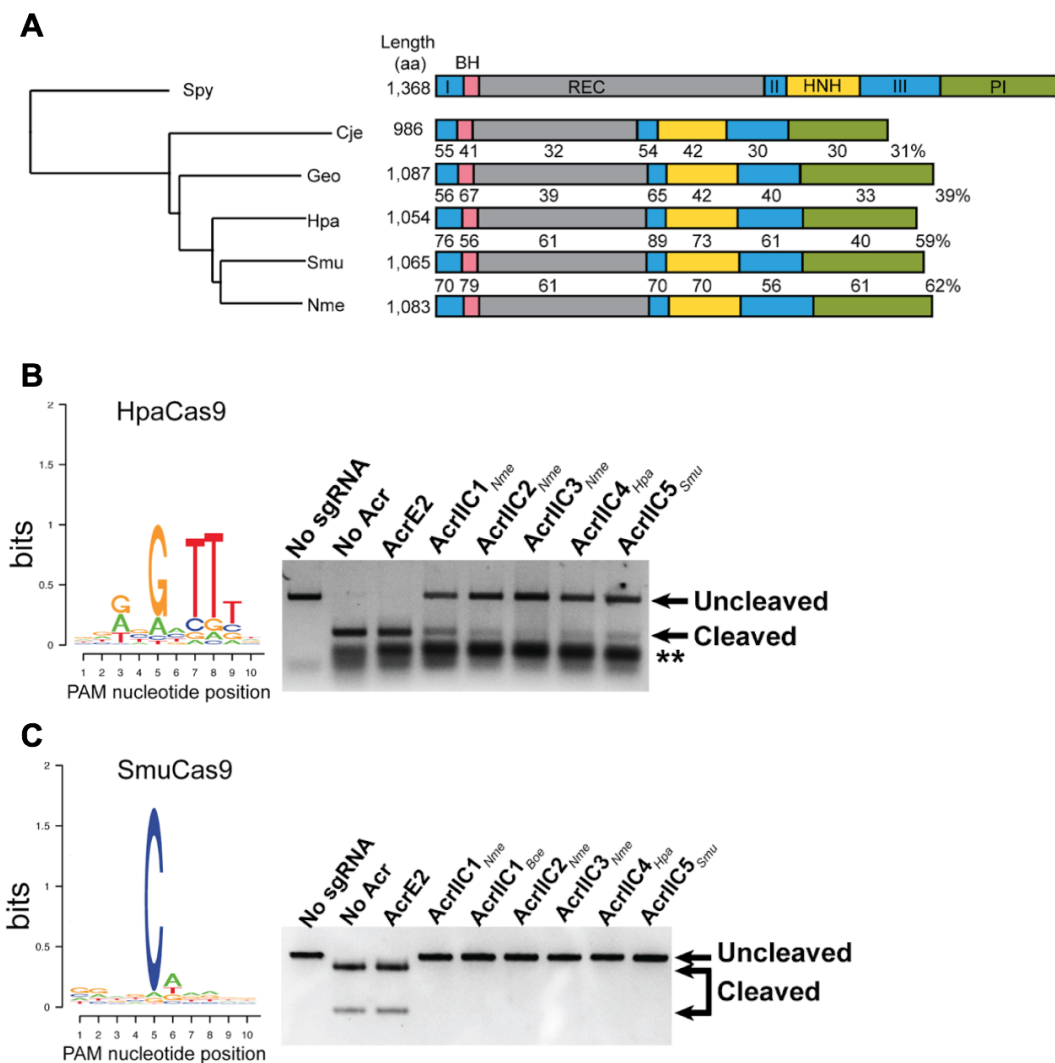


Figure 2.5 Characterization of new Type II-C Cas9 orthologs. (A) A phylogenetic tree of Type II Cas9 orthologs from *S. pyogenes*, *N. meningitidis*, *C. jejuni*, *G. stearothermophilus*, *H. parainfluenzae*, and *S. muelleri*. Domains are drawn to scale and colored as follows: blue, RuvC-I, -II, and -III nuclease domain; pink, bridge-helix (BH); gray, recognition lobe (REC); yellow, HNH nuclease domain; green, PAM-interacting domain (PI). Percent identities (%) of Type II-C orthologs to Nme1Cas9 are indicated. (B-C) PAM preferences for *H. parainfluenzae* (B) and *S. muelleri* (C) Cas9 orthologs. The frequency of nucleotides at each PAM position were calculated and plotted as a WebLogo. Validation of HpaCas9 and SmuCas9 cleavage activity and inhibition by anti-CRISPR proteins *in vitro*. The double asterisk (**) denotes sgRNA.

2.2.6 AcrIIIC4 and AcrIIIC5 inhibit genome editing in human cells

To assess the inhibition of Nme1Cas9 genome editing, we co-transfected HEK293T cells transiently with plasmids encoding Cas9, sgRNA, and anti-CRISPR and then used T7E1 digestion to estimate genome editing efficiency. In agreement with our *in vitro* data, the expression of AcrIIIC4_{Hpa} or AcrIIIC5_{Smu} reduced Nme1Cas9-mediated mutagenesis to undetectable levels (Figure 2.6A). In contrast, they had no effect on genome editing at the same genomic sites by SpyCas9 (Figure 2.6A). Additionally, we delivered a preformed RNP complex of Nme1Cas9, sgRNA, and each of the Acrs to HEK293T cells by electroporation. Then, we evaluated the inhibition of genome editing using tracking of indels by decomposition (TIDE) analysis (Brinkman et al., 2014) (Figure 2.6B). For more rigorous quantitation of Nme1Cas9 editing, we performed a titration experiment and used targeted deep sequencing at a distinct editing site (NTS1C) and its validated off-target site (Figure 2.6-D). We detected little to no editing at higher doses of AcrIIIC4_{Hpa} or AcrIIIC5_{Smu} plasmid transfections. Acrs displayed variations in their inhibitory activities with both plasmid and RNP delivery, suggesting that the differences in protein stability, off-rate, or other intrinsic properties may contribute to their efficacy in tested systems. Overall, both *in vitro* and in cells, AcrIIIC4_{Hpa} or AcrIIIC5_{Smu} consistently exhibited strong inhibitory potency comparable or superior to that of AcrIIIC3_{Nme}, which had previously been defined as the most potent Nme1Cas9 inhibitor in mammalian cells (Pawluk, Amrani, et al., 2016).

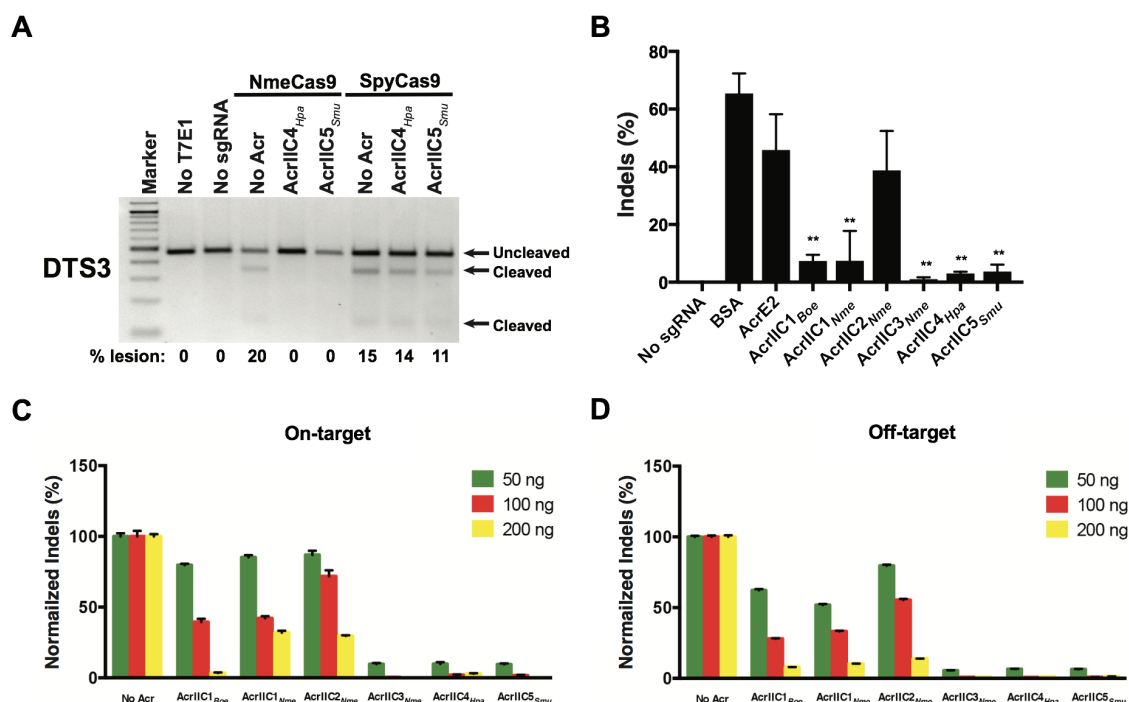


Figure 2.6 AcrIIC4_{Hpa} and AcrIIC5_{Smu} inhibit genome editing in human cells. (A) T7E1 assays of Nme1Cas9 or SpyCas9 editing efficiencies upon transient plasmid transfection of human HEK293T cells. Editing efficiency estimated by cleavage of target DNA (% lesion). (B) TIDE analysis upon RNP delivery of Nme1Cas9-sgRNA and Acr into HEK293T cells. Statistical significance was determined by two-tailed paired Student's t-test. Means and standard deviations from three biological replicates are indicated with lines (*, $P < 0.05$; **, $P < 0.01$; ***, $P < 0.001$). (C-D) Indel frequencies at on-target (C) and off-target (D) sites measured by targeted deep sequencing of PCR-amplified gDNA collected after transfection of Nme1Cas9 plasmid with or without Acrs at different dosages.

2.2.7 AcrIIC4 and AcrIIC5 prevent stable DNA binding by Nme1Cas9

Next, we attempted to dissect the mechanisms of Nme1Cas9 inhibition by AcrIIC4_{Hpa} and AcrIIC5_{Smu}. First, we checked whether sgRNA loading onto the Nme1Cas9 is inhibited by either of the anti-CRISPRs. We carried out electrophoretic mobility shift assays (EMSAs) by incubating Nme1Cas9 and sgRNA with or without Acr, and then visualizing sgRNA mobility after native gel electrophoresis followed by SYBR Gold staining. Without Acr or with AcrE2 negative control, incubation of Nme1Cas9 with its cognate sgRNA resulted in a gel shift that indicates the formation of a stable RNP complex (Figure 2.7A). Similarly, when incubated with AcrIIC4_{Hpa} and AcrIIC5_{Smu}, efficient Nme1Cas9:sgRNA complex formation was again observed, suggesting that neither Acr protein significantly affected the RNP assembly.

To test if the target DNA engagement by the Nme1Cas9:sgRNA complex is affected by the new anti-CRISPRs, we performed EMSA and fluorescence polarization assays after pre-incubating the RNP with each Acr and then adding the target DNA (Figure 2.7B). To inhibit DNA target cleavage, we omitted divalent metal ions from the reaction mixtures. While the target DNA exhibited the expected mobility shift in the absence of Acr, or in the presence of AcrE2 or AcrIIC1_{Nme} [as expected (Harrington, Doxzen, et al., 2017)], AcrIIC4_{Hpa} and AcrIIC5_{Smu} prevented binding of the Nme1Cas9 to the target DNA. In fluorescence polarization assays, we measured the equilibrium binding constants

of Nme1Cas9 RNP (0 to 2 μ M) to target DNA (8 nM) (Figure 2.7C). Both Acrs impaired the DNA binding activity of Nme1Cas9:sgRNA, confirming our EMSA results (Figure 2.7B).

To extend our findings from *in vitro* studies to mammalian cells, we evaluated the anti-CRISPR activity on stable dCas9 binding using previously established methods for live-cell imaging of telomeric foci (Figure 2.3A). We observed dNme1Cas9-(sfGFP)₃ foci in approximately 80% of the cells in the absence of any Acr protein, in 70% of the cells expressing AcrE2 protein (negative control), and in 0% of the cells in the presence of AcrIIC3_{Nme} (as a positive control) (Figure 2.7D). In conditions where the two novel anti-CRISPRs were co-expressed, we did not detect any cells with foci formation (Figure 2.7D). These results confirm that AcrIIC4_{Hpa} and AcrIIC5_{Smu} inhibit stable DNA binding of dNme1Cas9 in cellular context, indicating their potential utility as potent off-switches for dNme1Cas9-based applications.

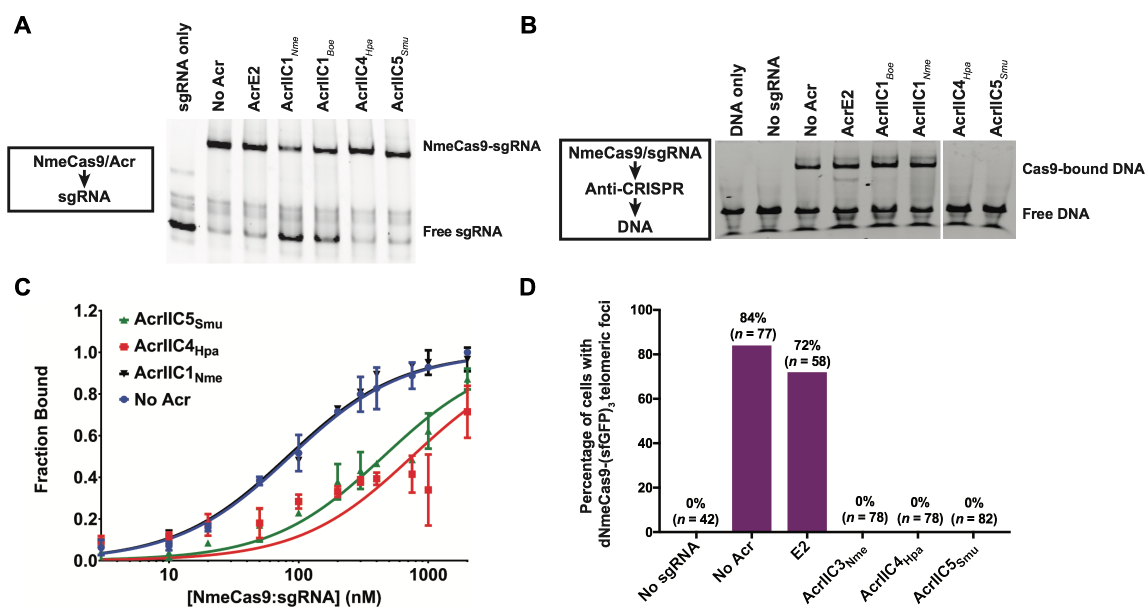


Figure 2.7 Mechanistic insights into AcrIIc4_{Hpa} and AcrIIc5_{Smu} inhibition.

(A) A native gel of the sgRNA visualized by SYBR gold staining after co-incubation of Cas9 and anti-CRISPR protein and then the addition of sgRNA. **(B)** A native gel of the FAM-labeled target DNA after co-incubation of Nme1Cas9:sgRNA complex with Acr and then the addition of the target DNA. **(C)** Binding of Nme1Cas9 to partially duplexed DNA measured by fluorescence polarization assays with or without the indicated Acrs. The graph shows the average values (\pm SD) of three replicates. The curve was fitted to the equation shown in Materials and Methods, and the resulting KD values (nM) for AcrIIc5_{Smu}, AcrIIc4_{Hpa}, AcrIIc1_{Nme}, and “No Acr” were 450.7 ± 47.6 , 749.6 ± 157.7 , 82.4 ± 6.5 , and 85.9 ± 3.9 , respectively. **(D)** Quantitation of dNme1Cas9-(sfGFP)₃ telomeric foci, as judged by colocalization with dSpyCas9-(mCherry)₃ telomeric foci in live-cell fluorescence imaging of U2OS cells. Foci were scored blinded, i.e., without the experimenter knowing the sample identities. n, the number of cells that were scored under each condition over three biological replicates.

2.2.8 AcrIIA5 inhibits Cas9 from both Type II-A and -C systems

A few known anti-CRISPR proteins such as AcrIIC1 and AcrVA1 can inhibit closely related Cas proteins, but their maximal inhibitory activity is generally restricted to specific Cas9 homologs belonging within the same subtype. To facilitate the practical exploitation of multiple Cas9 homologs, here we show that the previously reported AcrIIA5 (Hynes et al., 2017) potently inhibits nine diverse Type II-A and Type II-C Cas9 homologs, including those currently used for genome editing. Based on our observation of sgRNA cleavage *in vivo*, we speculate that the mechanism of AcrIIA5 inhibition involves RNA interaction.

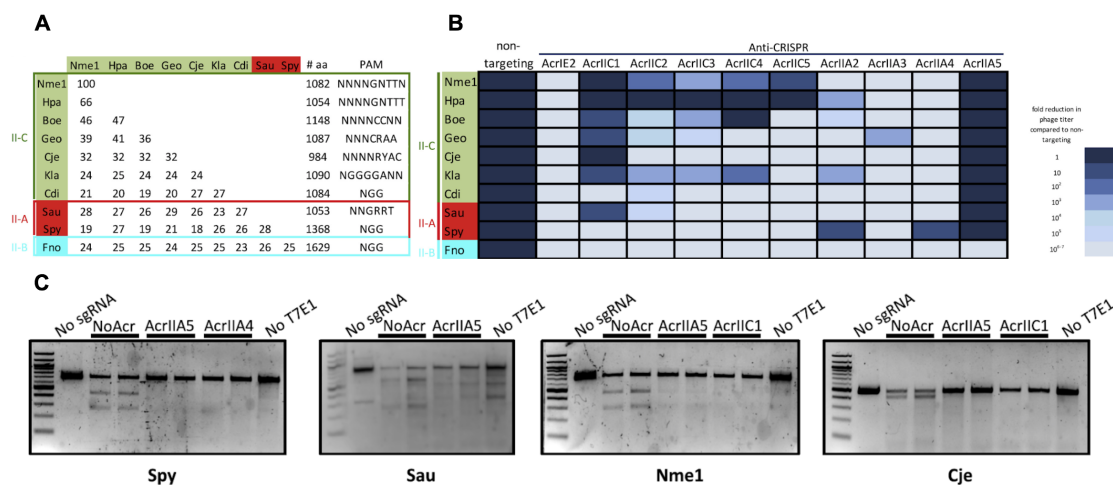


Figure 2.8 AcrIIA5 displays a broad-spectrum inhibition against Type II Cas9 proteins.

(A) Summary of Cas9 proteins used in the phage Mu targeting assays. The length in amino acids, a subtype classification, PAM sequences, and all-versus-all pairwise sequence identities are shown. **(B)** *E. coli* phage Mu plaque assays for Cas9 systems. The inhibitory activity of all tested anti-CRISPRs against diverse Cas9 homologs is represented based on the ten-fold serial dilutions of phage Mu lysate. The darkness of the cell in the table indicates the degree of inhibition of the Cas9 by the indicated anti-CRISPR, with the darkest cell representing $>10^6$ -fold inhibition of the Cas9 system (i.e., plaquing efficiency of phage Mu increases $>10^6$ -fold in the presence of the anti-CRISPR). The lightest-shaded cells indicate that the given anti-CRISPR displayed no inhibition of the Cas9. This figure represents data obtained through at least three biological replicates of each assay. **(C)** Genome editing in the HEK293T cells analyzed by T7E1 assays. AcrIIA5 and AcrIIA4 are used as positive controls for Nme1/CjeCas9 and SpyCas9 inhibition, respectively. The image shown has two technical replicates and is representative of at least three biological replicates.

To quantitatively compare the specificity profiles of a large number of anti-CRISPR proteins, we used a phage-targeting assay in which Cas9 is co-expressed with the sgRNA that targets phage Mu and prevents its replication by cleaving its genome (Harrington, Doxzen, et al., 2017). We expressed a diverse group of Cas9 homologs (Figure 2.8A) in *E. coli* with a cognate sgRNA to target phage Mu. These Cas9 homologs include SpyCas9, SauCas9, CjeCas9, and Nme1Cas9 as well as Cas9 homologs distributed across the phylogeny of Cas9s representing all three subtypes (II-A, II-B, and II-C), which range in pairwise sequence identity from 19% to 66% and use a variety of PAM sequences (Figure 2.8A). We tested 10 previously identified anti-CRISPRs in the phage Mu targeting assay, including four that were shown to inhibit Type II-A and five that inhibit Type II-C CRISPR-Cas systems. The level of phage Mu plaquing in the presence of a particular Cas9/anti-CRISPR combination provides a quantitative measure of the effectiveness of the anti-CRISPR in inhibiting a given Cas9 homolog. The targeted cleavage activity of Cas9 proteins reduced the plaquing efficiency of phage Mu by at least 10^5 -fold compared to strains expressing the same Cas9 proteins with non-targeting sgRNA (lighter shade; Figure 2.8B). The co-expression of anti-CRISPRs can have a range of effects on the Cas9-mediated reduction of plaquing efficiency. In some cases, the co-expression of anti-CRISPRs caused no increase or only a partial increase in plaquing efficiency. While some anti-CRISPRs, such as AcrIIA4, are highly specific, inhibiting one or a few CRISPR-Cas9 systems, others, such as AcrIIC1_{Nme}, inhibit

many Type II-C Cas9s (Figure 2.8B). Overall, the strength and specificity of anti-CRISPRs may vary over multiple orders of magnitude. In contrast to all of the other anti-CRISPRs tested, AcrIIA5 was able to completely inhibit every Type II-A and II-C Cas9 including a highly divergent *Corynebacterium diphtheria* (CdiCas9), emphasizing its unusually broad activity. It failed to block only the Type II-B Cas9 from *Francisella novicida* (Figure 2.8B). AcrIIA5 previously has been shown to inhibit CjeCas9 and a homolog of AcrIIA5 to inhibit Nme1Cas9 *in vitro* (Marshall et al., 2018). The uniquely broad specificity of AcrIIA5 inspired us to further investigate its properties.

Although AcrIIA5 was previously shown to inhibit genome editing mediated by SpyCas9 and *S. thermophilus* Cas9 (St1Cas9) in mammalian cells (Hynes et al., 2017), its activity against other Cas9 proteins in genome-editing applications had not been tested. To determine if AcrIIA5 could inhibit genome editing mediated by the four Cas9 homologs commonly used for genome-editing purposes in mammalian cells, we transiently co-transfected HEK293T cells with plasmids expressing anti-CRISPR proteins, Cas9s and their respective sgRNAs designed to target specific genomic sites. AcrIIA5 inhibited the activities of SpyCas9, Nme1Cas9, SauCas9, and CjeCas9 as confirmed by the T7E1 assay (Figure 2.8C). Collectively, these results show that AcrIIA5 efficiently inhibits the genome-editing activity of four diverse Cas9 proteins in both bacterial and mammalian cells. Furthermore, AcrIIA5 inhibits genome editing with similar potency to previously reported anti-CRISPRs.

2.2.9 AcrIIA5 activity prevents DNA binding and leads to sgRNA cleavage

To investigate how AcrIIA5 inhibits Cas9 activity, we developed a luminescence-based bioassay in which we targeted the catalytically inactive dSpyCas9 (Gilbert et al., 2014) to a constitutively expressed artificial promoter that drives expression of the luxCDABE luminescence genes in *E. coli* (Figure 2.9A). Binding of dSpyCas9 to the promoter of the luxCDABE operon repressed transcription, and no luminescence was detected in the absence of anti-CRISPR proteins (Figure 2.9B). The expression of AcrIIA5 relieved this repression, leading to an increase in luminescence and suggesting that DNA binding was inhibited. Similarly, the expression of AcrIIA4, which was previously shown to inhibit SpyCas9 DNA binding (Dong et al., 2017; Shin et al., 2017; H. Yang & Patel, 2017), also led to an increase in luminescence. By contrast, the expression of AcrIIC1, which does not inhibit SpyCas9, showed no increase in luminescence, as expected. These results demonstrate that AcrIIA5 blocks binding of dSpyCas9 to target DNA and impedes its function as a transcriptional repressor.

Although Nme1Cas9 lost its cleavage activity *in vitro* after the co-expression of His₆-tagged Nme1Cas9 and AcrIIA5, AcrIIA5 did not co-elute with Nme1Cas9, while a control, AcrIIC1, did co-elute (Figure 2.9C). Thus, the co-expression of AcrIIA5 with Nme1Cas9 caused a loss of activity even though the anti-CRISPR did not form a stable complex with Nme1Cas9. Surprisingly, when we examined

sgRNA bound to the Nme1Cas9 purified in the presence of AcrIIA5, a sizable proportion was smaller compared to the sgRNA bound to the Nme1Cas9 expressed without AcrIIA5 or with AcrIIC1 (Figure 2.9C, bottom gel). The full-length and cleaved sgRNA molecules seen in these gels were excised, reverse transcribed into DNA, and sequenced. We found that a portion of the Nme1Cas9 co-expressed with AcrIIA5 was bound to full-length sgRNAs that were indistinguishable from that of Nme1Cas9 controls. In addition, it was also frequently bound to truncated forms as mapped to stem-loops 1 and 2 of the sgRNA (Figure 2.9D). We tested whether Nme1Cas9 is responsible for the sgRNA cleavage as previously reported for RNA cleavage activity of the HNH endonuclease domain of Nme1Cas9 (Rousseau et al., 2018). However, the formation of the truncated sgRNA molecules was not mediated by either of the nuclease domains of Nme1Cas9 (Figure 2.9E). When the Nme1Cas9 mutants were co-expressed with AcrIIA5, the sgRNA was still cleaved in the same manner as with the wild-type Nme1Cas9. These results show that the nuclease domains of Nme1Cas9 do not catalyze the AcrIIA5-induced cleavage of sgRNA. The cleavage of sgRNA induced by AcrIIA5 and its close homologs is also observed for SpyCas9 [data not shown; (Garcia et al., 2019)]. Overall, AcrIIA5 functions as a broad-spectrum anti-CRISPR, and its co-expression with Nme1Cas9 results in the truncation of sgRNAs from the 3' ends. This phenomenon was observed consistently in six different AcrIIA5 family homologs for both Nme1Cas9 and SpyCas9.

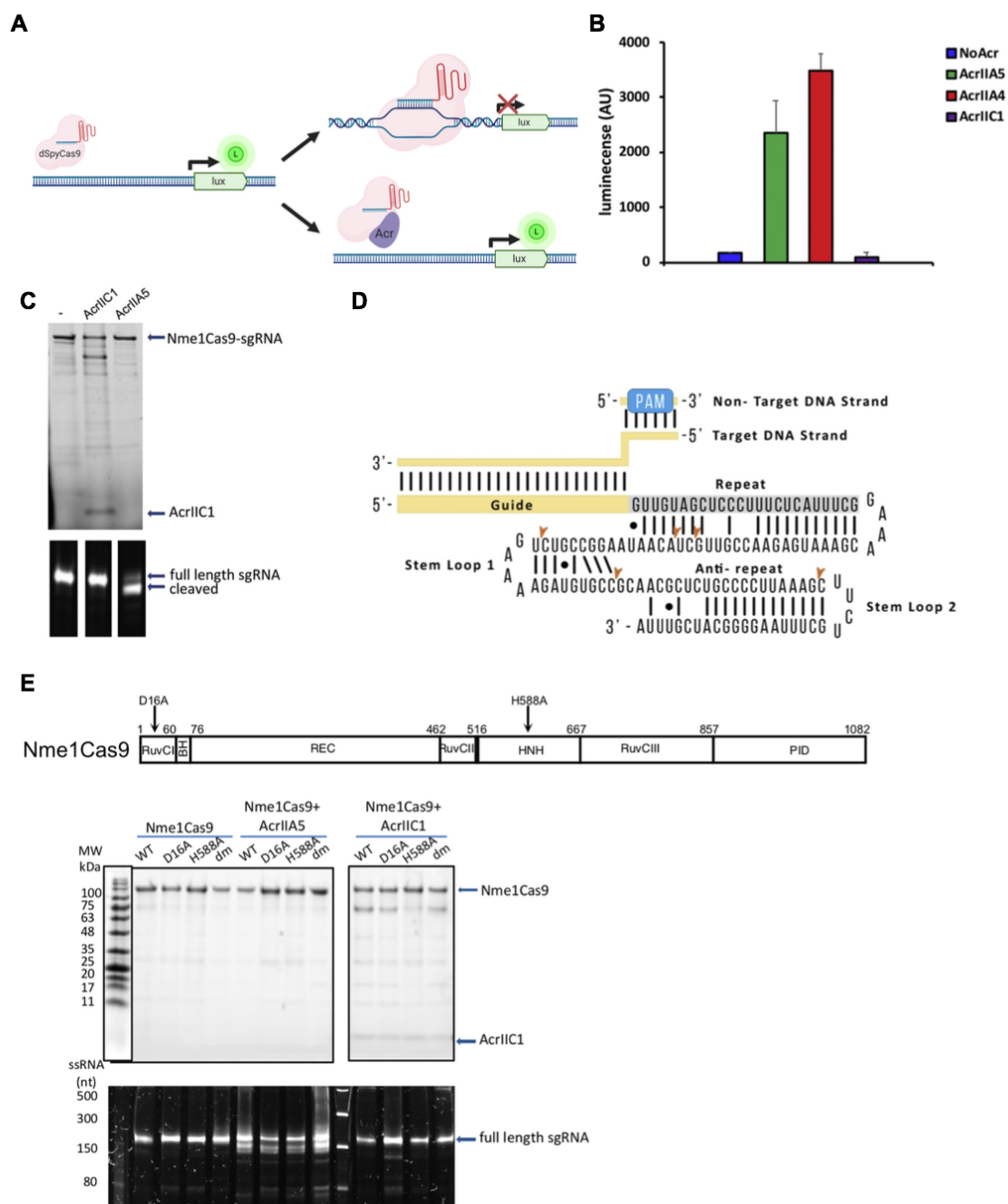


Figure 2.9 AcrIIA5 prevents DNA binding and leads to sgRNA cleavage

(A) Overview of CRISPRi luminescence assay. A constitutively active promoter controls the lux expression and its transcription is blocked when dSpyCas9 binds, resulting in no luminescence. Anti-CRISPR proteins can inhibit the binding of dSpyCas9 to the target DNA and restore the transcription and expression of the lux cassette. **(B)** The luminescence signal (AU, arbitrary units) is measured from cells expressing dSpyCas9 targeting the lux promoter in the presence of the indicated anti-CRISPRs. Data represent the mean and SD of luminescence measurements for three replicates. **(C)** His₆-Nme1Cas9 was co-expressed and co-purified without anti-CRISPR (-), or with AcrIIIC1 or AcrIIA5. Ribonucleoprotein complexes were analyzed by SDS-PAGE gel (top) and polyacrylamide/Urea gel (bottom). **(D)** A schematic of the Nme1Cas9 sgRNA with the target DNA is shown. The sgRNA secondary structure is predicted from other Cas9-sgRNA structures. Arrows indicate the positions of RNA cleavage in the sgRNA bound to the Nme1Cas9 co-expressed with AcrIIA5. The image is representative of at least three replicates of sequencing using the NEBnext Small RNA kit. **(E)** A domain architecture of Nme1Cas9 protein with amino acid substitutions in the RuvC domain (D16A), the HNH domain (H588A), and the double mutant (dm) with substitutions in both domains (D16A/H588A). Nme1Cas9 variants were co-expressed without Acr, or with AcrIIIC1 or AcrIIA5, and then purified by Ni-NTA chromatography. Ribonucleoprotein complexes were analyzed by a 15% Tris-tricine polyacrylamide gel using SDS-PAGE and visualized by stain-free imaging (top). For sgRNA visualization complexes were resolved on a 12.5% polyacrylamide/Urea gel and by SYBRTM Gold staining (bottom).

2.3 Discussion

CRISPR-Cas systems and anti-CRISPR proteins that inactivate them are in strong accord with the Red Queen hypothesis, which proposes that bacteria must evolve new mechanisms to resist invaders while the invaders simultaneously evolve countermeasures (Labrie et al., 2010). The widespread prevalence, extreme diversity, and sometimes co-occurrence of CRISPR-Cas systems in prokaryotic genomes, as well as the adaptive nature of the resulting defenses, pose a significant challenge to phages and other MGEs. An *in vitro* evolution study showed that the only way for phages to escape CRISPR-mediated extinction is by the expression of an anti-CRISPR gene (van Houte et al., 2016). Anti-CRISPR proteins provide phages with an effective tactic to inactivate CRISPR-Cas systems and likely contribute to phage persistence in the face of host defense mechanisms.

For the first time, we report the existence of the inhibitors of CRISPR interference in Type II systems (AcrIIC1-3 families for Nme1Cas9) (Pawluk, Amrani, et al., 2016). As a continuous exploration to uncover anti-CRISPR proteins, we report AcrIIC4 and AcrIIC5 that inhibit Nme1Cas9, HpaCas9, and SmuCas9. With time, our lab and others subsequently found that AcrIIC1-3 families of the Type II-C system inhibit Cas9 with varying potency and specificity by employing unique mechanisms of actions. Some Type II-C proteins have a narrow spectrum of inhibition while others demonstrate a broad-spectrum inhibition. Cross-species

inhibition may be graded depending on the similarity of the Cas9 orthologs. One prominent example of a broad-spectrum anti-CRISPR is AcrIIIC1, which inactivates multiple Type II-C Cas9 orthologs (Harrington, Doxzen, et al., 2017). This is likely because it binds to the highly conserved HNH domain, whereas other Type II-C Acrs may bind to Cas9 domains that are less conserved. On the other hand, AcrIIIC2 and AcrIIIC3 can inhibit only Nme1Cas9 by interfering with sgRNA loading and DNA binding and cleavage, respectively (Thavalingam et al., 2019; Zhu et al., 2019). It remains to be tested whether AcrIIIC4 and AcrIIIC5 prevent DNA binding by precluding initial recognition of the PAM, by interfering with the R-loop formation and Cas9 structural rearrangement, or a combination of both.

Anti-CRISPR proteins that can inhibit Cas9s across different subtypes (e.g. Type II-A, II-B, and II-C) are uncommon. We show that AcrIIIA5 can inhibit 9 different Cas9 orthologs of both Type II-A and II-C systems, displaying the specificity broader than that of AcrIIIC1_{Nme} and has a unique feature of resulting in sgRNA truncation. However, based on the heterogeneous population of truncated sgRNAs that vary in the abundance and identity as well as the presence of a full-length sgRNA indistinguishable from that bound to Nme1Cas9 in the absence of AcrIIIA5, we conclude that sgRNA cleavage alone cannot account for the inhibitory activity of AcrIIIA5. Instead, AcrIIIA5 may partially dislodge the sgRNA from Cas9, leaving it prone to digestion by intracellular RNases. The portion of the sgRNA that we observed to be digested, stem-loops 1 and 2, are the more

exposed parts of the sgRNA in the Cas9-sgRNA complex. We speculate that the sgRNA truncation may be due to a conformational change in Cas9 that alters the integrity of sgRNAs. It may not necessarily be the inhibitory mechanism per se but rather results from the interaction between AcrIIA5 and Cas9.

Another group reported that AcrIIA5 inhibits the RuvC domain of SpyCas9 while DNA binding is unaffected (G. Song et al., 2019). We and others previously reported that AcrIIA5 hinders DNA binding activity and such discrepancy may have resulted because the function of AcrIIA5 was assessed based on the indirect measurements by monitoring a reporter gene (Garcia et al., 2019; J. Li et al., 2018; Nakamura et al., 2019). The expression and stability of heterologous proteins in tested systems may have also influenced the varying results. For example, the expression of AcrIIA5 has been shown to reduce the reporter gene expression regardless of matching sgRNAs in a dCas9 binding assay (Marshall et al., 2018; G. Song et al., 2019). Moreover, we had difficulty purifying AcrIIA5 in the active form due to a low expression level of AcrIIA5, which has also been documented by Song et al. (2019). Therefore, the results should be interpreted with caution. Recently, An et al. reported that a solution structure of AcrIIA5 has an N-terminal intrinsically disordered region (IDR) and performed extensive truncation and substitution experiments to understand its role in inhibition of Cas9 (An et al., 2020). Based on their findings, the length of IDR mediates the interaction between the AcrIIA5 and Cas9-sgRNA while the amino acid content of AcrIIA5 dictates the catalytic efficiency of the inhibitory complex (An et al., 2020).

The conformational plasticity of the IDR may contribute to the broad-spectrum inhibition of multiple Cas9 effectors. To tie all the pieces together, AcrIIA5 may bind to the guide RNA binding region of Cas9 and the N-terminal IDR may extend toward the RuvC domain to inhibit the nuclease activity of Cas9. A co-crystal structure may help us better understand the whole picture of the inhibitory mechanism of AcrIIA5 in the future.

Although most studies are in agreement with one another, some discrepancies are notable as the Acrs may have multiple inhibitory mechanisms and one or the other may be revealed depending on how the studies are conducted. Extensive efforts combining different approaches spanning from *in vitro* biochemical studies to structural analyses are ongoing to dissect the mechanisms of many anti-CRISPR proteins that may surprise us with new exciting biology.

Beyond the host-phage arms race, anti-CRISPR proteins also hold immense potential for biotechnological uses. We demonstrate that the anti-CRISPR proteins can be used as potent off-switches for mammalian genome engineering for both Cas9 and dCas9 applications. Many such applications stand to benefit from increasing the numbers, specificities, and inhibitory mechanisms of anti-CRISPRs, for instance, through combinatorial control over multiple Cas9/dCas9 proteins. For example, both broad-spectrum (e.g., AcrIIC1, AcrIIA5) and highly-specific (e.g., AcrIIC3-5) anti-CRISPR proteins could be used to control multiple Cas9s simultaneously, or specific Cas9s but not others, upstream or downstream

of target recognition, to achieve maximal flexibility of both genome manipulation and regulation. Applications of genetically encoded anti-CRISPR inhibitors to provide a means to spatially, temporally, or conditionally control Cas9 activity are discussed in the next chapters.

2.4 Materials and Methods

Bioinformatics searches for anti-CRISPR proteins

Putative anti-CRISPR genes were identified using the guilt-by-association bioinformatic method. Briefly, BLAST searches were conducted using *aca2* and *aca3* as the query and orthologs of *aca* genes that had a small, uncharacterized hypothetical ORF immediately upstream were curated manually.

Plasmid vector construction

Appendix Table 1 contains the protein sequences of Cas9 and anti-CRISPR proteins. Appendix Table 2 summarizes plasmids used in this chapter. Plasmid maps and sequences are available on Addgene.

Expression vectors for bacterial expression

Nme1Cas9 sgRNA was synthesized by GenScript and cloned into the pMCSG7 expression vector downstream of the Nme1Cas9 ORF. DNA sequences encoding candidate anti-CRISPR proteins were synthesized by either GenScript and subcloned into pHAT4 vector or IDT and subcloned into the pMCSG7 vector.

Expression vectors for mammalian expression

Each Acr ORF was synthesized as a gene block (IDT) and then inserted into the pCSDest2 vector (Addgene). The resulting plasmids placed the Acr-encoding

genes under the control of the CMV-IE94 promoter. Cas9 expression vectors, also pCSDest2 under CMV-IE94 promoter, were identical in all respects except for the respective Cas9 ORFs. Similarly, plasmids for the expression of sgRNAs in pLKO.1 vectors for each Cas9 ortholog were also identical in all respects except for the sgRNA sequences themselves.

Vectors for fluorescence microscopy

pHAGE-TO-DEST dSpyCas9-(mCherry)₃ and dNme1Cas9-(sfGFP)₃ plasmids (Ma et al., 2015) were purchased from Addgene and used directly for no-sgRNA control experiments. All-in-one versions that also included the sgRNA-expressing cassette for targeting telomeric repeats were made by inserting the U6 promoter/sg-telomere cassette into its cognate dCas9 plasmid via Gibson assembly (NEB). To make the Acr plasmids, we amplified a mTagBFP2 cassette and incorporated it into pCSDest2 with ACR ORFs by Gibson assembly. To generate the control, simply Acr OF was removed and re-ligated.

Purification of recombinant proteins

6xHis-tagged recombinant proteins were expressed in E. coli BL21 (DE3). Cells were grown in either LB or TB medium at 37 °C to an optical density (OD₆₀₀ nm). Protein expression was induced by the addition of 1 mM IPTG for 16 hr at 16 °C. Cells were lysed by sonication in 50 mM Tris pH 7.5, 500 mM NaCl, 20 mM imidazole, 0.5 mM DTT and 5% glycerol supplemented with 0.5 mM PMSF,

lysozyme and protease inhibitor cocktail (Sigma). Clarified lysates were bound in batch to Ni-NTA agarose (Qiagen), and the bound protein was eluted with 300 mM imidazole. After elution from Ni-NTA resin, anti-CRISPR proteins were dialyzed in 10 mM Tris pH 7.5, 250mM NaCl, and 5mM b-mercaptoethanol and incubated with His-tagged Tobacco Etch Virus (TEV) protease overnight at 4°C. The second round of Ni-NTA purification was used to isolate successfully cleaved, untagged anti-CRISPRs by collecting the unbound fraction. Cas9s were further purified using cation exchange chromatography using a Sepharose HiTrap column (GE Life Sciences). Size exclusion chromatography was used to purify Nme1Cas9 further in 20 mM HEPES-KOH (pH 7.5), 300 mM KCl and 1 mM TCEP.

In vitro DNA cleavage

sgRNA was generated by *in vitro* T7 transcription (Epicentre). Cas9 was incubated with purified, recombinant anti-CRISPR protein in cleavage buffer [20 mM HEPES-KOH (pH 7.5), 150 mM KCl, 10% glycerol, 1 mM DTT, and 10 mM MgCl₂] for 10 min. Next, sgRNA was added and the mixture was incubated for another 15 min. For target DNA, a plasmid containing the protospacer was linearized by enzyme digestion or amplified by PCR. The reactions were incubated at 37°C for 30-60 min, treated with proteinase K, and visualized after electrophoresis in a 1% agarose/1xTAE gel.

Mammalian genome editing

Transient transfection

Plasmids for mammalian expression of Cas9s, their respective sgRNAs, and the anti-CRISPR proteins were transiently transfected in approximately 1.5×10^5 mid-passage HEK293T cells [cultured at 37 °C, 5% CO₂ in DMEM (Gibco) + 10% FBS(Sigma) + 1% Penicillin/Streptomycin (Sigma)] in a 24-well plate using PolyFect (Qiagen). The total amount of DNA was equal in all transfections (e.g., for the no-sgRNA controls, the sgRNA-expressing plasmids were replaced with the same mass of an irrelevant plasmid). 72 hr after transfection, cells were harvested and gDNA was extracted with the DNeasy Blood and Tissue kit (Qiagen) and then was used for PCR amplification [High Fidelity 2X PCR Master Mix (NEB)] with primers flanking the targeted site. PCR products were heat-denatured, re-annealed, and digested with T7 Endonuclease I (NEB). The samples were visualized in a 2.5% agarose/1xTAE gel and quantified with the ImageMaster-TotalLab program. Indel percentages (“% lesion” in the figures) were calculated as previously described (Guschin et al., 2010). Alternatively, indel frequencies were estimated by Sanger sequencing followed by TIDE (Brinkman et al., 2014) or the Next-generation sequencing followed by analysis with custom scripts.

Ribonucleoprotein Delivery

RNP delivery of Nme1Cas9 was performed using a Neon electroporation system following the manufacturer’s instructions (ThermoFisher). Briefly, in a 10 µl

reaction volume, 15 pmol of Nme1Cas9 and 150 pmol of anti-CRISPR protein were mixed in buffer R and incubated at room temperature for 20 min. Then, 20 pmol of T7 *in vitro*-transcribed sgRNA was added to the Cas9-Acr complex and incubated at room temperature for 30 min. Approximately 50,000 to 100,000 cells were mixed with the RNP-Acr-sgRNA complex, electroporated (Neon nucleofection system), and then plated in 24-well plates. After gDNA collection, PCR amplification of the target sites, and column purification, PCR products were sent for Sanger sequencing (Genewiz), and trace files (ab1 files) were analyzed using TIDE (Brinkman et al., 2014).

Targeted deep sequencing analysis

We used a two-step PCR amplification approach to produce DNA fragments for each on-target and off-target site. In the first step, we used locus-specific primers bearing universal overhangs with ends complementary to the TruSeq adaptor sequences. DNA was amplified with High Fidelity 2× PCR Master Mix (NEB) using appropriate annealing temperatures for the on-target (NTS1C) and off-target (NTS1C-OT1) sites. In the second step, the purified PCR pool was amplified with a universal forward primer and an indexed reverse primer to

reconstitute the TruSeq adaptors. Full-size products (~250bp in length) were extracted using AMPure beads (Beckman Coulter). The purified library was deep sequenced using a paired-end 150bp MiSeq run. High-throughput sequencing data are available at the NCBI Sequence Read Archive (accession no.

PRJNA505886)

Fluorescence microscopy

U2OS cells were cultured at 37 °C (5% CO₂) in DMEM (Gibco) supplemented with 10% FBS (Sigma) and 1% Pen/Strep (Sigma). For imaging, cells were grown on 170 µm, 35 x 10mm glass-bottom dishes (Eppendorf). Cells were co-transfected with all-in-one plasmids. sgRNA-expressing plasmids, and anti-CRISPR/mTagBFP2 plasmid using PolyFect (Qiagen). The additional sgRNA-only plasmid was included because we found the levels of sgRNAs expressed from the all-in-one plasmid alone to be sub-saturating. For the no-sgRNA control experiments, the additional sgRNA-only plasmids were excluded, and the sgRNA cassette was also excluded from the cognate dCas9-expressing plasmid. After 24 hr of incubation, live cells were imaged with a Leica DMI8 microscope equipped with a Hamamatsu camera (C11440-22CU), a 63x oil objective lens, and Microsystems software (LASX). Further imaging processing was done with Fiji-ImageJ. For the blinded experiments to score cells with telomeric foci, each

condition was coded by one experimenter and then scored by another who did not know which set of cells were from which condition. Only cells that exhibited mTagBFP2 and sfGFP fluorescence, as well as dSpyCas9-(mCherry)₃ telomeric foci, were assessed for the presence or absence of co-localizing dNme1Cas9-(sfGFP)₃ telomeric foci, and all such imaged cells were included in the quantifications.

PAM determination assay

A library of a protospacer with randomized PAM sequences was generated using overlapping PCRs, with the forward primer containing the 10-nt randomized sequence flanking the protospacer. The library was subjected to *in vitro* cleavage by purified recombinant HpaCas9 or SmuCas9 proteins as well as *in vitro*-transcribed sgRNAs. The segment of a gel where the cleavage products were expected to be was purified and subjected to library preparation as described previously (Z. Zhang et al., 2012). The library was sequenced using the Illumina NextSeq500 sequencing platform and analyzed with custom scripts.

Electrophoretic mobility shift assay (EMSA)

Nme1Cas9 (1 μ M) was incubated with 1 μ M sgRNA in 1 \times binding buffer (20 mM Tris-HCl [pH 7.5], 150 mM KCl, 2 mM EDTA, 1 mM DTT, 5% glycerol, 50 μ g/ml heparin, 0.01% Tween 20, 100 μ g/ml BSA) for 20 min at room temperature to form the RNP complex. Acrs were added to a final concentration of 10 μ M and

incubated for an additional 20 min. Finally, the FAM-tagged NTS4B protospacer oligonucleotide was added to the mixture and incubated at 37°C for 1 hr. The mixture was loaded onto a native 6% acrylamide gel, and the FAM-tagged DNA was visualized using a Typhoon imager.

sgRNA EMSA

Nme1Cas9 (1.5 μ M) and anti-CRISPR (20 μ M) proteins were preincubated in 1 \times binding buffer for 10 min, and then sgRNA (0.15 μ M) was added to the reaction mixture for an additional 10 min. The complexes were resolved on a 6% polyacrylamide native gel, stained by SYBR Gold (ThermoFisher), and visualized with a Typhoon imager.

Fluorescence polarization assay

Preformed RNP complex of Nme1Cas9 and sgRNA was added to 1 \times binding buffer (20 mM Tris-HCl [pH 7.5], 150 mM KCl, 5 mM EDTA, 5 mM MgCl₂, 1 mM DTT, 5% [vol/vol] glycerol, 50 μ g/ml heparin, 0.01% Tween 20, and 100 μ g/ml BSA) and incubated for 30 min followed by the addition of 10 μ M Acrs. This mixture was incubated for 30 min followed by the addition of an 8 nM FAM-tagged NTS4B protospacer (34 bp containing only 8-bp PAM duplex). After an incubation of 30 min the polarization measurements were made on Victor3 multilabel plate counters (Perkin Elmer). To calculate fraction-bound values, data were normalized by setting the lowest anisotropy to 0 and highest to 1. The curve fitting was performed in GraphPad Prism using the following equation:

$$Y = \frac{(|\text{DNA}| + |\text{RNP}| + K_d) - \sqrt{(|\text{DNA}| + |\text{RNP}| + K_d)^2 - (4 \times |\text{DNA}| \times |\text{RNP}|)}}{2 \times |\text{DNA}|}$$

In vivo phage Mu plaquing assays

E. coli BB101 cells were co-transformed with plasmids expressing Cas9-sgRNA combinations targeting phage Mu and a pCDF-1b plasmid expressing the different anti-CRISPR proteins. Cells containing both plasmids were sub-cultured in LB supplemented with chloramphenicol and streptomycin and grown for 2 hr, at which point anti-CRISPR expression was induced with 0.01mM IPTG for 3 hr. Cells were then mixed with soft LB-agar and top-plated on LB supplemented with both antibiotics and 200 ng/mL aTc, 0.2% arabinose, and 10 mM MgSO₄. Serial dilutions of phage Mu were spotted on top and the plates were incubated overnight at 37°C. Experiments were performed in triplicate.

dSpyCas9 binding luminescence assay

A plasmid in which the J23119 artificial promoter drives constitutive expression of the *luxCDABE* operon from *Photobacterium luminescens* (Winson et al., 1998) was targeted by dSpyCas9 with its crRNA, which was cloned into the BsaI site of the pCRISPathBrick plasmid (Cress et al., 2015). The target DNA plasmid was co-transformed into *E. coli* BL21 cells with pCM-str, a pCDF-1b plasmid expressing the anti-CRISPR proteins and a protospacer targeting the J23119 promoter. Cells containing the three plasmids were grown in LB supplemented

with kanamycin, chloramphenicol and streptomycin until they reached OD₆₀₀ nm of 0.6. The cultures were then diluted to an OD₆₀₀ of 0.1 in LB containing 200 ng/mL aTc, 0.2% arabinose and 0.01 mM IPTG, and 100 µl was dispensed into a 96-well plate. The plate was incubated with shaking at 37°C using a Synergy H1 reader controlled by Gen5 2.09 software (BioTek Instruments Inc.), and the OD₆₀₀ and luminescence was monitored for 24 hr.

Co-expression and co-purification of Nme1Cas-/sgRNA and anti-CRISPR

E. coli BB101 cells were co-transformed with 6x-His-tagged Nme1Cas9-sgRNA in pMCSG7 or 6x-His-tagged SpyCas9-sgRNA in pMCSG7 and a pCDF-1b vector encoding untagged anti-CRISPR protein. Cells were grown in LB at 37°C to an OD₆₀₀ of 0.8. Protein expression was induced by the addition of 1mM IPTG, and the cells were incubated for an additional 3 hr at 37°C. Cells were collected by centrifugation, resuspended in binding buffer [50 mM Tris-HCl (pH 7.5), 200 mM NaCl, 5% glycerol, 20 mM imidazole], and lysed by sonication. Clarified lysates were incubated with Ni-NTA agarose (Qiagen) for 30 min at 4°C, washed with binding buffer supplemented with 30 mM imidazole, and bound protein was eluted with binding buffer supplemented with 300 mM imidazole. The purified ribonucleoprotein complexes were analyzed by SDS-PAGE using a 15% Tris-Tricine gel, and the proteins were visualized using Coomassie stain. The co-purifying sgRNA was examined using a denaturing 12.5% polyacrylamide/Urea gel and visualized by SYBR™ Gold (ThermoFisher Scientific) staining.

RNA cloning and sequencing

sgRNAs bound to affinity-purified Nme1Cas9 in the presence or absence of AcrIIA5 or in the presence of AcrIIC1 were electrophoresed on a denaturing 12.5% polyacrylamide/Urea gel and visualized by SYBR™ Gold (ThermoFisher Scientific) staining. Bands corresponding to full-length sgRNAs were excised for each sample and bands with higher mobility than the full-length sgRNAs were excised from the sample of Nme1Cas9 purified from the cells grown in the presence of AcrIIA5. The gel slices were soaked in 250 µL of DNA Gel Elution Buffer (NEB) supplemented with 1:100 SUPERase·In RNase Inhibitor (ThermoFisher Scientific) and rotated overnight at 4°C. The eluate was filtered through a Nanosep® MF 0.45 µm column (Pall Laboratory, ODM45C35). RNA was ethanol precipitated and reconstituted in ultrapure water. Libraries were prepared with the NEBNext Small RNA Library Prep Set for Illumina (NEB) following the protocol provided by the manufacturer. The resulting DNA library was visualized using 8% PAGE and bands corresponding to the sgRNA fragments were excised. DNA was eluted from the excised bands by rotating overnight in the DNA Gel Elution buffer at room temperature. The eluate was filtered through a Nanosep® MF 0.45 µm column and the DNA was ethanol precipitated and resuspended in ultrapure water. DNA fragments were then ligated to the TOPO Blunt vector (ThermoFisher Scientific), DNA was purified from single colonies, and inserts were sequenced using the M13F or M13R primers.

Chapter 3 Applications of anti-CRISPR proteins for genome engineering

3.1 Introduction

Although RNA-programmable CRISPR-Cas9 genome engineering has revolutionized biological research and promises to do so for clinical applications, limitations and safety issues remain (Doudna, 2020). The discovery of anti-CRISPR proteins provides the opportunity to exploit their ability to inhibit Cas9 and to address some of the limitations of Cas9 genome engineering (Marino et al., 2020). In this chapter, I describe a method of improving HDR efficiency and controlling various genome editors using anti-CRISPR proteins to demonstrate the broader utility of Acrs in genome engineering applications.

3.1.1 Precise gene editing using HDR is inefficient

One of the limitations of the Cas9 genome editing is the inefficiency of precise DNA insertions, deletions, or substitutions by HDR due to the competing NHEJ repair pathway (Jasin & Rothstein, 2013). To achieve a precise integration of the target DNA efficiently, various approaches have been used to promote HDR, inhibit NHEJ, or both (M. Liu et al., 2018; Yeh et al., 2019). One of the drawbacks of such approaches is that they directly interfere with the cellular DNA repair machinery, possibly jeopardizing the cell's ability to repair endogenous DNA breaks in the genome. Studies of DSB repair pathways in eukaryotic cells support that the repair pathway choice is largely dependent on the cell-cycle phase: HDR is active in late S/G2 phases and suppressed in other cell cycle phases whereas NHEJ is active in all cycle phases (Hustedt & Durocher, 2016).

Suppressing the NHEJ or enhancing the activity of HDR by gene knockdown, small molecules (Chu et al., 2015; Maruyama et al., 2015; Pinder et al., 2015; Robert et al., 2015; J. Song et al., 2016; Srivastava et al., 2012; Yu et al., 2015), or engineered proteins (Canny et al., 2018; M. Charpentier et al., 2018; Nambiar et al., 2019) can improve the efficiency of HDR (Yeh et al., 2019). To increase the effectiveness of HDR by using the cell-cycle dependence of repair pathway choice, different chemical inhibitors have been used to synchronize the cell cycle.

They function to arrest the cells in G2 and/or M phase and narrow down the timing of Cas9 editing (S. Lin et al., 2014; D. Yang et al., 2016). Although this

cell-cycle synchronization strategy improves HDR efficiency, it will be difficult to implement in animals and humans. An alternate approach to enhance the HDR efficiency is an endogenous regulation to control Cas9 activity by restricting the Cas9 editing to S/G2 phases and inhibiting Cas9 in the G1 phase by anti-CRISPR proteins.

To this end, we adopted the FUCCI (Fluorescence Ubiquitin Cell Cycle Indicator) system developed originally by Sakaue-Sawano et al. (2008) for degron-mediated proteolysis of Cas9 and anti-CRISPR proteins. The FUCCI technology takes advantage of two components of the DNA replication control system: the licensing factor Cdt1 and its inhibitor Geminin (Sakaue-Sawano et al., 2008; Zielke & Edgar, 2015). Cdt1 and Geminin protein abundance oscillate during the cell cycle: Geminin levels are high during S/G2 phase, but low in M/G1 phase while Cdt1 protein peaks in the G1 phase (with a steep decline in the S phase) (Arias & Walter, 2007). This reciprocal expression of Geminin and Cdt1 is mediated by E3 ubiquitin ligases APC/CCdh1 and SCFSkp2, respectively. In the FUCCI system, degron sequences derived from Geminin (hGem₁₋₁₁₀) and Cdt1 (hCdt1₃₀₋₁₂₀) are fused to fluorescent proteins to monitor the cell cycle progression (Sakaue-Sawano et al., 2008; Zielke & Edgar, 2015). We repurposed this system so that the degrons are transferred to Cas9 and anti-CRISPR proteins to improve HDR efficiency by restricting Cas9 editing to S/G2 phases and preventing the editing in other phases using anti-CRISPRs. The degrons will promote the degradation of each protein in the respective cell cycle

phases: Cas9 with M/G1-specific hGem₁₋₁₁₀ degron will be degraded in the M/G1 phase and Acr with S/G2-specific hCdt1₃₀₋₁₂₀ degron will be degraded in the S/G2 to permit Cas9 editing and HDR. This approach will be described in more detail in the section 3.2.1.

3.1.2 Enhancing target specificity often requires engineering nucleases

Another challenge of using CRISPR-Cas9 is a safety concern over off-target gene editing. For instance, studies have shown that high expression of Cas9s leads to a prolonged activity and increased off-target cleavages (Cameron et al., 2017; Hsu et al., 2013; S. Kim et al., 2014) and limiting Cas9 concentration may help reduce off-target activity (Cameron et al., 2017; Hsu et al., 2013; S. Kim et al., 2014). Unlike traditional gene editors such as ZFNs or TALENs, which are designer nucleases that have been optimized for highly specific DNA targeting via protein engineering, CRISPR systems, though easily programmable, are often prone to off-target editing. Various methods have been developed to improve the specificity by modifying either guide RNA scaffolds or nucleases themselves (D. Kim et al., 2019).

One interesting protein engineering approach is to combine the CRISPR nuclease with a programmable DNA binding domain (pDBD; such as ZFNs or another Cas9 ortholog) to ensure enhanced specificity while retaining the robust on-target activity (Bolukbasi et al., 2015, 2018). In this platform, Cas9 has reduced binding affinity to the target DNA due to the mutations introduced in the residues involved in PAM recognition. A PAM-attenuated SpyCas9 (SpyCas9^{MT3}) fused to a pDBD enables SpyCas9 binding to be dependent on the pDBDs (Bolukbasi et al., 2015). The first step is mediated by pDBD recognition of a sequence downstream of the PAM. The increased local concentration of

SpyCas9^{MT} upon pDBD binding facilitates the recognition of the PAM and unwinding of the target DNA (R-loop formation) and subsequent DNA cleavage based on the sufficient complementarity between the sgRNA and the target site. These additional licensing steps, therefore, restrict editing by the Cas9 nuclease to the intended on-target site while suppressing off-target editing. ZFNs, TALENs, or orthogonal dCas9s can serve as the pDBD (Bolukbasi et al., 2015, 2018). The biggest advantage of using a pDBD is the enhancement of target binding and near elimination of off-target activity of Cas9. Although Nme1Cas9 is intrinsically hyper-accurate, an extra layer of accuracy can help eliminate even a low risk of off-target activities where precision is paramount as is in gene therapy applications. For this reason, we previously developed a Nme1Cas9-pDBD platform based on the SpyCas9 system (Amrani et al., in preparation). In section 3.2.2, we show that the inhibition of Nme1Cas9 by anti-CRISPRs proteins can be also extended to the chimera Nme1Cas9-pDBD, validating that these anti-CRISPR proteins can be used as potent off-switches for a large fusion protein in genome engineering applications.

3.2 Results

3.2.1 Anti-CRISPRs with cell-cycle-dependent degrons improve HDR

In eukaryotes, DSB repair pathway choice is largely dependent on the cell cycle: HDR is active only in S/G2 phases whereas NHEJ is active throughout the cell cycle (Hustedt & Durocher, 2016) (Figure 3.1A). To enhance the efficiency of HDR with minimal perturbations in cells, we took advantage of the cell-cycle dependence of DSB repair pathway choice and degron-mediated proteolysis (Figure 3.1B). One of the proteins that oscillates during the cell cycle is Geminin, an inhibitor of a replication licensing factor, Cdt1. Geminin is a direct substrate of the anaphase-promoting complex (APC)/Cdh1, a protein-ubiquitin ligase that is active in late M/G1 phases and promotes degradation of target substrates by ubiquitination (Arias & Walter, 2007). Previously, SpyCas9 was fused to the first 110 amino acids of Geminin containing a destruction box motif, designated as a human Geminin degron (hGem₁₋₁₁₀) (Gutschner et al., 2016). This increased the HDR efficiency by promoting degradation of SpyCas9 in the G1 phase when HDR is not active; however, the effects were modest (<2-fold), probably due to residual SpyCas9 activity from the incomplete degradation (Gutschner et al., 2016). Cas9 editing in the G1 phase may result in indels if DSBs are repaired by NHEJ and can reduce the number of available sites that can be targeted for HDR (Figure 3.1B). To further restrict Cas9 editing to S/G2 phases by preventing its activity in G1 phase, we used anti-CRISPR proteins to inactivate Cas9 in the G1

phase, but permit editing in the S/G2 phases by fusing Acr to a degron from the licensing factor, Cdt1. 30-120 aa of human Cdt1 (hCdt₁₃₀₋₁₂₀) is targeted for ubiquitination and degradation by Skp, Cullin, F-box containing complex (SCF)/Skp2 in S/G2 phases (Zielke & Edgar, 2015). We hypothesized that restricting the activity of Cas9 strictly to the S/G2 phases will enhance HDR efficiency.

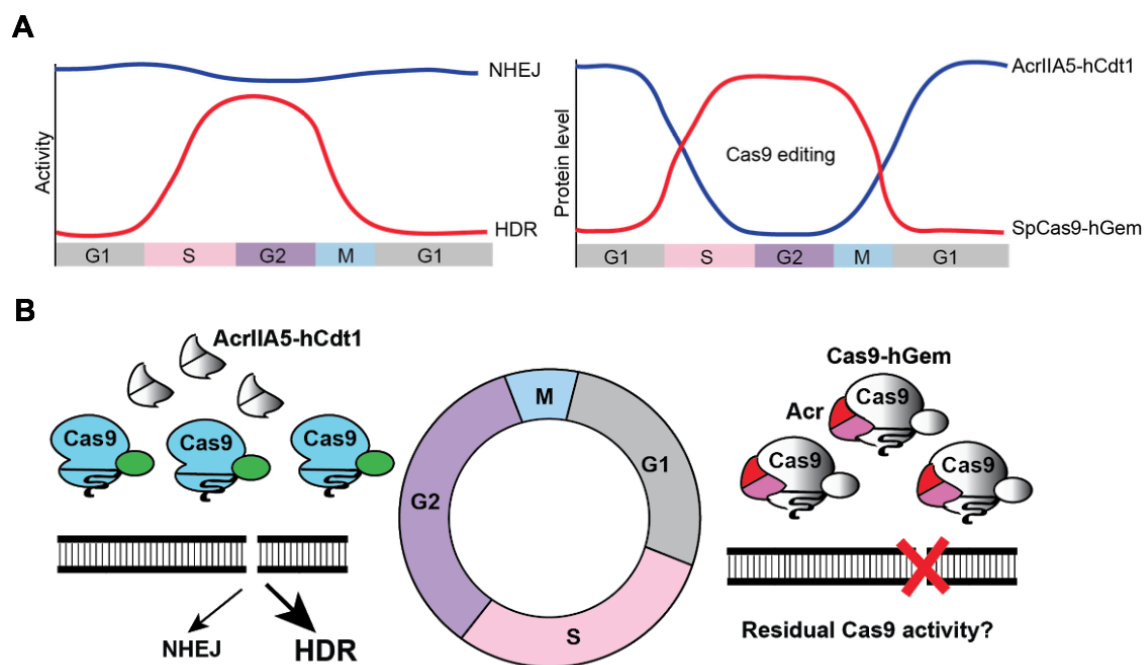


Figure 3.1 Cell-cycle dependence of DSB repair pathways. (A) Left: Cell-cycle dependent DSB repair: NHEJ (blue) and HDR (red). Right: Cas9 editing window can be tailored to mirror HDR activity throughout the cell cycle. While SpyCas9-hGem is degraded in the M/G1 phase, AcrIIA5-hCdt1 is degraded in the S/G2 phase when HDR activity is high. The activity of protein-ubiquitin proteases APC/Cdh1 and SCF/Skp2 that mediate cell-cycle progression is responsible for cell-cycle-dependent degradation of hGem and hCdt1 fused proteins, respectively. **(B)** A schematic of how Cas9 and anti-CRISPR deconjugation fusion proteins would help increase the HDR:NHEJ ratio throughout the cell cycle.

Engineering AcrIIA5-hCdt1 for cell-cycle-dependent inhibition of Cas9

Since SpyCas9-hGem construct is already validated and available to test our hypothesis using Type II-A anti-CRISPR proteins, we chose to engineer AcrIIA5 for cell-cycle dependent degradation (Figure 3.2A). AcrIIA5 can work not only against SpyCas9 but also other types of Cas9 that are commonly used in genome editing, therefore maximizing its utility. Although Acrs are generally small and do not require an NLS for efficient nuclear import, we added an NLS on the C-terminus of Acr as well as a FLAG epitope tag, followed by hCdt1 degron sequences.

To estimate the efficiency of HDR and NHEJ, we took advantage of the TLR-MCV1.0 cell line, a modified traffic-light reporter (TLR) system (Certo et al., 2011; Iyer, Mir, et al., 2019) (Figure 3.2B). Briefly, a TLR locus consists of a broken eGFP cassette interrupted by an artificial fragment of target sites for different Cas effector proteins and an out-of-frame mCherry ORF downstream of the eGFP and a self-cleaving peptide T2A. Providing Cas9 and sgRNA targeting the broken eGFP will result in indels that can be repaired by either NHEJ or HDR if the eGFP donor is supplied. Therefore, a DSB will result in eGFP fluorescence if repaired by HDR, or mCherry if repaired by NHEJ (Figure 3.2B) (Certo et al., 2011; Iyer, Mir, et al., 2019; Mir, Alterman, et al., 2018). This system allows us to easily evaluate the efficiencies of each repair outcome based on the green or red fluorescence by flow cytometry.

We generated a stable HEK293T cell line expressing the TLR system as well as AcrIIA5-hCdt1 (Figure 3.2B). Then SpyCas9 or SpyCas-hGem plasmids were transiently transfected in these cell lines along with donor templates. We tested the effect of different exogenous eGFP DNA donor types: a plasmid donor, a linear dsDNA, or a TEG-modified dsDNA (Figure 3.2C).

A plasmid dsDNA donor was used as a template to generate a linear dsDNA and a TEG donor by PCR amplification. For TEG donors, custom primers with the 5' end modification were used for PCR. The TEG donor consists of 2'OMe-RNA::TEG at both 5' ends of the DNA donor. The 5' addition of either TEG or 2'OMe-RNA has been shown to dramatically improve HDR potency and these modifications retain its high potency across dsDNA, ssDNA, and ssODN donors (Ghanta et al., 2018).

Next, we tested combinations of the following: 1) TLR cell line or mTLR-AcrIIA5-hCdt1 cell line, 2) SpyCas9 or SpyCas9-hGem, and 3) plasmid, linear, or TEG donor. We then used flow cytometry to score the efficiencies of HDR (GFP+) and NHEJ (mCherry+) in the total cell population to determine the absolute and relative HDR efficiencies (Figure 3.2D).

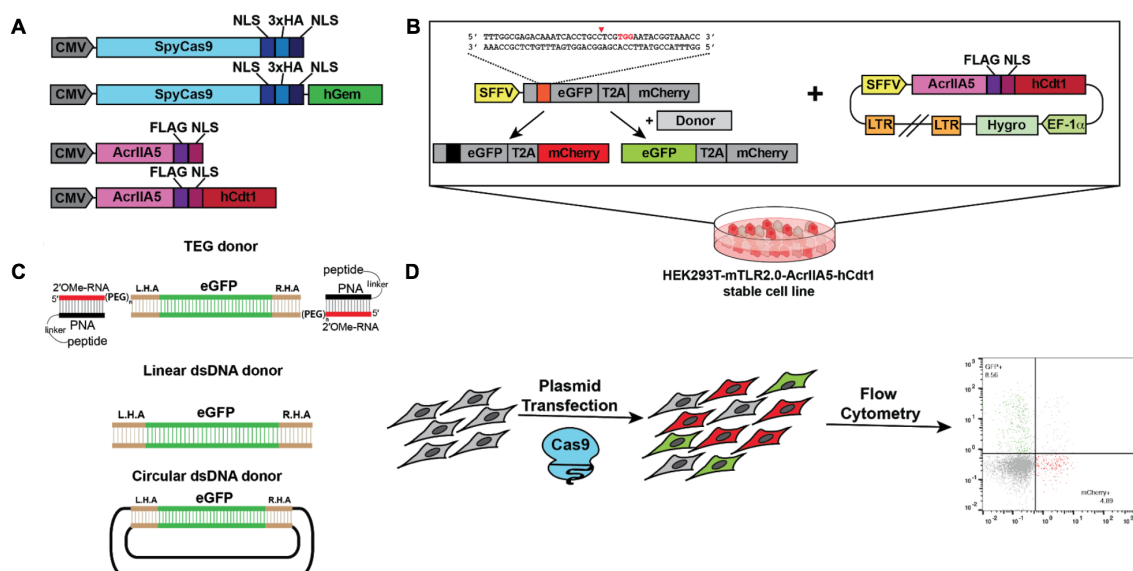
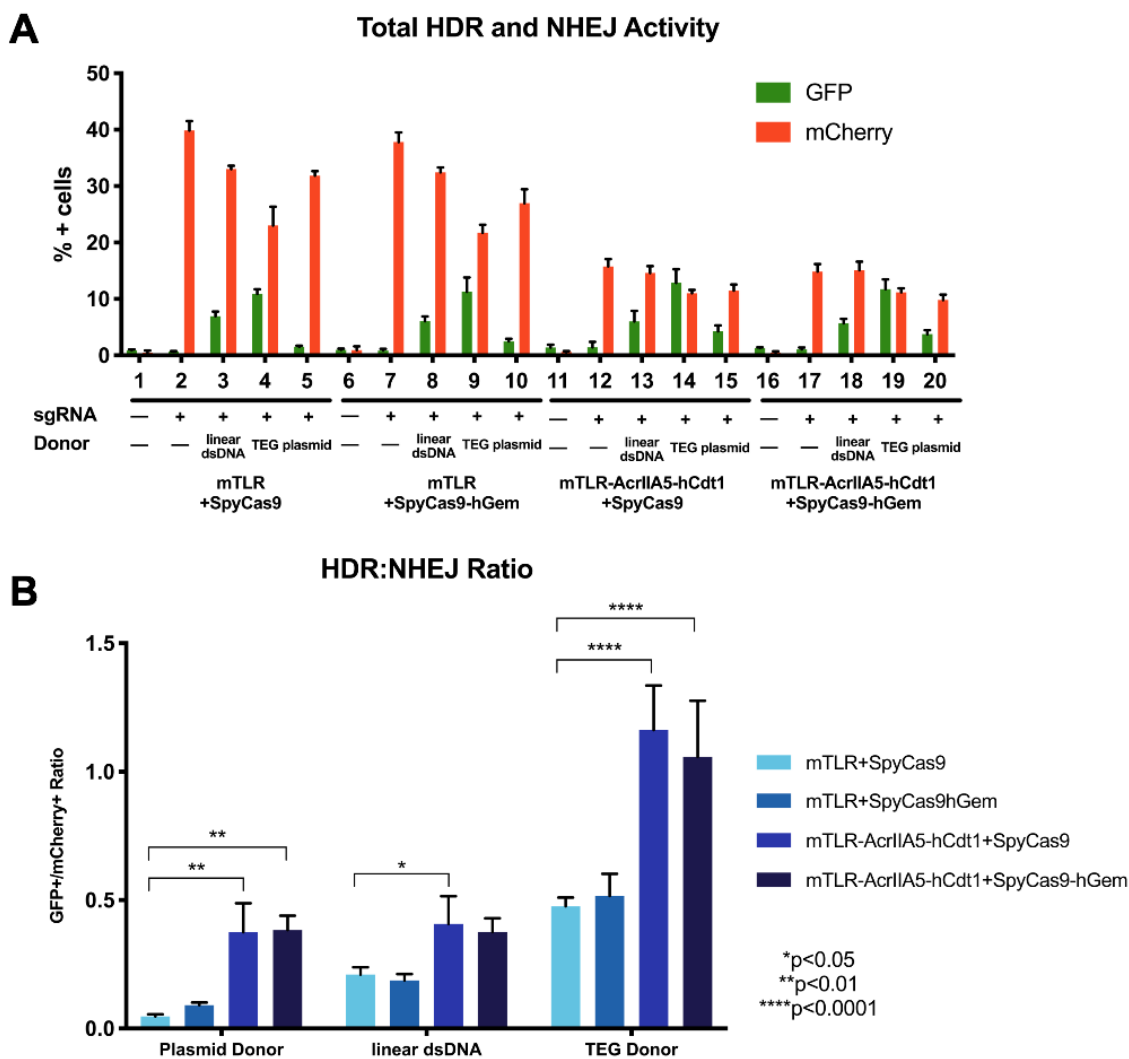


Figure 3.2 Experimental overview of testing Cas9 and anti-CRISPR proteins with cell-cycle-dependent degrons. (A) Schematic of plasmids constructs. NLS, nuclear localization signal; HA, Hemagglutinin tag; FLAG, Flag epitope tag. (B) Generation of a stable cell line by a lentiviral transduction of a variation of a traffic-light reporter (TLR) system from Certo et al. (2011). Resulting HEK293T-mTLR2.0 expresses AcrIIA5-hCdt1 (mTLR-AcrIIA5-hCdt1). (C) Schematic representation of donor types tested in the current study. TEG donor, dsDNA donor with 2'OMe-RNA::TEG moieties covalently attached to 5' ends of each DNA strand and PNA::NLS is annealed to the RNA overhangs. Linear dsDNA donor is produced by PCR amplification of the circular dsDNA plasmid donor. (D) The workflow of transfecting the stable cell lines with plasmids expressing SpyCas9 variants and sgRNA targeting the TLR locus and analyzing cells by flow cytometry.

A combination of AcrIIA5-hCdt1 and TEG donor improve HDR:NHEJ ratio

To evaluate the effect of SpyCas-hGem in our system, the TLR reporter cell line was transiently transfected with either SpyCas9 or SpyCas9-hGem along its sgRNA targeting the TLR locus. A TLR cell line expressing AcrIIA5-hCdt1 (mTLR-AcrIIA5-hCdt1) was also tested with SpyCas9 and SpyCas9-hGem to determine if we can observe the effect of AcrIIA5-hCdt1 alone and additive or synergistic effects from the combination of two degen systems for Cas9 and anti-CRISPR proteins. AcrIIA5 in the stable TLR cell line decreased (~50% reduction) the editing efficiencies (mCherry) compared to that of the TLR cell line without the AcrIIA5 (Figure 3.3A). The overall editing efficiencies may be decreased due to the incomplete degradation of AcrIIA5-hCdt1 in S/G2 phases that still may inhibit Cas9 editing. To better visualize the relative efficiency of HDR occurrences and the inhibition of NHEJ by AcrIIA5-hCdt1, we calculated the ratio of GFP positive cells to mCherry positive cells (HDR:NHEJ) (Figure 3.3B). We observed increased events of HDR compared to NHEJ in the following order: SpyCas9 = SpyCas9-hGem < SpyCas9 + AcrIIA5-hCdt1 = SpyCas9-hGem + AcrIIA5-hCdt1. We anticipated either synergistic or additive effects from combining both SpyCas9-hGem and AcrIIA5-hCdt1, however, we could not detect any improvement from SpyCas9-hGem alone, to begin with. Therefore, we observed a maximum of ~3-fold improvement of HDR:NHEJ ratio primarily due to the AcrIIA5-hCdt1 contribution.

Based on the HDR:NHEJ ratios for each tested condition, TEG donors outperformed other types of donors by ~4-fold (Figure 3.3B). AcrIIA5-hCdt1 improved the ratio significantly regardless of the donor types, confirming its compatibility for various types of applications. The editing with TEG donors alone can increase HDR:NHEJ ratio, but in conjunction with AcrIIA5-hCdt1, further improvement can be achieved.



3.2.2 Application of anti-CRISPR proteins for Cas9 fusion platforms

Cas9-pDBD fusion proteins improve activity and precision of Cas9

A PAM attenuated SpyCas9 fused to a pDBD offers an expanded platform for high specificity and targeting range (Bolukbasi et al., 2015, 2018). Similarly, mutations in some residues in the PID attenuate Nme1Cas9 binding to target DNA (Amrani et al., in preparation). We used a single mutant (R1025A) and the double mutant (K1013A/R1025A) [referred to as single mutant (SM) and double mutant (DM), respectively] that show the most prominent weakening of Nme1Cas9 intrinsic DNA binding affinity with the canonical PAM (Amrani et al., in preparation). Reduced affinity for PAM recognition of Cas9 variants requires an additional DNA binding domain to bind and cleave target DNA, which bolsters the high binding affinity and accuracy of the nuclease. We tethered Nme1Cas9 mutants to ZFPs, which are DNA-binding domains that would theoretically augment the efficiency and precision of target recognition. This platform dramatically improved the precision and efficiency of Nme1Cas9 targeting in mammalian genome editing (Amrani et al., in preparation). We tested whether these large fusion proteins are still amenable to anti-CRISPR inhibition.

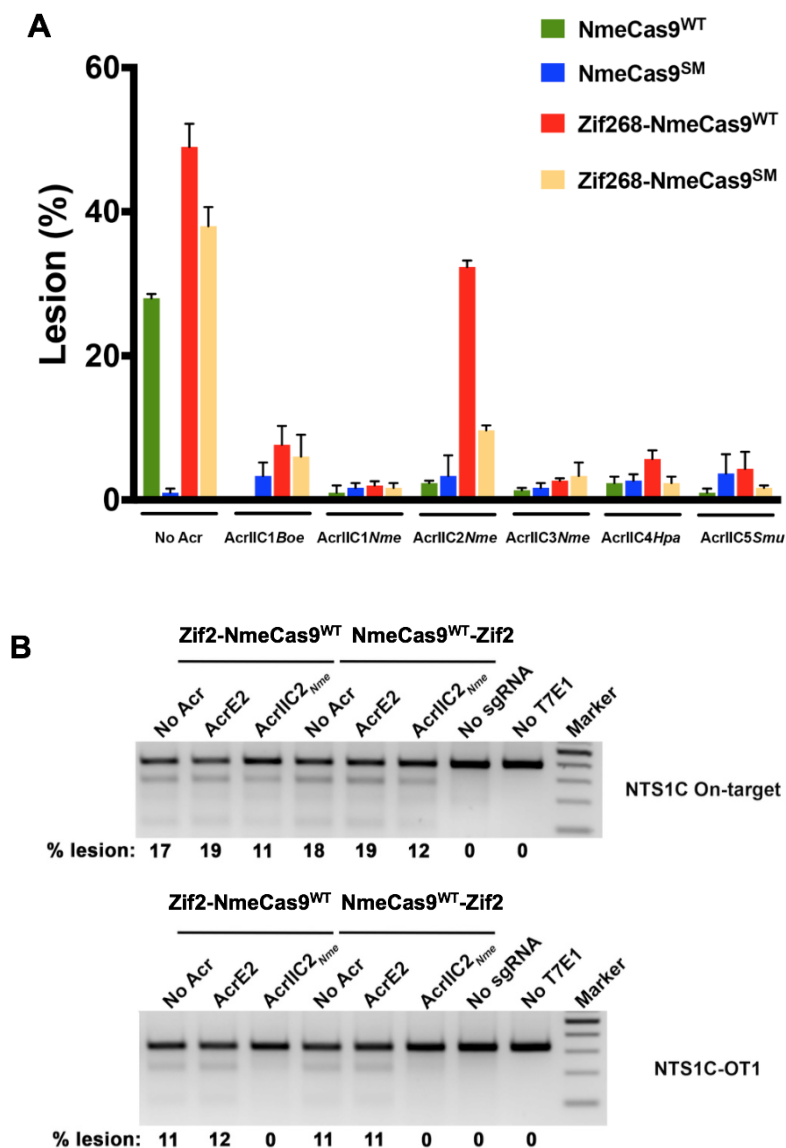


Figure 3.4 Type II-C anti-CRISPRs inhibit Nme1Cas9-pDBD fusion proteins. (A) Lesion frequencies from NTS25 genomic site by Nme1Cas9 and Nme1Cas9SM-Zif268 fusions. TIDE analysis shows that all AcrIIIC families inhibit Nme1Cas9^{WT} editing, however, AcrIIIC2_{Nme} has no inhibitory effect on Zif268-Nme1Cas9^{WT} while potently inhibiting attenuated Zif268-Nme1Cas9SM. Error bars indicate \pm s.e.m. from three independent biological replicates. (B) AcrIIIC2_{Nme} has no inhibition effect on Nme1Cas9^{WT} pDBD fusions at the NTS1C on-target site (top) but can inhibit pDBD-Nme1Cas9^{WT} at the NTS1C-OT1 off-target site (bottom).

Inhibition of Cas9-pDBD proteins by anti-CRISPR proteins

To examine the ability of Type II-C Acr proteins to inhibit Nme1Cas9-pDBD genome editing, we co-transfected HEK293T cells transiently with plasmids expressing the anti-CRISPR protein, Nme1Cas9, and sgRNA targeting the NTS25 genomic site. We then used both T7E1 and TIDE to estimate genome editing efficiencies (Figure 3.4). In agreement with our previous findings, the expression of Acrs dramatically reduced Nme1Cas9-mediated mutagenesis in the presence of Nme1Cas9^{WT} (Figure 3.4A). As expected for Nme1Cas9SM, we did not observe any editing even without any anti-CRISPR proteins since Nme1Cas9SM without the pDBD cannot bind to the target DNA. Upon tethering the ZFP to Nme1Cas9SM (Zif268-Nme1Cas9SM), the activity of Cas9 cleavage is restored and even augmented in the absence of Acrs. The observed increase in editing efficiency is nearly eliminated in the presence of anti-CRISPR proteins (Figure 3.4B). All Type II-C Acrs, except AcrIIIC2_{Nme}, inhibited the cleavage activity of the wild-type as well as the ZFP-Nme1Cas9 fusion protein (Figure 3.4A). Surprisingly, while AcrIIIC2_{Nme} inhibits Nme1Cas9^{WT}, it fails to inhibit Nme1Cas9^{WT} fused to a ZFP. This observation motivated us to test whether AcrIIIC2_{Nme} could prevent off-targeting activities of Nme1Cas9^{WT} fused to a pDBD without inhibiting on-target site editing. We chose NTS1C genomic site and its validated off-target site (NTS1C-OT1) to test how AcrIIIC2_{Nme} affects the editing efficiency at two distinct sites. We used one of programmed five-finger domains (Zif2) to recognize sequences located downstream of GATT PAM of the NTS1C

target site. Indeed, when AcrIIIC2_{Nme} was co-expressed, Nme1Cas9^{WT} fused to either N-terminal or C-terminal ZFP was still able to edit the NTS1C on-target site but not the NTS1C-OT1 off-target site (Figure 3.4B).

Cas9-Cas9 fusion proteins expand the utility of Cas9 genome editing

In the chimera between the PAM-interaction attenuated Cas9 and pDBD, the pDBD provides an additional stage of target site licensing prior to cleavage, thus enhancing the targeting range, efficiency, and specificity (Bolukbasi et al., 2015; Amrani et al., in preparation). However, the generation of functional pDBD fusions is not as easy as Cas9's programmability using guide RNAs. To this end, orthogonal Cas9-Cas9 fusion proteins have also been developed to facilitate the adoption of the RNA-programmable binding platform of Cas9 instead of pDBD (Bolukbasi et al., 2018). In a single- or a dual-nuclease format, Cas9-Cas9 fusions have an expanded targeting range as well as high specificity for genome editing. In particular, a pair of orthogonal wild-type Cas9s have been combined to facilitate precise segmental deletions via simultaneous DNA cleavage events by the fused Cas9 orthologs (including SpyCas9-Nme1Cas9) (Bolukbasi et al., 2018). Since there are anti-CRISPR proteins for a variety of Cas9 orthologs, we anticipate their utility in these platforms as well.

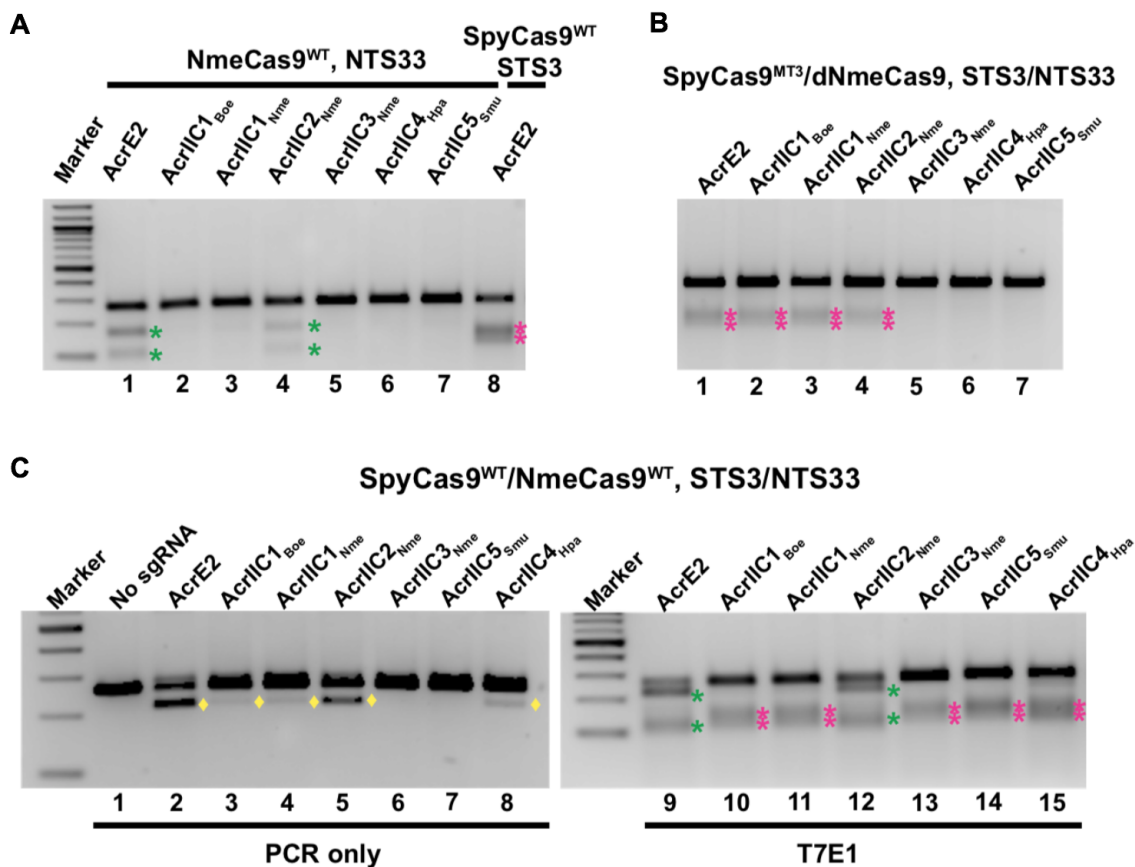


Figure 3.5 Inhibition of Cas9-Cas9 fusion proteins by anti-CRISPR proteins. (A) T7E1 digestion shows editing patterns of wild-type (WT) Nme1Cas9 (lane 1,4; green asterisks) and SpyCas9 (lane 8; magenta asterisks) at their NTS33 and STS3 genomic target sites, respectively. (B) With a PAM-attenuated version of SpyCas9 (SpyCas9^{MT3}) fused to dNme1Cas9, genome editing by the nuclease activity of SpyCas9 was prevented by AcrII-C3_{Nme}, AcrII-C4_{Hpa}, or AcrII-C5_{Smu}. (C) Type II-C anti-CRISPR proteins specifically block Nme1Cas9^{WT} editing in a fusion of wild-type Cas9 proteins (SpyCas9^{WT}/Nme1Cas9^{WT}). Left: A deletion of genomic DNA resulting from active SpyCas9^{WT}/Nme1Cas9^{WT} is detected by PCR (yellow diamonds). Right: The same PCR amplicon analyzed by T7E1 digestion shows distinguishable editing patterns of each Cas9. Nme1Cas9 editing (green asterisks) is only seen with AcrE2 or AcrII-C2_{Nme} (the least potent inhibitor in mammalian cells), while SpyCas9 editing is observed in the presence of all the Type II-C Acrs.

Inhibition of orthogonal Cas9-Cas9 fusion proteins by anti-CRISPR proteins

When the wild-type Nme1Cas9 and SpyCas9 were expressed separately as a monomeric form, each Cas9 ortholog efficiently cleaved at the respective target site within the vicinity of each other as indicated by the unique band cleavage patterns for each nuclease (Figure 3.5A). Nme1Cas9^{WT} is inhibited by all AcrIIC families (AcrIIC1-5), though less efficiently by AcrIIC2. When SpyCas9^{MT3} fused to dNme1Cas9 (in place of pDBD) was expressed along with its cognate sgRNA, only AcrIIC3_{Nme}, AcrIIC4_{Hpa}, and AcrIIC5_{Smu} inhibited genome editing since AcrIIC3-5 interfere with DNA binding activity of Nme1Cas9 (Figure 3.5B). The suppression of genome editing by SpyCas9^{MT3}-dNme1Cas9 indicates that these Type II-C anti-CRISPRs can serve as SpyCas9 editing off-switches in this context. As expected, AcrIIC1 orthologs do not inhibit editing by SpyCas9^{MT3}-dNme1Cas9 since AcrIIC1 does not affect the dNme1Cas9 binding. (Figure 3.5B). Furthermore, we tested anti-CRISPR proteins against dual-nuclease fusion proteins (SpyCas9^{WT}/Nme1Cas9^{WT}) that can create a segmental deletion (Figure 3.5C). With non-cognate AcrE2 or a weak inhibitor such as AcrIIC2, a band corresponding to the size of the deletion can be detected by PCR (Figure 3.5C). On the other hand, type II-C anti-CRISPRs that inhibit editing activity of Nme1Cas9 in the fusion context led to the appearance of small indels at the SpyCas9 site rather than a segmental deletion as shown by the T7E1 assay (Figure 3.5C). These data from mammalian cells confirm the potential utility of

Type II anti-CRISPRs proteins for modulating Cas9-dependent genome engineering.

3.3 Discussion

Unintentional DSBs can induce genomic instability by disrupting gene structure and function or by inducing chromosomal rearrangements (Kosicki et al., 2018), therefore numerous cellular machinery is in place for immediate repair (Ciccia & Elledge, 2010). In principle, all DSB repair pathways may compete for access to free DNA ends. However, the two major DSB repair pathways, canonical NHEJ and HDR, are dominant in the repair of a conventional DSB. In addition to two major DSB repair pathways, there are other competing error-prone pathways such as single-stranded annealing (SSA), alternative end-joining (a-EJ), or microhomology-mediated end-joining (MMEJ) (Scully et al., 2019). The choice of repair pathway is dependent on various cellular factors including the cell-cycle stages and the local chromatin environment (Chapman et al., 2012).

In the first half of this chapter, our goal was to take advantage of the cell-cycle-dependence of the HDR pathway for controlling Cas9 activity to improve precise genome editing. We adopted the degron-mediated FUCCI system (Sakaue-Sawano et al., 2008) to sync the expression of Cas9 and anti-CRISPR proteins to cell cycles. Using a TEG-modified donor and AcrIIA5-hCdt1 with SpyCas9, HDR increased up to 2.4-fold. A TEG donor showed the highest ratio of HDR:NHEJ compared to plasmid or linear dsDNA donors. Previously, SpyCas9-hGem has been shown to improve HDR by ~1.8-fold in mammalian cells (Gutschner et al., 2016), however, we did not observe any improvement using

SpyCas9-hGem alone. We believe this may be a result of overexpression of SpyCas9-hGem due to the nature of transient transfection, while AcrIIA5-hCdt1 is expressed at lower levels from endogenous loci in a stable cell line.

The current study is limited to testing in an artificial reporter cell line, therefore making it difficult to generalize the overall performance of our system. Future studies will require testing in different model systems (e.g. cell lines, organisms) as well as at endogenous loci for different target sites to thoroughly investigate the efficacy of using the cell-cycle-dependent degron system. Variations in different sites and cell lines will reflect how differences in genomic architecture and cellular DNA repair availability affect HDR.

Although we observed improvement of the HDR:NHEJ ratio using AcrIIA5-hCdt1, we also lost overall editing activity. One way to mitigate the issue of improving HDR efficiency at the cost of reduced overall editing efficiency is to use a weaker promoter to drive Acr expression or a less potent Acr in mammalian cells. This fine-tuning process will optimize Acr activity to inhibit Cas9 in the G1 phase, but allow maximal editing in other cell cycle stages for efficient HDR.

Although the HDR:NHEJ ratio increased when AcrIIA5-Cdt1 was used, the slight increments did not achieve significant improvement with this strategy. Current methods were proposed to minimize the external perturbation to the systems, as a balance of DSB repair pathways is necessary for maintaining genomic stability in normal cellular states (Ciccia & Elledge, 2010). Harnessing the cellular repair

machinery and pathway choice to our advantage may require complementary methods such as NHEJ inhibitors or HDR promoting small molecules (Chu et al., 2015; G. Li et al., 2017; Maruyama et al., 2015; Yeh et al., 2019). Overall, we have demonstrated that anti-CRISPRs can be fused to a cell-cycle-dependent degron to increase HDR events relative to NHEJ in human cells.

In the second half of this chapter, we show evidence that engineered variants of Cas9 nucleases are amenable to anti-CRISPR off-switches, demonstrating their utility across multiple applications and editors. Catalytically inactive Cas9 enabled the expansion of numerous applications for tethering any types of effector proteins of interest (Adli, 2018). In addition to the platforms that rely on dCas9 fused to heterologous proteins such as fluorescent proteins, transcriptional regulators, and epigenetic modifiers, there are other Cas9 fusion platforms. One such example is a chimeric protein between PAM-attenuated SpyCas9 and a pDBD that has been shown to increase targetability and accuracy (Bolukbasi et al., 2015).

We show that the fusion of a pDBD likewise augments the binding and nuclease activity of Nme1Cas9 (Amrani et al., in preparation). Although Nme1Cas9 is naturally hyper-accurate, Nme1Cas9 generally exhibits lower nuclease activity than SpyCas9, possibly due to inefficient unwinding of the target DNA (E. Ma et al., 2015). Tethering a pDBD confers Nme1Cas9 high-affinity binding to suboptimal genomic sites to provide sufficient residence time to facilitate the

efficient R-loop formation. Thus, Nme1Cas9^{WT}-pDBD chimera can serve as both an efficient and precise editor.

From our studies, all known Type II-C Acrs dramatically reduced Zinf268-Nme1Cas9^{WT} mediated mutagenesis except AcrIIC2_{Nme}. A plausible explanation for this observation may be attributed to how AcrIIC2_{Nme} inhibits Nme1Cas9. AcrIIC2_{Nme} interacts with the bridge helix motif of Nme1Cas9, thereby interfering with sgRNA loading onto the Cas9 and binding to the target DNA. For this reason, as well as a low level of protein accumulation, AcrIIC2_{Nme} has been previously documented as the weakest inhibitor among the Type II-C Acrs (Pawluk, Amrani, et al., 2016). It is plausible that the Nme1Cas9 brought to the target site via a ZFP increases the local concentration of the Nme1Cas9 that could lead to cleavage when engaged with its sgRNA. AcrIIC2_{Nme} inhibits Nme1Cas9^{WT} but fails to completely inhibit Zinf268-Nme1Cas9^{WT}, suggesting that the binding conferred by the ZFP may help Cas9 overcome the AcrIIC2_{Nme} inhibitory barrier and increase the probability of engaging with the target site for cleavage.

A combination of Nme1Cas9^{WT}-pDBD and AcrIIC2_{Nme} could be useful for reducing off-target editing without inhibiting cleavage of the on-target site. Since off-target sites lack ZFP binding sites, Nme1Cas9^{WT}-pDBD fusion protein most probably does not lead to off-target editing, however, using anti-CRISPR proteins in this context will also reduce the efficiency of on-target editing. Unlike other

potent Acrs, AcrIIIC2_{Nme} still permits editing by Nme1Cas9^{WT}-pDBD since Cas9 can recognize the PAM, bind to a target DNA, and uses the sgRNA complementarity for cleavage of the on-target site. This observation is somewhat analogous to reducing off-target editing using an artificially weakened anti-CRISPR protein fused to SpyCas9 (Aschenbrenner et al., 2020). Using a relatively weaker anti-CRISPR protein allows editing at the on-target site, but not at the off-target site, due to differential Cas9 binding affinity and cleavage kinetics. Such strategies can be useful alternatives since they bypass the difficulty faced in other approaches such as timed delivery of anti-CRISPR proteins to reduce off-targeting (Shin et al., 2017).

Furthermore, the specificity of an anti-CRISPR protein to inhibit its cognate Cas9 in the orthogonal Cas9-Cas9 fusion context enables precise control of the Cas9 of interest to achieve the desired editing outcome. For instance, the co-expression of Acrs for both Cas9 orthologs will inhibit deletion altogether, while the expression of only one Acr for each Cas9 will result in indels.

In summary, we demonstrate that the inhibition of Nme1Cas9 by anti-CRISPR proteins can be extended to Nme1Cas9-pDBD, specifically, Nme1Cas9 fused to a ZFP or to another orthogonal Cas9. Validating that these anti-CRISPR proteins can be used as potent off-switches for larger fusion Cas9 proteins opens the door to regulating broad applications in the genome engineering field.

3.4 Materials and Methods

Plasmid vector construction

Appendix Table 2 contains plasmids used in this chapter.

Plasmid vectors for Cas9 and anti-CRISPR with cell-cycle-dependent degra-

A pCSDest2-SpyCas9-hGem construct is a gift from Dr. Scot A. Wolfe. AcrIIA5 sequence was codon-optimized for mammalian expression and ordered as a gene block (IDT). To make AcrIIA5-hCdt1 expression plasmid, the hCdt1 sequence was amplified from an ES-FUCCI plasmid, a gift from Pierre Neveu (Addgene #62451) and inserted into the pEJS1004-pCSDest2-AcrIIA5-FLAG-NLS vector by Gibson assembly (NEB). For a lentiviral transduction plasmid, pLenti-vector with a hygromycin selection marker was used to make a version that has hCdt1 using Gibson assembly (NEB), resulting in pEJS1033-pLenti-AcrIIA5-Cdt1-HygR.

HDR donor constructs

An eGFP plasmid donor is pEJS716-GFP from the Sontheimer lab. The linear dsDNA donor was generated by PCR amplification using the plasmid donor. The TEG donor was similarly made but using custom primers that have 5' end modifications for each primer (IDT). After amplification, PCR fragments were directly used after column purification.

Plasmid vectors for Nme1Cas9-pDBD experiments

An all-in-one plasmid was used for the expression of Nme1Cas9 variants and sgRNAs for NTS25 or NTS1C target sites (Amrani et al., 2018). Anti-CRISPR expressing vectors are the same as plasmids previously described in Chapter 2.

Cell culture

Lentiviral transduction

A version of a traffic light reporter in HEK293T cells (mTLR-MCV2.0) was previously generated in the Sontheimer lab. The lentiviral transduction was performed as follows. Viruses were produced and collected by transfecting HEK293T (ATCC) with the lentiviral vector plasmid pEJS1033-pLenti-AcrIIA5-Cdt1-HygR that expresses AcrIIA5-hCdt1 and packaging helper plasmids (VSV-G and Δ R8.2). HEK293T-mTLR-MCV2.0 target cells were transduced with the viruses and then selected with hygromycin, resulting in the mTLR-AcrIIA5-hCdt1 cell line.

Transient transfection

For mTLR reporter experiments, stable cell lines were transiently transfected with SpyCas9 or SpyCas9-hGem, sgRNA targeting the TLR locus (pEJS760-Spy.sgRNA.STS118), and donor templates (plasmids or PCR fragments) using PolyFect (Qiagen). For genome editing experiments, plasmids for Cas9s,

respective sgRNAs, and anti-CRISPRs were transiently transfected in HEK293T cells using PolyFect (Qiagen). The total amount of DNA was equal in all transfections.

Flow Cytometry

48 hr post-transfection cells were analyzed on a MACSQuant® VYB from Miltenyi Biotec. FlowJo® v10.4.1. was used for gating single cells based on FSC-A and FSC-H. The percentage of cells expressing mCherry and GFP was used to estimate the Cas9-mediated editing efficiency of NHEJ and HDR, respectively.

Genome editing assay

72 hr post-transfection, cells were harvested and gDNA was extracted with the DNeasy Blood and Tissue kit (Qiagen) and then was used for PCR amplification [High Fidelity 2X PCR Master Mix (NEB)] with primers flanking the targeted site. PCR products were heat-denatured, re-annealed, and digested with T7 Endonuclease I (NEB). For the detection of a deletion outcome, T7E1 was omitted. The samples were visualized in a 2.5% agarose/1xTAE gel and quantified with the ImageMaster-Totallab program. Indel percentages were calculated as previously described (Guschin et al., 2010). Alternatively, indel frequencies were estimated by Sanger sequencing followed by analysis using TIDE (Brinkman et al., 2014) or ICE (Synthego).

Chapter 4 Tissue-restricted genome editing *in vivo* by miRNA-repressible anti-CRISPRs

4.1 Introduction

Despite Cas9's potential in gene therapy, many hurdles must be overcome before it can be used in clinical applications: delivery of Cas9, off-target editing, non-target tissue editing, and persistent activity after the intended editing (Carroll, 2014). Therapeutic uses of Cas9 often require editing only in certain cell types or tissues, which have been aided by use of tissue-specific promoters and AAVs that have some selectivity in tissue tropism. However, these promoters can be weak or leaky and AAV serotypes still have imperfect tissue specificity (Kanegae et al., 2011; Zincarelli et al., 2008). Tissue-specific Cas9 editing is necessary to protect against undesired chromosomal breaks in non-target tissues. For example, Cas9-induced DSB can elicit translocations, which are often associated with heritable disorders or various kinds of cancer (J. Jiang et al., 2016; Maddalo et al., 2014). Although tissue-specific promoters can be used, some target tissues lack promoters that are highly specific and strong enough to drive a transgene expression (Kanegae et al., 2011). Moreover, tissue tropic AAV serotypes widely used for delivery of therapeutic transgenes can still infect a broad range of tissues *in vivo* (Gao et al., 2004), necessitating additional methods of regulation to enforce tissue specificity. Acrs will provide another

safeguard against the undesired editing in non-target tissues by inhibiting Cas9 activity in all ancillary tissues.

4.1.1 Background on AAV

An rAAV is widely used for therapeutic gene delivery due to its minimal immunogenicity, rare integration events in the host genome, and long-term expression of transgenes (D. Wang et al., 2019). Notably, there is already an rAAV gene therapy drug (Luxturna) approved by the US Food and Drug Administration (FDA) (Russell et al., 2017) and many other rAAV platforms are currently in clinical trials (Mendell et al., 2017). AAVs can package a single-stranded DNA genome of ~ 4.7kb and specify a tissue-tropism by capsid proteins. The single-stranded rAAV (ssAAV) genome is released in the nucleus and then converted into a double-stranded form by second-strand synthesis or strand annealing (Nakai et al., 2000; Zhong et al., 2008; Zhou et al., 2008). This step is required for transcription and is a rate-limiting step. Alternatively, a self-complementary rAAV genome (scAAV), which has a mutated ITR, enables faster and higher gene expression than ssAAV albeit of a half the size of the packaging capacity (~2.3kb) (McCarty et al., 2003; Z. Wang et al., 2003). After intra- and inter-molecular circularization and concatemerization of dsDNA, the AAV genome persists as episomal DNA (D. Duan et al., 1998, 1999).

4.1.2 Enhancing tissue-specificity of transgene expression

Many natural tropisms of AAVs are useful for gene therapy programs that focus mainly on the liver, muscles, and the Central Nervous System (CNS) (D. Wang et al., 2019). Almost all natural AAV capsids can transduce the liver efficiently and some other serotypes such as AAV8 and AAV9 can have broader tropisms, targeting multiple muscle types throughout the body (D. Wang et al., 2014).

Gene expression in off-target tissues or cell types may lead to toxicity or trigger an unwanted immune response. Conventional strategies to confine the gene expression to targets of interest include using tissue- or cell type-specific promoters (Gray et al., 2011). Tissue-specific promoters drive the expression of transcripts under the control of native or composite promoters. A native or minimal promoter is composed of a core promoter and its natural 5' untranslated region (UTR) (sometimes containing an intron), whereas a composite promoter is engineered by combining different promoter elements (e.g. enhancers). More compact promoters that usually do not exhibit high specificity are often used for gene editing due to the large size of Cas proteins and sometimes guide RNAs as well as the donor.

4.1.3 A strategy for miRNA-mediated transgene de-targeting

Another method of restricting transgene expression is using a class of small non-coding RNAs known as microRNAs (miRNAs), which were first discovered in *Caenorhabditis elegans* (R. C. Lee et al., 1993; Wightman et al., 1993). The miRNAs regulate gene expression posttranscriptionally by directing Argonaute (AGO) proteins to bind to and repress complementary mRNA targets (Bartel, 2018; Jonas & Izaurralde, 2015). The mammalian genome encodes four AGO proteins (Ago1-4) and Ago2 is the only AGO protein able to cleave the target that is fully complementary to the guide strand of the miRNA (J. Liu et al., 2004). Some miRNAs are often produced only in specific cell or tissue types (Lagos-Quintana et al., 2002). Among many other potential miRNA therapeutics, a “de-targeting” strategy using such tissue-specific miRNAs has opened a new avenue in gene therapy to ensure the expression of the therapeutic transgene in the correct tissue types while minimizing its expression elsewhere (Broderick & Zamore, 2011). The de-targeting strategies incorporate miRNA binding sites in the 3'-UTR of a transgene to prevent its expression in cells that are enriched for the miRNA while the transgene will be expressed in the intended cell type in which the miRNA is not expressed (Brown et al., 2006; Geisler et al., 2011; Qiao et al., 2011; Xie et al., 2011).

4.2 Results

4.2.1 A strategy for microRNA-regulated anti-CRISPR proteins

Delivery of Cas9 and sgRNA via AAV has the potential to induce editing in multiple transduced tissues (e.g., heart, skeletal muscle, and elsewhere); however, co-delivery of the miRNA-repressible Acr will inhibit editing in such non-target tissues due to the latter's lack of particular tissue-specific miRNAs. Key advantages of regulating the anti-CRISPR expression in the target tissue post-transcriptionally using tissue-specific, endogenous miRNAs include: 1) strong repression will be achieved via mRNA cleavage by using perfectly complementary miRNA response elements (MREs), which have been used to efficiently repress the expression of transgenes *in vivo* (Geisler et al., 2011; Qiao et al., 2011; Xie et al., 2011); 2) there is a well-established repository for tissue-specific miRNAs (Landgraf et al., 2007; Ludwig et al., 2016; Rahman et al., 2020); 3) the system provides the flexibility to switch or multiplex tissue specificities by simply changing or combining different MREs; 4) the short length of MRE sequences (~22nt) do not burden the packaging capacity of an AAV vector. As an example of endogenous miRNA-mediated, post-transcriptional repression of anti-CRISPR protein for liver-specific editing, we took advantage of microRNA-122 (miR-122), a well-validated miRNA that is highly expressed only in hepatic cells. In the target liver tissue, the *acr* gene with miR-122 MREs (used interchangeably with miRNA binding sites) will be repressed, enabling Cas9-

mediated editing while extrahepatic tissues that lack miR-122 will fail to silence the Acr expression (Figure 4.1A). To validate this concept, we chose two well-established Cas9-Acr combinations: AcrIIC3_{Nme} and Nme1Cas9/Nme2Cas9 (Type II-C) as well as AcrIIA4_{Lmo} and SpyCas9 (Type II-A). For our *in vitro* validations, Acr expression vectors were identical in every aspect except for the presence or absence of MREs in the 3' UTR. We placed three tandem miR-122 binding sites (3xmiR122BS) in the 3' UTR of each *Acr* gene, which also included a carboxy-terminal mCherry fusion to enable expression to be detected by fluorescence microscopy or flow cytometry (Figure 4.1B).

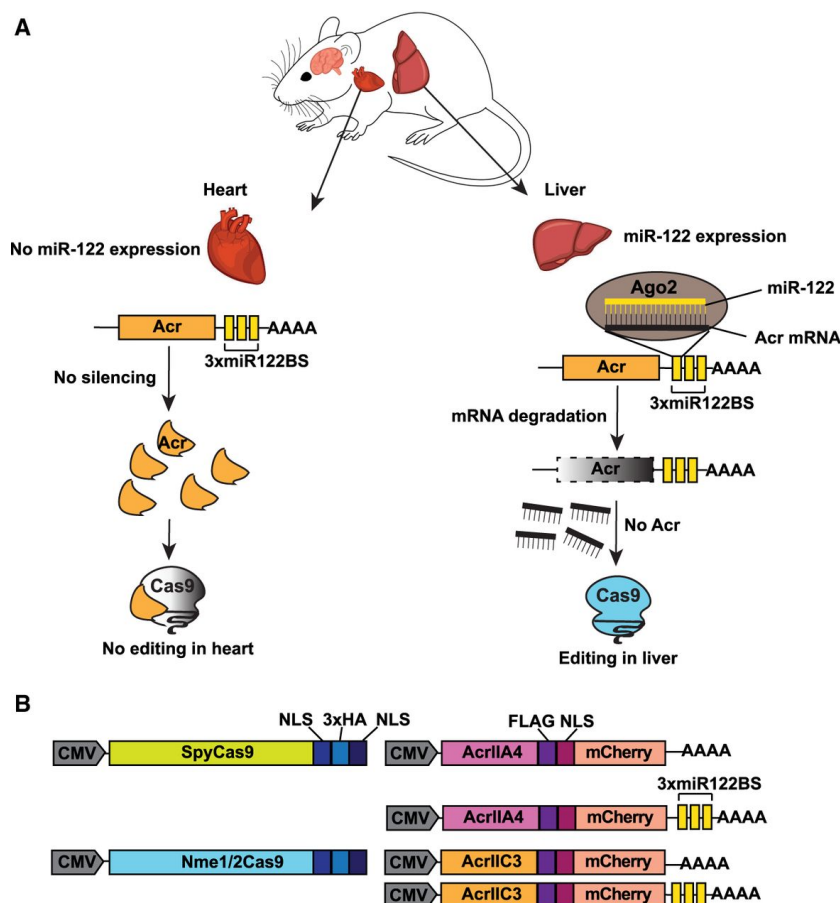


Figure 4.1 Overview of the Cas9 and microRNA-repressible anti-CRISPR system. (A) An example of achieving liver-specific editing using the anti-CRISPR repressible by miR-122. Upon systemic delivery of Cas9 *in vivo* (e.g., via viral vectors), tissues receiving Cas9 and sgRNA potentially result in genome editing; however, co-delivery of miRNA-repressible anti-CRISPR proteins will prevent such editing in non-target tissues that lack miR-122, as depicted in the heart (left). In the liver, anti-CRISPR transcripts with perfectly complementary miR-122 binding sites will undergo Ago2-mediated mRNA degradation, and the resulting silencing of the Acr will permit Cas9 editing in the liver (right). **(B)** A schematic of expression vectors for Cas9 orthologs from Type II-A (SpyCas9) and II-C (Nme1Cas9 and Nme2Cas9) systems, along with their respective anti-CRISPR proteins, AcrIIA4 and AcrIIC3. The Acr expression constructs were generated with or without three tandem, perfectly complementary miRNA-122 binding sites in the 3' UTR. CMV, cytomegalovirus promoter; NLS, nuclear localization signal; AAAA, poly(A) tail.

4.2.2 *In vitro* validation of microRNA-repressible anti-CRISPR vectors

We used a human hepatocellular carcinoma cell line (Huh-7) that expresses miR-122 in high levels in contrast to non-hepatic cell lines such as human embryonic kidney (HEK293T) cells (Fukuhara et al., 2012). We transfected cells with plasmids expressing AcrIIC3-Flag-mCherry-3xmiR122BS, AcrIIA4-Flag-mCherry-3xmiR122BS, or their respective control vectors lacking the miR-122 binding sites (Figure 4.1B). A separate GFP expression plasmid was also included to indicate transfection efficiency in each cell line. When these vectors were transiently transfected, the expression of mCherry-fused Acr with miR-122 MREs was dramatically suppressed in Huh7 cells whereas Acr-mCherry lacking the 3xmiR122BS cassette was still well expressed (Figure 4.2A). In HEK293T cells, there was no discernible difference in mCherry signal from the Acr and Acr-3xmiR122BS constructs based on both fluorescence microscopy and flow cytometry (Figure 4.2B). The Acr expression was also confirmed by anti-Flag western blot analysis. Compared to HEK293T cells, transfection efficiency was lower in Huh-7 cells as indicated by a decrease in the overall GFP and mCherry signals (Figure 4.2). Nevertheless, fluorescence microscopy, flow cytometry, and western blot analysis consistently revealed effective reductions of both AcrIIC3-3xmiR122BS and AcrIIA4-3xmiR122BS expression in Huh-7, but not in HEK293T cells. The expression of Acrs lacking miR-122 MREs was unaffected in both cell lines, consistent with effective regulation of Acr by miR-122 only in hepatic cells.

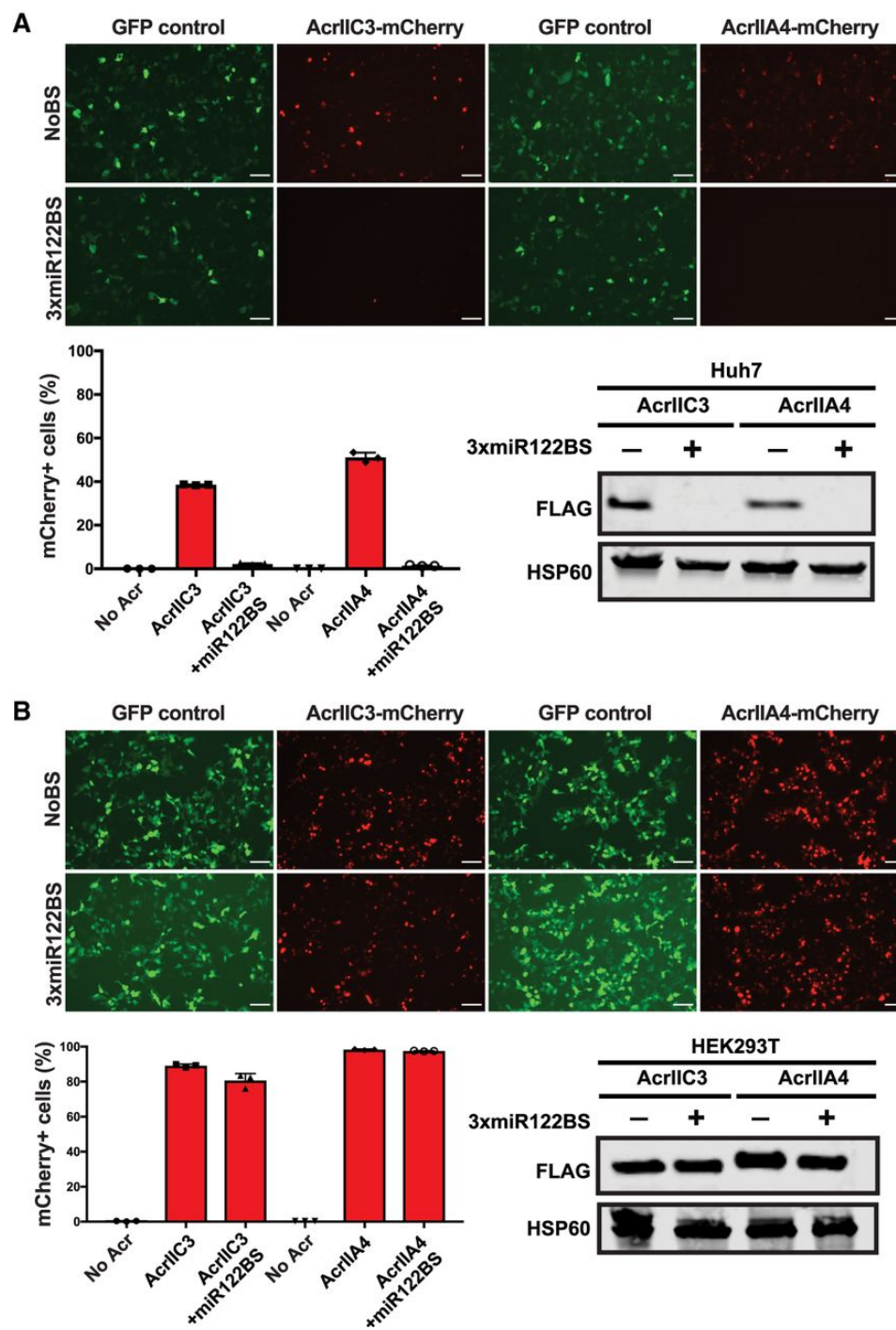


Figure 4.2 Validation of miRNA regulation of anti-CRISPR expression in cultured cells.

(A,B) Hepatocyte-specific silencing of anti-CRISPR expression. Plasmid vectors encoding either AcrIIIC3-mCherry or AcrIIIA4-mCherry, with or without miR-122 MREs, were transfected into **(A)** Huh7 cells or **(B)** non-hepatic HEK293T cells; only the former express miR-122. The expression of mCherry and GFP was visualized by fluorescence microscopy (top) and analyzed by flow cytometry (bottom left). The percentage of mCherry-positive cells in each transfection was normalized to the transfection of the control GFP-expressing plasmid. Anti-CRISPR protein expression was also confirmed by western blot against the 1xFlag epitope (bottom right). Heat shock protein 60 (HSP60) was used as a loading control. Scale bar, 100 μ m.

4.2.3 Acr repression by miR-122 precludes inhibition in hepatocytes

Having demonstrated that anti-CRISPR repression in hepatocyte-derived cells can be conferred by miR-122 MREs, we then tested whether this repression is sufficient to allow genome editing by Cas9 orthologs (Nme1Cas9, Nme2Cas9, and SpyCas9). We transiently transfected separate expression plasmids for each Cas9, its respective sgRNA, and the cognate Acr, with the latter construct either including or omitting miR-122 binding sites. We chose validated, endogenous sites in the human genome for each Cas9 ortholog (Figure 4.3). In HEK293T cells, AcrIIIC3 and AcrIIA4 robustly inhibited genome editing by Nme1/2Cas9 and SpyCas9, respectively (Figure 4.3). The presence or absence of miR-122 MREs had no significant effect on editing inhibition in HEK293T cells lacking miR-122 expression. Despite the overall lower transfection efficiencies and variable editing efficiency among Cas9 orthologs at the tested target sites, AcrIIIC3 and AcrIIA4 also prevented editing in Huh7 cells when expressed from constructs that lack miR-122 MREs. In contrast, Acr plasmids bearing miR-122 MREs in the 3'UTRs failed to inhibit Cas9 editing in Huh-7 cells, as indicated by editing efficiencies that were similar to the no-Acr control (Figure 4.3). This observation was true for all three Cas9 orthologs tested.

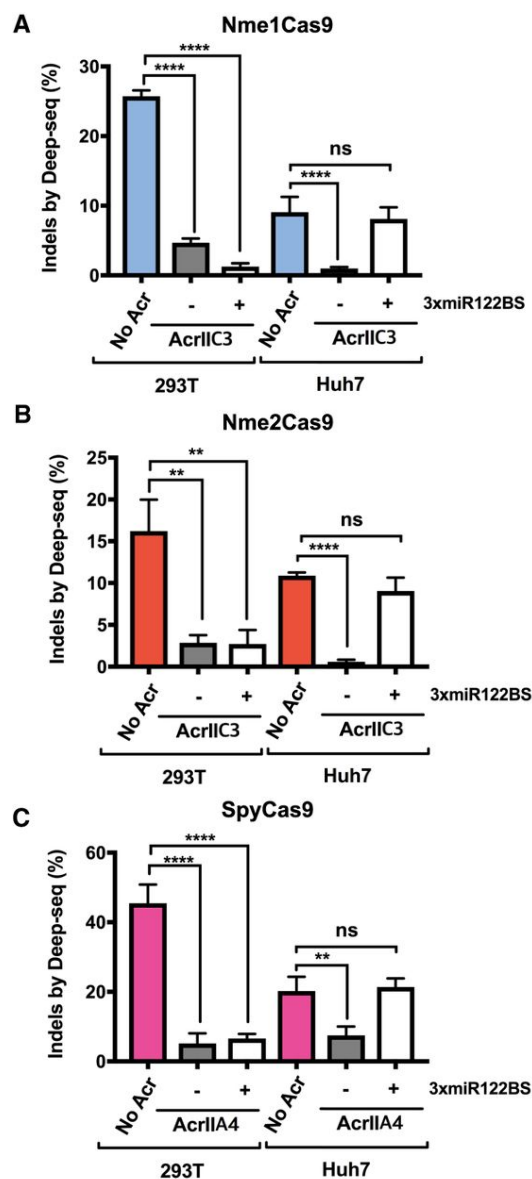


Figure 4.3 Hepatocyte-specific genome editing by Cas9 orthologs.

(A-C) HEK293T and Huh7 cells were transiently transfected with plasmids encoding cognate sgRNAs for **(A)** Nme1Cas9, **(B)** Nme2Cas9, and **(C)** SpyCas9. **(A, B)** AcrIIC3 constructs with or without 3xmiR122BS were co-transfected. **(C)** AcrIIA4 with or without 3xmiR122BS were co-transfected with SpyCas9. Data represent mean \pm SD with at least three replicates. Editing efficiencies are measured by targeted deep sequencing.

4.2.4 MiR-122-dependent genome editing conferred by Acrs *in vivo*

For our *in vivo* tests, we focused on Nme2Cas9 due to its compact size, high target site density, and relative lack of off-target editing (Edraki et al., 2018), all of which are advantageous for therapeutic development. We used a previously validated all-in-one AAV vector that expresses Nme2Cas9 from the minimal U1a promoter, as well as a U6 promoter-driven sgRNA targeting *Rosa26* (Figure 4.4A) (Edraki et al., 2018; Ibraheim et al., 2018). We also generated AcrIIc3 expression plasmids driven by the strong CB-PI promoter that is composed of a chicken-beta actin promoter and an intron from SV40 to enhance its ubiquitous and robust expression. In addition, these AcrIIc3 constructs either included or omitted the three tandem miR-122 MREs in the 3'-UTR (Figure 4.4A). For *in vivo* delivery, we first used hydrodynamic tail vein injection, which is a nonviral method of transient hepatocyte transfection that allows expression from naked DNA plasmids (G. Zhang et al., 1999). This injection method delivers DNA to ~10%-20% of hepatocytes for transient expression and leads to minimal transgene expression in organs other than the liver. Since miR-122 is abundant in the liver, and because Cas9 delivered to the liver by hydrodynamic injection can induce editing (Xue et al., 2014), this experimental approach enables tests of liver-specific editing and inhibition of editing in the presence or absence of Acr expression. Plasmids were injected into adult, wild-type C57BL/6 mice via tail vein and liver tissues were collected at 7 days post-injection (Figure 4.4B). To determine the effective dose of Acr plasmid needed to inhibit Nme2Cas9 editing

in vivo, we coinjected varying Cas9:Acr plasmid ratios (1:1, 1:1.5, and 1:2). AcrIIIC3 efficiently inhibited Nme2Cas9 editing at all ratios tested (Figure 4.4C). Once we defined the necessary plasmid dose, we subjected three groups of mice to hydrodynamic injection with plasmid combinations that included Nme2Cas9 with (i) no Acr, (ii) AcrIIIC3, and (iii) AcrIIIC3-3xmiR122BS (Figure 4.4A). In the livers of mice receiving no Acr, Nme2Cas9 yielded a mean editing efficiency of $5.2 \pm 1.7\%$ ($n = 6$ mice), similar to levels seen previously with this and other Cas9 orthologs upon hydrodynamic injection (Ibraheim et al., 2018; Xue et al., 2014). As expected, the coinjection of AcrIIIC3 plasmid strongly reduced the editing efficiency to $0.33 \pm 0.09\%$ ($P < 0.0001$). In contrast, AcrIIIC3-3xmiR122BS failed to inhibit Nme2Cas9 editing, with the indel efficiency comparable to no Acr group ($7.1 \pm 3.5\%$, Fig. 4D). In accordance with our results in human Huh-7 cells, endogenous miR-122 in mouse hepatocytes *in vivo* can be exploited to repress Acr expression, and therefore allow tissue-specific Cas9 genome editing, in the liver.

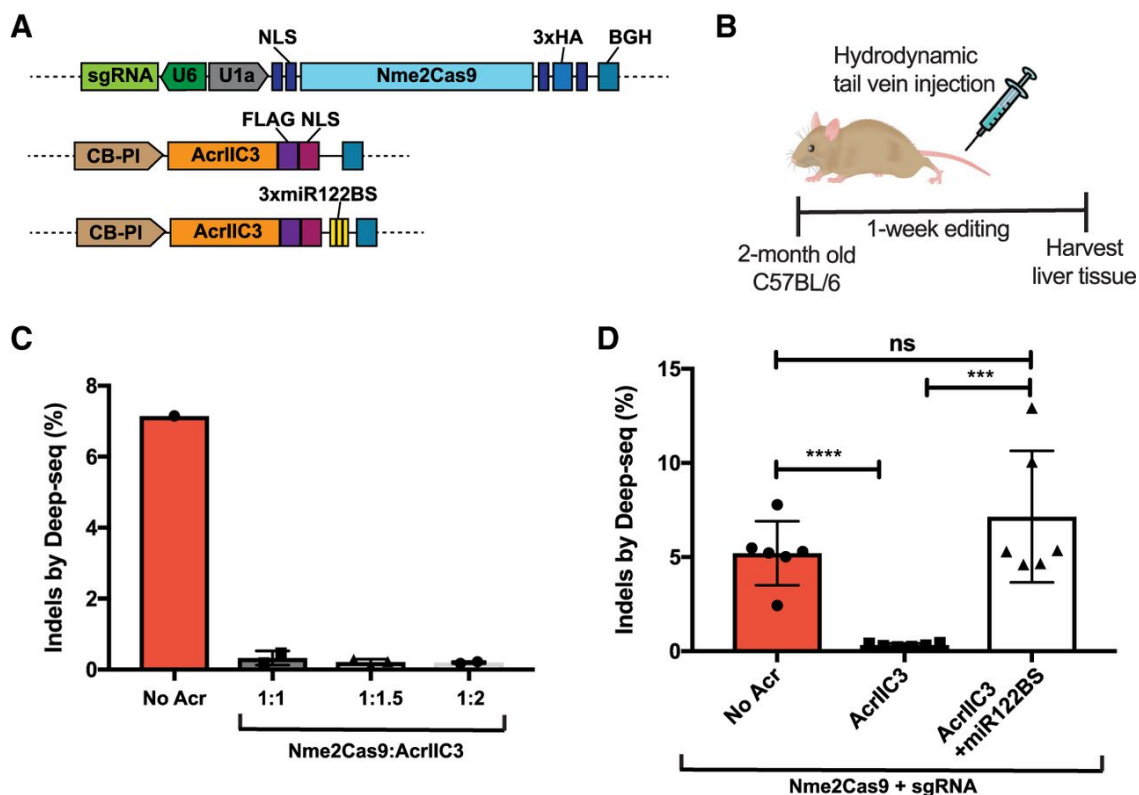


Figure 4.4 Anti-CRISPR inhibition of Nme2Cas9 editing *in vivo* is released by liver-specific miR-122. (A) Plasmids used for *in vivo* studies to drive the expression of Nme2Cas9 + sgRNA and AcrIIIC3, respectively. U1a, murine promoter; BGH, bovine growth hormone poly(A) signal; CB-PI, cytomegalovirus-enhancer, chicken β -actin (CB) promoter with SV40-derived mini-intron. (B) A schematic of mouse tail vein injection studies. Plasmid vectors shown in (A) are administered into 8- to 10-wk-old C56BL/6 mice by hydrodynamic injection. Liver tissues were collected 1 wk after injection. (C) Dose titration of Nme2Cas9 + sgRNA plasmid to AcrIIIC3 plasmid *in vivo*. The percentage of indels at the *Rosa26* target in the livers of C57Bl/6 mice was measured by targeted deep sequencing after hydrodynamic injection of Nme2Cas9 + sgRNA and AcrIIIC3 plasmids at mass ratios of 1:1, 1:1.5, and 1:2. (D) Genome editing in the liver by Nme2Cas9 is inhibited by AcrIIIC3 but restored when AcrIIIC3-3xmiR122BS is silenced. Indel percentages at the *Rosa26* locus in the livers of C57Bl/6 mice were measured by targeted deep sequencing after hydrodynamic injection of Nme2Cas9 + sgRNA plasmid, along with AcrIIIC3 plasmids with or without 3xmiR122BS. $n = 6$ mice per group. ns = not significant, $P < 0.05$ by unpaired, two-tailed t-test.

4.2.5 MiRNA-repressible anti-CRISPR inhibits off-tissue genome editing

To demonstrate that the miRNA-repressible anti-CRISPR proteins can inhibit editing in a non-target tissue upon systemic delivery, we designed a dual-AAV system in which a ssAAV vector expressing Nme2Cas9 is co-delivered with a scAAV expressing an anti-CRISPR protein and a cognate sgRNA (Figure 4.5A). We used the scAAV for AcrIIIC3 expression to enable the earlier onset of transcription (before second-strand synthesis) (McCarty et al., 2003; Z. Wang et al., 2003). This expedited AcrIIIC3 expression maximizes the likelihood that inhibitory levels of the anti-CRISPRs can accumulate before significant ssAAV-based Nme2Cas9 expression occurs since the latter requires prior synthesis of the complementary vector strand. Furthermore, we transferred the U6-driven sgRNA cassette from our previously developed all-in-one ssAAV-Nme2Cas9 vector (Edraki et al., 2018) to the Acr-expressing scAAV vector to ensure that editing cannot occur in cells that fail to receive the *Acr* transgene. These vectors were packaged as serotype AAV9, which is known to have a particularly broad tissue tropism in mice (Zincarelli et al., 2008). The tail veins of three groups of mice were injected with 4×10^{11} genome copies (GC) of ssAAV9-Nme2Cas9 vector, along with 4×10^{11} GC of either (i) scAAV9-AcrIIIC3-sgRNA, (ii) scAAV9-AcrIIIC3-3xmiR122BS-sgRNA, or (iii) scAAV9-AcrIIA4-sgRNA vector (Figure 4.5B). AcrIIA4 was used as a non-cognate, negative-control anti-CRISPR. Both liver and heart tissue samples were collected for indel analysis and histology at 5-wk post-injection. Consistent with *in vivo* delivery by hydrodynamic injection,

editing in the liver was inhibited by AcrIIIC3 but not by AcrIIIC3-3xmiR122BS, in accord with miRNA silencing of the latter in hepatocytes (Figure 4.5C). In contrast, off-target tissue editing in the heart was inhibited by both AcrIIIC3 and AcrIIIC3-3xmiR122BS vectors, indicating that the latter was effectively expressed in the absence of miR-122 in cardiomyocytes (Figure 4.5D).

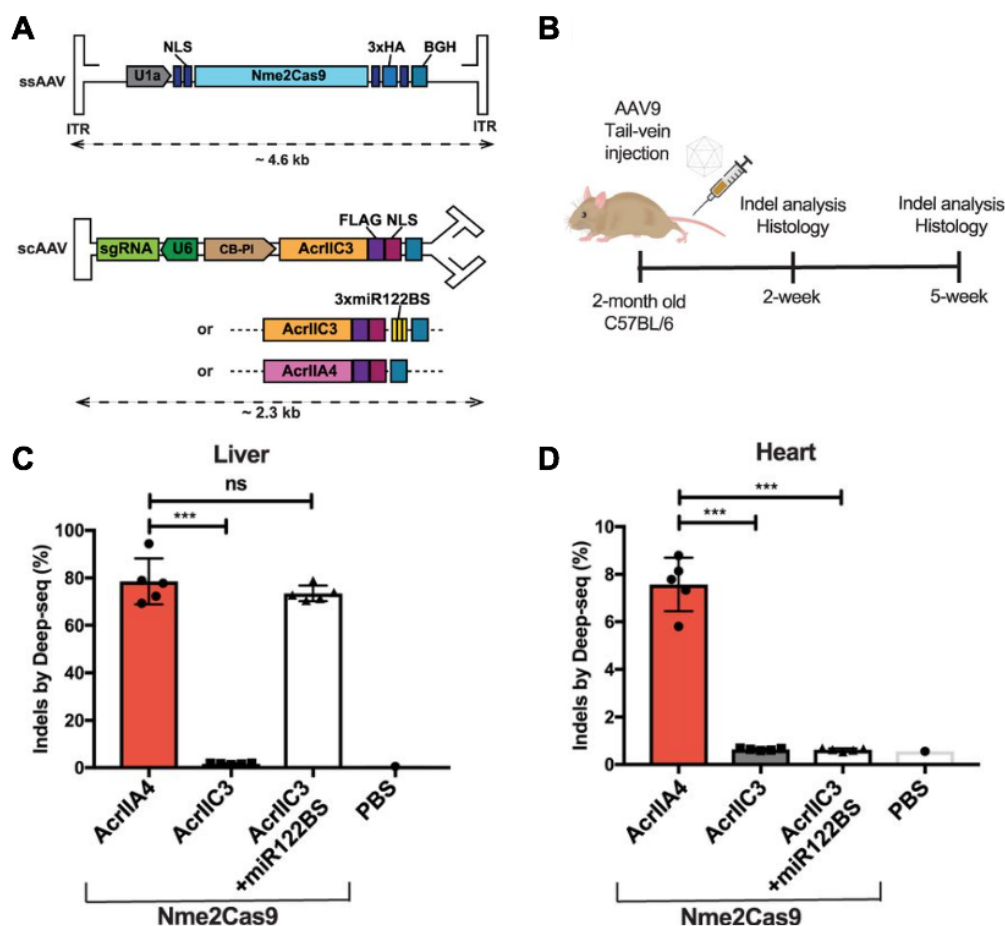


Figure 4.5 AAV delivery of a miRNA-repressible AcrIIA3 inhibits Nme2Cas9 editing in non-target tissue. (A) Design of a dual-AAV9 system for the expression of Nme2Cas9, sgRNA, and anti-CRISPR. A ssAAV9 vector encodes Nme2Cas9 and a scAAV9 vector encodes an anti-CRISPR protein (AcrIIA3, AcrIIA3-3xmiR122BS, or AcrIIA4) as well as a U6-driven sgRNA targeting *Rosa26*. **(B)** A schematic of mouse studies for AAV9 delivery of the dual AAV system shown in **(A)**. Liver and heart tissue samples were collected at 2- and 5-wk post-injection. **(C)** Genome editing in liver and heart tissue samples 5-wk after AAV delivery. Indel percentages at the *Rosa26* locus were measured by targeted deep sequencing. For the 5-wk time points, n = 5 mice per group. ns = not significant; P < 0.05 by unpaired, two-tailed t-test. Control, PBS-injected.

4.2.6 Lack of editing *in vivo* is not due to lack of Nme2Cas9 expression

We confirmed the expression of Nme2Cas9 in all three groups by immunohistochemistry (IHC) against the 3xHA epitope (Figure 4.6A). Robust Nme2Cas9 expression detected by IHC in the liver as well as the cardiac muscles at both time points indicates that the lack of editing was indeed due to AcrIIIC3 inhibition and not due to lack of Nme2Cas9 expression. We were unable to detect AcrIIIC3 by IHC against the Flag epitope in mice injected with AcrIIIC3, likely because antibody binding by the 1xFlag tag is too weak for IHC detection under these conditions. However, we ruled out the possibility of injection failures by using RT-PCR to confirm mRNA expression of *Acr* transcripts both in the liver and heart tissues (Figure 4.6B). Collectively, these results demonstrate that Type II anti-CRISPRs can be used as AAV-deliverable off-switches for genome editing *in vivo*, and that they can be effectively rendered miRNA-repressible to enforce the tissue specificity of genome editing activity.

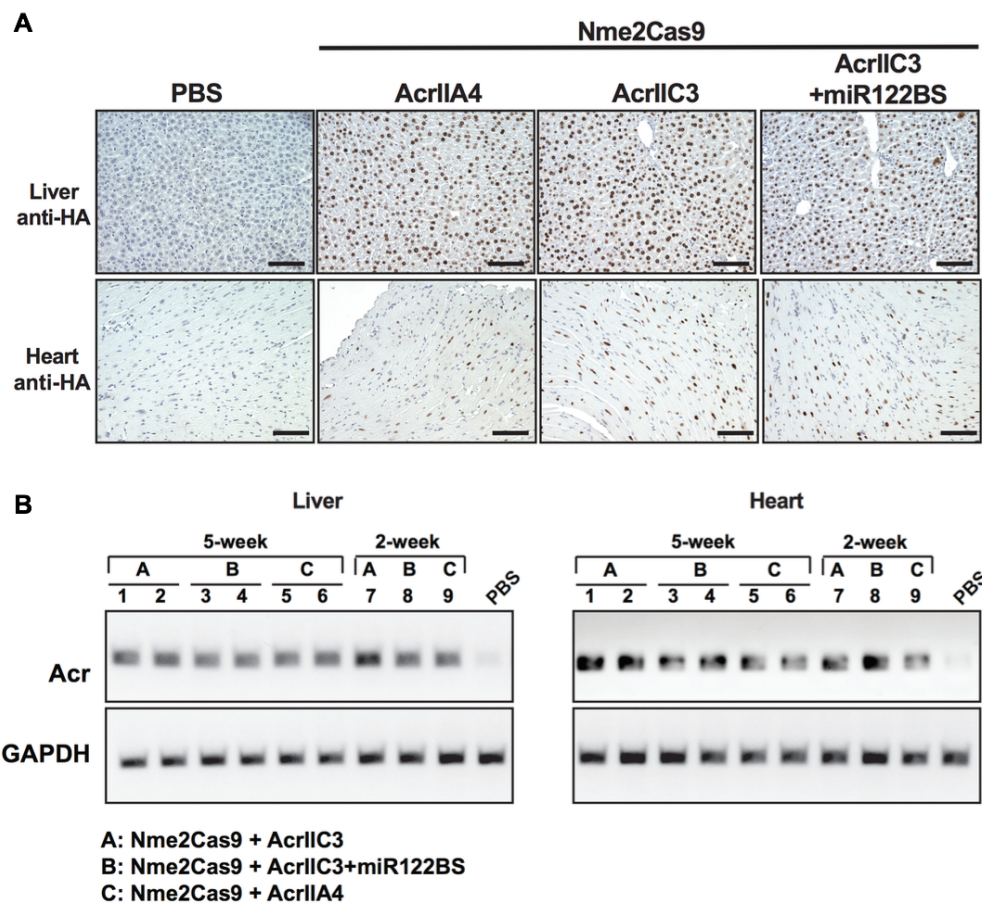


Figure 4.6 Confirmation of Nme2Cas9 expression and Acr transcripts. (A) IHC of the liver and heart tissues from mice injected with dual AAV9 vectors expressing Nme2Cas9 and either AcrIIA4, AcrIIC3, or AcrIIC3-3xmiR122BS. Anti-HA was used for 3xHA-tagged Nme2Cas9 detection. Control, PBS-injected. Scale bar, 100 μ m. **(B)** RT-PCR analysis of AcrIIC3 or AcrIIA4 mRNA using primers specific for each Acr. GAPDH was used as an internal control. Tissue samples collected at both 2-week (n = 1) and 5-week (n = 2) time points were analyzed.

4.2.7 Expression of anti-CRISPRs *in vivo* does not elicit adverse effects

To our knowledge, this is the first demonstration of *in vivo* expression of Acr proteins in a vertebrate model to inhibit Cas9 editing activity. No apparent liver and cardiac muscle damage were detected from staining with hematoxylin and eosin (H&E) when we co-delivered AAV9 expressing Nme2Cas9 and anti-CRISPR proteins (Figure 4.7A). To investigate the immunogenicity of anti-CRISPR and Nme2Cas9 expression, we looked for humoral IgG₁ immune response in injected mice using enzyme-linked immunosorbent assay (ELISA) (Figure 4.7B). Similar to previous reports of antibodies raised against SpyCas9 and SauCas9 (Charlesworth et al., 2019; Simhadri et al., 2018; Wagner et al., 2019), we detected the reactivity indicative of immunoglobulins raised against Nme2Cas9 (Figure 4.7C). In contrast, we could not detect any signals for AcrIIIC3 or AcrIIA4 (Figure 4.7D). From this study, we did not observe overt toxicity in the examined tissues, although the safety and immunogenicity profiles of delivered Acr proteins will need to be investigated over longer periods of time and in additional biological contexts.

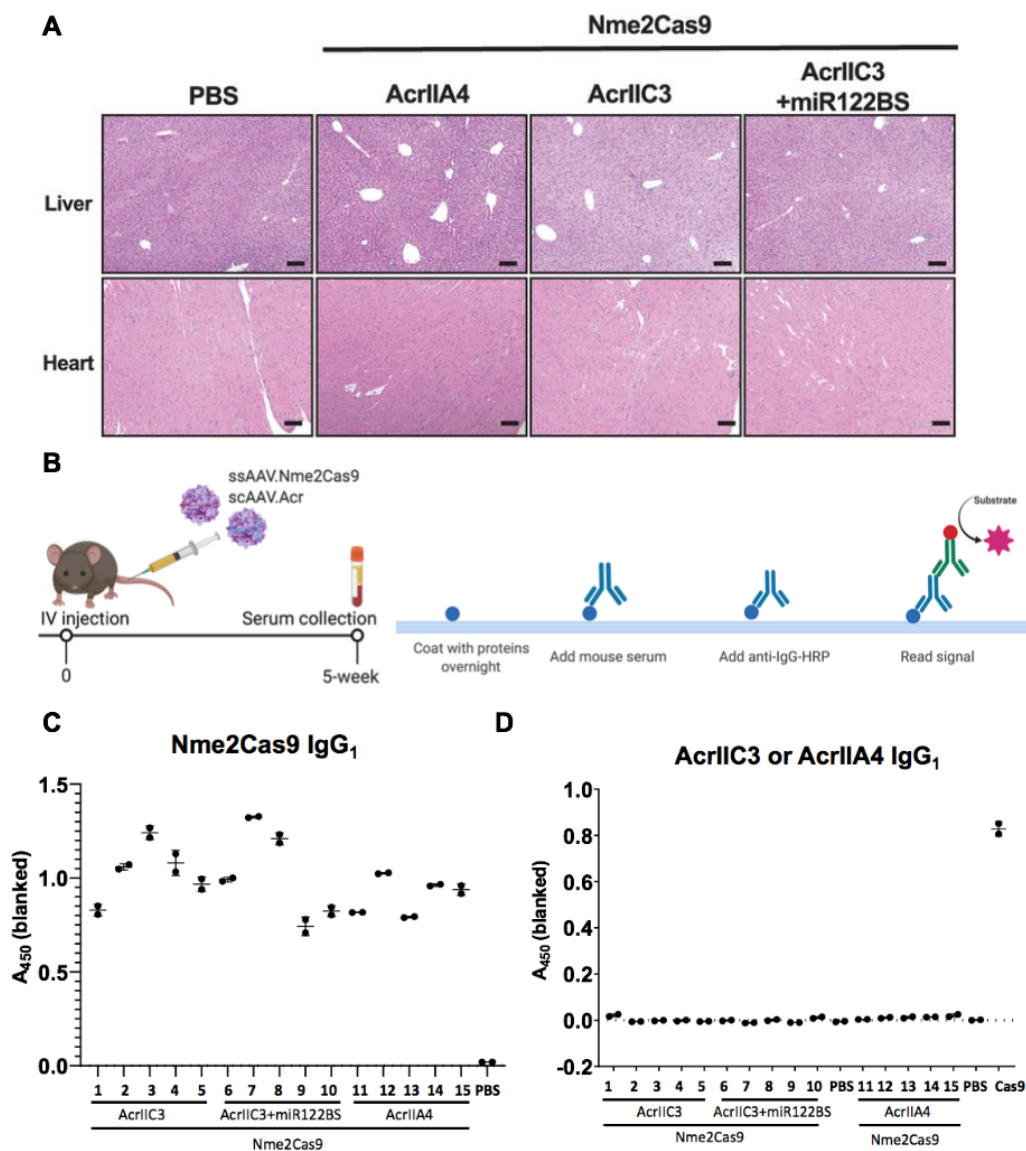


Figure 4.7 Acr and Cas9 expression *in vivo* has no overt adverse effects. (A) H&E staining of liver and heart tissue sections collected from mice 5-wk after AAV9 injection. Scale bar, 100 μ m. (B) Experimental overview of serum collection and ELISA. Serum from injected mice were added to the wells of the pre-coated plate with purified proteins (Nme2Cas9, AcrIIC3 or AcrIIA4). (C-D) ELISA to detect anti-Nme2Cas9 (C) and anti-AcrIIC3/anti-AcrIIA4 (D). Data are presented as mean \pm SD of two technical replicates. The number indicates the individual mouse coinjected with Nme2Cas9 and AcrIIC3 (1-5), AcrIIC3+miR122BS (6-10), or AcrIIA4 (11-15). PBS, PBS-injected mouse serum was used as a control.

4.3 Discussion

Despite Cas9's potential in gene therapy, many hurdles must be overcome in order for it to be used in clinical applications. Safeguarding against undesired, persistent editing in non-target tissues and protecting all ancillary tissues are paramount to ensure the clinical safety profile of CRISPR-based therapeutics for *in vivo* applications. Although AAV capsids with different tissue tropisms can be used, they often differ only in the tropism strength but not absolute specificity. Serotypes widely used for the delivery of therapeutic transgenes can still infect a broad range of tissues *in vivo* (Gao et al., 2004). Moreover, tissue-specific promoters are not always a viable option as some target tissues lack promoters that are highly specific and strong enough to drive transgene expression. Anti-CRISPR proteins are powerful off-switches for Cas nucleases and have potential advantages for implementation as regulators. Since anti-CRISPR proteins are genetically encodable, they can be used for long-term inactivation of Cas9. Preventing the persistence of Cas9 expression and activity after the AAV delivery will require likewise durable and effective inhibitors. To this end, we exploited anti-CRISPR proteins and endogenous tissue-specific miRNAs to restrict Cas9-mediated genome editing to a target tissue as a complementary method of reinforcing tissue specificity of genome editing *in vivo*.

In preliminary work, we demonstrated that miRNA-mediated inhibition of anti-CRISPRs bearing hepatocyte-specific miR-122 MREs allows genome editing in human hepatocytes but inhibits editing in a non-hepatic cell line. The miRNA-

repressible Acr system affords great flexibility in changing the Cas9-Acr pairs, given the discovery of new Acrs for different nucleases, as well as changing the tissue specificity, given the ease of swapping MREs. Furthermore, because MREs are so small, this approach is well-suited for AAV delivery and could confer specificity for some tissues that lack vector-compatible, tissue-specific promoters.

Previously, the endogenous miRNA repertoire has been combined with the CRISPR-Cas machinery to regulate the expression of Cas9 itself (Hirosawa et al., 2017; Senís et al., 2014). Delivery to tissues that highly express the miRNA will silence Cas protein expression, whereas other tissues lacking the miRNA will express the Cas protein for genome editing. For example, de-targeting Cas9 expression from the liver (e.g. with miR-122) allows editing everywhere but the liver, while our strategy will instead restrict Cas9 activity to the liver itself and protect other tissues from unwanted editing events. It will be particularly useful to restrict Cas9 genome editing to a single desired tissue following systemic Cas9 delivery by AAV. Our results complement a strategy that exploits miRNAs to release sgRNAs from longer, inactive precursors (X.-W. Wang et al., 2019), though this approach has not yet been validated in tissue-specific editing applications *in vivo*. While our manuscript was in preparation and revision, two reports also described miRNA-regulated Acr strategies that enable cell-type-specific editing in cultured hepatocytes and myocytes (Hirosawa et al., 2019; Hoffmann et al., 2019).

Our studies extend this work by establishing that miRNA-repressible anti-CRISPRs indeed enforce the tissue specificity of genome editing in discrete organs of adult mammals *in vivo*. To our knowledge, this is the first documentation of anti-CRISPR efficacy during Cas9-mediated editing *in vivo* in adult mammals. We did not observe any adverse tissue damage in the examined tissues or humoral responses against the foreign proteins. The inability to detect immunoglobulins against anti-CRISPRs does not necessarily mean a lack of their existence. The safety and immunity profiles of delivered Acr proteins will need to be further investigated over longer periods of time and in additional biological contexts. In case of immunogenicity of bacterial and viral proteins, we can apply a similar de-targeting strategy using miR-142-3p to mitigate immune response by preventing exogenous protein expression in antigen-presenting cells (APCs) (Boisgerault et al., 2013; Majowicz et al., 2013; Xiao et al., 2019).

In summary, we have developed a “plug-and-play” miRNA-repressible anti-CRISPR platform to confine Cas9 activity to target cells and tissues of interest. This is particularly useful in the context of clinical development as it is highly desirable to prevent unforeseen adverse effects associated with off-tissue and off-target editing *in vivo*.

4.4 Materials and Methods

Appendix Table 2 contains plasmids used in this chapter. Plasmid maps and sequences are available on Addgene.

Vector construction

Codon-optimized AcrIIC3 and AcrIIA4 sequences were ordered as gBlocks (IDT) and amplified using the primers with overhangs to the pCSDest vector by NEBuilder HiFi DNA Assembly (NEB). Similarly, an mCherry ORF was fused to the carboxyl terminus of each Acr by HiFi DNA assembly (NEB). To insert 3xmiR122 MREs in the 3' UTR of each Acr, top and bottom strands were ordered as oligos (IDT) with restriction sites for SacI and HindIII and annealed before ligating into the vector linearized with the same restriction enzymes. For *in vivo* experiments involving a hydrodynamic injection, we used the Nme2Cas9-sgRNA_Rosa26 all-in-one AAV vector (Edraki et al. 2018). To make scAAV vectors expressing Acr proteins, the original scAAV plasmid encoding an EGFP ORF [a kind gift from Jun Xie and Guangping Gao (UMass Medical School)] and pCSDest-Acr plasmids were digested with SacI and AgeI restriction enzymes and then ligated. For AAV vector preparation, a U6-driven sgRNA cassette was removed from the Nme2Cas9 vector by restriction digestion with MluI and assembled into linearized scAAV-EGFP by Hifi DNA assembly (NEB). This vector was digested with SacI and AgeI for AcrIIC3, AcrIIC3-3xmiR122BS, or

AcrIIA4 inserts made from pCSDest plasmids using the same restriction enzymes.

Cell culture and transfection

HEK293T and Huh-7 cell lines were cultured in Dulbecco's modified Eagle's medium supplemented with 10% fetal bovine serum (Sigma) and 1% penicillin-streptomycin (Gibco). For editing experiments *in vitro*, a total of 150 ng of Cas9, 150 ng of sgRNA, and 50 ng of Acr or an empty plasmid were transiently transfected in a 24-well format using Lipofectamine 2000 (Invitrogen) according to the manufacturer's protocol. The total DNA amount was kept constant by adding a stuffer plasmid in all cases. For western blot and flow cytometry analysis, 500,000 cells/well were seeded onto a six-well plate, and 500 ng of each Acr vector and GFP plasmid (the latter used as a transfection control) were transfected using Lipofectamine 2000 (Invitrogen) following the manufacturer's protocol. Prior to flow cytometry analysis, cells were imaged using an EVOS Cell Imaging System (Thermo Fisher).

Flow cytometry

Cells were trypsinized 48 hr post-transfection, washed with PBS, and resuspended in PBS. A total of 100,000 cells were analyzed on a MACSQuant® VYB (Miltenyi Biotec). A yellow laser (561 nm) with a 615/20 nm filter and a blue laser (488 nm) with a 525/50 nm filter were used for mCherry and GFP detection, respectively. Subsequent analysis was performed using FlowJo v10.4.1. Cells

were first sorted based on forward and side scattering (FSC-A vs. SSC-A), and then single cells were gated using FSC-A and FSC-H. Finally, mCherry-positive cells were recorded to estimate the expression level of anti-CRISPR proteins after gating for GFP-positive (transfected) cells.

Western blots

Proteins were collected 48 hr post-transfection and their concentrations were measured using the Pierce BCA Protein Assay Kit (Thermo Fisher Scientific). Western blots were performed as described previously (Lee et al. 2018) with primary mouse anti-Flag (AbClonal, 1:5000) used for Acr detection and rabbit anti-HSP60 (1:5000) used for loading control. After incubation with secondary anti-Rabbit or anti-Mouse antibodies (LI-COR IRDye, 1:20,000), blots were visualized using a LI-COR imaging system.

Mouse studies

C57BL/6 mice were obtained from Jackson Laboratory and all animal maintenance and procedures were performed following the guidelines of the Institutional Animal Care and Use Committee of the University of Massachusetts Medical School. Plasmids for hydrodynamic tail vein injection were prepared using the EndoFreeMaxi kit (Qiagen). For hydrodynamic liver injection, a total of 90 µg of endotoxin-free plasmids was suspended in 2 mL of injection-grade saline and injected via the tail vein into 8- to 10-wk-old C57BL/6 mice. Mice were euthanized 7-day post-injection and liver tissues were collected and stored at

-80°C for analysis. For AAV injection, 4×10^{11} GC of ssAAV-Nme2Cas9 and 4×10^{11} GC of scAAV-U6_sgRNA-Acr (a total of 8×10^{11} GC per mouse) were resuspended in 200 μ L PBS and administered via tail vein injection. Tissue samples from heart and liver were collected and stored at -80°C for indel analysis and histology at 2- and 5-wk post-injection.

Indel analysis

Genomic DNA from cells or tissues were collected using a DNeasy Blood and Tissue Kit (Qiagen). Indel frequencies were measured by targeted deep sequencing. Targeted deep sequencing analyses were done as previously described (Bolukbasi et al. 2015). Briefly, target sites were amplified using High Fidelity 2 \times PCR Master Mix (NEB) in a two-step PCR amplification with locus-specific primers in the first step and then with universal index primers to reconstitute TruSeq adapters. Full-size products were gel-extracted and purified using a DNA Clean and Concentrator Kit (Zymo). The purified library was sequenced using a paired-end 150 bp MiniSeq run using a Mid-output cartridge (Illumina).

Immunohistochemistry

Liver tissues were fixed in 4% formalin overnight, paraffin-embedded, and sectioned at the UMass Morphology Core. For Figure 5C and Supplemental Figure S2A, sectioned slides were stained with H&E for pathology analysis. For IHC, liver sections were dewaxed, rehydrated, and stained following standard

protocols previously described (W. Xue et al., 2011) with primary antibodies against 3xHA-tagged Nme2Cas9 (anti-HA; Cell Signaling) and mCherry (anti-RFP; Rockland). Representative images are shown.

RT-PCR analysis

Total RNA (0.5-1 µg) from mouse tissues were collected by TRIzol (Invitrogen) and then reverse-transcribed to cDNA using random hexamer primers and SuperScript III First-Strand Synthesis System (Invitrogen) following the manufacturers' protocols. cDNA templates were directly used for PCR amplification using primers specific for (1) Nme2Cas9, (2) AcrIIIC3, and (3) GAPDH. The resulting RT-PCR amplicons were visualized by 2.5% agarose/1×TAE gel electrophoresis.

ELISA

Humoral IgG₁ immune response to Nme2Cas9 and anti-CRISPR proteins was measured by ELISA (Bethyl; Mouse IgG1 ELISA Kit, E99-105) following the manufacturer's protocol with a few modifications. In a 96-well plate (Corning Costar 3603 Polystyrene), each well was coated with 0.5 µg of a recombinant protein in 150 µL of coating buffer (Bethyl, cat#E107) for 12 hr on rocker at 4°C. The wells were washed 3× times for 5 min, blocked with 1× BSA Blocking Solution (Bethyl cat#E104) for 2 hr at room temperature, then washed again 3× times. Serum samples (diluted 1:40) were added in duplicate and incubated at 4 °C for 5 hr. Then, the plates were washed 3× times for 5 min and 100 µL of

HRP-conjugated anti-mouse IgG₁ antibody (Bethyl; 1: 100,000 in 1 x BSA Blocking Solution) was added to each well. After incubating for 1 hr at room temperature, the plates were washed 3× times and 100 µL of TMB substrate was added. After development 20 min in dark at room temperature, 100 µL of ELISA Stop Solution was added to each well. The absorbance was measured at 450 nm using a BioTek Synergy HT microplate reader.

Statistical analysis

Standard deviations are derived from each group that has a minimum of three independent replicates unless otherwise noted. Unpaired, two-tailed *t*-tests were used to determine the statistical significance between each group. Resulting *P* values <0.05, 0.01, 0.001, 0.0001 are indicated by one, two, three, or four asterisks, respectively.

Chapter 5 Discussion

5.1 The prospects of CRISPR genome engineering

5.1.1 A summary of CRISPR-Cas applications

The CRISPR-based toolbox has greatly expanded to enable genome editing, base editing, gene regulation, and other uses (Anzalone et al., 2020; Doudna, 2020; Porteus, 2019). In typical gene editing applications, RNA-guided Cas9 or Cas12a introduces a DSB that can be resolved by cellular repair mechanisms to yield an insertion or deletion via NHEJ or integration or replacement of a donor DNA via HDR (Pickar-Oliver & Gersbach, 2019). In base editing, a fused deaminase domain converts a single base through deamination and followed by repair, which allows C to T or A to G transitions (Komor et al., 2018; Rees & Liu, 2018b; B. Yang et al., 2019). Moreover, gene regulation can be modulated by fusing other domains such as transcriptional activators or repressors and epigenetic modifiers (Adli, 2018; Dominguez et al., 2016; Pickar-Oliver & Gersbach, 2019; Thakore et al., 2016). More recent advances in the field gave rise to platforms such as prime editing (Anzalone et al., 2019), Cascade effector complexes from Type I systems for large genomic deletions (Cameron et al., 2019; Dolan et al., 2019; Morisaka et al., 2019), as well as DNA insertion directed by CRISPR effectors and transposases (S. P. Chen & Wang, 2019; Klompe et al., 2019; Strecker et al., 2019). New tools will continue to emerge as

we uncover and harness the natural prokaryotic gold mine in this fast-moving field. The only limit is one's creativity.

5.1.2 Considerations for human therapeutics

In less than a decade, CRISPR gene editing technologies have rapidly advanced into or close to clinical trials (Finn et al., 2018; Maeder et al., 2019). Although *ex vivo* and *in vivo* therapeutic gene editing approaches using CRISPR have unprecedented potential for treating human diseases, a few important issues must be considered (Doudna, 2020). First, introducing proteins of bacterial origin raises immunogenicity issues that are currently under active investigation (Charlesworth et al., 2019; A. Li et al., 2020; Simhadri et al., 2018; Wagner et al., 2019). This will not be a concern for *ex vivo* approaches since cells are corrected *in vitro* and engrafted back into patients. Since the safety profile of an *ex vivo* approach is more appealing, the ongoing Phase 1/2 clinical trials for sickle cell diseases will likely have success if proven efficacious (CTX001; NCT04208529). Whether the pre-existing immunity will be problematic in humans remains to be revealed in future clinical trials involving direct delivery of editing reagents into patients. Other than blood disorders, many diseases affect tissues inside the body that cannot be removed, requiring *in vivo* editing. Among the many complications for *in vivo* therapeutics is the possibility of immunogenicity, though delivery of the editing reagents may be the biggest obstacle. An ideal delivery modality will combine the benefits of different strategies: cheap and easy production, efficient tissue targeting capabilities, and transient expression (Glass et al., 2018). To date, AAV is a clinically well-established delivery vector for *in vivo* transgene expression, however, AAV poses restrictions for CRISPR-

mediated gene editing because of its limited cargo size, potential genomic integration, and the likelihood of off-targeting due to long-term expression (D. Wang et al., 2019). To evaluate the clinical relevance of AAV-delivered Cas9, preclinical assessment must be conducted in large animal models such as dogs and nonhuman primates using clinical-grade AAV vectors. Furthermore, many factors should be considered to minimize potential immune responses in humans: the inflammatory nature of the AAV vector, the dose, the tissue-specific expression of transgene, as well as route of administration.

Last but not least, although the immediate outcomes of the therapeutic gene editing may be successful, no one can predict the unforeseeable consequences of gene editing without long-term evaluation, and only time will tell. Therefore, precaution should be taken at every step of CRISPR technology development and implementation in humans.

5.1.3 Heritable germline editing and ethics

Germline genome editing is already in widespread use in animals and plants and has been approved for research purposes only in human embryos (Fogarty et al., 2017; P. Liang et al., 2015; H. Ma et al., 2017; Tang et al., 2017). For therapeutic purposes, all genome editing technologies are currently directed at treating patients' somatic cells (Porteus, 2019). A distinction between somatic and germline editing is that the heritable genetic modifications will pass onto future generations in the germline editing. While correcting disease-causing mutations in the embryo may seem powerful, creating a "disease-free" baby, germline editing of a human embryo that resulted in pregnancy and birth of Chinese twin babies sparked widespread controversies (Baltimore et al., 2015; Lanphier et al., 2015). Human germline editing is faced with many challenges both scientifically and ethically (Ledford, 2019). Notably, the latest research suggests large genomic rearrangements or deletions induced by DSBs and underscores that we have not fully grasped DNA repair mechanisms in human embryos (Alanis-Lobato et al., 2020; D. Liang et al., 2020; Zuccaro et al., 2020). Moreover, studies based on germline editing in mice may not be easily translatable due to differences between mice and humans in early embryo development (Fogarty et al., 2017). This leads to the next point: while apprehension about embryo editing is understandable, human embryo editing in research must not be completely banned. With strict regulations in place for biomedical research, germline editing will facilitate research on possible future clinical applications (Araki & Ishii, 2014).

Lastly, the scientific community must address societal concerns and establish and comply with the appropriate guidelines. In the future, if the germline editing is ever used, we must ensure that the merit of an unmet medical need outweighs the risks by evaluating the urgency, safety, and ethical justification (Ormond et al., 2017).

5.2 The new and emerging field of anti-CRISPRs

5.2.1 The biology of anti-CRISPRs

Since the discovery of anti-CRISPRs in 2013, the number of published reports on this topic has dramatically increased in the past few years (Bondy-Denomy, 2018; Davidson et al., 2020; S. Hwang & Maxwell, 2019; Koonin & Makarova, 2018; Pawluk et al., 2018; Sontheimer & Davidson, 2017). Many aspects of anti-CRISPR research focused heavily on discovery for different types of CRISPR-Cas systems and dissecting their inhibitory mechanisms (Borges et al., 2017; Davidson et al., 2020; Stanley & Maxwell, 2018). The prevalence of anti-CRISPR proteins that inactivate almost all types of CRISPR-Cas systems (Types I, II, III, V, and VI), and the diversity in sequences and structures that perhaps explain the unique strategies they employ (Wiegand et al., 2020; Yuwei Zhu et al., 2018), suggest the importance of anti-CRISPR proteins in shaping the microbial world (Samson et al., 2013; Wiedenheft, 2013). More recently, we began to uncover the diversity of archaeal Acrs as well (Peng et al., 2020). Furthermore, studies are underway to understand how anti-CRISPRs operate in the host-pathogen interactions occurring in a more complex population of natural environments (Nussenzweig & Marraffini, 2018; van Gent & Gack, 2018). There is still so much unknown in this emergent field and future studies will be necessary to shed light on the evolutionary origins and their implications as well as on the discovery of anti-CRISPR proteins that function at different stages of CRISPR immunity such

as adaptation. The ongoing battle opens up the possibilities to more exciting discoveries such as “anti-anti-CRISPRs.”

5.2.2 A summary of anti-CRISPR protein applications

While CRISPR technologies are widely adopted for numerous applications (Anzalone et al., 2020), anti-CRISPR proteins have not yet been extensively used in genome engineering (Q. Liu et al., 2020; Marino et al., 2020). The versatility of anti-CRISPR proteins in regulating all types of CRISPR-based technologies warrants an enormous potential as a safeguard against undesired editing. For example, anti-CRISPR proteins can be used to eliminate editing at off-target sites (Aschenbrenner et al., 2020; Shin et al., 2017). In addition, undesired editing in non-target cell types (Hirosawa et al., 2019; Hoffmann et al., 2019) or tissues in vivo (J. Lee et al., 2019) can be achieved by using tissue-specific miRNAs that regulate the expression of anti-CRISPR proteins. Other methods of post-transcriptional regulation such as alternative splicing or mRNA stability and decay can be explored (Corbett, 2018). These processes have been implicated in gene regulatory potential in different cell or tissue types as well as healthy versus diseased conditions (Carey and Wickramasinghe, 2018) although implementing such complex system for transgene regulation may be tricky and require more extensive studies.

Furthermore, anti-CRISPR proteins may serve as a safety measure in reducing the cytotoxicity of the CRISPR/Cas9 complex in human hematopoietic stem cells (C. Li et al., 2018), or stopping the propagation of gene drive (Basgall et al., 2018). The application of Acrs is not limited to regulating gene editing, for

example, anti-CRISPR can be used as a ligand biosensor to detect and quantify the CRISPR-Cas9 RNP (Johnston et al., 2019). Applications of anti-CRISPR proteins may face similar challenges that CRISPR-Cas technologies currently have (Doudna, 2020). Alternative technologies are being developed to inhibit the activity of Cas9, such as nucleic acid-base inhibitors (Barkau et al., 2019) and small-molecule inhibitors (Maji et al., 2019). However, these inhibitors may require substantial efforts in proper designing through screening or optimization to minimize the risk of interaction with other targets in mammalian cells (Schneider, 2018). Overall, development of anti-CRISPR-based tools will provide a unique capacity to make CRISPR technologies more useful, effective, and safe. Applications of anti-CRISPR proteins are still at an early stage, and many innovations will arise moving forward.

Concluding Remarks

The overarching goal of this thesis was to mine for natural anti-CRISPR protein inhibitors of Cas9 (Chapter 2) and repurpose these proteins to complement current Cas9 technologies in basic and clinical research by developing anti-CRISPR application tools (Chapters 3 and 4).

Appendix

Appendix 1 Characterization of additional Type II-C anti-CRISPRs

In Chapter 2, we discovered anti-CRISPR proteins for Type II-C systems that can inhibit various Cas9 orthologs. After we published that AcrIIC5 inhibits the originally reported Nme1Cas9 (Hou et al., 2013), a closely related Nme2Cas9 from our lab was reported (Edraki et al., 2018). Nme1Cas9 and Nme2Cas9 share a high identity except for the divergent PID (Edraki et al., 2018). While all other previously reported AcrIIC families inhibit Nme2Cas9, AcrIIC5_{Smu} failed to inhibit gene editing (Edraki et al., 2018). We reported that there are few homologs of AcrIIC5 in different *Neisseria* species with varying percent identity (Figure A1.1A). We also tested a new Type II-C (AcrIIC6) from *Neisseria* spp. (HMSC056A03). Surprisingly when we evaluated genome editing inhibition by AcrIIC5 homologs and AcrIIC6, none of the anti-CRISPR proteins were able to inhibit Nme2Cas9 very efficiently in T7E1 assays while completely inhibiting Nme1Cas9 (Figure A1.1B). To measure the indel efficiencies more quantitatively, we performed TIDE analysis for Nme2Cas9 editing (Figure A1.1C). Similar to T7E1, tested anti-CRISPR proteins failed to completely inhibit Nme2Cas9 genome editing although at varying potency (Figure A1.1C). AcrIIC5_{N10} does not inhibit Nme2 and both AcrIIC5_{Nwa} and AcrIIC6 inhibit Nme2Cas9 modestly, although all three Acrs potently inhibit Nme1Cas9. Based on this observation, the inhibitory mechanism of AcrIIC5 may involve interaction with the PID of

Nme1Cas9, while the interaction of AcrIIC5 with the PID of Nme2Cas9 may be suboptimal. From our earlier investigation as presented in Chapter 2, AcrIIC5 most likely prevents Nme1Cas9 from binding to the target DNA. It remains to be elucidated whether AcrIIC5 interacts with the PID of Nme1Cas9 via DNA mimicry similar to AcrIIA4. Anti-CRISPRs from the current study must be accompanied by biochemical and/or structural studies for additional characterization. It will be interesting to further investigate how one of the two closely related Cas9 orthologs is susceptible to anti-CRISPR inhibition while the other escapes. This will help us understand the ongoing arms race in the battle between bacterial Cas9 and phage anti-CRISPRs.

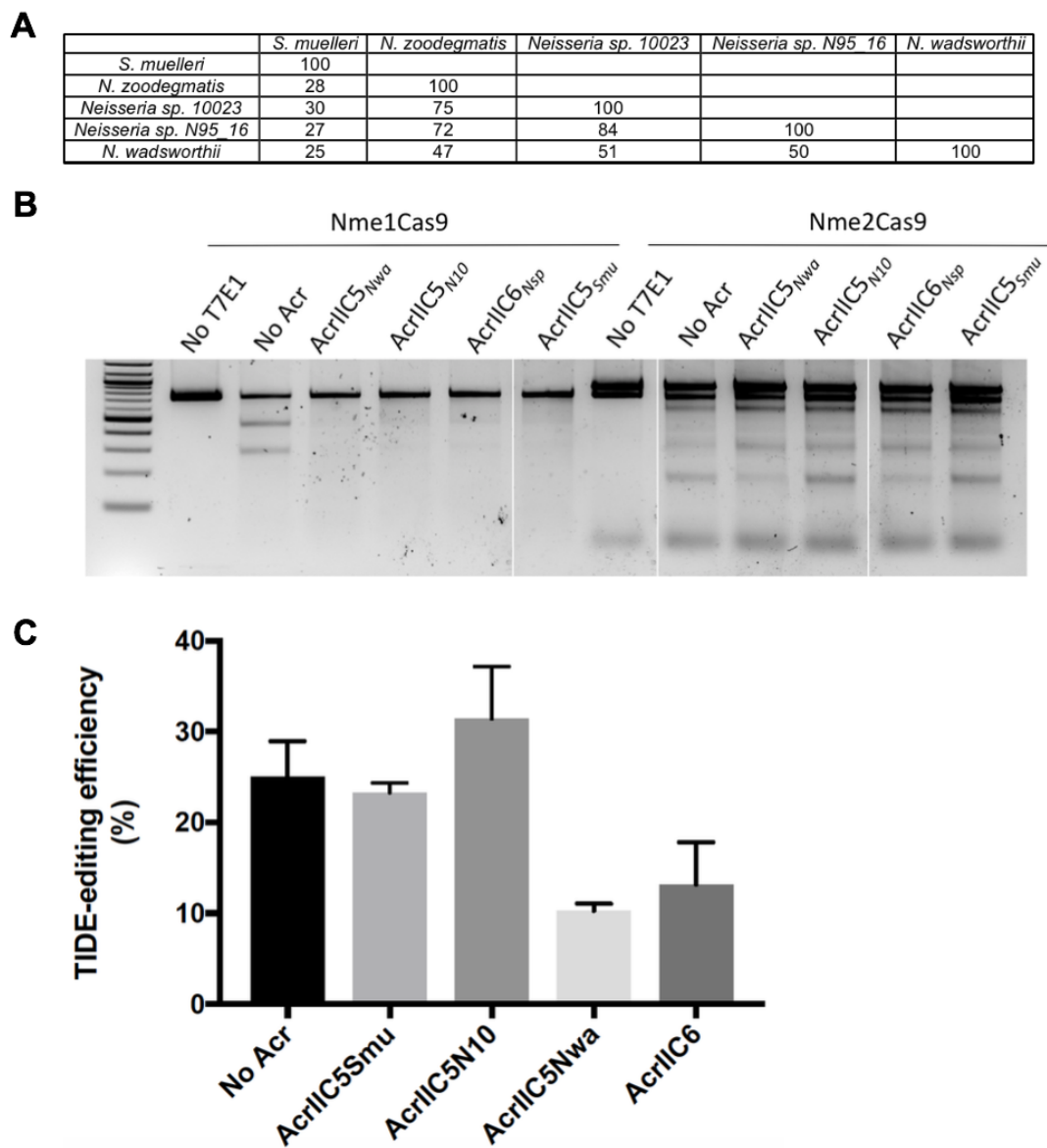


Figure A1.1 Type II-C anti-CRISPR inhibition of Nme1Cas9 and Nme2Cas9. (A) AcrIIIC5 homologs pairwise percent identity. (B) Comparison of inhibition of Nme1Cas9 (left) and Nme2Cas9 (right) by AcrIIIC5 homologs and AcrIIIC6 using T7E1 assays. (C) Indel frequency of Nme2Cas9 genome editing and inhibition by AcrIIIC5 homologs and AcrIIIC6 using TIDE analysis.

Appendix 2 Optimization of the miRNA-repressible anti-CRISPR system

In Chapter 4, we demonstrated robust repression of anti-CRISPRs by miR-122 in the liver. However, since many miRNAs are not expressed as highly as miR-122 in the liver, and certain miRNAs are differentially expressed in various tissues rather than an all-or-none fashion, we decided to investigate the effect of varying endogenous miRNA abundances on silencing efficiency. Moreover, we also aimed to optimize the existing strategy to be least disruptive for endogenous miRNAs and their target transcripts.

A2.1 Transgene repression requires a threshold level of miRNAs

To better understand the expression level (i.e. copy number of a specific miRNA) that is required for efficient repression of anti-CRISPR with MREs, we profiled miRNA abundance in a reporter cell line and evaluated miRNA representatives of different copy number groups (Figure A2.1).

We performed small RNA sequencing of a HEK293T reporter cell line (HEK293T-TLR-MCV) to profile miRNA abundance, then ranked and binned miRNAs into 5 groups depending on the miRNA molecules per cell: the highest (~20,000 molecules /cell) to the lowest (2 molecules /cell), with each bin representing a log fold difference. We estimated the number of miRNA molecules by including spike-in controls. Then a miRNA representing each bin was used to clone a vector expressing anti-CRISPR fused to mCherry and 3xMRE for each miRNA in the 3' UTR. We transfected the HEK293T-TLR-MCV reporter cells with these vectors by titrating the dosage of plasmids and performed flow cytometry (Figure A2.1).

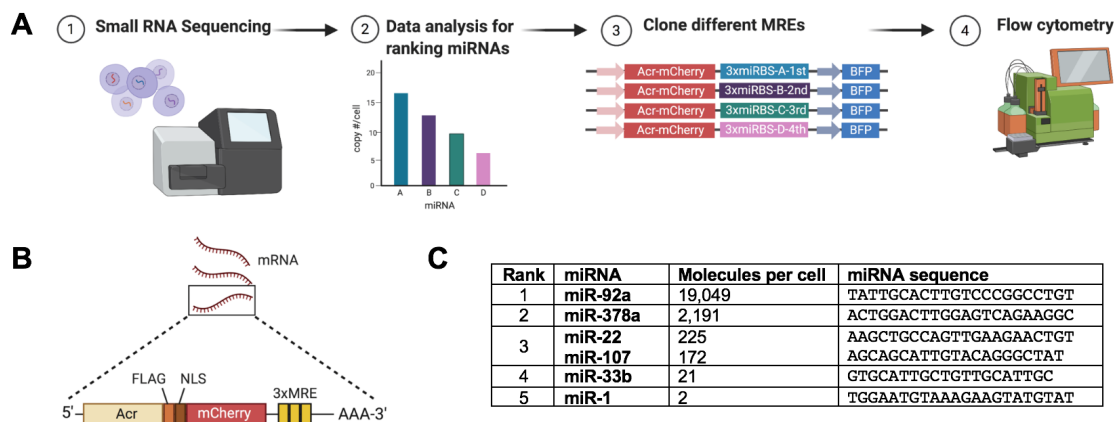


Figure A2.1 Experimental overview of miRNA profiling. (A) Workflow: after small RNA sequencing and data analysis, we ranked endogenous miRNAs in HEK293T-TLR-MCV based on their occurrences. To clone the anti-CRISPR protein-mCherry fusion construct, miRNAs that differ in abundance (~ 20,000 copies to 2 molecules per cell) were randomly chosen. We transiently transfected the HEK293T-TLR-MCV cells with each construct and evaluated the efficiency of repression by flow cytometry. **(B)** Schematic of AcrIIC3-mCherry-MRE transcripts. Three MRE sequences are placed in tandem with each MRE having a perfect complementarity to a full-length miRNA sequence. **(C)** Randomly picked 5 unique miRNAs from the rank of 10-fold difference in abundance.

As expected, the most abundant miR-92a showed the lowest level of mCherry expression, indicative of potent silencing activity. Similarly, the amount of the plasmid that expresses AcrIIIC3-mCherry-MRE affected the efficiency of silencing mCherry expression: fewer targets (low) available resulted in more efficient silencing. We observed efficient silencing for the highest miRNA group (~20,000 molecules /cell) while 2-2,000 molecules /cell did not significantly reduce the expression of mCherry. Although we could observe a general correlation, targets containing miR-22 MREs consistently showed no sign of silencing activity (Figure A2.2A). To test if miR-22 was an exception for low or undetectable silencing activity, we picked another miRNA from the same abundance ranking group (miR-107) and repeated the titration experiment (Figure A2.2B). This time, we observed a gradual increase of mCherry expression for targets containing less abundant miRNA, demonstrating the dosage effect of endogenous miRNAs indeed correlates with the silencing efficiency (Figure A2.2B). Based on our observation, we believe ~20,000 copies or more would be needed for potent silencing activity and a miRNA that has an abundance of fewer than 2,000 copies /cell may not be sufficient.

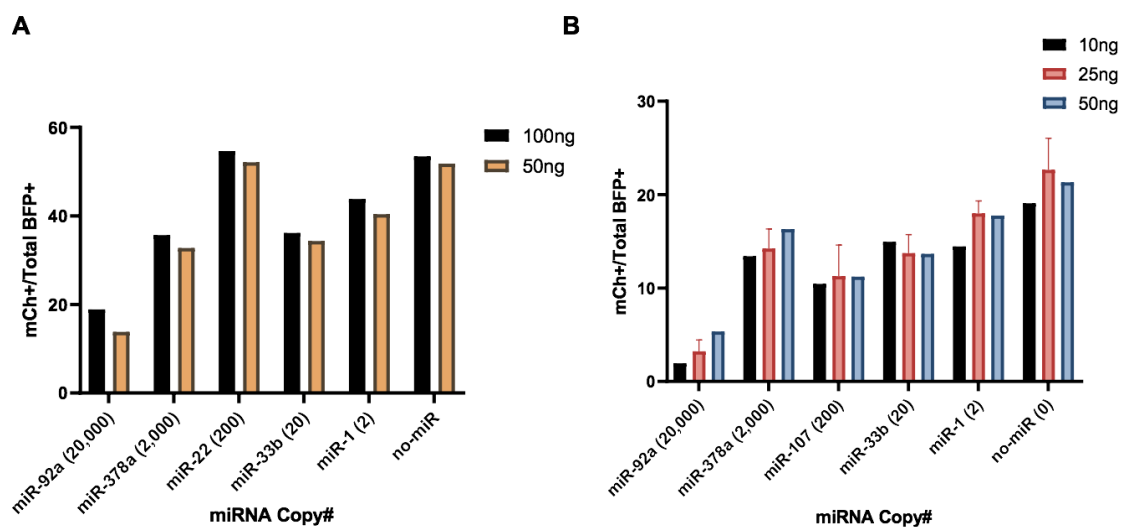


Figure A2.2 Effects of miRNA and target abundance on silencing activity. (A-B) AcrIIIC3-mCherry with fully complementary MREs for each miRNA was tested with miR-22 (A) and miR-107 (B) for a ranking group of 200 molecules /cell. The mCh+/total BFP+ ratio indicates miRNA silencing activity.

A2.2 Optimizing the length of the MRE to bypass the TDMD pathway

A competitive endogenous RNAs (ceRNAs) hypothesis proposes that strong overexpression of natural or artificial RNAs harboring miRNA target sites can act as sponges for miRNAs by titrating miRNAs away from natural targets and thereby de-repressing these transcripts (Ebert et al., 2007; Franco-Zorrilla et al., 2007; Hansen et al., 2013; Memczak et al., 2013; Mukherji et al., 2011). This presents a potential caveat of the miRNA-repressible anti-CRISPR system since the exogenous targets containing MREs may impact the endogenous transcripts that are regulated by the same miRNAs. Although the hypothesis is still debated, extensive studies on endogenous transcripts and miRNA regulation suggest that changes in target abundance are unlikely to cause significant effects on gene expression via a sponge effect (Denzler et al., 2014, 2016).

Another pathway in which the abundance of miRNA itself may be altered and potentially impact the de-repression of targets is target RNA-directed miRNA degradation (TDMD) (Ameres et al., 2010). When there is extensive pairing between the RNA target and miRNA, TDMD causes instability and depletion of miRNAs (Wightman et al., 2018; Pawlica et al., 2020). In the initial miRNA-repressible anti-CRISPR system, we used the full-length MRE that has perfect complementarity to the miRNA sequence (21-22nt) to achieve cleavage of mRNA targets for strong repression. When a miRNA and its target are perfectly complementary, Ago2 mediates cleavage of the target, which is then quickly

degraded by cellular exonucleases. However, when a target exhibits extensive 3' base-pairing, the miRNA becomes subjected to degradation by the cellular ribonucleases that function in TDMD (Wightman et al., 2018).

In light of the TDMD pathway, we questioned how we can design our targets to minimize the perturbations to the endogenous cellular miRNAs and their regulatory functions. To define the parameters for designing MREs that are effective in the target repression without eliciting TDMD, we decided to test shorter MREs. A previous study showed that complementarity past guide base g16 is unnecessary for efficient cleavage by mammalian AGO2 (Becker et al., 2019). Thus, based on the requirement for g2-g16 complementarity for target cleavage, we decided to test a shortened MRE instead of a full-length sequence.

Comparison between full-length vs. g2-g16 complementarity

We used the identical vectors and experimental setup that we used above for the sensitivity assay, but this time the vectors encoding AcrIIIC3-mCherry-MRE have g2-g16 complementarity to the miRNAs. We then compared side-by-side the silencing efficiency of each miRNA that only differs in MRE length (Figure A2.3A). We again observed that the miR-92a reduced mCherry expression the most for both short and full-length MRE containing vectors compared to other miRNAs that belong to less abundant groups. Shorter MREs were still able to efficiently silence the transgene albeit at slightly lower efficiency than the full-length MRE (Figure A2.3B)

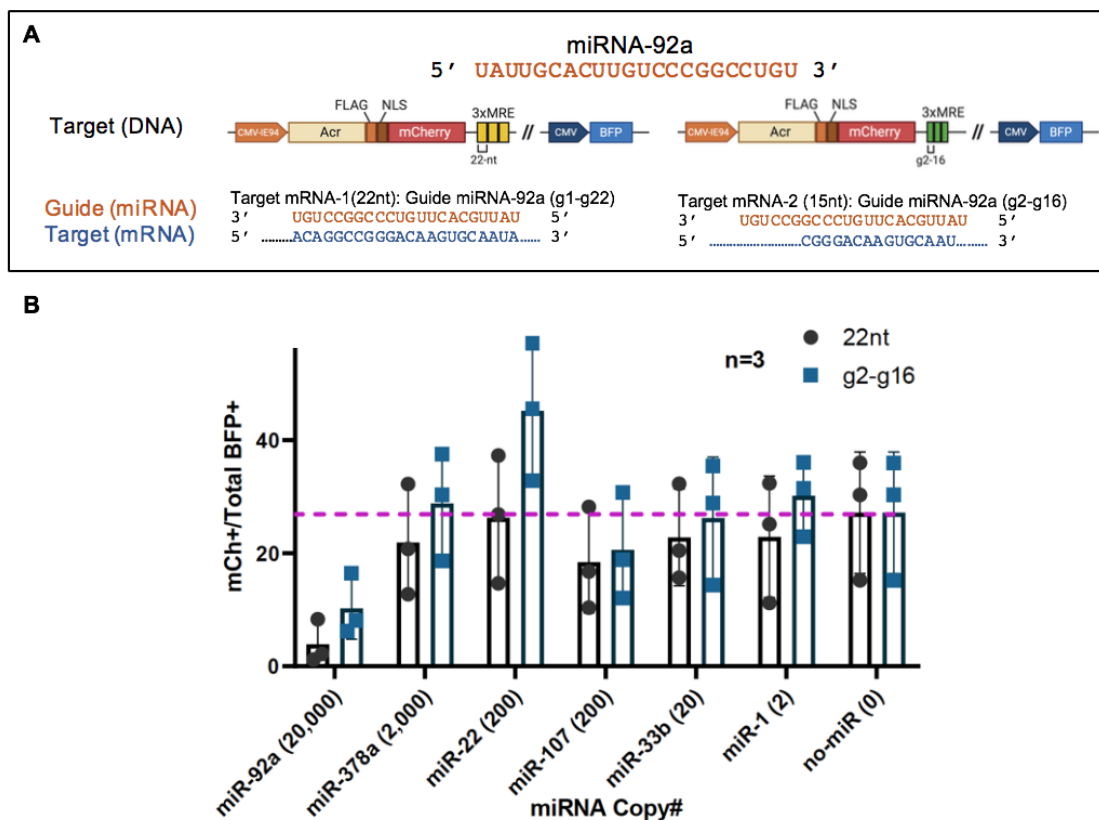


Figure A2.3 Comparison of full-length vs. g2-g16 MREs on silencing activity of miRNAs. (A) Schematic of DNA vectors that encode transcripts for AcrIIC3-mCherry with either full-length or g2-g16 MREs of miR-92a as an example. Target:Guide pairing is shown in blue and orange colors. **(B)** AcrIIC3-mCherry expression levels are compared between the 22nt and g2-g16 MREs for various miRNA copy numbers. mCh⁺/(Total BFP⁺) ratio indicates silencing efficiency.

Ultimately, the silencing of anti-CRISPR transcripts bearing MREs should enable Cas9-mediated genome editing. To evaluate the genome editing outcome of variable silencing efficiency seen with full-length and g2-g16 MREs, we transfected HEK293T-TLR-MCV cells with Nme2Cas9, sgRNA, and an AcrIIIC3 vector harboring 22nt or g2-g16 MREs (Figure A2.4). Without any anti-CRISPRs, ~10% of indels were seen at TS126, however, co-transfecting AcrIIIC3 that is regulated by different miRNAs reduced the editing efficiency. Only the full-length MRE containing AcrIIIC3 (miR-92a; Figure A2.4A) restored the editing levels comparable to cells that were transfected with only Nme2Cas9 and sgRNA (TS126; Figure A2.4A) while AcrIIIC3 bearing the g2-g16 MREs for miR-92a partially restored editing levels (Figure A2.4B).

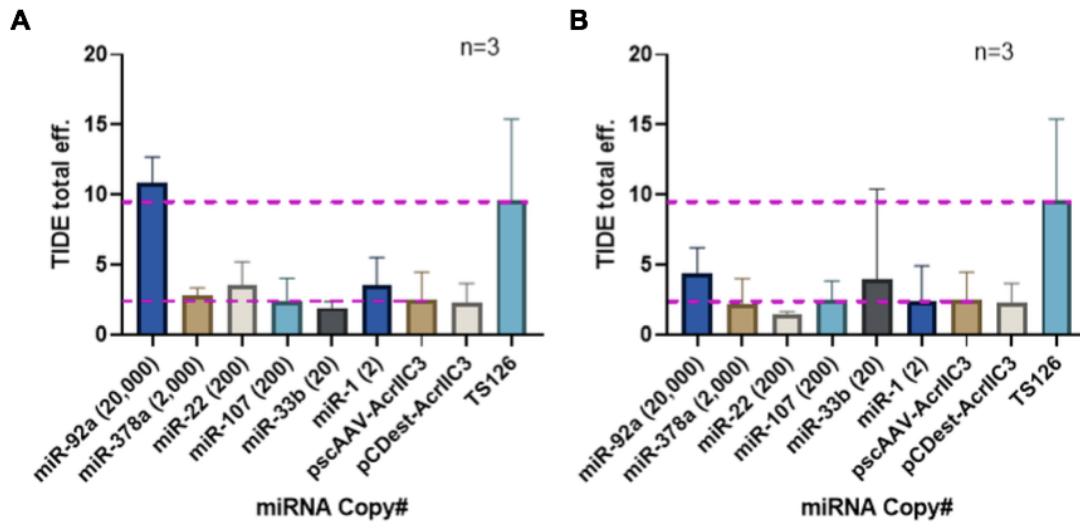


Figure A2.4 Anti-CRISPR repression by full-length or g2-g16 MREs leads to genome editing. (A) Nme2Cas9 and its sgRNA targeting TS126 were co-transfected with miRNA repressible AcrIIIC3-mCherry with either full-length **(A)** or g2-g16 MRE **(B)** constructs. TIDE analysis was performed to estimate the genome editing efficiency. pscAAV-AcrIIIC3 and pCDestAcrIIIC3 are used as AcrIIIC3 controls without MREs. TS126 indicates the Nme2Cas9 sgRNA target site without the expression of any Acr, serving as a ‘No Acr’ control.

A2.3 Future directions

In our studies, we attempted to address two main questions we initially raised:

- 1) What is the level of abundance required for robust repression of anti-CRISPR transgene to enable Cas9-mediated gene editing?
- 2) Will expressing exogenous targets bearing MREs affect endogenous miRNAs and their natural targets?

From our preliminary studies conducted in HEK293T reporter cells, it appears that ~20,000 copies of miRNA should be sufficient for anti-CRISPR silencing to allow genome-editing. We note that other contributing factors were not considered in the current study. Other determinants of target:miRNA interactions may depend on the genomic sequence context such as the location and accessibility of the miRNA binding sites (Grimson et al., 2007; Hausser & Zavolan, 2014). Therefore, exceptions may exist for different types of miRNAs. For example, we consistently observed that miR-22 did not perform as well as other less abundant miRNAs previously also seen by another group (Mullochandov et al., 2012), suggesting that the abundance alone cannot be the sole determinant for silencing efficiency. Due to the complexity of miRNA regulation, mechanisms responsible for differential miRNA activity are likely to be combinatorial effects of many factors. To select the best miRNA for relevant target

tissue or cell types of interest, future studies will require *in vivo* profiling of “functional” miRNAs (miRNome) (Mullokov et al., 2012).

Furthermore, we endeavored to optimize the MRE sequences to minimize any potential complications due to long-term expression of targets harboring perfectly complementary MREs from AAV vectors. One way such a case can potentially be an issue is the depletion of endogenous miRNAs via the TDMD pathway. Artificial targets with extensive complementarity to the miRNA can trigger TDMD through tailing and trimming of the miRNA 3' terminus (Ameres et al., 2010; Baccarini et al., 2011; de la Mata et al., 2015; Denzler et al., 2016; Xie et al., 2012). This raised our concern and we attempted to address this by changing the perfect complementarity of MREs to shorter g2-g16 lacking 3' extensive pairing to avoid being targeted for TDMD (Becker et al., 2019). We show that shorter MREs can repress the Acr1C3 to allow gene editing although not as efficiently as the full-length MREs we originally used. Further optimization may be needed for improving efficiency by other design parameters such as spacing between the MREs. It remains to be tested in the future whether there is a benefit of using g2-g16 at the cost of modest loss of silencing activity so that we can bypass TDMD that may perturb the endogenous miRNA pool and transcriptional regulation.

Appendix 3 Immunogenicity of anti-CRISPR proteins

To the best of our knowledge, the *in vivo* studies presented in Chapter 4 were the first to introduce anti-CRISPR proteins into mammalian models. The utility of anti-CRISPR proteins *in vivo* may be compromised if they are immunogenic or faced with pre-existing immunity (A. Li et al., 2020). During our 5-week study after AAV delivery, there was no apparent toxicity or abnormal tissue histology. We collected sera of mice injected with AAV expressing Nme2Cas9 and anti-CRISPR proteins (AcrIIC3 and AcrIIA4) and performed ELISA to test if there are any IgG antibodies raised against these foreign proteins. We did not observe any humoral immune response against AcrIIC3 and AcrIIA4, two of the most potent anti-CRISPR proteins that can inactivate NmeCas9 and SpyCas9, respectively. As previously reported for other Cas9 orthologs, a strong IgG response was observed for Nme2Cas9 as well. To further investigate whether we can raise antibodies against anti-CRISPR proteins, we performed an immunization assay (Figure A3.1).

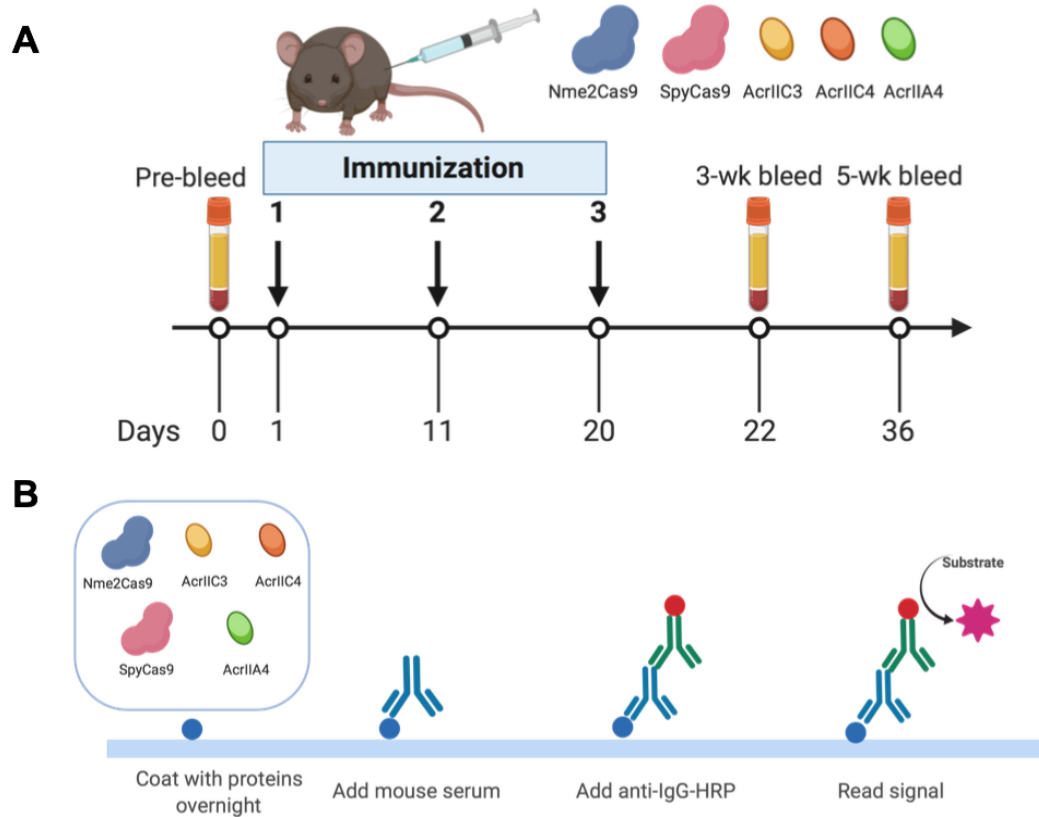


Figure A3.1 Immunization assay via subcutaneous injection of recombinant Cas9 and anti-CRISPR proteins. (A) A timeline of mouse immunization studies. Mice were pre-bled at day 0 before Intraperitoneal injections of recombinant proteins. Serum was collected at day 22 (3-wk) and 36 (5-wk). **(B)** Overview of ELSIA.

A3.1 No IgG immune response against anti-CRISPR proteins is detected

Groups of 4 mice each (sex- and gender-matched for each group) were bled before subcutaneous injection of five recombinant proteins: Nme2Cas9, SpyCas9, AcrIIIC3, AcrIIIC4, and AcrIIA4. PBS-injected mice served as our control group. Mice were then bled at 3- and 5-wk post-injection to collect serum, and ELISA was performed for detecting IgG in the serum (Figure A3.1). Consistent with our earlier observations, both Nme2Cas9 and SpyCas9 showed immunoreactivity, confirming the humoral response raised against Cas9 orthologs similar to AAV injected mice (Figure A3.2A-B). All PBS-injected mice did not show any signs of IgGs against the recombinant Cas9 proteins that we tested (Figure A3.2C-D).

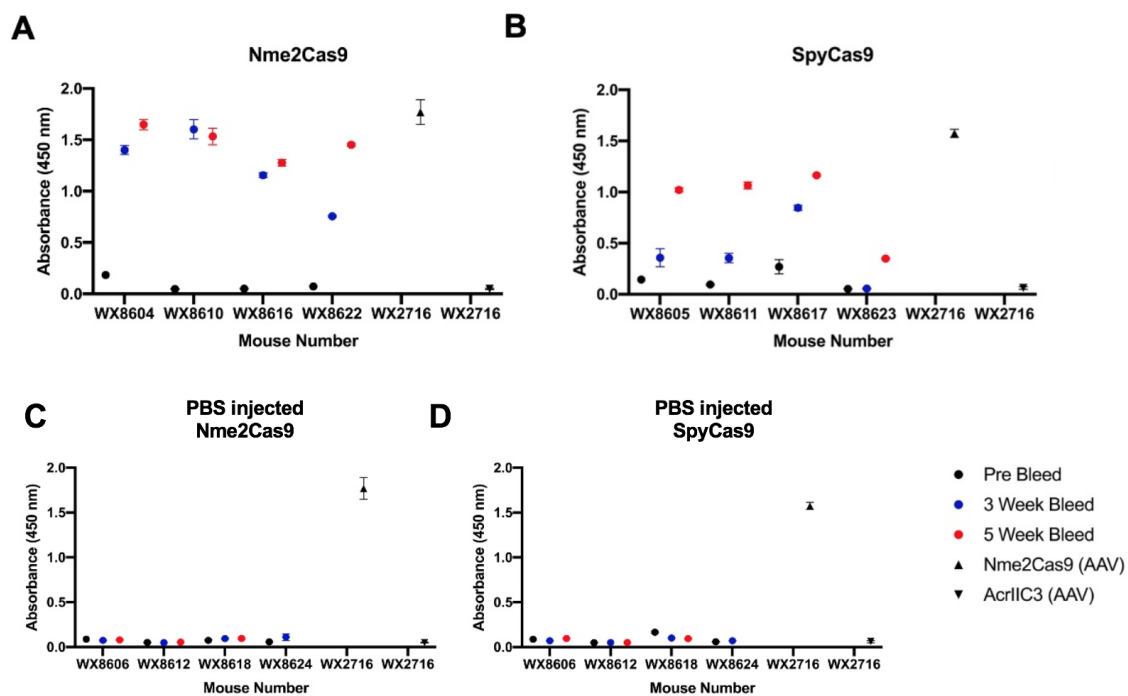


Figure A3.2 IgG immune response against Nme2Cas9 and SpyCas9 proteins. Serum was collected from each mouse injected with **(A)** Nme2Cas9 or **(B)** SpyCas9. Serum from 4 PBS injected mice were tested against **(C)** Nme2Cas9 and **(D)** SpyCas9 as well. As a reference, we plotted Nme2Cas9 (AAV) and AcrIIC3 (AAV) serum samples from mouse WX2716 injected with AAV from the previous experiment in Chapter 4 and used here as positive and negative controls, respectively.

Next, we assessed whether IgG immunoglobulins were raised against anti-CRISPR proteins that were introduced into mice by subcutaneous injection. We did not see significant signals for each of the tested anti-CRISPR proteins for most mice (Figure A3.3A-C), corroborating our results from mice that were injected with AAV. All PBS injected mice did not show any signs of IgGs against any of the recombinant proteins we tested (Figure A3.3D-F).

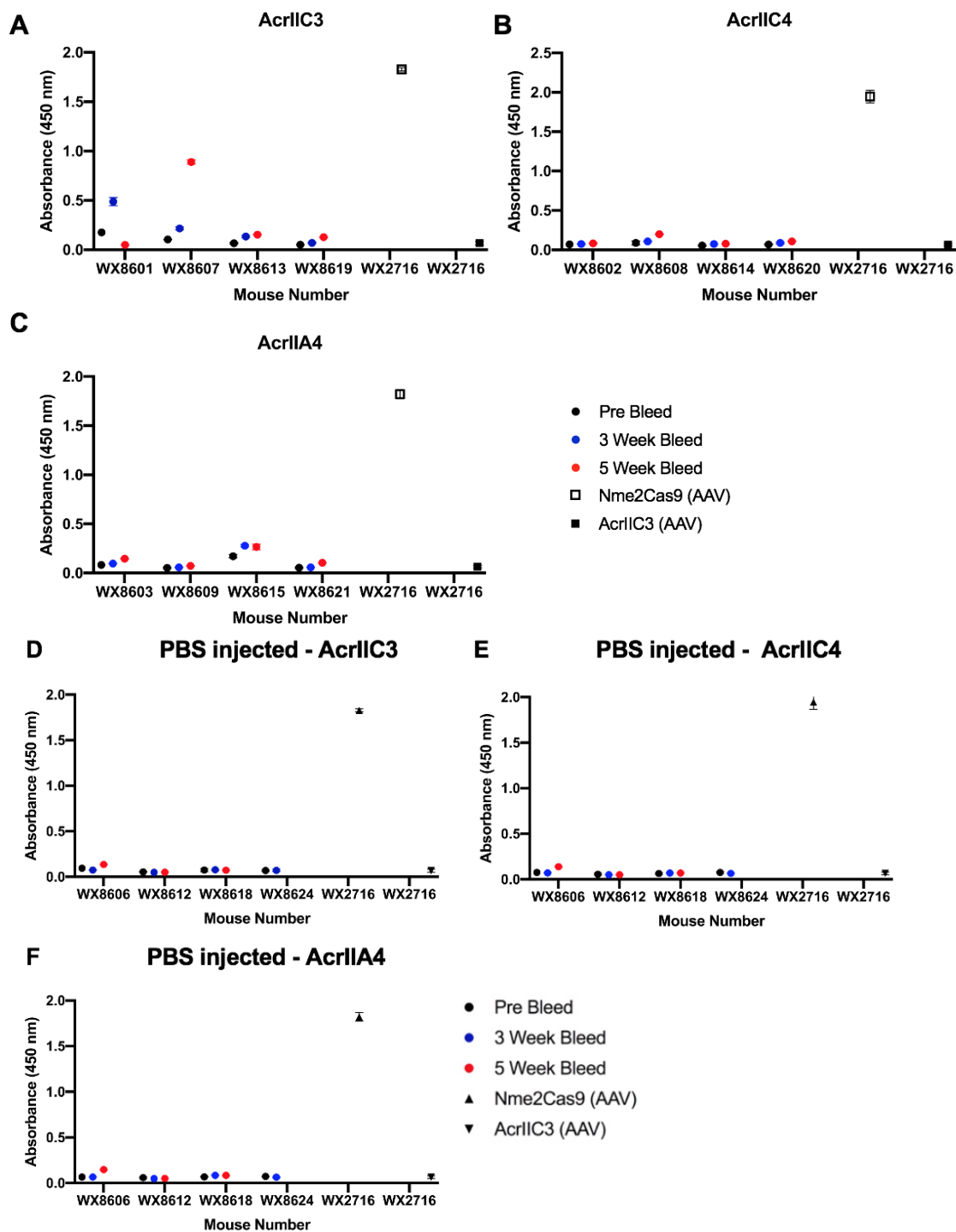


Figure A3.3 IgG immune response against anti-CRISPR recombinant proteins.

Serum was tested against **(A)** AcrIIIC3, **(B)** AcrIIC4, and **(C)** AcrIIA4 for any presence of IgG. Sera collected from PBS injected mice were also tested against **(D)** AcrIIC3, **(E)** AcrIIC4, and **(F)** AcrIIA4. Samples from an AAV-injected mouse (WX2716) were used as a reference for positive and negative signals.

A3.2 Future directions

Previous studies raised concern over pre-existing adaptive immunity against Cas9 (Charlesworth et al., 2019; A. Li et al., 2020; Simhadri et al., 2018; Wagner et al., 2019). Immune responses to Cas9 or anti-CRISPR proteins can be problematic as antibodies raised against the proteins can result in their clearance, affect their activities, have cross-reactivity with endogenous proteins, and cause anaphylactic reactions in serious cases (Sauna et al., 2018). From our preliminary studies on the immunogenicity of anti-CRISPR proteins, we primarily investigated the presence of IgGs using ELISA assays. However, we note that more systematic studies must be conducted to provide more conclusive evidence for the lack of antibodies against anti-CRISPR proteins. Since the anti-CRISPR proteins are much smaller than Cas9 proteins, ELISA optimization such as coating conditions may be necessary.

Moreover, future studies will require conducting assays for a comprehensive understanding of both humoral and cellular immunity. We used two different delivery methods: intravenous injection of AAV and subcutaneous injection of recombinant proteins. In the former case, delivery of AAV encoding DNA would produce intracellular proteins, and the peptides could potentially be processed by major histocompatibility complex (MHC) class I to elicit a cytotoxic CD8⁺ T cell response. In the latter, directly delivered exogenous proteins could potentially be

processed by MHC class II and engage with CD4+ T cells to elicit an antibody response.

Overall, whether there is a clinical relevance of humoral and cellular responses and how these may impact the efficacy and safety of CRISPR and anti-CRISPR reagents remains to be evaluated.

Appendix 4 Muscle-specific genome editing *in vivo* for DMD

A4.2 Background on Duchenne's Muscular Dystrophy

In Chapter 4, we showed liver-specific genome editing using a miRNA-repressible anti-CRISPR system as a proof-of-principle. To continue expanding our platform, we envisioned a therapeutic application. A few criteria were considered for choosing the next therapeutic target:

1. Well-validated microRNAs
2. Availability of disease models (cell lines, mouse models)
3. AAV deliverables

Tissue-specific editing is even more critical when therapeutic reagents must be delivered systemically to tissues impacted throughout the body such as in Duchenne's muscular dystrophy (DMD). DMD is a muscle degenerative disease affecting 1 in 5,000 newborn males every year in the United States (McGreevy et al., 2015; Mendell & Lloyd-Puryear, 2013). DMD arises from mutations in the dystrophin gene (*Dmd*), which is located on the X chromosome and is comprised of 79 exons. Diverse types of mutations are found in a large cohort of patients: deletion, insertion, duplication, or point mutations that change the reading frame or result in a premature stop codon (Flanigan et al., 2009). The current genetic interventions such as antisense oligonucleotides to skip mutated exons, delivery of mini-/micro-dystrophin, and CRISPR-Cas9-mediated exon deletion (Duan, 2018; Mendell & Rodino-Klapac, 2016; Mitropant et al., 2009), produce partially

functional proteins to create a less severe Becker muscular dystrophy phenotype. Since there is 1) a list of well-validated miRNAs that are expressed in high abundance specifically in muscle (e.g. miR-1), 2) availability of multiple murine models of DMD (e.g. *mdx*), and 3) a myriad of examples of CRISPR technologies being developed in the field using AAV, testing the miRNA-repressible strategy in cardiac/skeletal muscles as a new therapeutic target would be desirable. To this end, we decided to pursue therapeutic genome editing for DMD.

Exon skipping and deletion are two common strategies for therapeutic DMD gene correction that are currently being developed using CRISPR-Cas9 (Min et al., 2018) (Figure A4.1). Both strategies rely on the observation of a relatively mild disease course of Becker Muscular Dystrophy (BMD) patients with deletion mutations. This is also supported by the capacity of FDA-approved ASO drugs for DMD which mask splice donor or acceptor sequences of mutated exons in dystrophin mRNA to restore biologically active dystrophin proteins in humans (Kinali et al., 2009; van Deutekom et al., 2007).

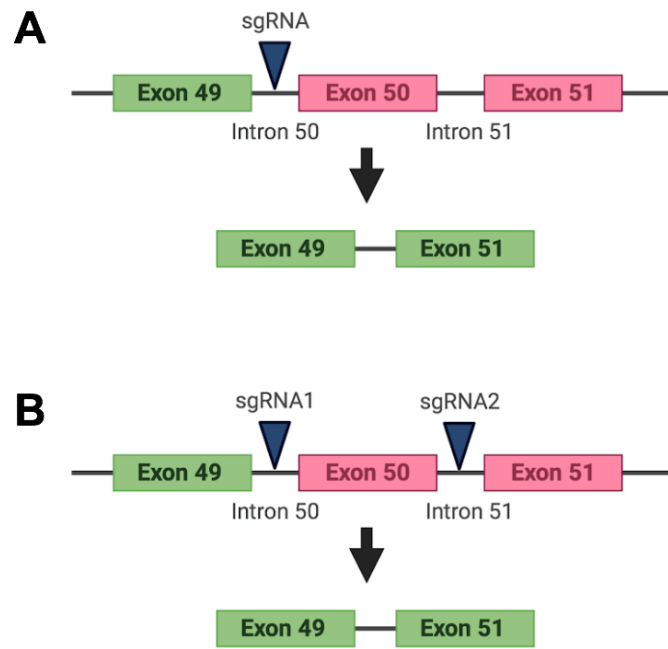


Figure A4.1 Two strategies for the therapeutic targeting of DMD. (A) Skipping of the mutated exon 50 in *Dmd* using a single sgRNA targeting the intron 50 is shown as an example. **(B)** Two sgRNAs targeting introns 50 and 51 flanking the mutated exon 50 will delete out the exon 50.

A4.2 Exon skipping strategy for therapeutic editing in DMD

With the initial success of CRISPR-Cas9 gene editing to induce exon skipping (Long et al., 2016; Nelson et al., 2016), different mutated exons have become targets of such a strategy with a prominent example of targeting exon 51 using SpyCas9 showing efficacy in preclinical studies of large animal models (Amoasii et al., 2018; Moretti et al., 2020). As rapid advances in a clinical setting are projected, we aim to incorporate highly accurate Nme2Cas9 and miRNA-repressible anti-CRISPR as safety measures. First, we designed several target sites in exon 51 for Nme2Cas9 that, in theory, should disrupt exonic splicing enhancer (ESE) elements and induce skipping of exon 51 (Figure A4.2A). To screen a highly active sgRNA we transfected HEK293T cells with seven different sgRNAs for Nme2Cas9 and measured editing efficiencies at each target site by targeted deep-sequencing (Figure A4.2B). We also included two validated SpyCas9 sgRNAs to use as a benchmark for Nme2Cas9 editing. Out of seven Nme2Cas9 sgRNAs, two (sgRNA #3 and 6) showed editing levels comparable to that of SpyCas9 (Figure A4.2B).

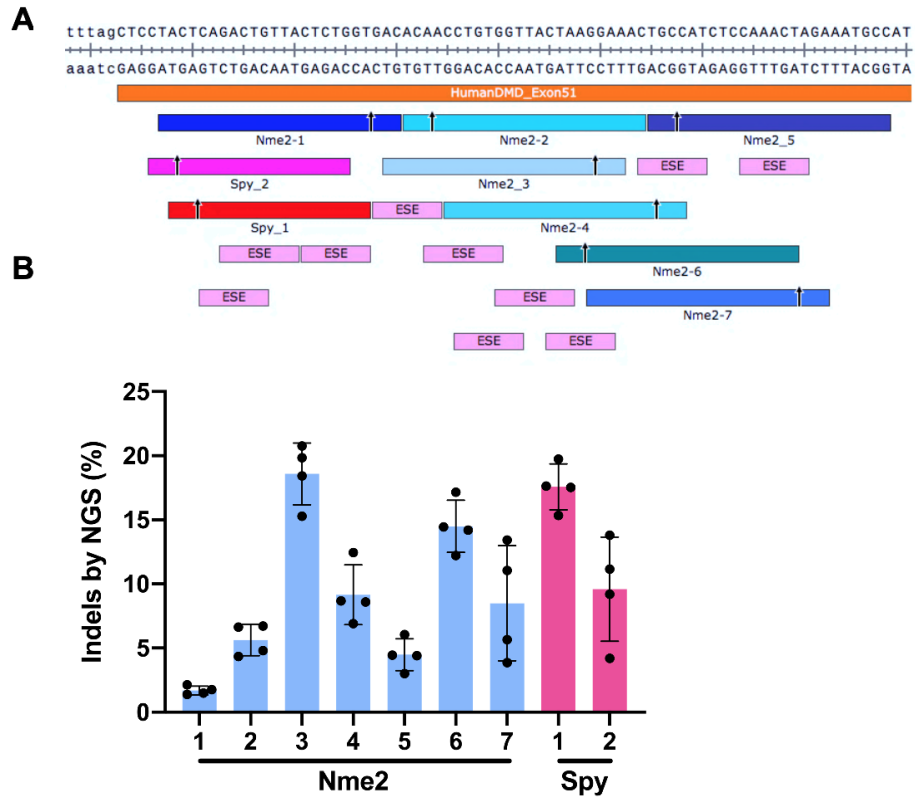


Figure A4.2 Exon 51 skipping strategy: target site design and validation. (A) Target sites for Nme2Cas9 and SpyCas9 for skipping exon 51. ESE, an exonic splicing enhancer annotated in Amoassi et al. (2017). Arrows indicate the cleavage site for Cas9. **(B)** Editing efficiency of each sgRNA for Nme2Cas9 and SpyCas9 is measured by targeted deep sequencing. Four biological replicates (N=4).

A4.3 Exon deletion strategy for therapeutic editing in DMD

As an alternative to exon skipping using a single sgRNA, two sgRNAs can be used simultaneously for introducing an exon deletion (Tabebordbar et al., 2016) (Figure A4.1B). Initially, we used a scAAV that expresses a single sgRNA driven by a U6 promoter along with a miRNA-repressible anti-CRISPR expression cassette (Figure A4.3A). Since scAAV has a packaging limit of ~2.5 kb, the current vector design can accommodate an extra sgRNA-expression cassette. Even after the addition of a second sgRNA, the “dual sgRNA scAAV” vector is ~2.4 kb, which is well within the packaging capacity (Figure A4.3B). To minimize recombination between highly similar sequences, we can take advantage of other pol III promoters such as the H1 promoter instead of U6.

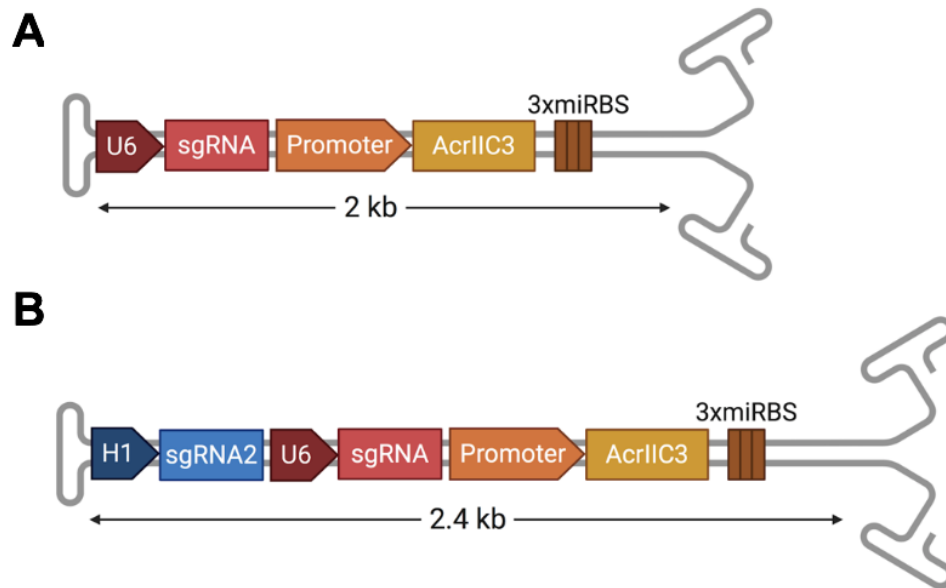


Figure A4.3 Exon deletion strategy: a design of a scAAV vector encoding two guides. (A) A schematic of a scAAV encoding a U6 driven sgRNA and a separate promoter driving AcrIIIC3 as in the original vector design. **(B)** A schematic of a scAAV encoding an additional H1 driven sgRNA cassette along with U6-sgRNA and anti-CRISPR expression cassettes.

A4.4 Future directions

To extend the existing platform for therapeutic application, we aimed to repurpose our tools to reinforce muscle-specific editing, which will greatly facilitate the treatment of DMD by Cas9. Following *in vitro* validation of guide RNAs in HEK293T cells, top-performing sgRNAs must be assessed to determine if the editing outcome indeed results in the skipping of exon 51 at the transcript level and truncated dystrophin at the protein level in relevant cell types. The next step is to test the sgRNAs in human patient-derived induced pluripotent stem cells (iPSCs) for evaluating exon skipping efficiency in differentiated myocytes. Lastly, it would be important to test whether myomiRs regulate the anti-CRISPR regulation in muscle cell lineages. Based on our preliminary data as well as another study showing myocyte-specific editing using miR-1 (Hoffmann et al., 2019), myomiR-repressible anti-CRISPR proteins (with miR-1 or miR-208) will be feasible for *in vivo* context for evaluating the efficacy in *mdx* or other DMD mouse models for AAV dual delivery as we have previously done for liver-specific editing.

In addition to multiplexing sgRNAs in a scAAV, MREs themselves can be easily swapped for targeting different tissues; for example, neuronal miRNAs such as astrocyte-specific miRNAs for targeting GFAP in Alexander disease (Jovičić et al., 2013) or endothelial cell-specific miR-126 for targeting cardiovascular diseases (S. Wang et al., 2008). Furthermore, the platform can be extended to

multiple tissues that are affected by a genetic disease, necessitating systemic delivery of therapeutic reagents as in the case of a Muscle-eye-brain (MEB) disease, also known as muscular dystrophy-dystroglycanopathy congenital with brain and eye anomalies A3 (MDDGA3). By multiplexing different miRNAs, for example, such as muscle- and brain- targeting miRNAs, we can restrict CRISPR-mediated genome editing to muscles and brain while avoiding off-target tissue editing in other tissues such as the liver. Numerous applications can be explored.

Appendix Table 1. Protein sequences of anti-CRISPR and Cas9

	Amino acid sequence (N→C)
<i>AcrIIC1_{Boe}</i>	MAKEVFKLKPELVTYKGCWALACIKDGEIIDLTYVRDLGIEEYDENFDGLEPEIYYDV VASQACKEVAYRYEEMGEFTFGLCSCWEFNVM
<i>AcrIIC1_{Nme}</i>	MANKTYKIGKNAGYDGCGLCLAAISENEAIKVKYLRDICPDYDGDKAEDWLRWGTDS RVKAAALEMEQYAYTSVGMASCWEFVEL
<i>AcrIIC2_{Nme}</i>	MASKNNIFNKYPTIIHGEARGENDEFVVHTRYPRFLARKSFDDNFTGEMPAKPVNGEL GQIGEPRLAYDSRLGLWLSDFIMLDNNKPKNMEWDLGQLKAACDRIAADDLMLNED AADLEGWDD
<i>AcrIIC3_{Nme}</i>	MAFKRAIIFTSFNGFEKVSRTKRRLAKIINARVSIIDEYLRAKDTNASLDGQYRAFLFN DESPAMTEFLAKLKAFASCTGISIDAWIEESEYVRLPVERRDFLAAANGKEIFKI
<i>AcrIIC4_{Hpa}</i>	MKITSSNFATIATSENFAKLSVLPKNHREPIKGLFKSAVEQFSSARDFFKNENYSKELAE KFNKEAVNEAVEKQLQKAIDLAEKQGIQF
<i>AcrIIC5_{Smu}</i>	MNNSIKFHVSYDGTARALFNTKEQAKEYCLVEEINDEMNGYKRKSWEEKLREENCAS VQDWVEKNYTSYSDFNICEIEVSSAGQLVKIDNTEVDDFVENCYGFTLEDDLEEFNK AKQYLQKFYAECEN
<i>HpaCas9</i>	MENKNLNYILGLDLGASVGVAVVEIDKENPLRLIDVGVRTFERAEVPKTGESLALS RLARSARRLTQRRVARLKAKRLLKSENILLSTDERLPHQVWQLRVEGLDHLKLERQEW AAVLLHLIKHRGYLSQRKNESKSENKELGALLSGVDNNHKLQKQATYRSPAELAVKKF EVEEGHIRNQQGAYTHTFSRLDLLAEMELLFSRQQHFGNPFASEKLENLTALLMWQK PALSGEAILKMLGKCTFEDEYKAAKNTYSAERFVWITKLNLRQENGLERALNDNERL ALMEQPYDKNRLFYSQVRSILKLSDEAIFKGLRYSGEDKKAIEKAVLMEMKAYHQIRK VLEGNNLKAWEAELKANPTLLDEIGTAFSLYKTDEDISAYLAGKLSQPVLNALLNLSFD KFIQLSLKALYKLLPLMQQGLRYDEACREIYGDHYGKKTEENHFLPQIPADEIRNPVVL RTLQARKVINGVVRLYGSPARIHIETGREVGKSYKDRRELEKQREENRKQRENAIKF KEYFPHFAGEPKAKDILKMRLYKQNAKCLYSGKPIELHRLLEKGYVEVDHALPFSRT WDDSFNNKVLVLANENQNKGNLTPFEWLDGKHNSERWRAFALVETSAPFYAKKQRI LSQKLEDEKGFIERNLNDTRYVARFLCNFIADNMHLTGEGKRKVFASNGQITALLRSRW GLAKSREDNDRHHALDAVVVACSTVAMQQKITRFVFEAGDVFTGERIDRETGEIPLH FPTPWQFFKQEVEIRIFSDNPKLELENRPLDRPQANHEFVQPLFVSRMPTRKMTGGG HMETVKSARKLNEGISVIKMLPTKLKLDLELMVNREREKLDYDTLAKARLEAFNDPAK AFAEPFIKGGGAIVKSVRVEQIQKSGVLVREGNGVADNASMVRVDVFTKGGKYFLVPIY TWQVAKGILPNKAATQYKDEEDWEVMDNSATFKFSLHPNDLVKLVTKKTLGYFNGL NRATGNIDIKEHDLKSKGKQGFIFEGVIGIKLALSFEKYQVDELGKNIRLCKPSKRQPVV
<i>SmuCas9</i>	MMMEKFHYVLGLDLGASVGVAAIEIDKETETSIGLLDCGVRTFERAEVPKTGDSLAKA RREARSTRRLIRRRSHRLLRLKRLKREIFRQPETFKDLPINAWQLRVKGLDSRLNEYE WAAVLLHLVKHRGYLSQRKSEMSETDSKSEMGRLLAGVAENHQLLQEQYRTPAELA LKKFVKHFRNKGGDYAHTFNRLDLQAEHLHLLFQKQRELGNPFTSPELERQVDDLLMTQ RSALQGDAIKMLGHCGFEPEQFKAANKTFSAEFIWLTCLNLRQDQGGKERALTAD ERTKLLDEPYKKSCLTYAQRKLLSLPQTAIFKGLRYDLEHDKKAENSTLMEMKSYHNI RQTEKSGLKTEWQSIATQPEILDAIGTAFSIYKTDEDISHELKTCRLPENVLNELLKNIN FDGFIQLSLTALRKILPLMEQGYRYDEACTQIYGNHHSGLSQEQSKFLPHIPIDDVRN PVVFRTLQARKVVNAIIRRYGSPARVHIEMARELGKSKSDRDRIEQQQKNKKEREN AVAKFKEDFPDFVGEPRGKDILKMRLYEQQHGKCLYSGHDIDINRLNEKGYVEIDHALP FSRTWDDSQNNKVLVLGSENQNKRNQTPDEYLDGANNQSRWLEFQARVQTCHFSY GKKQRIQLAKLDDETEKGFLERNLNDTRYIARFMCQFVQENLYLTGKGRKLVFASNGG MTATLRNLWGLRKYREDNDRHHALDAIVVACSTASMQQKITKAFRHFESIEYVDTEG EVKFRIPQPWDFRQEVMIKRVFSDQPCEDLVEKLSARPEALHNVTRPLSVRAPNRMK SGQGHELETIKSARKLSEENSMVKKPLTTLKLDIPEIVGYPSREPQLYAALKTRLETHDD DPIKAFKPFYKPNKNGELGALVRSVRVKGQNTGVMVHDGKGIADNATMVRVDVYT KAGKNYLVVYVWQVAQGILPNRAVTSKSEADWDLIDESFEFKFSLSRGDLVEMISN KGRIFGYNGLDRANGSIGIREHDLEKSKGKDGVHRVGVKTATAFNKYHVDPLGKEIH RCSSEPRPTLKIKSKK

Appendix Table 2. Plasmids used in Chapters 2, 3, and 4

Addgene #	Plasmid Name
Chapter 2	
87448	pEJS424-pCDEST2-NmeCas9-NLS-3XHA-NLS
85750	pEJS482-pCDEST2-AcrIIIC3Nme-mTagBFP2-IRES
85749	pEJS481-pCDEST2-AcrE2-mTagBFP2-IRES
85748	pEJS507-pCDEST2-noAcr-mTagBFP2-IRES
85717	pEJS477-pHAGE-TO-Spy dCas9 3XmCherry-SgRNA/Telomere-All-in-one
85716	pEJS476-pHAGE-TO-Nme dCas9 3XGFP-SgRNA/Telomere-All-in-one
85715	pEJS469-pLK.O1-SpySgRNA/DTS13-Telomere
85714	pEJS468-pLK.O1-NmeSgRNA/DTS13-Telomere
85713	pEJS443-pCDEST2-AcrIIIC3Nme
85712	pEJS436-pCDEST2-AcrIIIC2Nme
85679	pEJS433-pCDEST2-AcrIIIC1Nme
85678	pEJS430-pCDEST2-AcrIIIC1Boe
85677	pEJS427-pCDEST2-AcrE2
121541	pEJS1027-pMCSG7-SmuCas9
121540	pEJS1026-pMCSG7-HpaCas9
113441	pEJS664-pMCSG7-AcrIIIC5Smu
113440	pEJS663-pMCSG7-AcrIIIC4Hpa
113439	pEJS593-pCDEST2-AcrIIIC5Smu-BFPv2-IRES
113438	pEJS592-pCDEST2-AcrIIIC4Hpa-BFPv2-IRES
113437	pEJS583-pCDEST2-AcrIIIC5Smu-FLAG-NLS
113436	pEJS581-pCDEST2-AcrIIIC4Hpa-FLAG-NLS
113435	pEJS542-pCDEST2-AcrIIIC5Smu
113434	pEJS540-pCDEST2-AcrIIIC4Hpa
136514	pEJS1005-Lenti-mammalian c.o.AcrIIA5-FLAG-NLS-HygR
136513	pEJS1004-pCDEST2-AcrIIA5-NLS-FLAG
Chapter 3	
	pEJS430-pCDEST-AcrIIIC1-Boe
	pEJS433-pCDEST-AcrIIIC1-Nme
	pEJS436-pCDEST-AcrIIIC2-Nme
	pEJS443-pCDEST-AcrIIIC3-Nme
	pEJS540-pCDEST-AcrIIIC4-Hpa
	pEJS542-pCDEST-AcrIIIC5-Smu
	pEJS2-M427-stuffer plasmid
	pEJS323-pSimpleII-NmeCas9 SgRNA-N-T25
	pEJS324-pSimpleII-NmeCas9 R1025A SgRNA-N-TS25
	pEJS326-pSimpleII-N-termZinf268-NmeCas9 SgRNA-N-TS125
	pEJS327-pSimpleII-N-termZinf268-NmeCas9 R1025A SgRNA-N-TS25
	pEJS758-pCDEST2-SpyCas9-hGem
	pEJS24-pCDEST2-SpyCas9
	pEJS1004-pCDEST2-AcrIIA5-FLAG-NLS
	pEJS1033-pLenti-AcrIIA5-hCdt1-HygR
	pEJS716-GFP Donor plasmid
	pEJS760-pLKO.1-Spy-sgRNA-mTLR(STS118)
Chapter 4	
129534	pEJS1195-pssAAV.U1a.hNme2Cas9
129532	pEJS1194-scAAV-U6-Rosa26sgR_Nme2Cas9_CB-PI-AcrIIA4_FLAG-NLS
129531	pEJS1193-scAAV-U6-Rosa26sgR_Nme2Cas9_CB-PI-AcrIIIC3_FLAG-NLS-3XmiR122BS
129530	pEJS1192-scAAV-U6-Rosa26sgR_Nme2Cas9_CB-PI-AcrIIIC3_FLAG-NLS
126205	pEJS1149-pCDEST-AcrIIA4-mCherry-miR122BS
126204	pEJS1148-pCDEST-AcrIIA4-mCherry
126203	pEJS1147-pCDEST-AcrIIIC3Nme-mCherry-miR122BS

References

- Abudayyeh, O. O., Gootenberg, J. S., Essletzbichler, P., Han, S., Joung, J., Belanto, J. J., Verdine, V., Cox, D. B. T., Kellner, M. J., Regev, A., Lander, E. S., Voytas, D. F., Ting, A. Y., & Zhang, F. (2017). RNA targeting with CRISPR-Cas13. *Nature*, *550*(7675), 280–284.
- Ackerman, C. M., Myhrvold, C., Thakku, S. G., Freije, C. A., Metsky, H. C., Yang, D. K., Ye, S. H., Boehm, C. K., Kosoko-Thoroddsen, T.-S. F., Kehe, J., Nguyen, T. G., Carter, A., Kulesa, A., Barnes, J. R., Dugan, V. G., Hung, D. T., Blainey, P. C., & Sabeti, P. C. (2020). Massively multiplexed nucleic acid detection with Cas13. *Nature*. <https://doi.org/10.1038/s41586-020-2279-8>
- Adli, M. (2018). The CRISPR tool kit for genome editing and beyond. *Nature Communications*, *9*(1), 1911.
- Alanis-Lobato, G., Zohren, J., McCarthy, A., Fogarty, N. M. E., Kubikova, N., Hardman, E., Greco, M., Wells, D., Turner, J. M. A., & Niakan, K. K. (2020). Frequent loss-of-heterozygosity in CRISPR-Cas9-edited early human embryos. In *bioRxiv* (p. 2020.06.05.135913). <https://doi.org/10.1101/2020.06.05.135913>
- Amabile, A., Migliara, A., Capasso, P., Biffi, M., Cittaro, D., Naldini, L., & Lombardo, A. (2016). Inheritable Silencing of Endogenous Genes by Hit-and-Run Targeted Epigenetic Editing. *Cell*, *167*(1), 219–232.e14.
- Ameres, S. L., Horwich, M. D., Hung, J.-H., Xu, J., Ghildiyal, M., Weng, Z., & Zamore, P. D. (2010). Target RNA-Directed Trimming and Tailing of Small Silencing RNAs. In *Science* (Vol. 328, Issue 5985, pp. 1534–1539). <https://doi.org/10.1126/science.1187058>
- Amoasii, L., Hildyard, J. C. W., Li, H., Sanchez-Ortiz, E., Mireault, A., Caballero, D., Harron, R., Stathopoulou, T.-R., Massey, C., Shelton, J. M., Bassel-Duby, R., Piercy, R. J., & Olson, E. N. (2018). Gene editing restores dystrophin expression in a canine model of Duchenne muscular dystrophy. *Science*, *362*(6410), 86–91.
- Amrani, N., Gao, X. D., Liu, P., Edraki, A., Mir, A., Ibraheim, R., Gupta, A., Sasaki, K. E., Wu, T., Donohoue, P. D., Settle, A. H., Lied, A. M., McGovern, K., Fuller, C. K., Cameron, P., Fazzio, T. G., Zhu, L. J., Wolfe, S. A., & Sontheimer, E. J. (2018). NmeCas9 is an intrinsically high-fidelity genome-editing platform. *Genome Biology*, *19*(1), 214.
- An, S. Y., Ka, D., Kim, I., Kim, E.-H., Kim, N.-K., Bae, E., & Suh, J.-Y. (2020). Intrinsic disorder is essential for Cas9 inhibition of anti-CRISPR AcrIIA5. *Nucleic Acids Research*. <https://doi.org/10.1093/nar/gkaa512>
- Anzalone, A. V., Koblan, L. W., & Liu, D. R. (2020). Genome editing with CRISPR-Cas nucleases, base editors, transposases and prime editors. *Nature Biotechnology*. <https://doi.org/10.1038/s41587-020-0561-9>
- Anzalone, A. V., Randolph, P. B., Davis, J. R., Sousa, A. A., Koblan, L. W., Levy, J. M., Chen, P. J., Wilson, C., Newby, G. A., Raguram, A., & Liu, D. R. (2019). Search-and-replace genome editing without double-strand breaks or

- donor DNA. *Nature*, 576(7785), 149–157.
- Araki, M., & Ishii, T. (2014). International regulatory landscape and integration of corrective genome editing into in vitro fertilization. *Reproductive Biology and Endocrinology: RB&E*, 12, 108.
- Arias, E. E., & Walter, J. C. (2007). Strength in numbers: preventing rereplication via multiple mechanisms in eukaryotic cells. *Genes & Development*, 21(5), 497–518.
- Aschenbrenner, S., Kallenberger, S. M., Hoffmann, M. D., Huck, A., Eils, R., & Niopek, D. (2020). Coupling Cas9 to artificial inhibitory domains enhances CRISPR-Cas9 target specificity. *Science Advances*, 6(6), eaay0187.
- Athukoralage, J. S., McMahon, S. A., Zhang, C., Grüşchow, S., Graham, S., Krupovic, M., Whitaker, R. J., Gloster, T. M., & White, M. F. (2020). An anti-CRISPR viral ring nuclease subverts type III CRISPR immunity. *Nature*, 577(7791), 572–575.
- Baccarini, A., Chauhan, H., Gardner, T. J., Jayaprakash, A. D., Sachidanandam, R., & Brown, B. D. (2011). Kinetic analysis reveals the fate of a microRNA following target regulation in mammalian cells. *Current Biology: CB*, 21(5), 369–376.
- Baltimore, D., Berg, P., Botchan, M., Carroll, D., Charo, R. A., Church, G., Corn, J. E., Daley, G. Q., Doudna, J. A., Fenner, M., Greely, H. T., Jinek, M., Martin, G. S., Penhoet, E., Puck, J., Sternberg, S. H., Weissman, J. S., & Yamamoto, K. R. (2015). Biotechnology. A prudent path forward for genomic engineering and germline gene modification. *Science*, 348(6230), 36–38.
- Barkau, C. L., O'Reilly, D., Rohilla, K. J., Damha, M. J., & Gagnon, K. T. (2019). Rationally Designed Anti-CRISPR Nucleic Acid Inhibitors of CRISPR-Cas9. *Nucleic Acid Therapeutics*, 29(3), 136–147.
- Barrangou, R., Fremaux, C., Deveau, H., Richards, M., Boyaval, P., Moineau, S., Romero, D. A., & Horvath, P. (2007). CRISPR provides acquired resistance against viruses in prokaryotes. *Science*, 315(5819), 1709–1712.
- Bartel, D. P. (2018). Metazoan MicroRNAs. *Cell*, 173(1), 20–51.
- Basgall, E. M., Goetting, S. C., Goeckel, M. E., Giersch, R. M., Roggenkamp, E., Schrock, M. N., Halloran, M., & Finnigan, G. C. (2018). Gene drive inhibition by the anti-CRISPR proteins AcrIIA2 and AcrIIA4 in *Saccharomyces cerevisiae*. *Microbiology*, 164(4), 464–474.
- Becker, W. R., Ober-Reynolds, B., Jouravleva, K., Jolly, S. M., Zamore, P. D., & Greenleaf, W. J. (2019). High-Throughput Analysis Reveals Rules for Target RNA Binding and Cleavage by AGO2. *Molecular Cell*, 75(4), 741–755.e11.
- Bhoobalan-Chitty, Y., Johansen, T. B., Di Cianni, N., & Peng, X. (2019). Inhibition of Type III CRISPR-Cas Immunity by an Archaeal Virus-Encoded Anti-CRISPR Protein. In *Cell* (Vol. 179, Issue 2, pp. 448–458.e11). <https://doi.org/10.1016/j.cell.2019.09.003>
- Birkholz, N., Fagerlund, R. D., Smith, L. M., Jackson, S. A., & Fineran, P. C. (2019). The autoregulator Aca2 mediates anti-CRISPR repression. *Nucleic Acids Research*, 47(18), 9658–9665.

- Boisgerault, F., Gross, D.-A., Ferrand, M., Poupiot, J., Darocha, S., Richard, I., & Galy, A. (2013). Prolonged gene expression in muscle is achieved without active immune tolerance using microRNA 142.3p-regulated rAAV gene transfer. *Human Gene Therapy*, *24*(4), 393–405.
- Bolukbasi, M. F., Gupta, A., Oikemus, S., Derr, A. G., Garber, M., Brodsky, M. H., Zhu, L. J., & Wolfe, S. A. (2015). DNA-binding-domain fusions enhance the targeting range and precision of Cas9. *Nature Methods*, *12*(12), 1150–1156.
- Bolukbasi, M. F., Liu, P., Luk, K., Kwok, S. F., Gupta, A., Amrani, N., Sontheimer, E. J., Zhu, L. J., & Wolfe, S. A. (2018). Orthogonal Cas9-Cas9 chimeras provide a versatile platform for genome editing. *Nature Communications*, *9*(1), 4856.
- Bondy-Denomy, J. (2018). Protein Inhibitors of CRISPR-Cas9. *ACS Chemical Biology*, *13*(2), 417–423.
- Bondy-Denomy, J., Garcia, B., Strum, S., Du, M., Rollins, M. F., Hidalgo-Reyes, Y., Wiedenheft, B., Maxwell, K. L., & Davidson, A. R. (2015). Multiple mechanisms for CRISPR-Cas inhibition by anti-CRISPR proteins. *Nature*, *526*(7571), 136–139.
- Bondy-Denomy, J., Pawluk, A., Maxwell, K. L., & Davidson, A. R. (2013). Bacteriophage genes that inactivate the CRISPR/Cas bacterial immune system. *Nature*, *493*(7432), 429–432.
- Borges, A. L., Davidson, A. R., & Bondy-Denomy, J. (2017). The Discovery, Mechanisms, and Evolutionary Impact of Anti-CRISPRs. *Annual Review of Virology*, *4*(1), 37–59.
- Borges, A. L., Zhang, J. Y., Rollins, M. F., Osuna, B. A., Wiedenheft, B., & Bondy-Denomy, J. (2018). Bacteriophage Cooperation Suppresses CRISPR-Cas3 and Cas9 Immunity. *Cell*, *174*(4), 917–925.e10.
- Briner, A. E., Donohoue, P. D., Gomaa, A. A., Selle, K., Slorach, E. M., Nye, C. H., Haurwitz, R. E., Beisel, C. L., May, A. P., & Barrangou, R. (2014). Guide RNA functional modules direct Cas9 activity and orthogonality. *Molecular Cell*, *56*(2), 333–339.
- Brinkman, E. K., Chen, T., Amendola, M., & van Steensel, B. (2014). Easy quantitative assessment of genome editing by sequence trace decomposition. *Nucleic Acids Research*, *42*(22), e168.
- Broderick, J. A., & Zamore, P. D. (2011). MicroRNA therapeutics. *Gene Therapy*, *18*(12), 1104–1110.
- Brouns, S. J. J., Jore, M. M., Lundgren, M., Westra, E. R., Slijkhuis, R. J. H., Snijders, A. P. L., Dickman, M. J., Makarova, K. S., Koonin, E. V., & van der Oost, J. (2008). Small CRISPR RNAs guide antiviral defense in prokaryotes. *Science*, *321*(5891), 960–964.
- Brown, B. D., Venneri, M. A., Zingale, A., Sergi Sergi, L., & Naldini, L. (2006). Endogenous microRNA regulation suppresses transgene expression in hematopoietic lineages and enables stable gene transfer. *Nature Medicine*, *12*(5), 585–591.

- Bubeck, F., Hoffmann, M. D., Hartevelde, Z., Aschenbrenner, S., Bietz, A., Waldhauer, M. C., Börner, K., Fakhiri, J., Schmelas, C., Dietz, L., Grimm, D., Correia, B. E., Eils, R., & Niopek, D. (2018). Engineered anti-CRISPR proteins for optogenetic control of CRISPR-Cas9. *Nature Methods*, *15*(11), 924–927.
- Burstein, D., Harrington, L. B., Strutt, S. C., Probst, A. J., Anantharaman, K., Thomas, B. C., Doudna, J. A., & Banfield, J. F. (2017). New CRISPR-Cas systems from uncultivated microbes. *Nature*, *542*(7640), 237–241.
- Cameron, P., Coons, M. M., Klompe, S. E., Lied, A. M., Smith, S. C., Vidal, B., Donohoue, P. D., Rotstein, T., Kohrs, B. W., Nyer, D. B., Kennedy, R., Banh, L. M., Williams, C., Toh, M. S., Irby, M. J., Edwards, L. S., Lin, C.-H., Owen, A. L. G., Künne, T., ... Sternberg, S. H. (2019). Harnessing type I CRISPR–Cas systems for genome engineering in human cells. *Nature Biotechnology*, *37*(12), 1471–1477.
- Cameron, P., Fuller, C. K., Donohoue, P. D., Jones, B. N., Thompson, M. S., Carter, M. M., Gradia, S., Vidal, B., Garner, E., Slorach, E. M., Lau, E., Banh, L. M., Lied, A. M., Edwards, L. S., Settle, A. H., Capurso, D., Llaca, V., Deschamps, S., Cigan, M., ... May, A. P. (2017). Mapping the genomic landscape of CRISPR–Cas9 cleavage. *Nature Methods*, *14*(6), 600–606.
- Canny, M. D., Moatti, N., Wan, L. C. K., Fradet-Turcotte, A., Krasner, D., Mateos-Gomez, P. A., Zimmermann, M., Orthwein, A., Juang, Y.-C., Zhang, W., Noordermeer, S. M., Seclen, E., Wilson, M. D., Vorobyov, A., Munro, M., Ernst, A., Ng, T. F., Cho, T., Cannon, P. M., ... Durocher, D. (2018). Inhibition of 53BP1 favors homology-dependent DNA repair and increases CRISPR–Cas9 genome-editing efficiency. *Nature Biotechnology*, *36*(1), 95–102.
- Carey, K. T., & Wickramasinghe, V. O. (2018). Regulatory Potential of the RNA Processing Machinery: Implications for Human Disease. *Trends in Genetics: TIG*, *34*(4), 279–290.
- Carroll, D. (2014). Genome engineering with targetable nucleases. *Annual Review of Biochemistry*, *83*, 409–439.
- Carte, J., Wang, R., Li, H., Terns, R. M., & Terns, M. P. (2008). Cas6 is an endoribonuclease that generates guide RNAs for invader defense in prokaryotes. *Genes & Development*, *22*(24), 3489–3496.
- Certo, M. T., Ryu, B. Y., Annis, J. E., Garibov, M., Jarjour, J., Rawlings, D. J., & Scharenberg, A. M. (2011). Tracking genome engineering outcome at individual DNA breakpoints. *Nature Methods*, *8*(8), 671–676.
- Chapman, J. R., Taylor, M. R. G., & Boulton, S. J. (2012). Playing the end game: DNA double-strand break repair pathway choice. *Molecular Cell*, *47*(4), 497–510.
- Charlesworth, C. T., Deshpande, P. S., Dever, D. P., Camarena, J., Lemgart, V. T., Cromer, M. K., Vakulskas, C. A., Collingwood, M. A., Zhang, L., Bode, N. M., Behlke, M. A., Dejene, B., Cieniewicz, B., Romano, R., Lesch, B. J., Gomez-Ospina, N., Mantri, S., Pavel-Dinu, M., Weinberg, K. I., & Porteus, M. (2019). Efficient genome editing in human cells using CRISPR-Cas9. *Nature Biotechnology*, *37*(12), 1471–1477.

- M. H. (2019). Identification of preexisting adaptive immunity to Cas9 proteins in humans. *Nature Medicine*.
- Charpentier, E., Richter, H., van der Oost, J., & White, M. F. (2015). Biogenesis pathways of RNA guides in archaeal and bacterial CRISPR-Cas adaptive immunity. *FEMS Microbiology Reviews*, 39(3), 428–441.
- Charpentier, M., Khedher, A. H. Y., Menoret, S., Brion, A., Lamribet, K., Dardillac, E., Boix, C., Perrouault, L., Tesson, L., Geny, S., De Cian, A., Itier, J. M., Anegon, I., Lopez, B., Giovannangeli, C., & Concordet, J. P. (2018). CtIP fusion to Cas9 enhances transgene integration by homology-dependent repair. *Nature Communications*, 9(1), 1133.
- Chen, F., Alphonse, M., & Liu, Q. (2020). Strategies for nonviral nanoparticle-based delivery of CRISPR/Cas9 therapeutics. *WIREs Nanomedicine and Nanobiotechnology*, 12(3), 1.
- Cheng, A. W., Wang, H., Yang, H., Shi, L., Katz, Y., Theunissen, T. W., Rangarajan, S., Shivalila, C. S., Dadon, D. B., & Jaenisch, R. (2013). Multiplexed activation of endogenous genes by CRISPR-on, an RNA-guided transcriptional activator system. *Cell Research*, 23(10), 1163–1171.
- Chen, J. S., Ma, E., Harrington, L. B., Da Costa, M., Tian, X., Palefsky, J. M., & Doudna, J. A. (2018). CRISPR-Cas12a target binding unleashes indiscriminate single-stranded DNase activity. *Science*, 360(6387), 436–439.
- Chen, S. P., & Wang, H. H. (2019). An Engineered Cas-Transposon System for Programmable and Site-Directed DNA Transpositions. *The CRISPR Journal*, 2(6), 376–394.
- Chevallereau, A., Meaden, S., Fradet, O., Landsberger, M., Maestri, A., Biswas, A., Gandon, S., van Houte, S., & Westra, E. R. (2020). Exploitation of the Cooperative Behaviors of Anti-CRISPR Phages. *Cell Host & Microbe*, 27(2), 189–198.e6.
- Cho, S. W., Kim, S., Kim, J. M., & Kim, J.-S. (2013). Targeted genome engineering in human cells with the Cas9 RNA-guided endonuclease. *Nature Biotechnology*, 31(3), 230–232.
- Chu, V. T., Weber, T., Wefers, B., Wurst, W., Sander, S., Rajewsky, K., & Kühn, R. (2015). Increasing the efficiency of homology-directed repair for CRISPR-Cas9-induced precise gene editing in mammalian cells. *Nature Biotechnology*, 33(5), 543–548.
- Ciccia, A., & Elledge, S. J. (2010). The DNA damage response: making it safe to play with knives. *Molecular Cell*, 40(2), 179–204.
- Cong, L., Ran, F. A., Cox, D., Lin, S., Barretto, R., Habib, N., Hsu, P. D., Wu, X., Jiang, W., Marraffini, L. A., & Zhang, F. (2013). Multiplex genome engineering using CRISPR/Cas systems. *Science*, 339(6121), 819–823.
- Corbett, A. H. (2018). Post-transcriptional regulation of gene expression and human disease. *Current Opinion in Cell Biology*, 52, 96–104.
- Cox, D. B. T., Gootenberg, J. S., Abudayyeh, O. O., Franklin, B., Kellner, M. J., Joung, J., & Zhang, F. (2017). RNA editing with CRISPR-Cas13. *Science*, 358(6366), 1019–1027.

- Cress, B. F., Toparlak, Ö. D., Guleria, S., Lebovich, M., Stieglitz, J. T., Englaender, J. A., Jones, J. A., Linhardt, R. J., & Koffas, M. A. G. (2015). CRISPathBrick: Modular Combinatorial Assembly of Type II-A CRISPR Arrays for dCas9-Mediated Multiplex Transcriptional Repression in *E. coli*. *ACS Synthetic Biology*, 4(9), 987–1000.
- Crudele, J. M., & Chamberlain, J. S. (2018). Cas9 immunity creates challenges for CRISPR gene editing therapies. *Nature Communications*, 9(1), 3497.
- Davidson, A. R., Lu, W.-T., Stanley, S. Y., Wang, J., Mejdani, M., Trost, C. N., Hicks, B. T., Lee, J., & Sontheimer, E. J. (2020). Anti-CRISPRs: Protein Inhibitors of CRISPR-Cas Systems. *Annual Review of Biochemistry*. <https://doi.org/10.1146/annurev-biochem-011420-111224>
- de la Mata, M., Gaidatzis, D., Vitanescu, M., Stadler, M. B., Wentzel, C., Scheiffele, P., Filipowicz, W., & Großhans, H. (2015). Potent degradation of neuronal miRNAs induced by highly complementary targets. *EMBO Reports*, 16(4), 500–511.
- Deltcheva, E., Chylinski, K., Sharma, C. M., Gonzales, K., Chao, Y., Pirzada, Z. A., Eckert, M. R., Vogel, J., & Charpentier, E. (2011). CRISPR RNA maturation by trans-encoded small RNA and host factor RNase III. In *Nature* (Vol. 471, Issue 7340, pp. 602–607). <https://doi.org/10.1038/nature09886>
- Denzler, R., Agarwal, V., Stefano, J., Bartel, D. P., & Stoffel, M. (2014). Assessing the ceRNA hypothesis with quantitative measurements of miRNA and target abundance. *Molecular Cell*, 54(5), 766–776.
- Denzler, R., McGeary, S. E., Title, A. C., Agarwal, V., Bartel, D. P., & Stoffel, M. (2016). Impact of MicroRNA Levels, Target-Site Complementarity, and Cooperativity on Competing Endogenous RNA-Regulated Gene Expression. *Molecular Cell*, 64(3), 565–579.
- Deveau, H., Barrangou, R., Garneau, J. E., Labonté, J., Fremaux, C., Boyaval, P., Romero, D. A., Horvath, P., & Moineau, S. (2008). Phage response to CRISPR-encoded resistance in *Streptococcus thermophilus*. *Journal of Bacteriology*, 190(4), 1390–1400.
- Dolan, A. E., Hou, Z., Xiao, Y., Gramelspacher, M. J., Heo, J., Howden, S. E., Freddolino, P. L., Ke, A., & Zhang, Y. (2019). Introducing a Spectrum of Long-Range Genomic Deletions in Human Embryonic Stem Cells Using Type I CRISPR-Cas. *Molecular Cell*, 74(5), 936–950.e5.
- Dominguez, A. A., Lim, W. A., & Qi, L. S. (2016). Beyond editing: repurposing CRISPR-Cas9 for precision genome regulation and interrogation. *Nature Reviews. Molecular Cell Biology*, 17(1), 5–15.
- Dong, D., Guo, M., Wang, S., Zhu, Y., Wang, S., Xiong, Z., Yang, J., Xu, Z., & Huang, Z. (2017). Structural basis of CRISPR–SpyCas9 inhibition by an anti-CRISPR protein. *Nature*, 546(7658), 436–439.
- Doudna, J. A. (2020). The promise and challenge of therapeutic genome editing. *Nature*, 578(7794), 229–236.
- Duan, D. (2018). Systemic AAV Micro-dystrophin Gene Therapy for Duchenne Muscular Dystrophy. *Molecular Therapy: The Journal of the American*

- Society of Gene Therapy*, 26(10), 2337–2356.
- Duan, D., Sharma, P., Yang, J., Yue, Y., Dudus, L., Zhang, Y., Fisher, K. J., & Engelhardt, J. F. (1998). Circular intermediates of recombinant adeno-associated virus have defined structural characteristics responsible for long-term episomal persistence in muscle tissue. *Journal of Virology*, 72(11), 8568–8577.
- Duan, D., Yan, Z., Yue, Y., & Engelhardt, J. F. (1999). Structural analysis of adeno-associated virus transduction circular intermediates. *Virology*, 261(1), 8–14.
- Ebert, M. S., Neilson, J. R., & Sharp, P. A. (2007). MicroRNA sponges: competitive inhibitors of small RNAs in mammalian cells. *Nature Methods*, 4(9), 721–726.
- Edraki, A., Mir, A., Ibraheim, R., Gainetdinov, I., Yoon, Y., Song, C.-Q., Cao, Y., Gallant, J., Xue, W., Rivera-Pérez, J. A., & Sontheimer, E. J. (2018). A Compact, High-Accuracy Cas9 with a Dinucleotide PAM for In Vivo Genome Editing. *Molecular Cell*.
- Eitzinger, S., Asif, A., Watters, K. E., Iavarone, A. T., Knott, G. J., Doudna, J. A., & Minhas, F. U. A. A. (2020). Machine learning predicts new anti-CRISPR proteins. *Nucleic Acids Research*, 48(9), 4698–4708.
- Esvelt, K. M., Mali, P., Braff, J. L., Moosburner, M., Yaung, S. J., & Church, G. M. (2013). Orthogonal Cas9 proteins for RNA-guided gene regulation and editing. *Nature Methods*, 10(11), 1116–1121.
- Fajrial, A. K., He, Q. Q., Wirusanti, N. I., Slansky, J. E., & Ding, X. (2020). A review of emerging physical transfection methods for CRISPR/Cas9-mediated gene editing. *Theranostics*, 10(12), 5532–5549.
- Finn, J. D., Smith, A. R., Patel, M. C., Shaw, L., Youniss, M. R., van Heteren, J., Dirstine, T., Ciullo, C., Lescarbeau, R., Seitzer, J., Shah, R. R., Shah, A., Ling, D., Grove, J., Pink, M., Rohde, E., Wood, K. M., Salomon, W. E., Harrington, W. F., ... Morrissey, D. V. (2018). A Single Administration of CRISPR/Cas9 Lipid Nanoparticles Achieves Robust and Persistent In Vivo Genome Editing. *Cell Reports*, 22(9), 2227–2235.
- Flanigan, K. M., Dunn, D. M., von Niederhausern, A., Soltanzadeh, P., Gappmaier, E., Howard, M. T., Sampson, J. B., Mendell, J. R., Wall, C., King, W. M., Pestronk, A., Florence, J. M., Connolly, A. M., Mathews, K. D., Stephan, C. M., Laubenthal, K. S., Wong, B. L., Morehart, P. J., Meyer, A., ... Weiss, R. B. (2009). Mutational spectrum of DMD mutations in dystrophinopathy patients: application of modern diagnostic techniques to a large cohort. *Human Mutation*, 30(12), 1657–1666.
- Fogarty, N. M. E., McCarthy, A., Snijders, K. E., Powell, B. E., Kubikova, N., Blakeley, P., Lea, R., Elder, K., Wamaitha, S. E., Kim, D., Maciulyte, V., Kleinjung, J., Kim, J.-S., Wells, D., Vallier, L., Bertero, A., Turner, J. M. A., & Niakan, K. K. (2017). Genome editing reveals a role for OCT4 in human embryogenesis. *Nature*, 550(7674), 67–73.
- Fonfara, I., Le Rhun, A., Chylinski, K., Makarova, K. S., Lécrivain, A.-L.,

- Bzdrenga, J., Koonin, E. V., & Charpentier, E. (2014). Phylogeny of Cas9 determines functional exchangeability of dual-RNA and Cas9 among orthologous type II CRISPR-Cas systems. *Nucleic Acids Research*, *42*(4), 2577–2590.
- Forsberg, K. J., Bhatt, I. V., Schmidtke, D. T., Javanmardi, K., Dillard, K. E., Stoddard, B. L., Finkelstein, I. J., Kaiser, B. K., & Malik, H. S. (2019). Functional metagenomics-guided discovery of potent Cas9 inhibitors in the human microbiome. *eLife*, *8*. <https://doi.org/10.7554/eLife.46540>
- Franco-Zorrilla, J. M., Valli, A., Todesco, M., Mateos, I., Puga, M. I., Rubio-Somoza, I., Leyva, A., Weigel, D., García, J. A., & Paz-Ares, J. (2007). Target mimicry provides a new mechanism for regulation of microRNA activity. *Nature Genetics*, *39*(8), 1033–1037.
- Fuchs Wightman, F., Giono, L. E., Fededa, J. P., & de la Mata, M. (2018). Target RNAs Strike Back on MicroRNAs. *Frontiers in Genetics*, *9*, 435.
- Fukuhara, T., Kambara, H., Shiokawa, M., Ono, C., Katoh, H., Morita, E., Okuzaki, D., Maehara, Y., Koike, K., & Matsuura, Y. (2012). Expression of MicroRNA miR-122 Facilitates an Efficient Replication in Nonhepatic Cells upon Infection with Hepatitis C Virus. In *Journal of Virology* (Vol. 86, Issue 15, pp. 7918–7933). <https://doi.org/10.1128/jvi.00567-12>
- Gao, G., Vandenberghe, L. H., Alvira, M. R., Lu, Y., Calcedo, R., Zhou, X., & Wilson, J. M. (2004). Clades of Adeno-associated viruses are widely disseminated in human tissues. *Journal of Virology*, *78*(12), 6381–6388.
- Garcia, B., Lee, J., Edraki, A., Hidalgo-Reyes, Y., Erwood, S., Mir, A., Trost, C. N., Seroussi, U., Stanley, S. Y., Cohn, R. D., Claycomb, J. M., Sontheimer, E. J., Maxwell, K. L., & Davidson, A. R. (2019). Anti-CRISPR AcrIIA5 Potently Inhibits All Cas9 Homologs Used for Genome Editing. *Cell Reports*, *29*(7), 1739–1746.e5.
- Garneau, J. E., Dupuis, M.-È., Villion, M., Romero, D. A., Barrangou, R., Boyaval, P., Fremaux, C., Horvath, P., Magadán, A. H., & Moineau, S. (2010). The CRISPR/Cas bacterial immune system cleaves bacteriophage and plasmid DNA. *Nature*, *468*(7320), 67–71.
- Gasiunas, G., Barrangou, R., Horvath, P., & Siksnys, V. (2012). Cas9-crRNA ribonucleoprotein complex mediates specific DNA cleavage for adaptive immunity in bacteria. *Proceedings of the National Academy of Sciences of the United States of America*, *109*(39), E2579–E2586.
- Gaudelli, N. M., Komor, A. C., Rees, H. A., Packer, M. S., Badran, A. H., Bryson, D. I., & Liu, D. R. (2017). Programmable base editing of A•T to G•C in genomic DNA without DNA cleavage. *Nature*, *551*(7681), 464–471.
- Geisler, A., Jungmann, A., Kurreck, J., Poller, W., Katus, H. A., Vetter, R., Fechner, H., & Müller, O. J. (2011). microRNA122-regulated transgene expression increases specificity of cardiac gene transfer upon intravenous delivery of AAV9 vectors. In *Gene Therapy* (Vol. 18, Issue 2, pp. 199–209). <https://doi.org/10.1038/gt.2010.141>
- Ghanta, K. S., Dokshin, G. A., Mir, A., Krishnamurthy, P. M., Gneid, H., Edraki,

- A., Watts, J. K., Sontheimer, E. J., & C., C. (2018). 5' Modifications Improve Potency and Efficacy of DNA Donors for Precision Genome Editing. *bioRxiv*. <https://doi.org/10.1101/354480>
- Gilbert, L. A., Horlbeck, M. A., Adamson, B., Villalta, J. E., Chen, Y., Whitehead, E. H., Guimaraes, C., Panning, B., Ploegh, H. L., Bassik, M. C., Qi, L. S., Kampmann, M., & Weissman, J. S. (2014). Genome-Scale CRISPR-Mediated Control of Gene Repression and Activation. *Cell*, *159*(3), 647–661.
- Gilbert, L. A., Larson, M. H., Morsut, L., Liu, Z., Brar, G. A., Torres, S. E., Stern-Ginossar, N., Brandman, O., Whitehead, E. H., Doudna, J. A., Lim, W. A., Weissman, J. S., & Qi, L. S. (2013). CRISPR-mediated modular RNA-guided regulation of transcription in eukaryotes. *Cell*, *154*(2), 442–451.
- Glass, Z., Lee, M., Li, Y., & Xu, Q. (2018). Engineering the Delivery System for CRISPR-Based Genome Editing. *Trends in Biotechnology*, *36*(2), 173–185.
- Gootenberg, J. S., Abudayyeh, O. O., Lee, J. W., Essletzbichler, P., Dy, A. J., Joung, J., Verdine, V., Donghia, N., Daringer, N. M., Freije, C. A., Myhrvold, C., Bhattacharyya, R. P., Livny, J., Regev, A., Koonin, E. V., Hung, D. T., Sabeti, P. C., Collins, J. J., & Zhang, F. (2017). Nucleic acid detection with CRISPR-Cas13a/C2c2. *Science*, *356*(6336), 438–442.
- Gray, S. J., Foti, S. B., Schwartz, J. W., Bachaboina, L., Taylor-Blake, B., Coleman, J., Ehlers, M. D., Zylka, M. J., McCown, T. J., & Jude Samulski, R. (2011). Optimizing Promoters for Recombinant Adeno-Associated Virus-Mediated Gene Expression in the Peripheral and Central Nervous System Using Self-Complementary Vectors. In *Human Gene Therapy* (Vol. 22, Issue 9, pp. 1143–1153). <https://doi.org/10.1089/hum.2010.245>
- Grimson, A., Farh, K. K.-H., Johnston, W. K., Garrett-Engele, P., Lim, L. P., & Bartel, D. P. (2007). MicroRNA targeting specificity in mammals: determinants beyond seed pairing. *Molecular Cell*, *27*(1), 91–105.
- Guschin, D. Y., Waite, A. J., Katibah, G. E., Miller, J. C., Holmes, M. C., & Rebar, E. J. (2010). A rapid and general assay for monitoring endogenous gene modification. *Methods in Molecular Biology*, *649*, 247–256.
- Gutschner, T., Haemmerle, M., Genovese, G., Draetta, G. F., & Chin, L. (2016). Post-translational Regulation of Cas9 during G1 Enhances Homology-Directed Repair. *Cell Reports*, *14*(6), 1555–1566.
- Hale, C. R., Zhao, P., Olson, S., Duff, M. O., Graveley, B. R., Wells, L., Terns, R. M., & Terns, M. P. (2009). RNA-guided RNA cleavage by a CRISPR RNA-Cas protein complex. *Cell*, *139*(5), 945–956.
- Hampton, H. G., Watson, B. N. J., & Fineran, P. C. (2020). The arms race between bacteria and their phage foes. *Nature*, *577*(7790), 327–336.
- Hand, T. H., Das, A., & Li, H. (2019). Directed evolution studies of a thermophilic Type II-C Cas9. *Methods in Enzymology*, *616*, 265–288.
- Hand, T. H., Das, A., Roth, M. O., Smith, C. L., Jean-Baptiste, U. L., & Li, H. (2018). Phosphate Lock Residues of *Acidothermus cellulolyticus* Cas9 Are Critical to Its Substrate Specificity. *ACS Synthetic Biology*.
- Hanlon, K. S., Kleinstiver, B. P., Garcia, S. P., Zaborowski, M. P., Volak, A.,

- Spirig, S. E., Muller, A., Sousa, A. A., Tsai, S. Q., Bengtsson, N. E., Lööv, C., Ingelsson, M., Chamberlain, J. S., Corey, D. P., Aryee, M. J., Joung, J. K., Breakefield, X. O., Maguire, C. A., & György, B. (2019). High levels of AAV vector integration into CRISPR-induced DNA breaks. *Nature Communications*, *10*(1), 4439.
- Hansen, T. B., Jensen, T. I., Clausen, B. H., Bramsen, J. B., Finsen, B., Damgaard, C. K., & Kjems, J. (2013). Natural RNA circles function as efficient microRNA sponges. *Nature*, *495*(7441), 384–388.
- Harrington, L. B., Doxzen, K. W., Ma, E., Liu, J.-J., Knott, G. J., Edraki, A., Garcia, B., Amrani, N., Chen, J. S., Cofsky, J. C., Kranzusch, P. J., Sontheimer, E. J., Davidson, A. R., Maxwell, K. L., & Doudna, J. A. (2017). A Broad-Spectrum Inhibitor of CRISPR-Cas9. *Cell*, *170*(6), 1224–1233.e15.
- Harrington, L. B., Paez-Espino, D., Staahl, B. T., Chen, J. S., Ma, E., Kyrpides, N. C., & Doudna, J. A. (2017). A thermostable Cas9 with increased lifetime in human plasma. *Nature Communications*, *8*(1), 1424.
- Haurwitz, R. E., Jinek, M., Wiedenheft, B., Zhou, K., & Doudna, J. A. (2010). Sequence- and structure-specific RNA processing by a CRISPR endonuclease. *Science*, *329*(5997), 1355–1358.
- Hausser, J., & Zavolan, M. (2014). Identification and consequences of miRNA-target interactions--beyond repression of gene expression. *Nature Reviews. Genetics*, *15*(9), 599–612.
- He, F., Bhoobalan-Chitty, Y., Van, L. B., Kjeldsen, A. L., Dedola, M., Makarova, K. S., Koonin, E. V., Brodersen, D. E., & Peng, X. (2018). Anti-CRISPR proteins encoded by archaeal lytic viruses inhibit subtype I-D immunity. *Nature Microbiology*, *3*(4), 461–469.
- High, K. A., & Roncarolo, M. G. (2019). Gene Therapy. *The New England Journal of Medicine*, *381*(5), 455–464.
- Hirosawa, M., Fujita, Y., Parr, C. J. C., Hayashi, K., Kashida, S., Hotta, A., Woltjen, K., & Saito, H. (2017). Cell-type-specific genome editing with a microRNA-responsive CRISPR-Cas9 switch. *Nucleic Acids Research*, *45*(13), e118.
- Hirosawa, M., Fujita, Y., & Saito, H. (2019). Cell-type-specific CRISPR activation with microRNA-responsive AcrIIA4 switch. *ACS Synthetic Biology*. <https://doi.org/10.1021/acssynbio.9b00073>
- Hoffmann, M. D., Aschenbrenner, S., Grosse, S., Rapti, K., Domenger, C., Fakhiri, J., Mastel, M., Börner, K., Eils, R., Grimm, D., & Niopek, D. (2019). Cell-specific CRISPR-Cas9 activation by microRNA-dependent expression of anti-CRISPR proteins. *Nucleic Acids Research*. <https://doi.org/10.1093/nar/gkz271>
- Hou, Z., Zhang, Y., Propson, N. E., Howden, S. E., Chu, L.-F., Sontheimer, E. J., & Thomson, J. A. (2013). Efficient genome engineering in human pluripotent stem cells using Cas9 from *Neisseria meningitidis*. *Proceedings of the National Academy of Sciences of the United States of America*, *110*(39), 15644–15649.

- Hsu, P. D., Scott, D. A., Weinstein, J. A., Ran, F. A., Konermann, S., Agarwala, V., Li, Y., Fine, E. J., Wu, X., Shalem, O., Cradick, T. J., Marraffini, L. A., Bao, G., & Zhang, F. (2013). DNA targeting specificity of RNA-guided Cas9 nucleases. *Nature Biotechnology*, *31*(9), 827–832.
- Hustedt, N., & Durocher, D. (2016). The control of DNA repair by the cell cycle. *Nature Cell Biology*, *19*(1), 1–9.
- Hwang, S., & Maxwell, K. L. (2019). Meet the Anti-CRISPRs: Widespread Protein Inhibitors of CRISPR-Cas Systems. *The CRISPR Journal*, *2*(1), 23–30.
- Hwang, W. Y., Fu, Y., Reyon, D., Maeder, M. L., Tsai, S. Q., Sander, J. D., Peterson, R. T., Yeh, J.-R. J., & Joung, J. K. (2013). Efficient genome editing in zebrafish using a CRISPR-Cas system. *Nature Biotechnology*, *31*(3), 227–229.
- Hynes, A. P., Rousseau, G. M., Agudelo, D., Goulet, A., Amigues, B., Loehr, J., Romero, D. A., Fremaux, C., Horvath, P., Doyon, Y., Cambillau, C., & Moineau, S. (2018). Widespread anti-CRISPR proteins in virulent bacteriophages inhibit a range of Cas9 proteins. *Nature Communications*, *9*(1), 2919.
- Hynes, A. P., Rousseau, G. M., Lemay, M.-L., Horvath, P., Romero, D. A., Fremaux, C., & Moineau, S. (2017). An anti-CRISPR from a virulent streptococcal phage inhibits *Streptococcus pyogenes* Cas9. *Nat Microbiol*, *2*(10), 1374–1380.
- Ibraheim, R., Song, C.-Q., Mir, A., Amrani, N., Xue, W., & Sontheimer, E. J. (2018). All-in-one adeno-associated virus delivery and genome editing by *Neisseria meningitidis* Cas9 in vivo. *Genome Biology*, *19*(1), 137.
- Iyer, S., Mir, A., Vega-Badillo, J., Roscoe, B. P., Ibraheim, R., Zhu, L. J., Lee, J., Liu, P., Luk, K., Mintzer, E., de Brito, J. S., Zamore, P. D., Sontheimer, E. J., & Wolfe, S. A. (2019). Efficient Homology-directed Repair with Circular ssDNA Donors. In *bioRxiv* (p. 864199). <https://doi.org/10.1101/864199>
- Iyer, S., Suresh, S., Guo, D., Daman, K., Chen, J. C. J., Liu, P., Zieger, M., Luk, K., Roscoe, B. P., Mueller, C., King, O. D., Emerson, C. P., Jr, & Wolfe, S. A. (2019). Precise therapeutic gene correction by a simple nuclease-induced double-stranded break. *Nature*, *568*(7753), 561–565.
- Jarrett, K. E., Lee, C. M., Yeh, Y.-H., Hsu, R. H., Gupta, R., Zhang, M., Rodriguez, P. J., Lee, C. S., Gillard, B. K., Bissig, K.-D., Pownall, H. J., Martin, J. F., Bao, G., & Lagor, W. R. (2017). Somatic genome editing with CRISPR/Cas9 generates and corrects a metabolic disease. *Scientific Reports*, *7*, 44624.
- Jasin, M., & Rothstein, R. (2013). Repair of strand breaks by homologous recombination. *Cold Spring Harbor Perspectives in Biology*, *5*(11), a012740.
- Jiang, F., Liu, J.-J., Osuna, B. A., Xu, M., Berry, J. D., Rauch, B. J., Nogales, E., Bondy-Denomy, J., & Doudna, J. A. (2018). Temperature-Responsive Competitive Inhibition of CRISPR-Cas9. *Molecular Cell*.
- Jiang, J., Zhang, L., Zhou, X., Chen, X., Huang, G., Li, F., Wang, R., Wu, N., Yan, Y., Tong, C., Srivastava, S., Wang, Y., Liu, H., & Ying, Q.-L. (2016).

- Induction of site-specific chromosomal translocations in embryonic stem cells by CRISPR/Cas9. *Scientific Reports*, 6, 21918.
- Jiang, W., Bikard, D., Cox, D., Zhang, F., & Marraffini, L. A. (2013). RNA-guided editing of bacterial genomes using CRISPR-Cas systems. *Nature Biotechnology*, 31(3), 233–239.
- Jiang, W., Maniv, I., Arain, F., Wang, Y., Levin, B. R., & Marraffini, L. A. (2013). Dealing with the evolutionary downside of CRISPR immunity: bacteria and beneficial plasmids. *PLoS Genetics*, 9(9).
<https://www.ncbi.nlm.nih.gov/pmc/articles/pmc3784566/>
- Jinek, M., Chylinski, K., Fonfara, I., Hauer, M., Doudna, J. A., & Charpentier, E. (2012). A programmable dual-RNA-guided DNA endonuclease in adaptive bacterial immunity. *Science*, 337(6096), 816–821.
- Jinek, M., East, A., Cheng, A., Lin, S., Ma, E., & Doudna, J. (2013). RNA-programmed genome editing in human cells. *eLife*, 2, e00471.
- Johnston, R. K., Seamon, K. J., Saada, E. A., Podlevsky, J. D., Branda, S. S., Timlin, J. A., & Harper, J. C. (2019). Use of anti-CRISPR protein AcrIIA4 as a capture ligand for CRISPR/Cas9 detection. *Biosensors & Bioelectronics*, 141, 111361.
- Jonas, S., & Izaurralde, E. (2015). Towards a molecular understanding of microRNA-mediated gene silencing. *Nature Reviews. Genetics*, 16(7), 421–433.
- Jovičić, A., Roshan, R., Moiso, N., Pradervand, S., Moser, R., Pillai, B., & Luthi-Carter, R. (2013). Comprehensive expression analyses of neural cell-type-specific miRNAs identify new determinants of the specification and maintenance of neuronal phenotypes. *The Journal of Neuroscience: The Official Journal of the Society for Neuroscience*, 33(12), 5127–5137.
- Kanegae, Y., Terashima, M., Kondo, S., Fukuda, H., Maekawa, A., Pei, Z., & Saito, I. (2011). High-level expression by tissue/cancer-specific promoter with strict specificity using a single-adenoviral vector. In *Nucleic Acids Research* (Vol. 39, Issue 2, pp. e7–e7). <https://doi.org/10.1093/nar/gkq966>
- Kazlauskiene, M., Kostiuk, G., Venclovas, Č., Tamulaitis, G., & Siksnys, V. (2017). A cyclic oligonucleotide signaling pathway in type III CRISPR-Cas systems. *Science*, 357(6351), 605–609.
- Kim, D., Luk, K., Wolfe, S. A., & Kim, J.-S. (2019). Evaluating and Enhancing Target Specificity of Gene-Editing Nucleases and Deaminases. *Annual Review of Biochemistry*. <https://doi.org/10.1146/annurev-biochem-013118-111730>
- Kim, E., Koo, T., Park, S. W., Kim, D., Kim, K., Cho, H.-Y., Song, D. W., Lee, K. J., Jung, M. H., Kim, S., Kim, J. H., Kim, J. H., & Kim, J.-S. (2017). In vivo genome editing with a small Cas9 orthologue derived from *Campylobacter jejuni*. *Nature Communications*, 8, 14500.
- Kim, I., Jeong, M., Ka, D., Han, M., Kim, N.-K., Bae, E., & Suh, J.-Y. (2018). Solution structure and dynamics of anti-CRISPR AcrIIA4, the Cas9 inhibitor. *Scientific Reports*, 8(1), 3883.

- Kim, S., Kim, D., Cho, S. W., Kim, J., & Kim, J.-S. (2014). Highly efficient RNA-guided genome editing in human cells via delivery of purified Cas9 ribonucleoproteins. In *Genome Research* (Vol. 24, Issue 6, pp. 1012–1019). <https://doi.org/10.1101/gr.171322.113>
- Kim, Y., Lee, S. J., Yoon, H.-J., Kim, N.-K., Lee, B.-J., & Suh, J.-Y. (2019). Anti-CRISPR AcrIIIC3 discriminates between Cas9 orthologs via targeting the variable surface of the HNH nuclease domain. *The FEBS Journal*. <https://doi.org/10.1111/febs.15037>
- Kinali, M., Arechavala-Gomez, V., Feng, L., Cirak, S., Hunt, D., Adkin, C., Guglieri, M., Ashton, E., Abbs, S., Nihoyannopoulos, P., Garralda, M. E., Rutherford, M., McCulley, C., Popplewell, L., Graham, I. R., Dickson, G., Wood, M. J. A., Wells, D. J., Wilton, S. D., ... Muntoni, F. (2009). Local restoration of dystrophin expression with the morpholino oligomer AVI-4658 in Duchenne muscular dystrophy: a single-blind, placebo-controlled, dose-escalation, proof-of-concept study. *Lancet Neurology*, 8(10), 918–928.
- Klompe, S. E., Vo, P. L. H., Halpin-Healy, T. S., & Sternberg, S. H. (2019). Transposon-encoded CRISPR–Cas systems direct RNA-guided DNA integration. *Nature*, 571(7764), 219–225.
- Knott, G. J., Cress, B. F., Liu, J.-J., Thornton, B. W., Lew, R. J., Al-Shayeb, B., Rosenberg, D. J., Hammel, M., Adler, B. A., Lobba, M. J., Xu, M., Arkin, A. P., Fellmann, C., & Doudna, J. A. (2019). Structural basis for AcrVA4 inhibition of specific CRISPR-Cas12a. *eLife*, 8. <https://doi.org/10.7554/eLife.49110>
- Knott, G. J., Thornton, B. W., Lobba, M. J., Liu, J.-J., Al-Shayeb, B., Watters, K. E., & Doudna, J. A. (2019). Broad-spectrum enzymatic inhibition of CRISPR-Cas12a. *Nature Structural & Molecular Biology*, 26(4), 315–321.
- Komor, A. C., Badran, A. H., & Liu, D. R. (2018). Editing the Genome Without Double-Stranded DNA Breaks. *ACS Chemical Biology*, 13(2), 383–388.
- Komor, A. C., Kim, Y. B., Packer, M. S., Zuris, J. A., & Liu, D. R. (2016). Programmable editing of a target base in genomic DNA without double-stranded DNA cleavage. *Nature*, 533(7603), 420–424.
- Konermann, S., Lotfy, P., Brideau, N. J., Oki, J., Shokhirev, M. N., & Hsu, P. D. (2018). Transcriptome Engineering with RNA-Targeting Type VI-D CRISPR Effectors. *Cell*, 173(3), 665–676.e14.
- Koonin, E. V., & Makarova, K. S. (2018). Anti-CRISPRs on the march [Review of *Anti-CRISPRs on the march*]. *Science*, 362(6411), 156–157.
- Kosicki, M., Tomberg, K., & Bradley, A. (2018). Repair of double-strand breaks induced by CRISPR–Cas9 leads to large deletions and complex rearrangements. *Nature Biotechnology*, 36(8), 765–771.
- Krooss, S. A., Dai, Z., Schmidt, F., Rovai, A., Fakhiri, J., Dhingra, A., Yuan, Q., Yang, T., Balakrishnan, A., Steinbrück, L., & Others. (2020). *Ex Vivo/In vivo Gene Editing in Hepatocytes Using*. <https://repository.helmholtz-hzi.de/handle/10033/622113>
- Labrie, S. J., Samson, J. E., & Moineau, S. (2010). Bacteriophage resistance

- mechanisms. *Nature Reviews. Microbiology*, 8(5), 317–327.
- Lagos-Quintana, M., Rauhut, R., Yalcin, A., Meyer, J., Lendeckel, W., & Tuschl, T. (2002). Identification of tissue-specific microRNAs from mouse. *Current Biology: CB*, 12(9), 735–739.
- Landgraf, P., Rusu, M., Sheridan, R., Sewer, A., Iovino, N., Aravin, A., Pfeffer, S., Rice, A., Kamphorst, A. O., Landthaler, M., Lin, C., Socci, N. D., Hermida, L., Fulci, V., Chiaretti, S., Foà, R., Schliwka, J., Fuchs, U., Novosel, A., ... Tuschl, T. (2007). A mammalian microRNA expression atlas based on small RNA library sequencing. *Cell*, 129(7), 1401–1414.
- Landsberger, M., Gandon, S., Meaden, S., Rollie, C., Chevallereau, A., Chabas, H., Buckling, A., Westra, E. R., & van Houte, S. (2018). Anti-CRISPR Phages Cooperate to Overcome CRISPR-Cas Immunity. *Cell*, 174(4), 908–916.e12.
- Lanphier, E., Urnov, F., Haecker, S. E., Werner, M., & Smolenski, J. (2015). Don't edit the human germ line. *Nature*, 519(7544), 410–411.
- Ledford, H. (2019). CRISPR babies: when will the world be ready? *Nature*, 570(7761), 293–296.
- Lee, J., Mir, A., Edraki, A., Garcia, B., Amrani, N., Lou, H. E., Gainetdinov, I., Pawluk, A., Ibraheim, R., Gao, X. D., Liu, P., Davidson, A. R., Maxwell, K. L., & Sontheimer, E. J. (2018). Potent Cas9 Inhibition in Bacterial and Human Cells by AcrIIc4 and AcrIIc5 Anti-CRISPR Proteins. *mBio*, 9(6).
- Lee, J., Mou, H., Ibraheim, R., Liang, S.-Q., Liu, P., Xue, W., & Sontheimer, E. J. (2019). Tissue-restricted genome editing in vivo specified by microRNA-repressible anti-CRISPR proteins. *RNA*, 25(11), 1421–1431.
- Lee, R. C., Feinbaum, R. L., & Ambros, V. (1993). The *C. elegans* heterochronic gene *lin-4* encodes small RNAs with antisense complementarity to *lin-14*. *Cell*, 75(5), 843–854.
- Liang, D., Gutierrez, N. M., Chen, T., Lee, Y., Park, S.-W., Ma, H., Koski, A., Ahmed, R., Darby, H., Li, Y., Van Dyken, C., Mikhalchenko, A., Gonmanee, T., Hayama, T., Zhao, H., Wu, K., Zhang, J., Hou, Z., Park, J., ... Mitalipov, S. (2020). FREQUENT GENE CONVERSION IN HUMAN EMBRYOS INDUCED BY DOUBLE STRAND BREAKS. In *bioRxiv* (p. 2020.06.19.162214). <https://doi.org/10.1101/2020.06.19.162214>
- Liang, P., Xu, Y., Zhang, X., Ding, C., Huang, R., Zhang, Z., Lv, J., Xie, X., Chen, Y., Li, Y., Sun, Y., Bai, Y., Songyang, Z., Ma, W., Zhou, C., & Huang, J. (2015). CRISPR/Cas9-mediated gene editing in human tripronuclear zygotes. *Protein & Cell*, 6(5), 363–372.
- Li, A., Tanner, M. R., Lee, C. M., Hurley, A. E., De Giorgi, M., Jarrett, K. E., Davis, T. H., Doerfler, A. M., Bao, G., Beeton, C., & Lagor, W. R. (2020). AAV-CRISPR Gene Editing Is Negated by Pre-existing Immunity to Cas9. *Molecular Therapy: The Journal of the American Society of Gene Therapy*, 28(6), 1432–1441.
- Li, C., Psatha, N., Gil, S., Wang, H., Papayannopoulou, T., & Lieber, A. (2018). HDAd5/35++ Adenovirus Vector Expressing Anti-CRISPR Peptides

- Decreases CRISPR/Cas9 Toxicity in Human Hematopoietic Stem Cells. *Molecular Therapy. Methods & Clinical Development*, 9, 390–401.
- Lieber, M. R. (2010). The mechanism of double-strand DNA break repair by the nonhomologous DNA end-joining pathway. *Annual Review of Biochemistry*, 79, 181–211.
- Li, G., Zhang, X., Zhong, C., Mo, J., Quan, R., Yang, J., Liu, D., Li, Z., Yang, H., & Wu, Z. (2017). Small molecules enhance CRISPR/Cas9-mediated homology-directed genome editing in primary cells. *Scientific Reports*, 7(1), 8943.
- Li, J., Xu, Z., Chupalov, A., & Marchisio, M. A. (2018). Anti-CRISPR-based biosensors in the yeast *S. cerevisiae*. *Journal of Biological Engineering*, 12, 11.
- Lin, P., Qin, S., Pu, Q., Wang, Z., Wu, Q., Gao, P., Schettler, J., Guo, K., Li, R., Li, G., Huang, C., Wei, Y., Gao, G. F., Jiang, J., & Wu, M. (2020). CRISPR-Cas13 Inhibitors Block RNA Editing in Bacteria and Mammalian Cells. *Molecular Cell*. <https://doi.org/10.1016/j.molcel.2020.03.033>
- Lin, S., Staahl, B. T., Alla, R. K., & Doudna, J. A. (2014). Enhanced homology-directed human genome engineering by controlled timing of CRISPR/Cas9 delivery. *eLife*, 3, e04766.
- Liu, J., Carmell, M. A., Rivas, F. V., Marsden, C. G., Thomson, J. M., Song, J.-J., Hammond, S. M., Joshua-Tor, L., & Hannon, G. J. (2004). Argonaute2 is the catalytic engine of mammalian RNAi. *Science*, 305(5689), 1437–1441.
- Liu, J.-J., Orlova, N., Oakes, B. L., Ma, E., Spinner, H. B., Baney, K. L. M., Chuck, J., Tan, D., Knott, G. J., Harrington, L. B., Al-Shayeb, B., Wagner, A., Brötzmann, J., Staahl, B. T., Taylor, K. L., Desmarais, J., Nogales, E., & Doudna, J. A. (2019). Author Correction: CasX enzymes comprise a distinct family of RNA-guided genome editors. *Nature*, 568(7752), E8–E10.
- Liu, L., Yin, M., Wang, M., & Wang, Y. (2018). Phage AcrIIA2 DNA Mimicry: Structural Basis of the CRISPR and Anti-CRISPR Arms Race. *Molecular Cell*.
- Liu, M., Rehman, S., Tang, X., Gu, K., Fan, Q., Chen, D., & Ma, W. (2018). Methodologies for Improving HDR Efficiency. *Frontiers in Genetics*, 9, 691.
- Liu, Q., Zhang, H., & Huang, X. (2020). Anti-CRISPR proteins targeting the CRISPR-Cas system enrich the toolkit for genetic engineering. *The FEBS Journal*, 287(4), 626–644.
- Liu, X. S., Wu, H., Ji, X., Stelzer, Y., Wu, X., Czauderna, S., Shu, J., Dadon, D., Young, R. A., & Jaenisch, R. (2016). Editing DNA Methylation in the Mammalian Genome. *Cell*, 167(1), 233–247.e17.
- Liu, X. S., Wu, H., Krzisch, M., Wu, X., Graef, J., Muffat, J., Hnisz, D., Li, C. H., Yuan, B., Xu, C., Li, Y., Vershkov, D., Cacace, A., Young, R. A., & Jaenisch, R. (2018). Rescue of Fragile X Syndrome Neurons by DNA Methylation Editing of the FMR1 Gene. *Cell*, 172(5), 979–992.e6.
- Li, Y., Glass, Z., Huang, M., Chen, Z.-Y., & Xu, Q. (2020). Ex vivo cell-based CRISPR/Cas9 genome editing for therapeutic applications. *Biomaterials*,

- 234, 119711.
- Long, C., Amoasii, L., Mireault, A. A., McAnally, J. R., Li, H., Sanchez-Ortiz, E., Bhattacharyya, S., Shelton, J. M., Bassel-Duby, R., & Olson, E. N. (2016). Postnatal genome editing partially restores dystrophin expression in a mouse model of muscular dystrophy. *Science*, *351*(6271), 400–403.
- Ludwig, N., Leidinger, P., Becker, K., Backes, C., Fehlmann, T., Pallasch, C., Rheinheimer, S., Meder, B., Stähler, C., Meese, E., & Keller, A. (2016). Distribution of miRNA expression across human tissues. *Nucleic Acids Research*, *44*(8), 3865–3877.
- Maddalo, D., Machado, E., Concepcion, C. P., Bonetti, C., Vidigal, J. A., Han, Y.-C., Ogradowski, P., Crippa, A., Rekhman, N., de Stanchina, E., Lowe, S. W., & Ventura, A. (2014). In vivo engineering of oncogenic chromosomal rearrangements with the CRISPR/Cas9 system. *Nature*, *516*(7531), 423–427.
- Maeder, M. L., Linder, S. J., Cascio, V. M., Fu, Y., Ho, Q. H., & Joung, J. K. (2013). CRISPR RNA-guided activation of endogenous human genes. *Nature Methods*, *10*(10), 977–979.
- Maeder, M. L., Stefanidakis, M., Wilson, C. J., Baral, R., Barrera, L. A., Bounoutas, G. S., Bumcrot, D., Chao, H., Ciulla, D. M., DaSilva, J. A., Dass, A., Dhanapal, V., Fennell, T. J., Friedland, A. E., Giannoukos, G., Gloskowski, S. W., Glucksmann, A., Gotta, G. M., Jayaram, H., ... Jiang, H. (2019). Development of a gene-editing approach to restore vision loss in Leber congenital amaurosis type 10. *Nature Medicine*.
- Ma, E., Harrington, L. B., O'Connell, M. R., Zhou, K., & Doudna, J. A. (2015). Single-Stranded DNA Cleavage by Divergent CRISPR-Cas9 Enzymes. *Molecular Cell*, *60*(3), 398–407.
- Ma, H., Marti-Gutierrez, N., Park, S.-W., Wu, J., Lee, Y., Suzuki, K., Koski, A., Ji, D., Hayama, T., Ahmed, R., Darby, H., Van Dyken, C., Li, Y., Kang, E., Park, A.-R., Kim, D., Kim, S.-T., Gong, J., Gu, Y., ... Mitalipov, S. (2017). Correction of a pathogenic gene mutation in human embryos. *Nature*, *548*(7668), 413–419.
- Maji, B., Gangopadhyay, S. A., Lee, M., Shi, M., Wu, P., Heler, R., Mok, B., Lim, D., Siriwardena, S. U., Paul, B., Dančík, V., Vetere, A., Mesleh, M. F., Marraffini, L. A., Liu, D. R., Clemons, P. A., Wagner, B. K., & Choudhary, A. (2019). A High-Throughput Platform to Identify Small-Molecule Inhibitors of CRISPR-Cas9. *Cell*, *177*(4), 1067–1079.e19.
- Majowicz, A., Maczuga, P., Kwikkers, K. L., van der Marel, S., van Logtenstein, R., Petry, H., van Deventer, S. J., Konstantinova, P., & Ferreira, V. (2013). Mir-142-3p target sequences reduce transgene-directed immunogenicity following intramuscular adeno-associated virus 1 vector-mediated gene delivery. *The Journal of Gene Medicine*, *15*(6-7), 219–232.
- Makarova, K. S., Wolf, Y. I., Iranzo, J., Shmakov, S. A., Alkhnbashi, O. S., Brouns, S. J. J., Charpentier, E., Cheng, D., Haft, D. H., Horvath, P., Moineau, S., Mojica, F. J. M., Scott, D., Shah, S. A., Siksnyts, V., Terns, M.

- P., Venclovas, Č., White, M. F., Yakunin, A. F., ... Koonin, E. V. (2020). Evolutionary classification of CRISPR-Cas systems: a burst of class 2 and derived variants. *Nature Reviews. Microbiology*, 18(2), 67–83.
- Mali, P., Aach, J., Stranges, P. B., Esvelt, K. M., Moosburner, M., Kosuri, S., Yang, L., & Church, G. M. (2013). CAS9 transcriptional activators for target specificity screening and paired nickases for cooperative genome engineering. *Nature Biotechnology*, 31(9), 833–838.
- Malone, L. M., Warring, S. L., Jackson, S. A., Warnecke, C., Gardner, P. P., Gummy, L. F., & Fineran, P. C. (2020). A jumbo phage that forms a nucleus-like structure evades CRISPR–Cas DNA targeting but is vulnerable to type III RNA-based immunity. *Nature Microbiology*, 5(1), 48–55.
- Mani, R.-S., & Chinnaiyan, A. M. (2010). Triggers for genomic rearrangements: insights into genomic, cellular and environmental influences. *Nature Reviews. Genetics*, 11(12), 819–829.
- Marino, N. D., Pinilla-Redondo, R., Csörgő, B., & Bondy-Denomy, J. (2020). Anti-CRISPR protein applications: natural brakes for CRISPR-Cas technologies. *Nature Methods*. <https://doi.org/10.1038/s41592-020-0771-6>
- Marino, N. D., Zhang, J. Y., Borges, A. L., Sousa, A. A., Leon, L. M., Rauch, B. J., Walton, R. T., Berry, J. D., Joung, J. K., Kleinstiver, B. P., & Bondy-Denomy, J. (2018). Discovery of widespread type I and type V CRISPR-Cas inhibitors. *Science*, 362(6411), 240–242.
- Marraffini, L. A., & Sontheimer, E. J. (2008). CRISPR Interference Limits Horizontal Gene Transfer in Staphylococci by Targeting DNA. *Science*, 322(5909), 1843–1845.
- Marshall, R., Maxwell, C. S., Collins, S. P., Jacobsen, T., Luo, M. L., Begemann, M. B., Gray, B. N., January, E., Singer, A., He, Y., Beisel, C. L., & Noireaux, V. (2018). Rapid and Scalable Characterization of CRISPR Technologies Using an E. coli Cell-Free Transcription-Translation System. *Molecular Cell*, 69(1), 146–157.e3.
- Maruyama, T., Dougan, S. K., Truttmann, M. C., Bilate, A. M., Ingram, J. R., & Ploegh, H. L. (2015). Increasing the efficiency of precise genome editing with CRISPR-Cas9 by inhibition of nonhomologous end joining. *Nature Biotechnology*, 33(5), 538–542.
- Mathony, J., Hartevelde, Z., Schmelas, C., Belzen, J. U. zu, Aschenbrenner, S., Sun, W., Hoffmann, M. D., Stengl, C., Scheck, A., Georgeon, S., Rosset, S., Wang, Y., Grimm, D., Eils, R., Correia, B. E., & Niopek, D. (2020). Computational design of anti-CRISPR proteins with improved inhibition potency. In *Nature Chemical Biology*. <https://doi.org/10.1038/s41589-020-0518-9>
- McCarty, D. M., Fu, H., Monahan, P. E., Toulson, C. E., Naik, P., & Samulski, R. J. (2003). Adeno-associated virus terminal repeat (TR) mutant generates self-complementary vectors to overcome the rate-limiting step to transduction in vivo. In *Gene Therapy* (Vol. 10, Issue 26, pp. 2112–2118). <https://doi.org/10.1038/sj.gt.3302134>

- McCullough, K. T., Boye, S. L., Fajardo, D., Calabro, K. R., Peterson, J. J., Strang, C. E., Chakraborty, D., Gloskowski, S., Haskett, S., Samuelsson, S., Jiang, H., Witherspoon, C. D., Gamlin, P. D., Maeder, M. L., & Boye, S. (2018). Somatic gene editing of GUCY2D by AAV-CRISPR/Cas9 alters retinal structure and function in mouse and macaque. *Human Gene Therapy*.
- McGinn, J., & Marraffini, L. A. (2019). Molecular mechanisms of CRISPR-Cas spacer acquisition. *Nature Reviews. Microbiology*, 17(1), 7–12.
- McGreevy, J. W., Hakim, C. H., McIntosh, M. A., & Duan, D. (2015). Animal models of Duchenne muscular dystrophy: from basic mechanisms to gene therapy. In *Disease Models & Mechanisms* (Vol. 8, Issue 3, pp. 195–213). <https://doi.org/10.1242/dmm.018424>
- Meeske, A. J., Jia, N., Cassel, A. K., Kozlova, A., Liao, J., Wiedmann, M., Patel, D. J., & Marraffini, L. A. (2020). A phage-encoded anti-CRISPR enables complete evasion of type VI-A CRISPR-Cas immunity. *Science*. <https://doi.org/10.1126/science.abb6151>
- Meeske, A. J., Nakandakari-Higa, S., & Marraffini, L. A. (2019). Cas13-induced cellular dormancy prevents the rise of CRISPR-resistant bacteriophage. In *Nature* (Vol. 570, Issue 7760, pp. 241–245). <https://doi.org/10.1038/s41586-019-1257-5>
- Memczak, S., Jens, M., Elefsinioti, A., Torti, F., Krueger, J., Rybak, A., Maier, L., Mackowiak, S. D., Gregersen, L. H., Munschauer, M., Loewer, A., Ziebold, U., Landthaler, M., Kocks, C., le Noble, F., & Rajewsky, N. (2013). Circular RNAs are a large class of animal RNAs with regulatory potency. *Nature*, 495(7441), 333–338.
- Mendell, J. R., Al-Zaidy, S., Shell, R., Dave Arnold, W., Rodino-Klapac, L. R., Prior, T. W., Lowes, L., Alfano, L., Berry, K., Church, K., Kissel, J. T., Nagendran, S., L'Italien, J., Sproule, D. M., Wells, C., Cardenas, J. A., Heitzer, M. D., Kaspar, A., Corcoran, S., ... Kaspar, B. K. (2017). Single-Dose Gene-Replacement Therapy for Spinal Muscular Atrophy. In *New England Journal of Medicine* (Vol. 377, Issue 18, pp. 1713–1722). <https://doi.org/10.1056/nejmoa1706198>
- Mendell, J. R., & Lloyd-Puryear, M. (2013). Report of MDA muscle disease symposium on newborn screening for Duchenne muscular dystrophy. *Muscle & Nerve*, 48(1), 21–26.
- Mendell, J. R., & Rodino-Klapac, L. R. (2016). Duchenne muscular dystrophy: CRISPR/Cas9 treatment [Review of *Duchenne muscular dystrophy: CRISPR/Cas9 treatment*]. *Cell Research*, 26(5), 513–514.
- Miller, D. G., Petek, L. M., & Russell, D. W. (2004). Adeno-associated virus vectors integrate at chromosome breakage sites. *Nature Genetics*, 36(7), 767–773.
- Min, Y.-L., Bassel-Duby, R., & Olson, E. N. (2018). CRISPR Correction of Duchenne Muscular Dystrophy. *Annual Review of Medicine*.
- Mingozzi, F., & High, K. A. (2013). Immune responses to AAV vectors:

- overcoming barriers to successful gene therapy. *Blood*, 122(1), 23–36.
- Mir, A., Alterman, J. F., Hassler, M. R., Debacker, A. J., Hudgens, E., Echeverria, D., Brodsky, M. H., Khvorova, A., Watts, J. K., & Sontheimer, E. J. (2018). Heavily and fully modified RNAs guide efficient SpyCas9-mediated genome editing. *Nature Communications*, 9(1), 2641.
- Mir, A., Edraki, A., Lee, J., & Sontheimer, E. J. (2018). Type II-C CRISPR-Cas9 Biology, Mechanism, and Application. *ACS Chemical Biology*, 13(2), 357–365.
- Mitropant, C., Adams, A. M., Meloni, P. L., Muntoni, F., Fletcher, S., & Wilton, S. D. (2009). Rational design of antisense oligomers to induce dystrophin exon skipping. *Molecular Therapy: The Journal of the American Society of Gene Therapy*, 17(8), 1418–1426.
- Mojica, F. J. M., Díez-Villaseñor, C., García-Martínez, J., & Almendros, C. (2009). Short motif sequences determine the targets of the prokaryotic CRISPR defence system. *Microbiology*, 155(Pt 3), 733–740.
- Moreno, A. M., Palmer, N., Alemán, F., Chen, G., Pla, A., Jiang, N., Chew, W. L., Law, M., & Mali, P. (2019). Immune-orthogonal orthologues of AAV capsids and of Cas9 circumvent the immune response to the administration of gene therapy. In *Nature Biomedical Engineering* (Vol. 3, Issue 10, pp. 806–816). <https://doi.org/10.1038/s41551-019-0431-2>
- Moretti, A., Fonteyne, L., Giesert, F., Hoppmann, P., Meier, A. B., Bozoglu, T., Baehr, A., Schneider, C. M., Sinnecker, D., Klett, K., Fröhlich, T., Rahman, F. A., Haufe, T., Sun, S., Jurisch, V., Kessler, B., Hinkel, R., Dirschinger, R., Martens, E., ... Kupatt, C. (2020). Somatic gene editing ameliorates skeletal and cardiac muscle failure in pig and human models of Duchenne muscular dystrophy. *Nature Medicine*, 26(2), 207–214.
- Morisaka, H., Yoshimi, K., Okuzaki, Y., Gee, P., Kunihiro, Y., Sonpho, E., Xu, H., Sasakawa, N., Naito, Y., Nakada, S., Yamamoto, T., Sano, S., Hotta, A., Takeda, J., & Mashimo, T. (2019). CRISPR-Cas3 induces broad and unidirectional genome editing in human cells. *Nature Communications*, 10(1), 5302.
- Mukherji, S., Ebert, M. S., Zheng, G. X. Y., Tsang, J. S., Sharp, P. A., & van Oudenaarden, A. (2011). MicroRNAs can generate thresholds in target gene expression. *Nature Genetics*, 43(9), 854–859.
- Mulloikandov, G., Baccarini, A., Ruzo, A., Jayaprakash, A. D., Tung, N., Israelow, B., Evans, M. J., Sachidanandam, R., & Brown, B. D. (2012). High-throughput assessment of microRNA activity and function using microRNA sensor and decoy libraries. *Nature Methods*, 9(8), 840–846.
- Myhrvold, C., Freije, C. A., Gootenberg, J. S., Abudayyeh, O. O., Metsky, H. C., Durbin, A. F., Kellner, M. J., Tan, A. L., Paul, L. M., Parham, L. A., Garcia, K. F., Barnes, K. G., Chak, B., Mondini, A., Nogueira, M. L., Isern, S., Michael, S. F., Lorenzana, I., Yozwiak, N. L., ... Sabeti, P. C. (2018). Field-deployable viral diagnostics using CRISPR-Cas13. *Science*, 360(6387), 444–448.
- Nakai, H., Storm, T. A., & Kay, M. A. (2000). Recruitment of Single-Stranded

- Recombinant Adeno-Associated Virus Vector Genomes and Intermolecular Recombination Are Responsible for Stable Transduction of Liver In Vivo. In *Journal of Virology* (Vol. 74, Issue 20, pp. 9451–9463). <https://doi.org/10.1128/jvi.74.20.9451-9463.2000>
- Nakamura, M., Srinivasan, P., Chavez, M., Carter, M. A., Dominguez, A. A., La Russa, M., Lau, M. B., Abbott, T. R., Xu, X., Zhao, D., Gao, Y., Kipniss, N. H., Smolke, C. D., Bondy-Denomy, J., & Qi, L. S. (2019). Anti-CRISPR-mediated control of gene editing and synthetic circuits in eukaryotic cells. *Nature Communications*, *10*(1), 194.
- Nambiar, T. S., Billon, P., Diedenhofen, G., Hayward, S. B., Tagliatela, A., Cai, K., Huang, J.-W., Leuzzi, G., Cuella-Martin, R., Palacios, A., Gupta, A., Egli, D., & Ciccia, A. (2019). Stimulation of CRISPR-mediated homology-directed repair by an engineered RAD18 variant. *Nature Communications*, *10*(1), 3395.
- Nateghi Rostami, M. (2020). CRISPR/Cas9 gene drive technology to control transmission of vector-borne parasitic infections. *Parasite Immunology*, e12762.
- Nelson, C. E., Hakim, C. H., Ousterout, D. G., Thakore, P. I., Moreb, E. A., Castellanos Rivera, R. M., Madhavan, S., Pan, X., Ran, F. A., Yan, W. X., Asokan, A., Zhang, F., Duan, D., & Gersbach, C. A. (2016). In vivo genome editing improves muscle function in a mouse model of Duchenne muscular dystrophy. *Science*, *351*(6271), 403–407.
- Nelson, C. E., Wu, Y., Gemberling, M. P., Oliver, M. L., Waller, M. A., Bohning, J. D., Robinson-Hamm, J. N., Bulaklak, K., Castellanos Rivera, R. M., Collier, J. H., Asokan, A., & Gersbach, C. A. (2019). Long-term evaluation of AAV-CRISPR genome editing for Duchenne muscular dystrophy. *Nature Medicine*.
- Niewoehner, O., Garcia-Doval, C., Rostøl, J. T., Berk, C., Schwede, F., Bigler, L., Hall, J., Marraffini, L. A., & Jinek, M. (2017). Type III CRISPR–Cas systems produce cyclic oligoadenylate second messengers. *Nature*, *548*(7669), 543–548.
- Nishida, K., Arazoe, T., Yachie, N., Banno, S., Kakimoto, M., Tabata, M., Mochizuki, M., Miyabe, A., Araki, M., Hara, K. Y., Shimatani, Z., & Kondo, A. (2016). Targeted nucleotide editing using hybrid prokaryotic and vertebrate adaptive immune systems. *Science*, *353*(6305).
- Nobrega, F. L., Costa, A. R., Kluskens, L. D., & Azeredo, J. (2015). Revisiting phage therapy: new applications for old resources. *Trends in Microbiology*, *23*(4), 185–191.
- Nussenzweig, P. M., & Marraffini, L. A. (2018). Viral Teamwork Pushes CRISPR to the Breaking Point [Review of *Viral Teamwork Pushes CRISPR to the Breaking Point*]. *Cell*, *174*(4), 772–774.
- Ormond, K. E., Mortlock, D. P., Scholes, D. T., Bombard, Y., Brody, L. C., Faucett, W. A., Garrison, N. A., Hercher, L., Isasi, R., Middleton, A., Musunuru, K., Shriner, D., Virani, A., & Young, C. E. (2017). Human

- Germline Genome Editing. *American Journal of Human Genetics*, 101(2), 167–176.
- Osuna, B. A., Karambelkar, S., Mahendra, C., Christie, K. A., Garcia, B., Davidson, A. R., Kleinstiver, B. P., Kilcher, S., & Bondy-Denomy, J. (2020). Listeria Phages Induce Cas9 Degradation to Protect Lysogenic Genomes. *Cell Host & Microbe*. <https://doi.org/10.1016/j.chom.2020.04.001>
- Osuna, B. A., Karambelkar, S., Mahendra, C., Sarbach, A., Johnson, M. C., Kilcher, S., & Bondy-Denomy, J. (2020). Critical Anti-CRISPR Locus Repression by a Bi-functional Cas9 Inhibitor. *Cell Host & Microbe*. <https://doi.org/10.1016/j.chom.2020.04.002>
- Palmer, D. J., Turner, D. L., & Ng, P. (2019). Production of CRISPR/Cas9-Mediated Self-Cleaving Helper-Dependent Adenoviruses. *Molecular Therapy. Methods & Clinical Development*, 13, 432–439.
- Pawlica, P., Sheu-Gruttadauria, J., MacRae, I. J., & Steitz, J. A. (2020). How Complementary Targets Expose the microRNA 3' End for Tailing and Trimming during Target-Directed microRNA Degradation. *Cold Spring Harbor Symposia on Quantitative Biology*. <https://doi.org/10.1101/sqb.2019.84.039321>
- Pawluk, A., Amrani, N., Zhang, Y., Garcia, B., Hidalgo-Reyes, Y., Lee, J., Edraki, A., Shah, M., Sontheimer, E. J., Maxwell, K. L., & Davidson, A. R. (2016). Naturally Occurring Off-Switches for CRISPR-Cas9. *Cell*, 167(7), 1829–1838.e9.
- Pawluk, A., Bondy-Denomy, J., Cheung, V. H. W., Maxwell, K. L., & Davidson, A. R. (2014). A new group of phage anti-CRISPR genes inhibits the type I-E CRISPR-Cas system of *Pseudomonas aeruginosa*. *mBio*, 5(2), e00896.
- Pawluk, A., Davidson, A. R., & Maxwell, K. L. (2018). Anti-CRISPR: discovery, mechanism and function. *Nature Reviews. Microbiology*, 16(1), 12–17.
- Pawluk, A., Staals, R. H. J., Taylor, C., Watson, B. N. J., Saha, S., Fineran, P. C., Maxwell, K. L., & Davidson, A. R. (2016). Inactivation of CRISPR-Cas systems by anti-CRISPR proteins in diverse bacterial species. *Nat Microbiol*, 1(8), 16085.
- Peng, X., Mayo-Muñoz, D., Bhoobalan-Chitty, Y., & Martínez-Álvarez, L. (2020). Anti-CRISPR Proteins in Archaea. *Trends in Microbiology*. <https://doi.org/10.1016/j.tim.2020.05.007>
- Perez-Pinera, P., Kocak, D. D., Vockley, C. M., Adler, A. F., Kabadi, A. M., Polstein, L. R., Thakore, P. I., Glass, K. A., Ousterout, D. G., Leong, K. W., Guilak, F., Crawford, G. E., Reddy, T. E., & Gersbach, C. A. (2013). RNA-guided gene activation by CRISPR-Cas9-based transcription factors. *Nature Methods*, 10(10), 973–976.
- Pickar-Oliver, A., & Gersbach, C. A. (2019). The next generation of CRISPR–Cas technologies and applications. *Nature Reviews. Molecular Cell Biology*, 20(8), 490–507.
- Pinder, J., Salsman, J., & Dellaire, G. (2015). Nuclear domain “knock-in” screen for the evaluation and identification of small molecule enhancers of CRISPR-

- based genome editing. *Nucleic Acids Research*, 43(19), 9379–9392.
- Porteus, M. H. (2019). A New Class of Medicines through DNA Editing. *The New England Journal of Medicine*, 380(10), 947–959.
- Qiao, C., Yuan, Z., Li, J., He, B., Zheng, H., Mayer, C., Li, J., & Xiao, X. (2011). Liver-specific microRNA-122 target sequences incorporated in AAV vectors efficiently inhibits transgene expression in the liver. In *Gene Therapy* (Vol. 18, Issue 4, pp. 403–410). <https://doi.org/10.1038/gt.2010.157>
- Qi, L. S., Larson, M. H., Gilbert, L. A., Doudna, J. A., Weissman, J. S., Arkin, A. P., & Lim, W. A. (2013). Repurposing CRISPR as an RNA-Guided Platform for Sequence-Specific Control of Gene Expression. In *Cell* (Vol. 152, Issue 5, pp. 1173–1183). <https://doi.org/10.1016/j.cell.2013.02.022>
- Rahman, R.-U., Liebhoff, A.-M., Bansal, V., Fiosins, M., Rajput, A., Sattar, A., Magruder, D. S., Madan, S., Sun, T., Gautam, A., Heins, S., Liwinski, T., Bethune, J., Trenkwalder, C., Fluck, J., Mollenhauer, B., & Bonn, S. (2020). SEAwEB: the small RNA Expression Atlas web application. In *Nucleic Acids Research* (Vol. 48, Issue D1, pp. D204–D219). <https://doi.org/10.1093/nar/gkz869>
- Ran, F. A., Ann Ran, F., Cong, L., Yan, W. X., Scott, D. A., Gootenberg, J. S., Kriz, A. J., Zetsche, B., Shalem, O., Wu, X., Makarova, K. S., Koonin, E. V., Sharp, P. A., & Zhang, F. (2015). In vivo genome editing using *Staphylococcus aureus* Cas9. In *Nature* (Vol. 520, Issue 7546, pp. 186–191). <https://doi.org/10.1038/nature14299>
- Rauch, B. J., Silvis, M. R., Hultquist, J. F., Waters, C. S., McGregor, M. J., Krogan, N. J., & Bondy-Denomy, J. (2017). Inhibition of CRISPR-Cas9 with Bacteriophage Proteins. *Cell*, 168(1-2), 150–158.e10.
- Razin, A., & Riggs, A. D. (1980). DNA methylation and gene function. *Science*, 210(4470), 604–610.
- Rees, H. A., & Liu, D. R. (2018a). Base editing: precision chemistry on the genome and transcriptome of living cells. *Nature Reviews. Genetics*, 19(12), 770–788.
- Rees, H. A., & Liu, D. R. (2018b). Publisher Correction: Base editing: precision chemistry on the genome and transcriptome of living cells. *Nature Reviews. Genetics*, 19(12), 801.
- Robert, F., Barbeau, M., Éthier, S., Dostie, J., & Pelletier, J. (2015). Pharmacological inhibition of DNA-PK stimulates Cas9-mediated genome editing. *Genome Medicine*, 7, 93.
- Rollie, C., Chevallereau, A., Watson, B. N. J., Chyou, T.-Y., Fradet, O., McLeod, I., Fineran, P. C., Brown, C. M., Gandon, S., & Westra, E. R. (2020). Targeting of temperate phages drives loss of type I CRISPR–Cas systems. In *Nature* (Vol. 578, Issue 7793, pp. 149–153). <https://doi.org/10.1038/s41586-020-1936-2>
- Rostøl, J. T., & Marraffini, L. A. (2019). Non-specific degradation of transcripts promotes plasmid clearance during type III-A CRISPR-Cas immunity. *Nat Microbiol*.

- Rouillon, C., Zhou, M., Zhang, J., Politis, A., Beilsten-Edmands, V., Cannone, G., Graham, S., Robinson, C. V., Spagnolo, L., & White, M. F. (2013). Structure of the CRISPR interference complex CSM reveals key similarities with cascade. *Molecular Cell*, *52*(1), 124–134.
- Rousseau, B. A., Hou, Z., Gramelspacher, M. J., & Zhang, Y. (2018). Programmable RNA Cleavage and Recognition by a Natural CRISPR-Cas9 System from *Neisseria meningitidis*. *Molecular Cell*, *69*(5), 906–914.e4.
- Russell, S., Bennett, J., Wellman, J. A., Chung, D. C., Yu, Z.-F., Tillman, A., Wittes, J., Pappas, J., Elci, O., McCague, S., Cross, D., Marshall, K. A., Walshire, J., Kehoe, T. L., Reichert, H., Davis, M., Raffini, L., George, L. A., Parker Hudson, F., ... Maguire, A. M. (2017). Efficacy and safety of voretigene neparvovec (AAV2-hRPE65v2) in patients with RPE65 -mediated inherited retinal dystrophy: a randomised, controlled, open-label, phase 3 trial. In *The Lancet* (Vol. 390, Issue 10097, pp. 849–860). [https://doi.org/10.1016/s0140-6736\(17\)31868-8](https://doi.org/10.1016/s0140-6736(17)31868-8)
- Sakaue-Sawano, A., Kurokawa, H., Morimura, T., Hanyu, A., Hama, H., Osawa, H., Kashiwagi, S., Fukami, K., Miyata, T., Miyoshi, H., Imamura, T., Ogawa, M., Masai, H., & Miyawaki, A. (2008). Visualizing spatiotemporal dynamics of multicellular cell-cycle progression. *Cell*, *132*(3), 487–498.
- Samson, J. E., Magadán, A. H., Sabri, M., & Moineau, S. (2013). Revenge of the phages: defeating bacterial defences. *Nature Reviews. Microbiology*, *11*(10), 675–687.
- Sapranaukas, R., Gasiunas, G., Fremaux, C., Barrangou, R., Horvath, P., & Siksnys, V. (2011). The *Streptococcus thermophilus* CRISPR/Cas system provides immunity in *Escherichia coli*. *Nucleic Acids Research*, *39*(21), 9275–9282.
- Sauna, Z. E., Lagassé, D., Pedras-Vasconcelos, J., Golding, B., & Rosenberg, A. S. (2018). Evaluating and Mitigating the Immunogenicity of Therapeutic Proteins. *Trends in Biotechnology*, *36*(10), 1068–1084.
- Schneider, G. (2018). Automating drug discovery. *Nature Reviews. Drug Discovery*, *17*(2), 97–113.
- Scully, R., Panday, A., Elango, R., & Willis, N. A. (2019). DNA double-strand break repair-pathway choice in somatic mammalian cells. *Nature Reviews. Molecular Cell Biology*, *20*(11), 698–714.
- Senís, E., Fatouros, C., Große, S., Wiedtke, E., Niopek, D., Mueller, A.-K., Börner, K., & Grimm, D. (2014). CRISPR/Cas9-mediated genome engineering: an adeno-associated viral (AAV) vector toolbox. *Biotechnology Journal*, *9*(11), 1402–1412.
- Shen, M. W., Arbab, M., Hsu, J. Y., Worstell, D., Culbertson, S. J., Krabbe, O., Cassa, C. A., Liu, D. R., Gifford, D. K., & Sherwood, R. I. (2018). Predictable and precise template-free CRISPR editing of pathogenic variants. *Nature*, *563*(7733), 646–651.
- Shin, J., Jiang, F., Liu, J.-J., Bray, N. L., Rauch, B. J., Baik, S. H., Nogales, E., Bondy-Denomy, J., Corn, J. E., & Doudna, J. A. (2017). Disabling Cas9 by

- an anti-CRISPR DNA mimic. *Science Advances*, 3(7), e1701620.
- Shmakov, S., Smargon, A., Scott, D., Cox, D., Pyzocha, N., Yan, W., Abudayyeh, O. O., Gootenberg, J. S., Makarova, K. S., Wolf, Y. I., Severinov, K., Zhang, F., & Koonin, E. V. (2017). Diversity and evolution of class 2 CRISPR-Cas systems. *Nature Reviews. Microbiology*, 15(3), 169–182.
- Simhadri, V. L., McGill, J., McMahon, S., Wang, J., Jiang, H., & Sauna, Z. E. (2018). Prevalence of Pre-existing Antibodies to CRISPR-Associated Nuclease Cas9 in the USA Population. *Mol Ther Methods Clin Dev*, 10, 105–112.
- Song, G., Zhang, F., Zhang, X., Gao, X., Zhu, X., Fan, D., & Tian, Y. (2019). AcrIIA5 Inhibits a Broad Range of Cas9 Orthologs by Preventing DNA Target Cleavage. *Cell Reports*, 29(9), 2579–2589.e4.
- Song, J., Yang, D., Xu, J., Zhu, T., Eugene Chen, Y., & Zhang, J. (2016). RS-1 enhances CRISPR/Cas9- and TALEN-mediated knock-in efficiency. In *Nature Communications* (Vol. 7, Issue 1). <https://doi.org/10.1038/ncomms10548>
- Sontheimer, E. J., & Davidson, A. R. (2017). Inhibition of CRISPR-Cas systems by mobile genetic elements. *Current Opinion in Microbiology*, 37, 120–127.
- Srivastava, M., Nambiar, M., Sharma, S., Karki, S. S., Goldsmith, G., Hegde, M., Kumar, S., Pandey, M., Singh, R. K., Ray, P., Natarajan, R., Kelkar, M., De, A., Choudhary, B., & Raghavan, S. C. (2012). An inhibitor of nonhomologous end-joining abrogates double-strand break repair and impedes cancer progression. *Cell*, 151(7), 1474–1487.
- Stanley, S. Y., Borges, A. L., Chen, K.-H., Swaney, D. L., Krogan, N. J., Bondy-Denomy, J., & Davidson, A. R. (2019). Anti-CRISPR-Associated Proteins Are Crucial Repressors of Anti-CRISPR Transcription. In *Cell* (Vol. 178, Issue 6, pp. 1452–1464.e13). <https://doi.org/10.1016/j.cell.2019.07.046>
- Stanley, S. Y., & Maxwell, K. L. (2018). Phage-Encoded Anti-CRISPR Defenses. *Annual Review of Genetics*, 52, 445–464.
- Stone, N. P., Hilbert, B. J., Hidalgo, D., Halloran, K. T., Lee, J., Sontheimer, E. J., & Kelch, B. A. (2018). A Hyperthermophilic Phage Decoration Protein Suggests Common Evolutionary Origin with Herpesvirus Triplex Proteins and an Anti-CRISPR Protein. *Structure*, 26(7), 936–947.e3.
- Strecker, J., Ladha, A., Gardner, Z., Schmid-Burgk, J. L., Makarova, K. S., Koonin, E. V., & Zhang, F. (2019). RNA-guided DNA insertion with CRISPR-associated transposases. *Science*, 365(6448), 48–53.
- Sun, W., Yang, J., Cheng, Z., Amrani, N., Liu, C., Wang, K., Ibraheim, R., Edraki, A., Huang, X., Wang, M., Wang, J., Liu, L., Sheng, G., Yang, Y., Lou, J., Sontheimer, E. J., & Wang, Y. (2019). Structures of *Neisseria meningitidis* Cas9 Complexes in Catalytically Poised and Anti-CRISPR-Inhibited States. *Molecular Cell*. <https://doi.org/10.1016/j.molcel.2019.09.025>
- Suzuki, K., Tsunekawa, Y., Hernandez-Benitez, R., Wu, J., Zhu, J., Kim, E. J., Hatanaka, F., Yamamoto, M., Araoka, T., Li, Z., Kurita, M., Hishida, T., Li, M., Aizawa, E., Guo, S., Chen, S., Goebel, A., Soligalla, R. D., Qu, J., ...

- Belmonte, J. C. I. (2016). In vivo genome editing via CRISPR/Cas9 mediated homology-independent targeted integration. *Nature*, *540*(7631), 144–149.
- Tabebordbar, M., Zhu, K., Cheng, J. K. W., Chew, W. L., Widrick, J. J., Yan, W. X., Maesner, C., Wu, E. Y., Xiao, R., Ran, F. A., Cong, L., Zhang, F., Vandenberghe, L. H., Church, G. M., & Wagers, A. J. (2016). In vivo gene editing in dystrophic mouse muscle and muscle stem cells. *Science*, *351*(6271), 407–411.
- Tang, L., Zeng, Y., Du, H., Gong, M., Peng, J., Zhang, B., Lei, M., Zhao, F., Wang, W., Li, X., & Liu, J. (2017). CRISPR/Cas9-mediated gene editing in human zygotes using Cas9 protein. *Molecular Genetics and Genomics: MGG*, *292*(3), 525–533.
- Teng, F., Cui, T., Feng, G., Guo, L., Xu, K., Gao, Q., Li, T., Li, J., Zhou, Q., & Li, W. (2018). Repurposing CRISPR-Cas12b for mammalian genome engineering. *Cell Discov*, *4*, 63.
- Terns, M. P. (2018). CRISPR-Based Technologies: Impact of RNA-Targeting Systems. *Molecular Cell*, *72*(3), 404–412.
- Thakore, P. I., Black, J. B., Hilton, I. B., & Gersbach, C. A. (2016). Editing the epigenome: technologies for programmable transcription and epigenetic modulation. *Nature Methods*, *13*(2), 127–137.
- Thavalingam, A., Cheng, Z., Garcia, B., Huang, X., Shah, M., Sun, W., Wang, M., Harrington, L., Hwang, S., Hidalgo-Reyes, Y., Sontheimer, E. J., Doudna, J., Davidson, A. R., Moraes, T. F., Wang, Y., & Maxwell, K. L. (2019). Inhibition of CRISPR-Cas9 ribonucleoprotein complex assembly by anti-CRISPR AcrIIIC2. *Nature Communications*, *10*(1), 2806.
- Thuronyi, B. W., Koblan, L. W., Levy, J. M., Yeh, W.-H., Zheng, C., Newby, G. A., Wilson, C., Bhaumik, M., Shubina-Oleinik, O., Holt, J. R., & Liu, D. R. (2019). Continuous evolution of base editors with expanded target compatibility and improved activity. *Nature Biotechnology*, *37*(9), 1070–1079.
- Tornabene, P., & Trapani, I. (2020). Can Adeno-Associated Viral Vectors Deliver Effectively Large Genes? *Human Gene Therapy*, *31*(1-2), 47–56.
- Tsui, T. K. M., Hand, T. H., Duboy, E. C., & Li, H. (2017). The Impact of DNA Topology and Guide Length on Target Selection by a Cytosine-Specific Cas9. *ACS Synthetic Biology*, *6*(6), 1103–1113.
- Uribe, R. V., van der Helm, E., Misiakou, M.-A., Lee, S.-W., Kol, S., & Sommer, M. O. A. (2019). Discovery and Characterization of Cas9 Inhibitors Disseminated across Seven Bacterial Phyla. *Cell Host & Microbe*.
- Urnov, F. D. (2020). Prime Time for Genome Editing? In *New England Journal of Medicine* (Vol. 382, Issue 5, pp. 481–484).
<https://doi.org/10.1056/nejmcibr1914271>
- van Belkum, A., Soriaga, L. B., LaFave, M. C., Akella, S., Veyrieras, J.-B., Barbu, E. M., Shortridge, D., Blanc, B., Hannum, G., Zambardi, G., Miller, K., Enright, M. C., Mugnier, N., Brami, D., Schicklin, S., Felderman, M., Schwartz, A. S., Richardson, T. H., Peterson, T. C., ... Cady, K. C. (2015).

- Phylogenetic Distribution of CRISPR-Cas Systems in Antibiotic-Resistant *Pseudomonas aeruginosa*. *mBio*, 6(6), e01796–15.
- van Deutekom, J. C., Janson, A. A., Ginjaar, I. B., Frankhuizen, W. S., Aartsma-Rus, A., Bremmer-Bout, M., den Dunnen, J. T., Koop, K., van der Kooij, A. J., Goemans, N. M., de Kimpe, S. J., Ekhart, P. F., Venneker, E. H., Platenburg, G. J., Verschuuren, J. J., & van Ommen, G.-J. B. (2007). Local Dystrophin Restoration with Antisense Oligonucleotide PRO051. In *New England Journal of Medicine* (Vol. 357, Issue 26, pp. 2677–2686). <https://doi.org/10.1056/nejmoa073108>
- van Gent, M., & Gack, M. U. (2018). Viral Anti-CRISPR Tactics: No Success without Sacrifice [Review of *Viral Anti-CRISPR Tactics: No Success without Sacrifice*]. *Immunity*, 49(3), 391–393.
- van Houte, S., Ekroth, A. K. E., Broniewski, J. M., Chabas, H., Ashby, B., Bondy-Denomy, J., Gandon, S., Boots, M., Paterson, S., Buckling, A., & Westra, E. R. (2016). The diversity-generating benefits of a prokaryotic adaptive immune system. *Nature*, 532(7599), 385–388.
- van Overbeek, M., Capurso, D., Carter, M. M., Thompson, M. S., Frias, E., Russ, C., Reece-Hoyes, J. S., Nye, C., Gradia, S., Vidal, B., Zheng, J., Hoffman, G. R., Fuller, C. K., & May, A. P. (2016). DNA Repair Profiling Reveals Nonrandom Outcomes at Cas9-Mediated Breaks. *Molecular Cell*, 63(4), 633–646.
- Wagner, D. L., Amini, L., Wendering, D. J., Burkhardt, L.-M., Akyüz, L., Reinke, P., Volk, H.-D., & Schmueck-Henneresse, M. (2019). High prevalence of *Streptococcus pyogenes* Cas9-reactive T cells within the adult human population. *Nature Medicine*, 25(2), 242–248.
- Wang, D., Tai, P. W. L., & Gao, G. (2019). Adeno-associated virus vector as a platform for gene therapy delivery. *Nature Reviews. Drug Discovery*, 18(5), 358–378.
- Wang, D., Zhang, F., & Gao, G. (2020). CRISPR-Based Therapeutic Genome Editing: Strategies and In Vivo Delivery by AAV Vectors. *Cell*, 181(1), 136–150.
- Wang, D., Zhong, L., Abu Nahid, M., & Gao, G. (2014). The potential of adeno-associated viral vectors for gene delivery to muscle tissue. In *Expert Opinion on Drug Delivery* (Vol. 11, Issue 3, pp. 345–364). <https://doi.org/10.1517/17425247.2014.871258>
- Wang, J., Dai, W., Li, J., Xie, R., Dunstan, R. A., Stubenrauch, C., Zhang, Y., & Lithgow, T. (2020). PaCRISPR: a server for predicting and visualizing anti-CRISPR proteins. *Nucleic Acids Research*. <https://doi.org/10.1093/nar/gkaa432>
- Wang, S., Aurora, A. B., Johnson, B. A., Qi, X., McAnally, J., Hill, J. A., Richardson, J. A., Bassel-Duby, R., & Olson, E. N. (2008). The endothelial-specific microRNA miR-126 governs vascular integrity and angiogenesis. *Developmental Cell*, 15(2), 261–271.
- Wang, X.-W., Hu, L.-F., Hao, J., Liao, L.-Q., Chiu, Y.-T., Shi, M., & Wang, Y.

- (2019). A microRNA-inducible CRISPR-Cas9 platform serves as a microRNA sensor and cell-type-specific genome regulation tool. *Nature Cell Biology*.
- Wang, Z., Ma, H.-I., Li, J., Sun, L., Zhang, J., & Xiao, X. (2003). Rapid and highly efficient transduction by double-stranded adeno-associated virus vectors in vitro and in vivo. In *Gene Therapy* (Vol. 10, Issue 26, pp. 2105–2111). <https://doi.org/10.1038/sj.gt.3302133>
- Wan, T., Niu, D., Wu, C., Xu, F.-J., Church, G., & Ping, Y. (2019). Material solutions for delivery of CRISPR/Cas-based genome editing tools: Current status and future outlook. *Materials Today*, 26, 40–66.
- Watters, K. E., Fellmann, C., Bai, H. B., Ren, S. M., & Doudna, J. A. (2018). Systematic discovery of natural CRISPR-Cas12a inhibitors. *Science*, 362(6411), 236–239.
- Westra, E. R., van Houte, S., Oyesiku-Blakemore, S., Makin, B., Broniewski, J. M., Best, A., Bondy-Denomy, J., Davidson, A., Boots, M., & Buckling, A. (2015). Parasite Exposure Drives Selective Evolution of Constitutive versus Inducible Defense. *Current Biology: CB*, 25(8), 1043–1049.
- Wiedenheft, B. (2013). In defense of phage: viral suppressors of CRISPR-mediated adaptive immunity in bacteria. *RNA Biology*, 10(5), 886–890.
- Wiegand, T., Karambelkar, S., Bondy-Denomy, J., & Wiedenheft, B. (2020). Structures and Strategies of Anti-CRISPR-Mediated Immune Suppression. *Annual Review of Microbiology*. <https://doi.org/10.1146/annurev-micro-020518-120107>
- Wightman, B., Ha, I., & Ruvkun, G. (1993). Posttranscriptional regulation of the heterochronic gene *lin-14* by *lin-4* mediates temporal pattern formation in *C. elegans*. *Cell*, 75(5), 855–862.
- Winson, M. K., Swift, S., Hill, P. J., Sims, C. M., Griesmayr, G., Bycroft, B. W., Williams, P., & Stewart, G. S. A. B. (1998). Engineering the *luxCDABE* genes from *Photobacterium luminescens* to provide a bioluminescent reporter for constitutive and promoter probe plasmids and mini-Tn5 constructs. *FEMS Microbiology Letters*, 163(2), 193–202.
- Xiao, Y., Muhuri, M., Li, S., Qin, W., Xu, G., Luo, L., Li, J., Letizia, A. J., Wang, S. K., Chan, Y. K., Wang, C., Fuchs, S. P., Wang, D., Su, Q., Nahid, M. A., Church, G. M., Farzan, M., Yang, L., Wei, Y., ... Gao, G. (2019). Circumventing cellular immunity by miR142-mediated regulation sufficiently supports rAAV-delivered OVA expression without activating humoral immunity. *JCI Insight*, 5. <https://doi.org/10.1172/jci.insight.99052>
- Xie, J., Ameres, S. L., Friedline, R., Hung, J.-H., Zhang, Y., Xie, Q., Zhong, L., Su, Q., He, R., Li, M., Li, H., Mu, X., Zhang, H., Broderick, J. A., Kim, J. K., Weng, Z., Flotte, T. R., Zamore, P. D., & Gao, G. (2012). Long-term, efficient inhibition of microRNA function in mice using rAAV vectors. *Nature Methods*, 9(4), 403–409.
- Xie, J., Xie, Q., Zhang, H., Ameres, S. L., Hung, J.-H., Su, Q., He, R., Mu, X., Seher Ahmed, S., Park, S., Kato, H., Li, C., Mueller, C., Mello, C. C., Weng,

- Z., Flotte, T. R., Zamore, P. D., & Gao, G. (2011). MicroRNA-regulated, systemically delivered rAAV9: a step closer to CNS-restricted transgene expression. *Molecular Therapy: The Journal of the American Society of Gene Therapy*, *19*(3), 526–535.
- Xu, C.-F., Chen, G.-J., Luo, Y.-L., Zhang, Y., Zhao, G., Lu, Z.-D., Czarna, A., Gu, Z., & Wang, J. (2019). Rational designs of in vivo CRISPR-Cas delivery systems. In *Advanced Drug Delivery Reviews*. <https://doi.org/10.1016/j.addr.2019.11.005>
- Xue, W., Chen, S., Yin, H., Tammela, T., Papagiannakopoulos, T., Joshi, N. S., Cai, W., Yang, G., Bronson, R., Crowley, D. G., Zhang, F., Anderson, D. G., Sharp, P. A., & Jacks, T. (2014). CRISPR-mediated direct mutation of cancer genes in the mouse liver. *Nature*, *514*(7522), 380–384.
- Xue, W., Meylan, E., Oliver, T. G., Feldser, D. M., Winslow, M. M., Bronson, R., & Jacks, T. (2011). Response and Resistance to NF- κ B Inhibitors in Mouse Models of Lung Adenocarcinoma. In *Cancer Discovery* (Vol. 1, Issue 3, pp. 236–247). <https://doi.org/10.1158/2159-8290.cd-11-0073>
- Xu, L., Wang, J., Liu, Y., Xie, L., Su, B., Mou, D., Wang, L., Liu, T., Wang, X., Zhang, B., Zhao, L., Hu, L., Ning, H., Zhang, Y., Deng, K., Liu, L., Lu, X., Zhang, T., Xu, J., ... Chen, H. (2019). CRISPR-Edited Stem Cells in a Patient with HIV and Acute Lymphocytic Leukemia. *The New England Journal of Medicine*, *381*(13), 1240–1247.
- Yang, B., Yang, L., & Chen, J. (2019). Development and Application of Base Editors. *The CRISPR Journal*, *2*(2), 91–104.
- Yang, D., Scavuzzo, M. A., Chmielowiec, J., Sharp, R., Bajic, A., & Borowiak, M. (2016). Enrichment of G2/M cell cycle phase in human pluripotent stem cells enhances HDR-mediated gene repair with customizable endonucleases. *Scientific Reports*, *6*, 21264.
- Yang, H., & Patel, D. J. (2017). Inhibition Mechanism of an Anti-CRISPR Suppressor AcrIIA4 Targeting SpyCas9. *Molecular Cell*, *67*(1), 117–127.e5.
- Yan, W. X., Hunnewell, P., Alfonse, L. E., Carte, J. M., Keston-Smith, E., Sothiselvam, S., Garrity, A. J., Chong, S., Makarova, K. S., Koonin, E. V., Cheng, D. R., & Scott, D. A. (2019). Functionally diverse type V CRISPR-Cas systems. *Science*, *363*(6422), 88–91.
- Yeh, C. D., Richardson, C. D., & Corn, J. E. (2019). Advances in genome editing through control of DNA repair pathways. *Nature Cell Biology*, *21*(12), 1468–1478.
- Yi, H., Huang, L., Yang, B., Gomez, J., Zhang, H., & Yin, Y. (2020). AcrFinder: genome mining anti-CRISPR operons in prokaryotes and their viruses. *Nucleic Acids Research*. <https://doi.org/10.1093/nar/gkaa351>
- Yin, H., Kanasty, R. L., Eltoukhy, A. A., Vegas, A. J., Dorkin, J. R., & Anderson, D. G. (2014). Non-viral vectors for gene-based therapy. *Nature Reviews. Genetics*, *15*(8), 541–555.
- Yu, C., Liu, Y., Ma, T., Liu, K., Xu, S., Zhang, Y., Liu, H., La Russa, M., Xie, M., Ding, S., & Qi, L. S. (2015). Small molecules enhance CRISPR genome

- editing in pluripotent stem cells. *Cell Stem Cell*, 16(2), 142–147.
- Zhang, G., Budker, V., & Wolff, J. A. (1999). High levels of foreign gene expression in hepatocytes after tail vein injections of naked plasmid DNA. *Human Gene Therapy*, 10(10), 1735–1737.
- Zhang, H., Li, Z., Daczkowski, C. M., Gabel, C., Mesecar, A. D., & Chang, L. (2019). Structural Basis for the Inhibition of CRISPR-Cas12a by Anti-CRISPR Proteins. *Cell Host & Microbe*.
<https://doi.org/10.1016/j.chom.2019.05.004>
- Zhang, Y. (2017). The CRISPR-Cas9 system in *Neisseria* spp. *Pathogens and Disease*, 75(4).
- Zhang, Y., Heidrich, N., Ampattu, B. J., Gunderson, C. W., Seifert, H. S., Schoen, C., Vogel, J., & Sontheimer, E. J. (2013). Processing-independent CRISPR RNAs limit natural transformation in *Neisseria meningitidis*. *Molecular Cell*, 50(4), 488–503.
- Zhang, Z., Theurkauf, W. E., Weng, Z., & Zamore, P. D. (2012). Strand-specific libraries for high throughput RNA sequencing (RNA-Seq) prepared without poly(A) selection. *Silence*, 3(1), 9.
- Zheng, N., Li, L., & Wang, X. (2020). Molecular mechanisms, off-target activities, and clinical potentials of genome editing systems. *Clinical and Translational Medicine*, 10(1), 412–426.
- Zhong, L., Zhou, X., Li, Y., Qing, K., Xiao, X., Samulski, R. J., & Srivastava, A. (2008). Single-polarity Recombinant Adeno-associated Virus 2 Vector-mediated Transgene Expression In Vitro and In Vivo: Mechanism of Transduction. In *Molecular Therapy* (Vol. 16, Issue 2, pp. 290–295).
<https://doi.org/10.1038/sj.mt.6300376>
- Zhou, X., Zeng, X., Fan, Z., Li, C., McCown, T., Jude Samulski, R., & Xiao, X. (2008). Adeno-associated Virus of a Single-polarity DNA Genome Is Capable of Transduction In Vivo. In *Molecular Therapy* (Vol. 16, Issue 3, pp. 494–499). <https://doi.org/10.1038/sj.mt.6300397>
- Zhu, Y., Gao, A., Zhan, Q., Wang, Y., Feng, H., Liu, S., Gao, G., Serganov, A., & Gao, P. (2019). Diverse Mechanisms of CRISPR-Cas9 Inhibition by Type IIC Anti-CRISPR Proteins. *Molecular Cell*, 74(2), 296–309.e7.
- Zhu, Y., Zhang, F., & Huang, Z. (2018). Structural insights into the inactivation of CRISPR-Cas systems by diverse anti-CRISPR proteins. *BMC Biology*, 16(1), 32.
- Zielke, N., & Edgar, B. A. (2015). Fucci sensors: powerful new tools for analysis of cell proliferation. *Wiley Interdisciplinary Reviews. Developmental Biology*, 4(5), 469–487.
- Zincarelli, C., Soltys, S., Rengo, G., & Rabinowitz, J. E. (2008). Analysis of AAV Serotypes 1–9 Mediated Gene Expression and Tropism in Mice After Systemic Injection. In *Molecular Therapy* (Vol. 16, Issue 6, pp. 1073–1080).
<https://doi.org/10.1038/mt.2008.76>
- Zuccaro, M. V., Xu, J., Mitchell, C., Marin, D., Zimmerman, R., Rana, B., Weinstein, E., King, R. T., Smith, M., Tsang, S. H., Goland, R., Jasin, M.,

- Lobo, R., Treff, N., & Egli, D. (2020). Reading frame restoration at the EYS locus, and allele-specific chromosome removal after Cas9 cleavage in human embryos. In *bioRxiv* (p. 2020.06.17.149237). <https://doi.org/10.1101/2020.06.17.149237>
- Zuris, J. A., Thompson, D. B., Shu, Y., Guilinger, J. P., Bessen, J. L., Hu, J. H., Maeder, M. L., Joung, J. K., Chen, Z.-Y., & Liu, D. R. (2015). Cationic lipid-mediated delivery of proteins enables efficient protein-based genome editing in vitro and in vivo. *Nature Biotechnology*, 33(1), 73–80.